Haptic Interface for the Simulation of Endovascular Interventions

Hafiz Rashidi b Harun

Department of Surgery and Cancer

Imperial College London

A thesis submitted in partial fulfillment of requirements for the degree of Doctor of Philosophy at Imperial College London

January 2017

Abstract

Endovascular interventions are minimally invasive surgical procedures that are performed to diagnose and treat vascular diseases. These interventions use a combination of long and flexible instruments known as guidewire and catheter. A popular method of developing the skills required to manipulate the instruments successfully is through the use of virtual reality (VR) simulators. However, the interfaces of current VR simulators have several shortcomings due to limitations in the instrument tracking and haptic feedback systems design. A major challenge of developing physics-based training simulations of endovascular interventional procedures is to unobtrusively access the central, co-axial guidewire for tracking and haptics. This work sets out to explore the state of the art, to identify and develop novel solutions to this concentric occlusion problem, and to perform a validation of a proof of concept prototype. This multi port haptic interface prototype has been integrated with a 3-D virtual environment and features novel instrument tracking and haptic feedback actuation systems. The former involves the use of an optical sensor to detect guidewire movements through a clear catheter, whereas the latter utilises the placement of a customised electromagnetic actuator within the catheter hub. During the proof of concept validation process, both systems received positive reviews. Whilst the haptic interface prototype designed in this work has met the original objectives, there are still important aspects which need to be addressed to improve its content and face validity. With further development, the prototype has the potential to evolve and become a significant improvement over the haptic interfaces that exist today.

Declaration of Originality

I hereby certify that the work presented in this thesis has not previously been submitted for a degree or diploma in any university. To the best of my knowledge and belief, the thesis contains no material previously published or written by another person except where due reference is made in the thesis itself.

Hafiz Rashidi b Harun

Copyright Declaration

Acknowledgements

Firstly, I would like to acknowledge the dozens of endovascular clinicians, who sacrificed their time to assist and provide valuable information that contributed to this thesis. I would also like to acknowledge the British Society of Interventional Radiology, which played an important role in the recruitment of many of the aforementioned clinicians. Thirdly, I would like to express gratitude to the academics at both Imperial College and Universiti Putra Malaysia for the expert assistance on the technical and engineering aspects of this project. Next, I would like to thank the friendly and helpful staff at the Department of Surgery and Cancer, the International Office and the Imperial College Research Ethics Committee for their continued assistance throughout the work of this thesis. A special thank you also to the good people at OSCO UK for providing various materials and support to me in this project. Lastly, I would like to acknowledge both universities, Universiti Putra Malaysia and Imperial College, for creating the Malaysia-Imperial Doctoral Programme (MIDP) and for giving me this opportunity to obtain a PhD degree at one of the best universities in the world.

Dedications

First and foremost, I would like to thank God for his infinite blessings onto me. I have been to many places in my efforts to complete this PhD, and I feel like He has been with me every step of the way and I am eternally grateful to Him.

Next, I would like to express my utmost gratitude to my main supervisor Dr Fernando Bello for giving me the opportunity of completing this PhD and for teaching me so much throughout this journey. Your wisdom, patience and guidance has been a continuous source of support and inspiration to me as a researcher and as a scientist. I hope that this PhD will prove to be just the beginning of a fruitful relationship of collaboration between our two universities in the future. Secondly, I would like to give my sincerest thanks to my co supervisors Dr Iqbal and Dr Norhisam, for their support and advice that led to the completion of this PhD. I am also very grateful to everyone at my Department of Electric and Electronic Engineering in the Faculty of Engineering of UPM for their patience and encouragement.

This thesis is dedicated to my wonderful mother, Bariah and my loving father, Dr Ramli, who have provided for me and loved me with everything they have and more. The scope of my gratitude and love for you both is not expressible by words.

Mama, I remember how you were so strict with me with my studies, my discipline and my character because you want me to succeed. You always believed that i can be better, and you showed me the way to be better but yet you somehow made me feel absolutely perfect and extremely loved at the same time. No matter how many times i forgot and left my bag at home, or wore two left sided shoes to school by mistake, or asked you to cook something up for me in the middle of the night or broke something in the house while playing football indoors. Thank you for loving me so selflessly and so purely. I love you with all my heart and you will always be my number one.

Papa, I have always felt lucky and proud to be your son. Thank you for always being there with your warm smile and your words of encouragement. I still remember the time you taught me how to play the games from our earliest computers, the Spectrum, and then Amiga, and the IBM. You were so patient with me as i asked you question after question about all the things i don't understand in the games. You taught me so much Dad: how to think, how to question everything, how family always comes first and much more. I love you and thank you so much for everything. I hope I can be as good a father as you have been to me.

I would also like to say thanks to my beautiful sisters, Marina and Noraida, for their love, support and advice and for all the laughter and the tears we shared together. Thank you also to my auntie, Auntie Yap who took such good care of me and my family throughout the years. We love you Aunty and we will always be grateful for all that you've given us.

Speaking of family, a most special thank you to my family in London: Alejandro, Niels, Peter, Korzen, Ally, Vincent, Jimmy, Diane, Fran and Zinah. I truly feel lucky to have known and worked with all of you. My heartiest thanks also, to my long time friends in Malaysia: Azlan, Faisal, Samantha, Aidid, Ratna, Linda, Shaf, Bobo, Dian, Mel and YC.

Last but not least, to my wife and best friend, Azwa, I still cannot believe how perfect you are for me and I am so thankful to have found you. Thank you for all of the support and love you have given me and for being such a fantastic mother to our little angel, Sarah Dahlia. Daddy loves you so much Sarah and watching you grow up will probably be the greatest joy of my life. Though i'm worried about how the world is shaping up to be, i'll always keep you safe and do my best to give you a great life.

This PhD definitely has been the most challenging, most life changing yet most rewarding task i have ever undertaken. The only reason I was able to enjoy its highs and endure its lows was because of the love and support of everyone i mentioned here and the many others that i did not manage to. Thank you and may God bless all of you.

List of Outputs

1. Filed Patent

   Applicant: 1) Universiti Putra Malaysia 2) Imperial College London

   Application Number: PI 2015702770

   Patent Title: A Multi Port Haptic Interface Prototype

   Filing Date: 20 August 2015

   Applicant's Reference Number: UPM/100-45/2(A)MIS1

2. Submitted Publication (Under Review)

   - **Journal:** IEEE Transactions on Haptics

     Paper Title: A Review of Haptic Interface Designs for an Endovascular Procedures Simulator

   - **Journal:** European Journal of Vascular and Endovascular Surgery (EJVES)

     Paper Title: A Study of Haptics in Endovascular Interventions

Contents

List of Figures

List of Tables

1

Introduction

1.1 Background

On average, there are 5 litres of blood being continuously pumped through the human body by the human heart. Every living cell, every piece of tissue, depends on the supply of oxygen and glucose that this flow of blood provides to ensure its continued survival and functionality. These essential components of life are delivered through a system of tubular structures that are known as vessels. These vast networks of vessels make up the human vascular system, also known as the human circulatory system.

The human circulatory system consists of three main parts that work together simultaneously at all times: pulmonary circulation, systemic circulation and coronary circulation. Blood is pumped from the heart to the lungs. In the lungs, the respiratory system fills the blood with oxygen before it is pumped back to the heart. This first circle is called the pulmonary circulation. Then, the oxygenated blood is delivered from the heart to the rest of the body and to the heart or cardiac tissues themselves through the systemic and coronary circulations, respectively. As the oxygen is transferred to each target cell, the deoxygenated blood is returned to the heart to complete the system loop.

It can be observed that the circulatory system is both complex and fragile. A single diseased vessel has the potential to negatively affect any of the human vital systems to the extent of causing death. In fact, cardiovascular diseases or CVD are the number one cause of death around the world. To put it in perspective, it is estimated that 17.3 million people died from CVDs in 2008 [1]. From this number, 7.3 million deaths were

due to diseased cardiac vessels and 6.2 million were due to stroke, caused by diseased blood vessels limiting the supply of blood to the brain [1]. The projected estimation is that this number will reach 23.3 million by 2030 as it continues to be the single leading cause of death in the future [1].

However, despite the grim statistics, patients diagnosed with vascular disease have a reasonably good prognosis due to the advancement of vascular surgery over the last several decades [2]. Perhaps the most significant of these is the advent of endovascular interventions, which was pioneered by Drs. Charles Dotter and Melvin Judkins [3] in 1964, and gained recognition/popularity in the 1970s [4]. This minimally invasive form of surgery enables the diagnosis and treatment of many major vascular diseases and has become a vital part of vascular health care today [2]. Unlike traditional open surgery, endovascular interventions involve the use of long, thin and tubular specialised instruments, called catheters and guidewires, that are inserted into the patient's vascular system via a small incision in the groin or arm that provides access to the vascular system. These instruments will then be guided through the vessels to reach the target area where the necessary diagnosis or treatment is performed. With this approach, patients suffer much less tissue trauma, which leads to faster recovery and reduced treatment costs since they can usually be treated as day surgery cases. Endovascular interventions are performed by different specialities. Interventional cardiologists tend exclusively to cardiac and coronary vessels, whilst vascular surgeons and interventional radiologists are surgically trained for the peripheral vessels such as the renal and carotid arteries. In this thesis, these specialists are regarded as interventionists. The interventionists require extensive training and practise because endovascular procedures demand not only detailed clinical knowledge of the vascular system, but also manual dexterity in handling the delicate guidewire and catheter tool, as well as good hand-eye coordination to navigate the tools guided by interventional imaging techniques.

Traditionally, interventionists are largely trained using the apprenticeship model, where the learning process is facilitated by a senior clinician (mentor) and the trainee (apprentice) learns first through observation, and then by progressively assisting and performing surgical procedures themselves under the direct supervision of the mentor. As the apprentice grows in skill, knowledge and confidence, the mentor gradually steps back into an advisory role until the trainee can stand on his or her own. While this training method is widely considered to be the most realistic, it is not necessarily the

most efficient or effective as it has several drawbacks. Firstly, the mentors providing the necessary training, while highly proficient, often find it difficult to articulate their surgical expertise or decision making process to the apprentice. Research shows that expert knowledge is highly automated [5] (due to large amounts of practice and repetition throughout an extended period of time) and not easily accessible to the expert. A good example is that an experienced bicycle rider would not even have to consciously engage his or her cognitive process when riding a bicycle, whereas a total novice would have no idea on how to even begin riding without falling down. This factor makes the transfer of expertise to the apprentice a challenging task since, theoretically, learners need to be taught decision making strategies to gain expertise [5]. Secondly, learning by progressing through cases in the operating room/cathlab, means that the occasions for learning are always continuously ongoing without having the opportunity to repeat procedures to correct errors, or pause to ask questions during critical points [5]. Thirdly, factors such as a small mentor to apprentice ratio, time in the operating room being costly, and introduction of working time directives, have significantly reduced training opportunities and case exposure for trainees.

All of this has led to the introduction of adjunct training methods in simulated environments, designed to complement the traditional apprenticeship model. Simulated training (and testing) environments aim to replicate a real world state of affairs or process, in order to allow deliberate practice in safety, remotely from patients, and to reliably transfer skills learnt in the training environment to actual invasive procedures [6, 7]. Commonly, simulated training is done with cadavers, animals (usually porcine), physical bench top models and virtual reality (VR) computer simulators. Cadavers and animal subjects raise a series of ethical and practical issues. They are also limited in number and, while similar in some respects, the feel of working with dead tissues is very different to that of live tissues. In [8, 9], the use of VR simulators was found to be more cost effective than that of porcine training, despite the considerable initial cost of commercial endovascular simulators, which can range from £50,000-£100,000. Physical bench top models can be useful but, unlike computer simulators, they are normally built with fixed anatomy or a particular disease in mind so that, once set up, they cannot be altered to simulate different anatomies, diseases or conditions.

Therefore, VR simulators have the potential for significant development as computational technology improves. Unconstrained by any physical factors, training in

the virtual realm offers many different possibilities. This includes the ability to load a number of training scenarios, featuring a variety of anatomical models on which to operate, with different types and severity of disease. Using Computerised Tomography (CT) imaging, these models can be rendered from real patients, making it possible to conduct virtual rehearsals for complicated cases [10, 11], where patient specific data is loaded into the simulator so that the interventionists operating the simulator (hereafter referred to as the operators) may practise the required procedures beforehand. Increased processing power also leads to improved implementation of haptic feedback (application of vibrations/forces to replicate real life stimulus to the touch senses), provided to the operators during simulation via electromechanical devices known as haptic interfaces. Moreover, VR simulators also have the ability to record and quantitatively measure the performance of the operator during the simulation. While research regarding the parameters to be measured (technical and non technical skills) is still ongoing, this would potentially enable the operator to be objectively assessed during simulation training in order to more easily identify his or her mistakes and learn from them [11]. Also, in other applications, VR simulators offer an avenue for clinicians to develop and trial new interventional instruments and techniques in a safe and risk-free environment.

However, learning in a simulated environment, specifically using VR simulators, also suffers from the fundamental problem of expert knowledge transfer mentioned earlier. This is because, most of the current VR simulators are designed by observing experts perform a certain task and listening to their descriptions and justifications of the actions being carried out, which can be ineffective since expert knowledge is highly automated [5]. One method of solving this problem would be to use a Cognitive Task Analysis (CTA) to deconstruct expert knowledge. CTA is defined in [12] as a set of methods for identifying cognitive skills, or mental demands, needed to perform a task proficiently. In [13], the usefulness of CTA is highlighted as it concludes that "the cognitive processes and structures involved in complex tasks are superior to behaviourally based systems for training". CTA is the process of deconstructing an experts knowledge of a task and adapting it to the needs of the educational model. CTA produces a document that can then be used to highlight the specific needs of the operator, the educational goals, and how the simulator design can best meet those goals [5]. It is claimed that CTA can potentially enhance the training efficiency as it has been suggested that 5 years of

advanced job knowledge is transferable to trainees in approximately 50 hours [14]. This would in turn produce benefits in terms of cost reduction [14].

Whilst CTA has been extensively applied to training and education in other critical industries such as air traffic control and nuclear power plants, its application in clinical medicine is relatively new. CTA in the field of Interventional Radiology was pioneered in [15], where CTA techniques were used to develop detailed protocols covering the physical and cognitive processes required to successfully execute certain key tasks: arterial puncture, nephrostomy, venous access, biopsy (ultrasound and CT guided) and percutaneous transhepatic cholangiogram. With full ethical approval, observations of each task were conducted both in situ and via recorded videos. This was followed by discussions between psychologists and the subject matter experts (SMEs) to obtain an understanding of tools and techniques used during the procedure; the aims of the procedure, and the individual movements identified on the video; as well as identification and discussion of "decision points" during the task. The output of this was the first draft of a CTA for each of the interventional procedures. The CTA process is very time-consuming. [15] states that "deconstructing 1 hour of focused expertise requires approximately 30 hours of effort by a trained cognitive task analyst". Attaining the desired training objectives requires an iterative process of validation throughout development and implementation. Therefore, the first draft was presented to a second expert to obtain his or her feedback on what was missing and how it could be further improved. This process was repeated with other experts to obtain external validation before the CTA draft was finalised.

At this point, it is worth mentioning that the work in this thesis does not involve the development of a simulator as an educational tool for the training and teaching of interventional procedures, but rather the focus is on the development of haptic interfaces to support the simulation of endovascular interventions. For this reason, although the CTA that is currently available is a valuable resource to aid in understanding the clinical procedures involved, expanding the CTA further is not within the scope of this project. Instead, the emphasis is on a specific engineering problem caused by the configuration of the instruments during interventional procedures. This problem, which will be detailed further in the next section, requires a technical investigation of haptic interface designs used in simulators of endovascular interventions.

1.1.1 Related Research on Haptic Interfaces

The earliest known haptic interface or force feedback system is the GROPE1 developed in 1971. This system was developed at the University of North Carolina and used a modified robot that could be directed to move in 2-D [16]. Due to limitations in computational power at the time, the project was abandoned and research in the field remained stagnant for more than a decade. In the 1990s, haptic interfacing became a widely popular field of research, as more computational power was made available at low cost with advancements in processor technology. This led to the development of the SensAble Phantom haptic interface device released in 1995. While there are similar products commercially available, by 2003, the Phantom had become the most popular haptic device for professional use and had sold 1600 units and this number reached 6000 units in 2007 [17]. The popularity and relatively inexpensive price of these haptic devices made them ideal for use in medical research.

One of the earliest attempts of applying haptic devices for such a purpose used a modified version of the Phantom to develop a virtual environment simulator for training laparoscopic surgical skills [18]. Besides that, the work in [19] used the Phantom to control a robot arm grasping laparoscopic tools in order to study the role of haptics or force feedback in the ability of a surgeon to characterize tissues correctly. In this case, the challenge lies in the viscoelastic nature of tissues, and the consequent difficulty of characterizing and correctly replicating their physical properties. The study concluded that haptic feedback was an important feature to have as the surgeons involved in the experiment were found to make significantly better assessments with both visual information and haptic information, instead of just either one of them separately. The Phantom was also used in the development of an incision simulator using an offline FEM simulation [20] and of a bone drilling simulator for orthopaedic surgery [21]. In both cases, a unique deformable model was developed in detail for a specific task and the haptic device was used to interact with the model. Similarly, the work in [22] used Phantom haptic devices to simulate the transducer and needle in a simulation for ultrasound-guided organ biopsy. Results of the study show that the visual renditions and haptic feedback can help improve the training and involvement of needle insertion. More recently, haptic devices have been used in the development of a prototype dental skills training simulator, not only for the purpose of training, but also to classify an

operator as either a novice or an expert based on his or her performance during the simulation [23].

While commercial haptic devices have often been utilised in medical simulators, they are not suitable for use in all simulators. Simulators of certain medical procedures require a haptic interface of a different design or specification. This has lead to the development of novel and highly specialised haptic interface devices. The work in [24, 25] developed a haptic interface with a modular and mechanical design for an endovascular simulator. The system could apply rotational and translational force feedback to the instruments through the use of motors in indirect contact with the instruments. A haptic interface for a colonoscopy simulator, which relays force feedback in both translational and rotational directions to the endoscope during the simulation, was developed in [26]. In a novel setup, DC motors are used to apply friction to the colonoscope and brakes are used to restrict movement to only one direction. Thus, current research focus in the field of haptic interfaces applied to medicine include the design and development of novel haptic interfaces for medical procedures in cases where the devices commercially available are not suitably designed for a specific procedure [24, 25]. Another challenge is to reduce the cost of the haptic interface in order to decrease the overall cost of a medical procedure simulator. One way to achieve this is to lower the quality of the haptic feedback of the interface as studies have shown that in some cases low fidelity haptics is sufficient to increase the training effectiveness of the simulators [27]. Whilst for other applications, such as in teleoperation with robots [28], haptics with high face validity is desired and is thus an ongoing area of research.

1.1.2 Related Research on Interventional Procedures Simulation

The development of interventional skills requires repetitive and considerably realistic training. The level of realism required would be dependent on the specific training objective or context of the real world task. Low fidelity simulation may be sufficient for training simple practical skills such as balloon and stent positioning within unchallenging anatomy [7]. For example, this would include part task simulation training using physical/phantom bench top models that have been sufficiently validated. However, in certain clinical situations, where very delicate manipulations are required to avoid complications, higher fidelity simulation may be required [7]. An important aspect of interventional procedures simulation fidelity is the replication of haptic cues (vibrations

detected by the operator's touch senses) or haptic feedback that are normally felt during interventions from the interaction of the instruments with each other and with the vascular anatomy [7]. Work in [29, 30] investigated the types and range of forces involved during the process of arterial puncture using both the CTA approach and in vivo force measurements. Similar published work for other stages of interventions are very limited. This could be due to fact that the process of producing the CTA and obtaining the specialised equipments as well as ethical consent to perform in vivo measurements are very challenging and time consuming.

With advancements in electronics and computer technology, several parties have turned to virtual environments or computer simulations to provide improved training experiences. Work in [31, 32] detailed the development of one of the earliest interventional procedures simulators. The simulator was used for training interventionists to perform endovascular repair of abdominal aortic aneurysm (AAA) and consisted of several components, which included an anatomically accurate physical model of the aneurysm that is based upon CT scans and angiograms of a live patient. It also features an imaging system that uses subtraction imaging methods and mimics X-Ray imaging. One of the major topics of research interest regarding endovascular simulators is the evaluation of their effectiveness as a training tool. VIST (Vascular Intervention Simulation Trainer − Mentice Corporation), one of the commercially available endovascular simulators, has been shown to offer the most benefit in a mentored training program to novice participants compared to the more experienced participants [33]. A separate study had similar conclusions that the simulator showed to be effective in assisting trainees or surgeons to acquire basic endovascular skills in the early phase of their training [34, 35]. More generally, several studies have found that experience with endovascular simulator training results in better performance in the Cath Lab [36–39]. However, the need for careful validation of the simulators to show that training objectives can be achieved and that the transfer of skill can be performed from simulation to real patients correctly was emphasised by the authors in [40], who also claim that none of the simulators available at the time have achieved such a level of validation.

Many parties have called for the integration of computer simulators into a curriculum of interventional training [38, 39, 41–44], although the methodology for its official inclusion into a curriculum is still being developed. Therefore, another active area of research is in developing computer simulators as tools to objectively assess or evaluate

the trainees endovascular skills. In [45], the proposed simulator (STRESS machine), was successfully able to classify candidates into three predetermined groups (novice, intermediate and expert) according to their skill with good inter-rater reliability. Similarly, the work in [46] used a general scale and statistical analysis in a virtual carotid artery stent (CAS) simulator to discriminate between candidates that were experienced with the CAS procedure and those that were not. More than a tool for training surgeons, recently, virtual reality (VR) simulators are also being used to test new endovascular techniques before they are used on patients [47].

As mentioned earlier, another potential application for endovascular simulators is in realising patient-specific mission rehearsal, in which the surgeon is able to practice a virtual surgery using 3D anatomical models built from patient imaging prior to the procedure. Some work has already been done in this respect [48], however, the time taken to reconstruct 3D models of patient-specific data is still too long for the mission rehearsal to be feasible for integration into the standard surgical workflow [49, 50]. In the near future, as the power of computer processors continues to increase and their price becomes more affordable, the concept of such a rehearsal could well become a standard routine for complicated surgical cases.

1.2 Problem Statement

During endovascular interventions, the guidewire is positioned concentrically within the catheter while it is navigated within the blood vessels. In order to recreate this setup in a computer simulated environment, the haptic interface must be able to detect any changes in the position and orientation of the instruments, as well as apply suitable forces to them. However, this is not a simple task since, due to the fact that the guidewire is largely inside the catheter, there is limited contact points and line of sight for sensors and actuators to operate on the instruments. In this work, this is regarded as the "concentric occlusion" problem, and it is one of the main challenges in the design and development of haptic interfaces for interventional procedures simulators.

Current and previous interface designs have attempted to overcome this problem by sacrificing certain elements of face validity of the simulation (i.e. the degree to which the interface is representative of the world it attempts to model). The Xitact Vascular Simulation Platform (VSP) [51] will be used to provide an example. The VSP interface

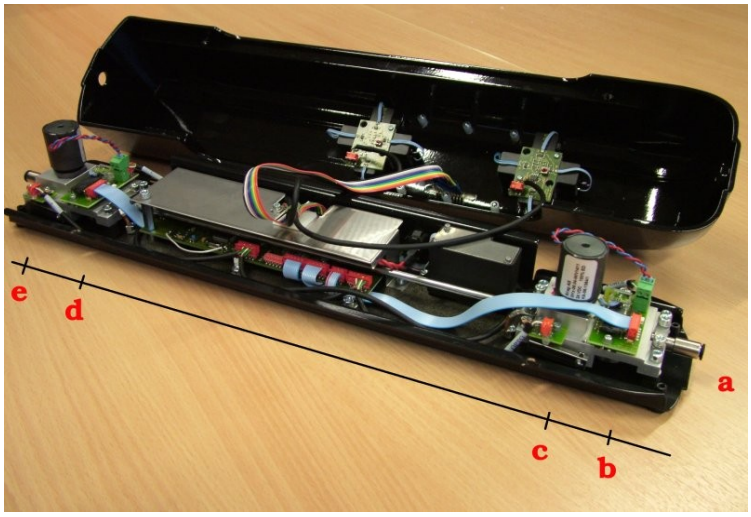

Figure 1.1: The Xitact VSP with chassis removed and components revealed

device is designed for portability, which explains its baguette-like appearance (Fig 1.1). The instruments are inserted at one end of the device and come out at the other end. At the entrance of the device is the sensor and actuator (in the form of a magnetic clip) for the catheter. At the other end of the device, about 30 centimetres away, is the sensor and actuator for the guidewire. While this arrangement of sensors and actuators manages to partly address the concentric occlusion problem, its creates a limit to the range of movement for the catheter. If the catheter is extended too far into the device, it will block the sensor for the guidewire, which will cause its positional information to be lost and disrupt the simulation.

Face validity in current simulators is also affected by the haptic feedback delivered to the operator by the haptic interface. Many senior clinicians claim that the haptic sensations are too basic and do not resemble the forces that are felt in real life close enough. Certain haptic cues occur where they should not have and vice versa. This can be due to the fact that hardware and software developers are trying to replicate forces or haptic feedback that they have never experienced themselves, with very little published evidence of the actual requirements for such devices.

1.3 Aims and Objectives

The aim of this project is to design and develop a haptic interface for the simulation of endovascular interventions that addresses several design issues in current haptic interfaces that affect the face validity of the simulation.

The specific objectives of the project are:

i. To design and develop a sensor system that continuously tracks the position and orientation of the guidewire and catheter during simulation.

ii. To study and understand the range and types of haptic feedback as perceived by the interventionists during an endovascular procedure.

iii. To design and develop a haptic actuation system that can deliver haptic feedback to both the catheter and guidewire.

iv. To combine both sensor and actuation systems into a prototype device.

v. To test and evaluate the prototype based on input from subject matter experts.

1.4 Project Contributions

Through the course of this project, several discoveries have been made either through literature review, experimental testing or the use of a questionnaire, that will be explained in greater detail in the subsequent chapters of this thesis. These discoveries are highlighted as the contributions of the project as follows:

Haptic Interface Design and Technology Review

A comprehensive review was performed in this study on the designs of various haptic interface devices related to the field of endovascular interventions simulation and also on the technology (sensors and actuators) implemented within each. While similar reviews have been performed previously [51], this review provides an introduction to a more technical understanding of the fundamental systems utilized in the haptic interfaces and also identifies shortcomings in the designs or technology used, such as the loss of instrument positional information and limited haptic feedback effects. These shortcomings highlight the need for further efforts to improve upon the current designs in order to provide a more immersive simulation experience.

Design and Implementation of a Concentric Guidewire Tracking Technique

Positional and rotational tracking of a concentric object is a highly challenging task due to the fact that there is minimal line of sight or points of contact for sensors to operate with. In this project, it was shown that it is possible to track the movements of a guidewire that is positioned concentrically within a catheter by using the combination of a highly reflective guidewire, a clear catheter and an optical sensor. The tracking performance achieved in the tests conducted was shown to be promising and a functional proof of concept. It is predicted that, utilizing this approach with custom made and professionally manufactured instruments in future work, should prove even more effective.

Investigations on Endovascular Haptic Feedback Effects

The production of a validated CTA and direct measurement of forces using in vivo techniques in an effort to study the endovascular haptic feedback effects were not considered feasible since both approaches present significant challenges (specialised instruments to enable force measurements, access to patients, ethical approvals, etc) that would not fit within the constraints of this project. As such, recognising the need to identify and recreate the haptic effects present in endovascular interventions, information regarding these effects was gathered from a number of Subject Matter Experts (SMEs) through interview sessions, questionnaires and an experimental test study. Whilst there are inherent limitations of using SMEs to obtain this information given its subjective nature, the details of existing haptic feedback was inferred using descriptive and statistical analysis. Also, the experiments conducted provided an estimate of the range of forces involved.

Design and Implementation of a Haptic Feedback Technique using a Custom Made Hub Actuator

A custom made actuator was developed in this project that provides haptic feedback to the guidewire using the electromagnetic actuator principle. The actuator is designed to be small enough to fit within the hub of a catheter to enable it to provide force to the guidewire while it is concentrically within the catheter. This novel approach to

concentric force actuation has been favorably received in the tests conducted and shows good potential for further development.

Development of a Haptic Interface Prototype Addressing the Concentric Occlusion Problem and Features Multiple Ports

A haptic interface device was produced in this project which manages to address the shortcomings of previous designs using novel approaches such as concentric guide wire tracking and force actuation. The prototype also features a multi port design where each port is tuned for different stages of intervention.

1.5 Thesis Layout

Chapter 2 presents a detailed literature review of the technology available that has been used in similar haptic interface devices. Chapter 3 studies the complexities of endovascular surgery, focusing on a detailed analysis of the requirements of its simulation from an engineering standpoint. In Chapter 4, the design and development process of the haptic interface prototype is described, with details on the different iterations and results that have led to the final version of the prototype. The final prototype is then put to the test both quantitatively and qualitatively based on the feedback of experienced endovascular clinicians, with the test results and expert reviews explained in Chapter 5. Lastly, Chapter 6 concludes on the work and contributions of this project, suggesting future work to further improve the haptic interface.

2

Interventional Procedures Simulator Haptic Interface: Design Reviews and Consideration of Alternatives

Traditionally, open surgery was the sole option in the diagnosis and treatment of vascular disease. During an operation, surgeons would make large incisions on the patient's body to gain direct access to the problematic vessel. As a result, patients would experience significant tissue trauma and blood loss. Furthermore, post operation, the patient would have to endure a lengthy period of recovery in the hospital ward and face a hefty medical bill due to the complexity of the surgery and the extended stay. However, in the last few decades, a minimally invasive approach to surgery was introduced and this quickly became the preferred form of medical treatment for vascular surgery. In this approach, long and tubular instruments are inserted into the vessel through small incisions on the patient's skin. This reduces patient tissue trauma leading to faster recovery times and reduced medical costs.

During an operation, the interventionist will make decisions and manipulate the instruments based on the fluoroscopic imaging feed that is available upon request. This approach to surgery is more challenging in some aspects because the interventionist does not have direct contact with or sight of the diseased vessel. He or she would have to make inferences from the images available and from the tiny tactile vibrations that travel through the instruments and are picked up by the receptors on their fingers. Also, the instruments themselves are very specialised to perform certain tasks in a particu-

lar way. As such, interventionists need to be extensively trained to build proficiency in handling the instruments and to build the required hand-eye coordination and dexterity to perform the procedures. Thus, whilst the focus of this research is on the development of haptic interfaces to support the simulation of endovascular interventions, the fundamental goal is to facilitate the training of core procedural skills through deliberate practice. This involves both cognitive and psychomotor aspects involved in manipulating the instruments (i.e. guidewire and catheter) based on image guidance and haptic information (from the sense of touch) [7]. The core skills, which will be described in context in the next sections, were identified through literature review [29, 52–54] and informal discussions with interventionists.

The instruments of endovascular interventions have a unique relationship with one another and they also react and respond actively to the endovascular environment in which they operate. Therefore, it is important to understand the mechanics of the instruments and the complexity of the tasks they perform if they are to be reproduced in a VR simulation environment. In the following section, the instruments that are involved in endovascular interventions are examined with some detail. This is followed by an illustrated explanation of the tasks performed during an intervention. Section 2.3 presents a detailed review and comparison of previous haptic interface designs, whilst Sections 2.4 and 2.5 discuss alternative sensor and actuator technologies.

2.1 Guidewires and Catheters

Whilst there are large variations in size, shape and rigidity, the core function of the guidewire and catheter remains the same. The role of the guidewire is to support and steer the catheter to a target. Upon arrival, the catheter then provides a conduit for diagnosis and/or therapy. Despite the physical similarities of being long and flexible, the two instruments are quite different and complement each other to enable successful interventions. In certain vascular interventions, it is necessary to use coaxial systems, such as microcatheters and vascular sheaths, in combination with guidewires and catheters. For instance, micro catheters are used when intervention is needed in the smallest, most tortuous vessels [53]. In these systems, there is usually more than one concentric instrument. For example, a guidewire is the innermost instrument and it is concentrically within a catheter which itself is concentrically within a second, larger catheter. This

adds significant complexity to the "concentric occlusion" problem described in Chapter 1. Thus, in the scope of this work, the focus is on having one single internal instrument (the guidewire) inside a single external instrument (the catheter).

Guidewires

Guidewire size or diameter is often measured in inches, where they can range from 0.014" to 0.038". Guidewires with diameter 0.014" to 0.018" are considered small caliber wires. Typically, in a majority of cases, the standard guidewire used is 0.035" in diameter. The length of a standard guidewire is commonly 180 cm but longer guide wires (up to 260cm) are needed for certain types of interventions [53] . The guidewire has a soft and atraumatic tip to prevent dissection of the vessel, whereas the end in contact with the operator is rigid. For example, a standard Amplatz wire has a "floppy" tip of 6cm. The length of the floppy tip can vary in different wires and the risk of dissection increases with a decrease in this tip length (minimum length of 1cm) [53].

Generally, there are two types of guidewires: steerable and non steerable. Steerable guidewires have shaped tips, hydrophilic coatings (to reduce friction) and are built to turn well to help traversing through narrowings and blockages in the vessels [53]. One of the most established steerable guidewires is the 0.035" diameter Terumo angled wire with hydrophilic coating (Fig 2.1(a)) which prevents friction and improves wire maneuverability. Non steerable guidewires are not equipped with any of those features, but they specialise in the ability to provide a support rail for catheter advancement.

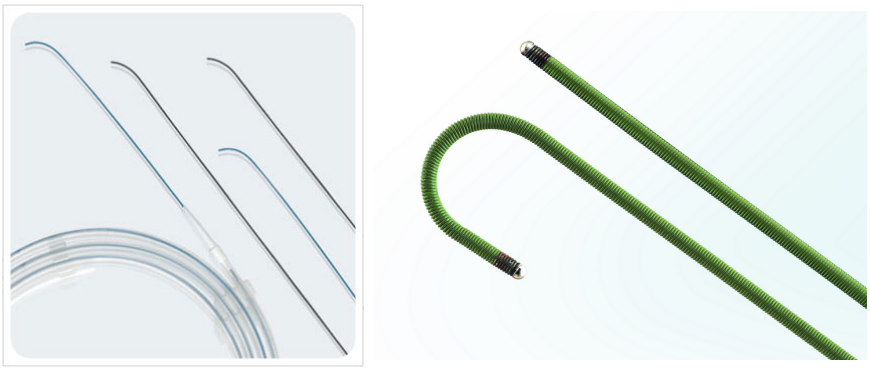

(a) (b)

Figure 2.1: Examples of (a) steerable guidewires [55] and (b) non steerable guide wires [56]

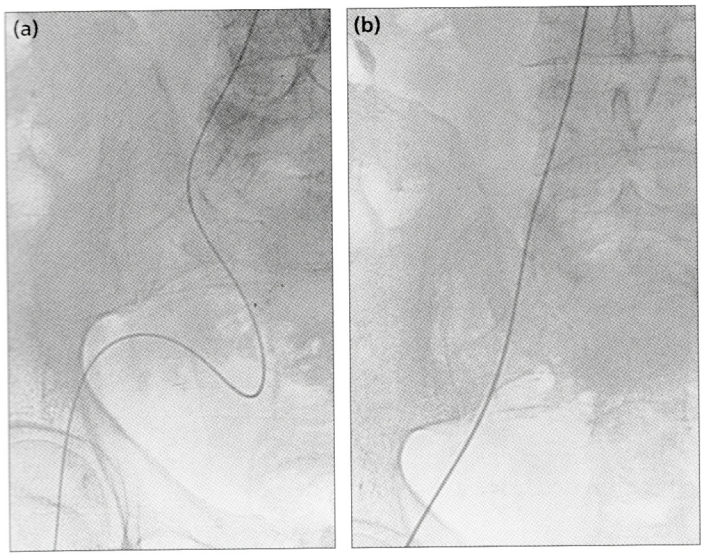

Figure 2.2: Straightening effect of a stiff guidewire on a tortuous vessel [53]

Examples of this wire type are the J guidewire and the straight wire, with the former being one the most commonly used wires (Fig 2.1(b)). Stiffness is an important factor in the selection of non steerable guidewires since it can vary from "floppy" to "unreasonably stiff" as each stiffness level could be suited to perform a specific task. It should also be noted that the stiffer the wire, the more likely that it will produce a straightening effect when passing through naturally tortuous blood vessels (Fig 2.2).

Catheters

The usable length of the tubular catheter is measured from the length of the catheter hub to the tip and it can range from 50-125 cm. Since some catheters can have multiple lumen, they are generally characterized or referred to by their outer diameter given in the unit French (Fr). The French size scale was introduced in the 19th century by Joseph Frederic Benoit Charriere, a surgical instrument maker based in Paris, France [57]. The outer diameter of a catheter would increase with its designated number in the French scale, which can range from 3 to 34. Conversion from the French scale to millimeters can be done by a division of 3. Typical catheters are in the range of 4-6 Fr or 1.333 - 2 mm. Catheter inner diameter, corresponding with its lumen size and the

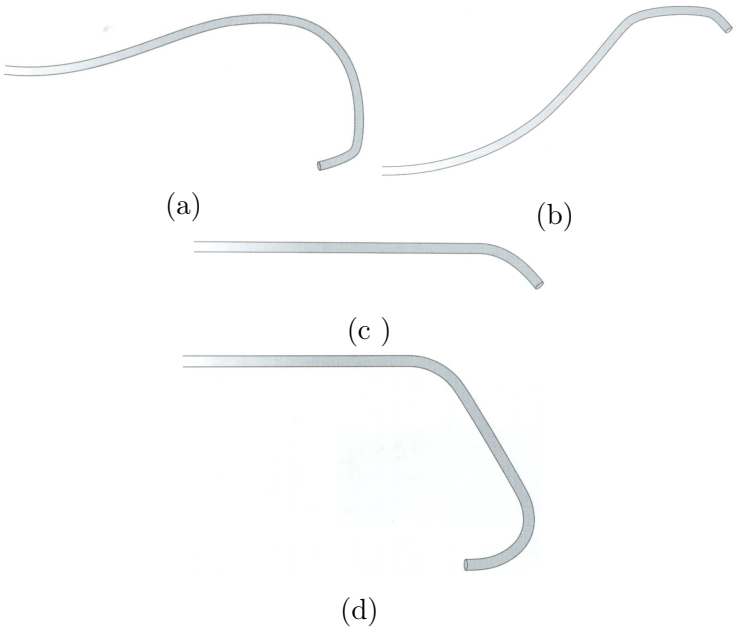

Figure 2.3: Selective catheters types (a) Cobra (b) Bernstein (c) Headhunter (d) Renal Double Curve [53]

maximum diameter of the wire/catheter passing within, is usually given in inches (e.g. 0.035") [53].

Similar to the guidewire, the catheter can also be categorized into two groups: selective and non-selective. Selective catheters are shaped to a wide variety of angles to allow for the catheterisation of branch vessels [53]. Some examples of the most popular selective catheters are shown in Figure 2.3 such as the Cobra, the Bernstein and the Headhunter. Each type of selective catheter also features catheter tips that are mild variations from the original as shown by the different types of Sidewinder catheters in Figure 2.4. Non-selective (flush) catheters can either be equipped with endholes and/or sideholes. The increased number of holes helps to stabilize the flow of contrast when injected into the catheter, especially when pump injection is used [53]. Non selective catheters are used to inject contrast in large and medium sized vessels as they have multiple side holes, which allow for increased contrast flow rate. One of the most popular non-selective catheters is the pigtail catheter (Fig 2.5), whose shape minimizes inadvertent catheterisation of small branch vessels. In smaller vessels where the pigtail would not fit, straight catheters are used as replacements [53]. Also, similar

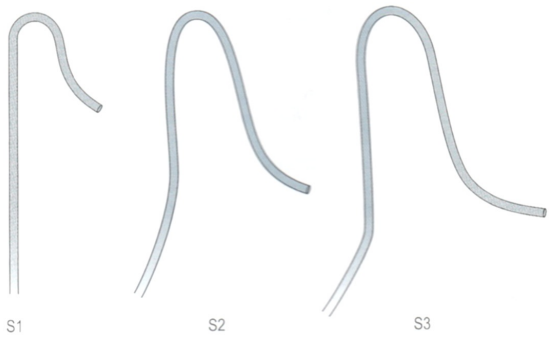

Figure 2.4: Different types of the Sidewinder tip catheter [53]

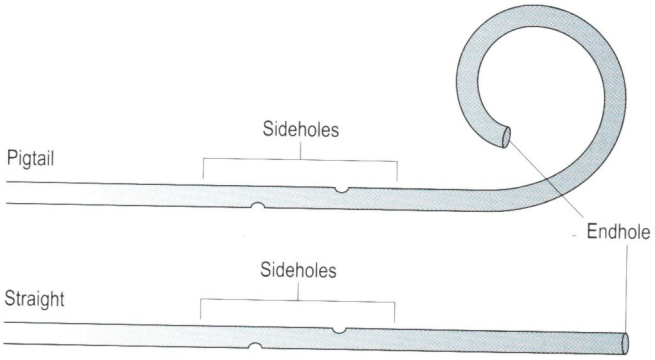

Figure 2.5: Pigtail and straight catheters with end and side holes [53]

to guidewires, catheters have hydrophilic coating to reduce friction. Table 2.1 shows the general differences between both types of instruments.

Table 2.1: Guidewire and Catheter Description

	Guidewire	Catheter
Function	Wire that provides support for tool (catheter/stent/etc) insertion into and progression through a blood vessel	Tube that creates a channel for the passage of fluid or entry of a medical device / tool
Length (cm)	140-300	50-125
Diameter	0.014 to 0.038 inches	4F to 10F (1.33 mm-3.33 mm)
Construction	Has an inner core that is made of tapered Mandril. Wound wire surrounding the Mandril forms the outer part. The safety wire is welded to both ends of Mandril	Made from different materials (polyethylene, poleyurethane, nylon, Teflon) that determine the behaviour and rigidity of the catheter
Tip shape	Has a floppy tip to prevent any perforation of the vessel wall. Initially, a wire with a J-shaped tip is used	Catheter tips are designed with a specific purpose in mind. Normally, a particular design is used that is better suited to reach or gain access to certain vessels

2.2 Endovascular Interventions

The particular goal of an intervention determines the selection of vessel puncture site, instrument type and specific tool manipulation techniques. In this section, the generic tasks for endovascular interventions are summarised. The intricacies and considerations for each task and subtasks/steps can be found in more detail in [53, 54] and the Cognitive Task Analysis developed by [29].

2.2.1 Task I: Arterial Puncture

Arterial puncture is commonly performed where the artery is found to be relatively fixed and can be compressed over bone to prevent or stop haemorrhage/bleeding. The most suitable vessel to access depends on several factors, such as location of the target zone and patient history, but the most frequently used site is the right Common Femoral Artery [53]. Arm approaches are also possible by accessing the brachial artery or the radial artery. The brachial artery is commonly used when the femoral approach is precluded and it is also the best route for performing procedures in the upper limb. Radial artery is often considered an alternative route for diagnostic angiography. It is more challenging to access compared to other vessels, but it has advantages for homeostasis (prevention or stopping of bleeding). Radial artery usually access does not require bed rest and thus it is most suitable for outpatient procedures [53].

Certain interventions require access to veins instead of arteries. Some of the common sites for venous puncture are the Common Femoral Vein (CFV) and the Internal Jugular Vein (IJV)[53]. Although it was noted that techniques and principles of venous access are similar to those for arterial access, compared to the arteries, veins are thin walled, highly compressible and prone to spasm. Thus, veins are more fragile and prone to dissection than a correspondingly sized artery [53]. The following list summarises the steps in performing this task [29].

i. Selection of site for procedure - For illustrative purposes, the puncture site chosen in this summary is the femoral artery.

ii. Checking of patient's pulse.

iii. Incision site is cleansed with antiseptic soaked swab.

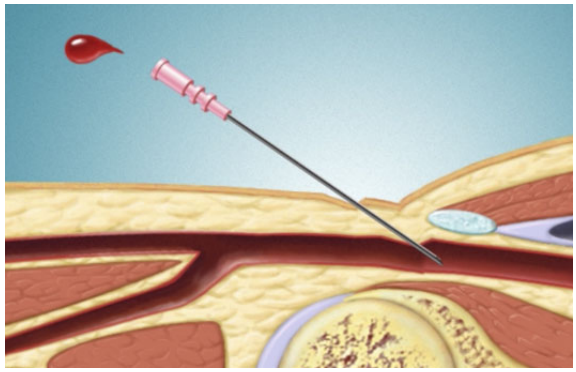

Figure 2.6: Free pulsatile back flow is indicative of successful arterial puncture [58]

iv. Sterile sheet is placed to expose incision site and its position is secured.

v. Image intensifier is prepared by the placement of a sterile cover over it.

vi. Preparation of syringe local anesthetic application.

vii. Preparation of guidewire - the guidewire is flushed as needed. Detailed preparations would depend on the specific type of guidewire selected.

viii. The femoral artery is located through palpation .

ix. Injection of local anesthetic.

x. Skin incision is performed.

xi. Preparation for puncture - Swab is placed to absorb blood.

xii. Needle adjustment and insertion - The needle is positioned at a 45 degrees angle to the artery prior to insertion. A successful needle puncture would produce free pulsatile back flow, which indicates the needle is intraluminal (Fig. 2.6) [53].

2.2.2 Task II: Passage of Guidewire

Following the puncture, a guidewire is then passed into the lumen through the needle. The most common wire used for initial insertion is the 0.035" 3 mm J guidewire, where 3 mm denotes the diameter of the curve of its J tip. The advantages of this wire is that it avoids disturbing lesions/plaque and prevents accidental insertions into smaller branch vessels [53]. The following list summarises the steps in performing this task.

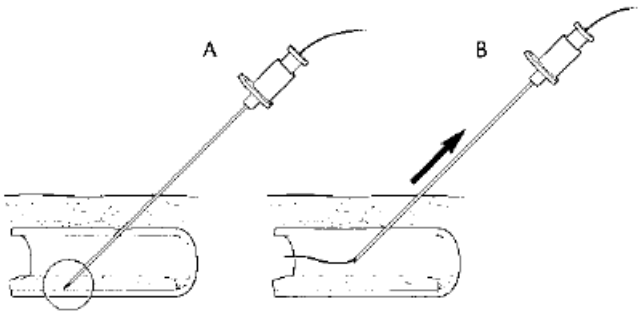

Figure 2.7: (a) Typically, when initially advancing the wire after the puncture, the guidewire will hit the arterial wall. (b) The needle needs to be retracted 1-2 mm before advancing the wire further to avoid the risk of puncturing the opposite arterial wall [54]

i. Adjustment of needle angle - Needle is tilted closer to the skin surface. This is to ensure the inserted guidewire will move into the artery without hitting the arterial wall or any formed lesions.

ii. Using the introducer, the guidewire is inserted into the needle hub - If unexpected resistance is felt, screening is used to ensure correct entry. Retraction of the needle 1-2 mm and reinsertion of the guidewire might be necessary to avoid collision with the arterial wall (Fig. 2.7) [54]. Instruments are checked to confirm that resistance is not caused by friction between the wire and the container during insertion [53].

iii. With the palpating hand, pressure is applied on the incision site to prevent bleeding

iv. Guide wire is held in place

v. Needle removal - Needle is withdrawn/pulled along the wire away from the patient

2.2.3 Task III: Introduction of Catheter

Once the needle is removed, a catheter is then introduced by passing it over the guidewire and into the vessel. It should be noted that, upon insertion, various factors can affect the handling of the catheter. These include catheter length, catheter material and degree of vessel tortuosity [54]. The following list summarises the steps in performing this task.

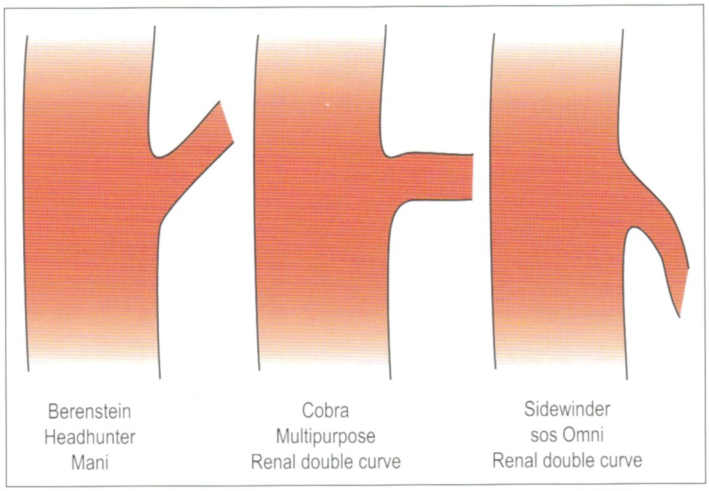

Figure 2.8: Illustration of suitable selective catheters for catheterisation of a vessel branch with a specific angle to its parent vessel [53]

i. Sufficient wire is inserted into the vessel

ii. Guidewire is held straight and under slight tension

iii. Catheter is held close to its tip within 1-2 cm of skin

iv. The catheter is pushed and twisted to advance it over the guidewire

v. The catheter is slided freely along the wire - If the catheter seems to stick and pulls on the wire, then the wire has kinked. Stop advancing and screening is used to show the problem and readjust position/advancement as required.

2.2.4 Task IV: Advancing to the Target Zone

In order to proceed to the target zone, the interventionist has to identify the specific instruments needed to gain access to the branch vessels leading to it. The most important factor to consider is the angle of the vessel as it connects to the parent vessel [53]. It is important to consult the imaging and select the most suitable instrument accordingly. Figure 2.8 illustrates the different types of selective catheters that can be used for the catheterisation of branch vessels of a certain angle and Figure 2.9 shows how the Sidewinder catheter is manipulated to place its tip within the vessel opening. Another

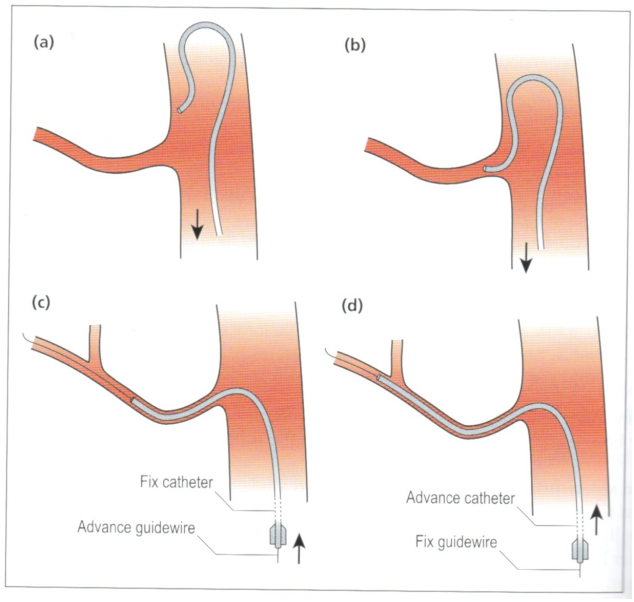

Figure 2.9: (a) The Sidewinder catheter is pulled back to place its tip into the vessel ostium (b) The catheter is pulled back more to advance its tip further into the vessel (c) Guidewire is advanced for deeper catheterisation (d) Catheter is pushed over the guidewire [53]

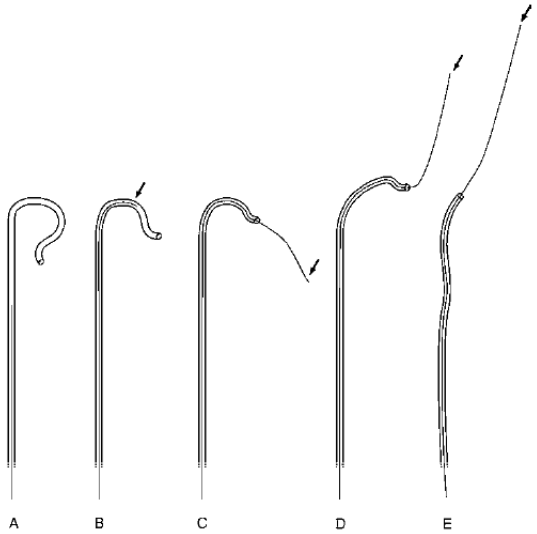

Figure 2.10: Example of altering the pre shaped tip of a catheter by passing a guidewire inside past the catheter tip [54]

technique that is useful in the catheterisation of branch vessels is the modification of the catheter tip shape by adjusting the position of the guidewire at the catheter's tip as shown in Figure 2.10. This allows the interventionist to increase the range of directions in which s/he can aim [53]. The following list summarises the steps in performing this task.

i. At this stage, the guidewire is positioned concentrically within the catheter in the femoral artery - Generally, in this configuration, the guidewire should always lead the catheter.

ii. The guidewire is advanced to lead the catheter to a branch vessel - The actual designation will depend on the area of study.

iii. The catheter is turned to point the guidewire to the correct direction such as the branch vessel ostium

iv. The guidewire is advanced into the vessel and then followed by the catheter.

v. This catheterisation process is continued en route to target area/vessel

vi. Instrument advancement is stopped immediately if an unexpected resistance is felt and/or if the guidewire is seen to buckle at any point on fluoroscopic imaging. Radiographic imaging techniques are then used to identify the cause of the problem. The solution might require approaching the vessel at a different angle or a change of instruments.

2.2.5 Task V: Angiography

Angiography enables the interventionist to examine the patient's vasculature to locate vessel abnormalities (Fig. 2.11). This is done by introducing contrast agent into the vessels by injecting fluoroscopic dye through a catheter using a hand syringe or a pump. This technique is mostly suited for examination of small-medium diameter vessels. In larger diameter vessels, or where controlled flow volume injection is needed, the syringe is replaced with an automated power injector [54]. Simultaneously during injection, X-Ray images are captured at the angiographic suite by engaging a foot pedal. The images can then be processed digitally to remove unwanted information, such as

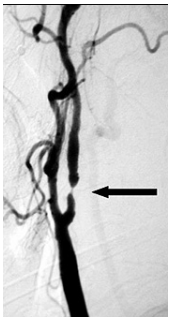

Figure 2.11: Example of an angiogram showing an abnormal narrowing of the vessel or stenosis [59]

producing a 'roadmap' of the vasculature through the Digital Subtraction Angiography (DSA) method. The following list summarises the steps in performing this task.

i. Preparation of syringe for fluoroscopic dye injection

ii. The catheter is held in place

iii. The guidewire is pulled out and withdrawn from within the catheter/vessel.

iv. The catheter is flushed with saline

v. Syringe with fluoroscopic dye is attached to the catheter hub

vi. The patient and image intensifier positions are ensured to obtain desired image angle

vii. Injection of fluoroscopic dye

viii. Foot pedal is immediately engaged to capture images

ix. Obtained images are checked for vascular abnormalities and diagnosis is made.

x. Task is repeated as needed for other angles or in other branch vessels to be investigated

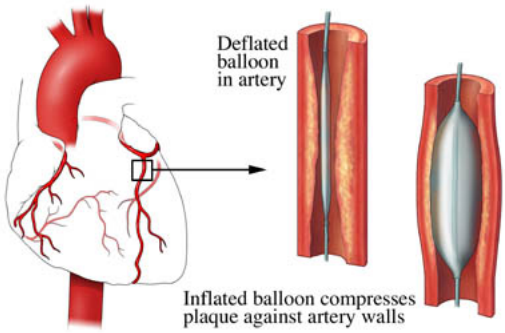

Figure 2.12: Illustration of successful balloon angioplasty in a coronary artery [60]

2.2.6 Task VI: Angioplasty/Stenting

In angioplasty, special catheters and wires are used to unblock stenosed/occluded vessels to repair or normalize the flow of blood passing through the vessel. The wires used can be a range of diameters and may be smaller than the 0.035" or 0.038" wires that are commonly used for access to be able to thread through the narrow lumen. Once past the stenosis, the wires are used to guide the balloon catheter into position amongst the plaque [53]. Commonly, the balloon catheter used in the Superficial Femoral Artery (SFA), Iliacs and etc. may be 5 French in diameter, but they may also be smaller for small vessels (e.g. coronary and tibial arteries).

The balloon's position is determined from X-ray imaging as its boundaries are marked with radio opaque material. The balloon is then inflated by hand using an inflation device that is connected to the balloon catheter hub [54]. The balloon flattens the lesions and this is repeated until blood flow in the vessel is restored to normal (Fig 2.12). In most cases, a stent is then placed at the treated area. The stent is a small wire mesh tube that is deployed during balloon inflation. Its main function is to hold open and keep the vessel from being blocked again [54]. Figure 2.13 illustrates this procedure known as "balloon stenting". The following list summarises the steps in performing this task.

i. Currently inserted instruments are exchanged for a 0.014"-0.018" guidewire and a balloon catheter.

ii. The guidewire is negotiated or threaded past the stenosis

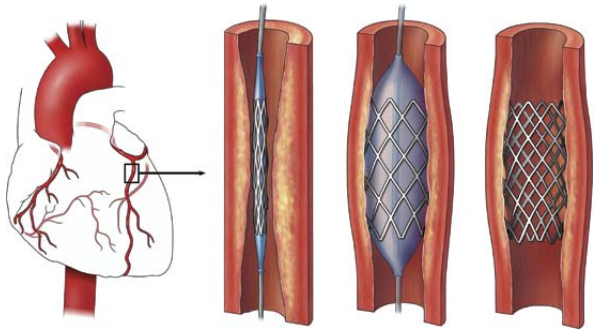

Figure 2.13: Illustration of successful stenting procedure in a coronary artery [61]

iii. The balloon catheter is advanced over the guidewire to place the balloon (mid-balloon is positioned at stenosis)

iv. A balloon catheter inflation device is attached to the balloon catheter hub

v. Balloon is inflated with the inflation device to flatten the lesions or plaque - This is repeated until the lesions have been cleared and there is optimal blood flow within the vessel.

vi. Angiography is performed to confirm the lesions have been cleared.

vii. The balloon catheter is then exchanged for a balloon catheter with a stent

viii. With the balloon catheter and stent in position, the balloon is inflated using the inflation device to deploy the stent

ix. The balloon is deflated once the stent is in place

x. Angiography is performed to confirm that the stent is positioned correctly

xi. Task is repeated as needed for other affected vessels

In this section, the instruments used in endovascular interventions have been studied. During an operation, the guidewire and catheter have a unique relationship with each other and combine to identify and treat diseased vessels. The tasks and subtasks involved in endovascular interventions have also been reviewed. While the particular tasks and subtasks and tools might be different from patient to patient, the key practice of using the guidewire and catheter in tandem to navigate through the vessel remains the

same. This is therefore considered to be a core skill to be developed by interventionists in training [29, 52–54].

Training of guidewire and catheter navigation skills on a benchtop or animal (porcine) model is relatively straightforward, but lacks the advantage of variability, feedback and assessment of a virtual environment, as well as suffering from wear and tear. Implementing such training within a virtual environment is more challenging as the operator will manipulate end effector tools that mimic actual guidewires and catheters to control the movements of the virtual equivalent, which should have a realistic look and feel, being able to recreate the subtle touch and visual feedback obtained during a real endovascular intervention.

The simulation software needs to know the position and orientation of the tools at all times so that it may react accordingly. Typically, this involves the use of sensor systems. However, it is difficult to design a sensor system to detect the fine and minute movements of the instruments with a limitation to the amount of line of sight or contact points available with the guidewire, since it largely moves concentrically within the catheter. This was referred to in Chapter 1 as the "concentric occlusion" problem. It also results in a significant challenge when attempting to reproduce the haptic effects felt by the operator during a real life endovascular intervention. They play an important role in the simulator's face and content validity, ensuring that an acceptable level of realism is maintained during the simulation of endovascular interventions [7] [62].

Based on this and taking into consideration the tasks and subtasks reviewed above, the functionality expected from a haptic interface in this context may be summarised as follows:

i. Allow the insertion of the guidewire and catheter

ii. Detect instruments immediately upon insertion into the virtual vessel

iii. Continuously track the position and orientation of the catheter at all times once detected

iv. Continuously track the position and orientation of the guidewire at all times once detected

v. Allow the instruments freedom of movement within the virtual vessel

vi. Apply translational force feedback to the instruments

vii. Apply rotational force feedback to the instruments

A more detailed explanation regarding haptic feedback will be provided in the next chapter. In the mean time, the following section presents a review of previous designs of haptic interfaces for the simulation of endovascular interventions, both commercial and academic. This will help to understand the work done and previous approaches to solving the concentric occlusion problem.

2.3 Review of Haptic Interface Designs

In examining the earlier designs of Endovascular Simulator Haptic Interfaces, the main focus is on identifying the different technologies used, namely the selection of actuators and sensors, and their configuration. The other common features that all the systems share, such as the power supply, 3-D model rendering algorithm of the vascular system and the processor or the controller unit are assumed to be the same and irrelevant for this review.

2.3.1 HT Medical-Accutouch-CathLabVR

A virtual simulator for endovascular procedures training was developed by HT Medical Systems Inc, an American based company, in the late 1990′s. They were granted patent

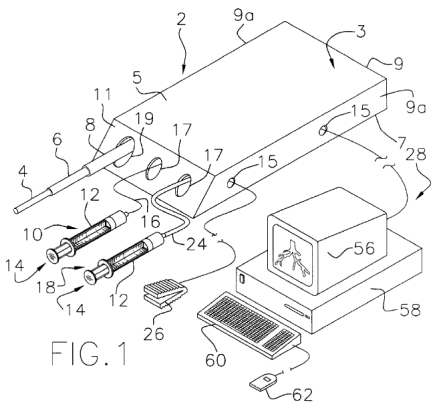

Figure 2.14: Illustration of device from HT Medical Systems Patent [63]

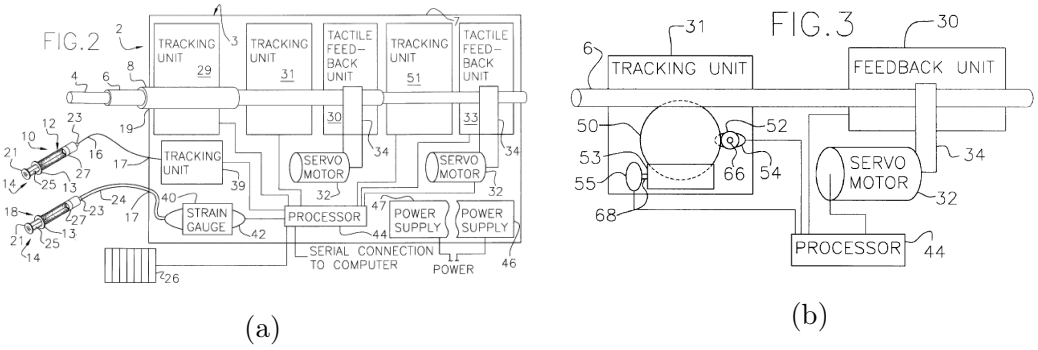

Figure 2.15: (a)Block diagram of device components (b) Design for the tracking and haptic unit for the device in [63]

US 6106301 A "Interventional Radiology Interface Apparatus and Method" [63]. The overall device, which has slots for four different input devices, can be seen in Figure 2.14. The first is the slot for nested tubular instruments, most commonly the most external instrument would be the sheath, followed by the catheter second, and the guide wire third. This is as indicated by numbers (4),(6) and (8) in slot (19). The second slot is for the syringe, indicated by (14),(10) and (12), that is used in the simulation of fluoroscopic dye injection during angiography. The last slot allows for the use of a balloon inflation device, (14),(12) and (24), in the simulation of an angioplasty. There is also a foot pedal, marked (26), that connects to the device through slot (15). The pedal is used in the simulation to control the capturing of radiographic images to be displayed. During real life procedures, the exposure of the patient to radiation must be minimised, and this vital lesson can be taught through this device.

The block diagram in Figure 2.15(a) shows the arrangement of the components that make up this haptic interface device and Figure 2.15(b) shows the haptic and tracking mechanisms. Within the device, there are tracking units and haptic units for the catheters and guide wires. The tracking units for the catheter and guide wire tools are made up of a roller ball (50) that is set to move with the instruments (6) upon insertion. The roller ball moves in two axis, rotationally and translationally. Its movement in each direction causes, in turn, the movement of another rolling mechanism that is coupled to an encoder that records the movements. The haptic unit is made up of a servo motor (32) that applies pressure onto the instruments (6) and (8) with the mechanical arm (34). Each tracking and haptic unit pair is specific to one instrument.

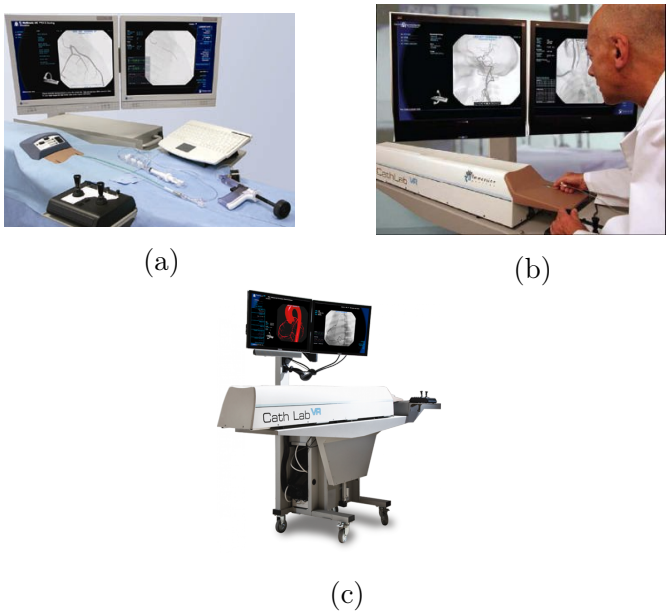

(a) (b) (c)

Figure 2.16: Photos of the (a) Accutouch (b) Immersion's CathLabVR and (c) CAE Healthcare's CathlabVR

The unit pair closest to the entry slot of the device detects movements of and applies haptic feedback to the most extrinsic instrument, the sheath. Further past the slot entrance, another two pairs of tracker and haptic units are placed to do the same for the catheter and guide wire. HT Medical merged with Immersion Inc. [64] in 2000. Immersion then developed the Accutouch Endovascular System commercially [65] where it became the CathLabVR in 2005 (Figure 2.16). In 2010, Immersion Medical was acquired by CAE Healthcare [66] , who are the current owners of its endovascular simulator technology.

2.3.2 DaVinci-Icard-Neurocath

The ICard system (Figure 2.17(b)) was developed by the Singapore Bioconsortium in partnership with the John Hopkins Medical Center [68]. The ICard follows the group′s first simulator known as the DaVinci [67] (Figure 2.17(a)), which is described as a prototype system that provides real time 2-D and simultaneous 3-D catheter navigation through simulated blood vessels registered with fluoroscopic image data. Unlike the DaVinci, which focused on peripheral vascular procedures, the ICard was designed to allow the user to familiarise with interventional cardiology procedures. The ICard allows

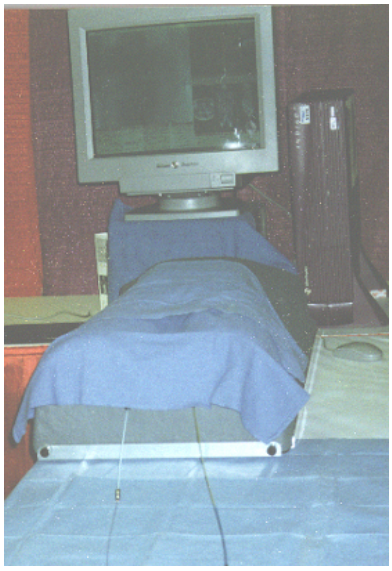

(a)

(b)

Figure 2.17: (a)Da Vinci and (b) ICard [67]

the user to interact with the virtual catheter by using directional buttons or by using the mock instruments in the Catheter Movement Sensing (CMS) Box. The CMS box contains the configuration shown in Figure 2.18. When the catheter is inserted, the distal tip of the catheter (in reference to the operator) will be gripped by a panel that slides along a pulley system. Pushing and pulling the catheter will cause the slide to move along the pulley axis. One of the pulleys is fixed with an encoder, encoder A, to detect the number of rotations as a means of recording catheter movement. The gripper will also turn with the catheter as it is rotated and its rotations will also be recorded by a second encoder, Encoder B. At the entrance of the unit, a stepper motor is placed. The arm of a stepper motor, that is placed at the entrance of the box, is actively controlled to put pressure on the catheter to resist its movement as a form of haptic feedback.

The group continued to develop the Da Vinci and ICard system further and this resulted in Patent US 6538634, titled "Apparatus for the simulation of image-guided surgery" [69]. As seen in Figure 2.19, the unit is rectangular in design with a pair of sensors and actuators located at each end. The device is designed to accept instruments (32) at the entrance of the device (150) located at one end. The sensor-actuator pair at the device entrance (152) and (112), is meant to track and apply haptic feedback to the

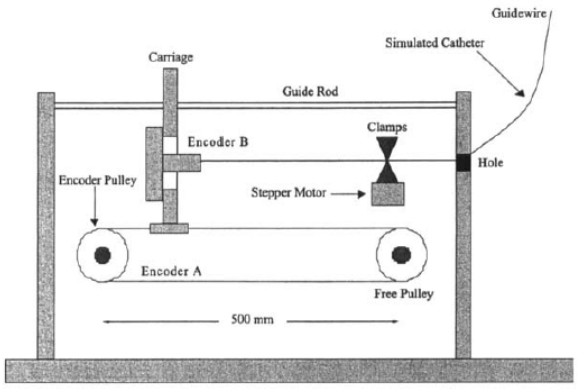

Figure 2.18: The Catheter Movement Sensing Box contains the instrument tracking and haptic feedback mechanisms for the ICard system[68]

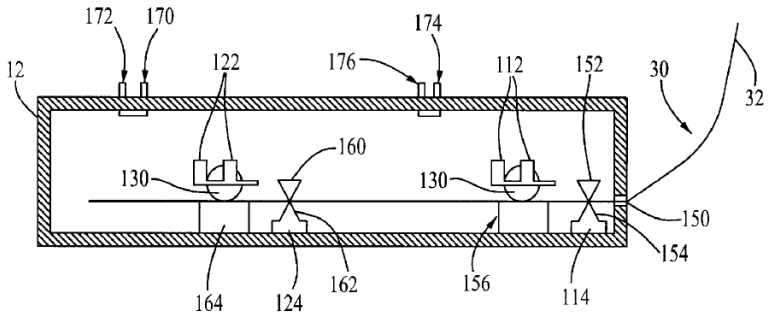

Figure 2.19: Illustration of the device design from patent [69]

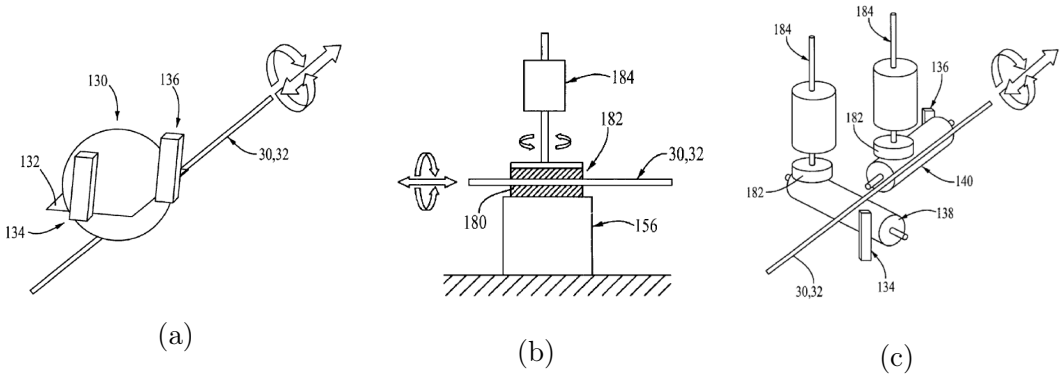

Figure 2.20: (a)Tracking mechanism used in patent (b)Haptic feedback mechanism used in patent (c) Design of integrated tracking and haptic feedback system from patent [69]

catheter, while the pair at the other end, (122) and (160), does the same for the guide wire. Figure 2.20(a) shows the tracking mechanism in more detail. The instruments come into contact with a roller ball (130). The roller ball's movement is detected by two rotary encoders, marked (134 and 136), one for each direction of movement. Figure 2.20(b) shows the haptic mechanism used, which comprises of a clamp (180) and (182), that is controlled by a stepper motor (184). Figure 2.20(c) shows an integration of both tracking and haptic feedback systems. In this configuration, the roller ball is replaced with two rollers (138) and (140). The sensors or encoders measure the rotation of the rollers to track movement of the instrument in each axis. For haptic feedback, the stepper motors (184) pressure the rollers with the cushion (182) to provide resistance to the instruments movement instead of pressuring the instruments directly.

The designs in the patent can be seen implemented in their next system, the Neurocath. The Neurocath uses two different units that can be used to track the individual movements of the two instruments, the guide wire and catheter [70]. These units are separated by a distance as shown in Figure 2.21. Each unit is called the Motion Tracking and Haptic Feedback Box (MFB) and contains sensors and actuators as shown in Figure 2.22. Similar to the design in the patent, the instruments (3) come into contact with two rollers or wheels upon insertion. Each wheel is arranged to move as the instrument is translated and rotated respectively. The wheels (4) and (8) are fit with an encoder that records the movements made as a measure of tracking instrument position and orientation. Every MFB unit is also fit with a servo motor (6) as opposed to the stepper motor mentioned in the patent, that is meant to press a friction surface (9)

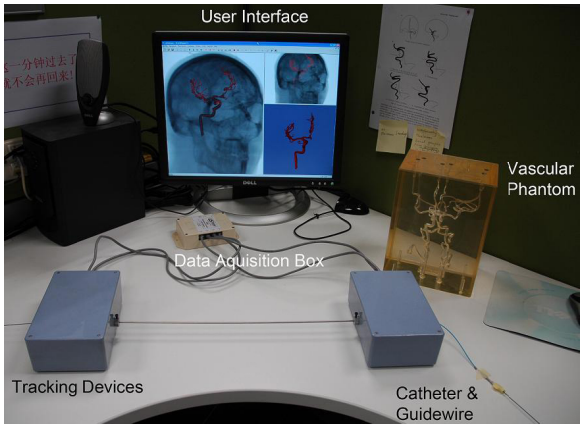

Figure 2.21: Neurocath system in action [70]

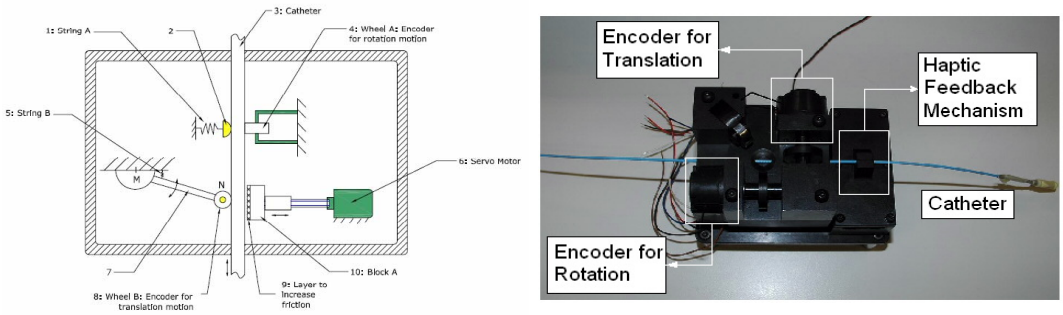

(a) (b)

Figure 2.22: (a)Illustration and (b) Photo of the MFB for the Neurocath [70]

on the instrument to produce resistance and haptic feedback. The strings A and B are mechanisms installed to prevent the user from pushing the instrument any further in scenarios where the user risks perforating a vessel in simulation. The Neurocath was still in development in 2007, however there is no evidence found that it was ever produced and sold commercially.

2.3.3 EVE

One of the earlier developers of endovascular procedures simulator systems is the Simulation Group at CIMIT (Center for Integration of Medicine and Innovative Technology). In 2004, they were working on a Real Time Endovascular Simulator (EVE) that focused on providing high fidelity interventional neuroradiology simulation for physician train-

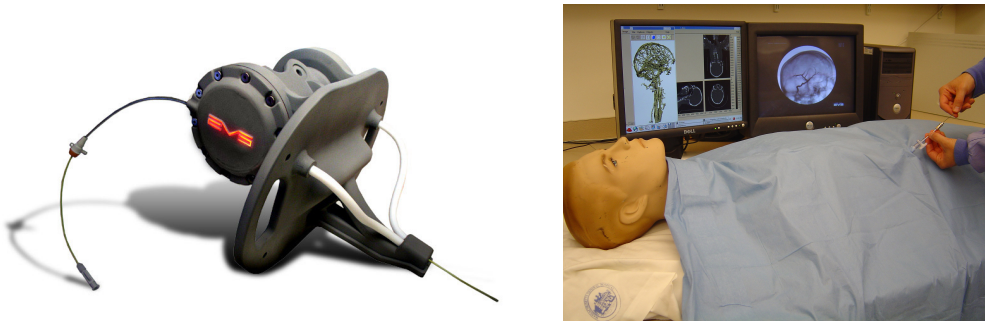

(a) (b)

Figure 2.23: (a) 3D representation of the EVE device by CIMIT (b) Implementation of EVE within mannequin [71]

ing. In 2005, they revealed that their prototype system (Figure 2.23(a)) implemented an optical system to track either guide wire or catheter movement [71] for the simulator interface. According to their publication, "only one instrument - catheter or guide wire - can be tracked at a time. A major difficulty, when tracking two or more nested devices, is that access to the inner device is mechanically impossible without modifying the instrument. " The tracking device is embedded within a mannequin (Figure 2.23(b)) and is connected to a physical vascular model that provides a passive type of haptic feedback to the instrument in the form of simple surface friction. Therefore, it does not have any mechanism for providing active haptic feedback. The EVE was still in development in 2009, but no updates have been reported since.

2.3.4 ICTS-VIST

Creators of the EVE, CIMIT also collaborated with the Medical Application Group at Mitsubishi Electric in the development of a simulator for cardiovascular procedures at the end of the 1990′s. The system was called the Interventional Cardiology Training System (ICTS) and allowed the use of real guide wire and catheters in its simulation [72]. The ICTS's interface (Figure 2.24(a)) uses electromechanical sensors to track the movements of both instruments, and servo motors for haptic feedback application. The configuration of these components was never illustrated in their publications. However, the design and technology of the ICTS was then acquired by Mentice Corp in 2005 who later launched the VIST or Vascular Intervention Simulation Trainer (Figure 2.24(b)).

(a) (b)

Figure 2.24: (a) The ICTS system [72] (b) The Procedicus VIST from Mentice [73]

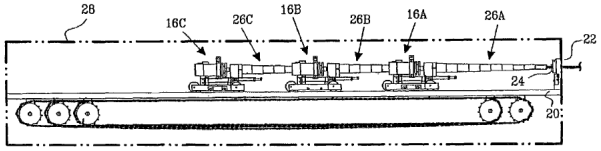

Figure 2.25: Overall design of device in [74]

The VIST became one of the most commercially successful simulators of its type, and is still popular today.

In 2006, Mentice was granted patent US 20060127864 A1 titled "Interventional Simulation Device". The designs in the patent are for a device in a simulator for interventional operation [74]. The system utilises serially interconnecting mobile carriages on a pulley system as shown in Figure 2.25. Instruments are inserted into the device through opening 22 entering the interconnecting member 26A, which is telescopic in this embodiment, and into the first carriage 16A. This carriage, like the others, is equipped with an optical sensor in the arrangement shown in Figure 2.26. The IR diode (104) emits light in the direction of the photodiode (106) past the passing instrument (108). The light that reaches the photodiode produces a current and the amount of light is linearly correlated to the current produced. This method is used to identify the endovascular tool's feature, namely its diameter, through the current signature produced. If the current signature is incorrect for the carriage, the mechanisms are kept deactivated and the instrument is allowed to exit the carriage and proceed to the next one. However, if

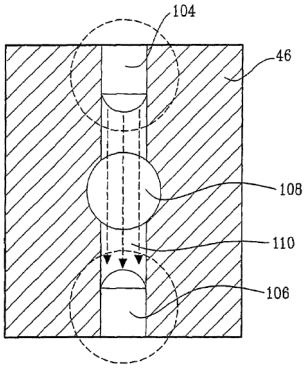

Figure 2.26: Arrangement of sensors onboard carriage [74]

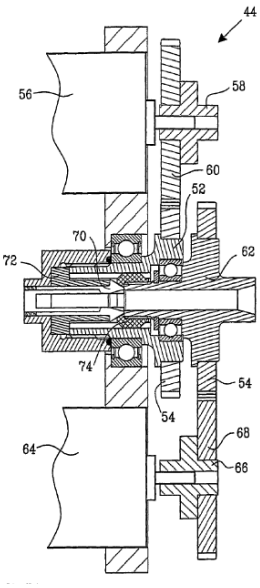

Figure 2.27: Locking and haptic feedback mechanism onboard carriage[74]

the right tool is recognised, the carriage will engage its instrument locking mechanism. This is shown in Figure 2.27 with the activation of both the torque motor (56) and lock motor (64) to start the locking sequence. The torque wheel (52) is fixed via the torque motor (56) and the lock wheel (62) rotates due to the lock motor (64). This pushes the crank block (74) towards the instrument and causes the collet to clamp around the instrument. Once locked, the instrument will then move translationally along the track with the carriage , as permitted by the interconnecting bodies, and rotational movements can be done as normal. Also, from that point on, the haptic feedback to the wire is controlled by the two motors based on the output of the simulation program to the force controller. The patent also states that in another preferred embodiment, the device comprises a processing unit for measuring a longitudinal movement and a movement of rotation of the instrument. While this mechanism was not illustrated, it is quite feasible that an could encoder be placed on the carriage that tracks its movements along the track or conveyor. An optical sensor can also be placed at another part of the carriage, with close proximity to the clamping unit, to track rotational motion. The number of carriages on the conveyor relates to the number of instruments that are used in the system. The carriage at the proximal end (nearest to the operator) is for the most external instrument and the carriages that are further away are for the instruments nested within the largest instrument. These could be used in the simulation of procedures that use multiple tools such as guide wire, catheter, balloons, stents and others.

Figure 2.28: The HERMES Angioplasty Simulator [75]

2.3.5 HERMES

Italian−based Perceptual Robotics (PERCRO) laboratory developed an angioplasty simulator called the HERMES (Hematology Research Medical Systems) in 2005 (Figure 2.28). The HERMES featured a haptic interface unit called the Hermes Haptic Interface or HHI [75]. Two different design configurations were considered in its development. The first, as shown in Figure 2.29(a) involves a pulley system (4) with a single mounted carriage (5) on top. The carriage's elastic joint (6) accepts and grips the inserted instrument and then slides along the pulley as the instrument is pushed and pulled. A motor (M2) is attached to one of the wheels in the pulley system at the entrance of the device. Simultaneously, a second pulley system (7 and 8) that runs normal to the first pulley is positioned at the entrance of the device and another motor, (M1), is attached to one of the wheels of this pulley system. The motors (M1) and (M2) are each fixed to a rotary encoder. Each pulley wheel will move when the instrument is translated or rotated respectively and this movement will be recorded by the encoders to track the instrument's position. Aside from that, the motors (M1) and (M2) can be activated to provide resistance or haptic feedback to resist the instrument's movement. The second design is very similar to the first, with the exception that the motor (M1), with its fixed encoder is mounted onto the carriage and its shaft is connected to the elastic joint (6) as seen in Figure 2.29(b). The mechanism for translational instrument tracking and haptic feedback is unchanged, but now the haptic feedback and rotational tracking is done directly by the motor (M1) and its encoder without the need for a second pulley system. The HERMES developers compared the two designs in a study and concluded that the second design was better since it is less complicated, cheaper to produce and has less friction. Thus the second design was implemented in the device. It should be pointed out that the "instrument" used in HERMES was a rigid rod and not an actual or original instrument. The rigid rod used was made to look similar to an actual catheter by enabling different terminal parts to replace the rod's interchangeable grip. In a first validation study for the HERMES, the feedback received from a surgeon concluded that this substitution of instruments is acceptable without affecting the realism of the simulation. Examination of the PERCRO laboratory website reveals that the HERMES is no longer in development at the time of writing.

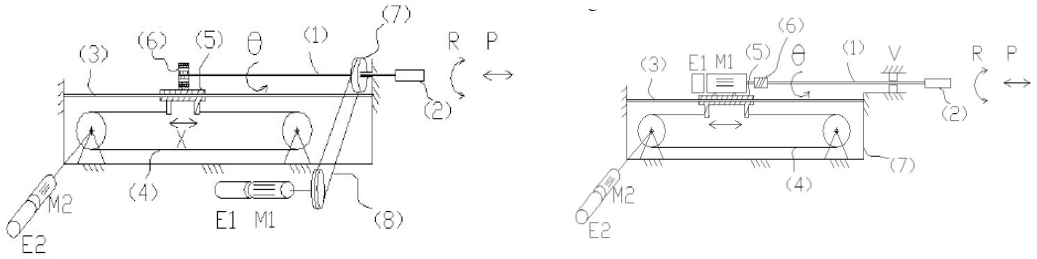

(a) (b)

Figure 2.29: The (a) first and (b) second designs for the HERMES [75]

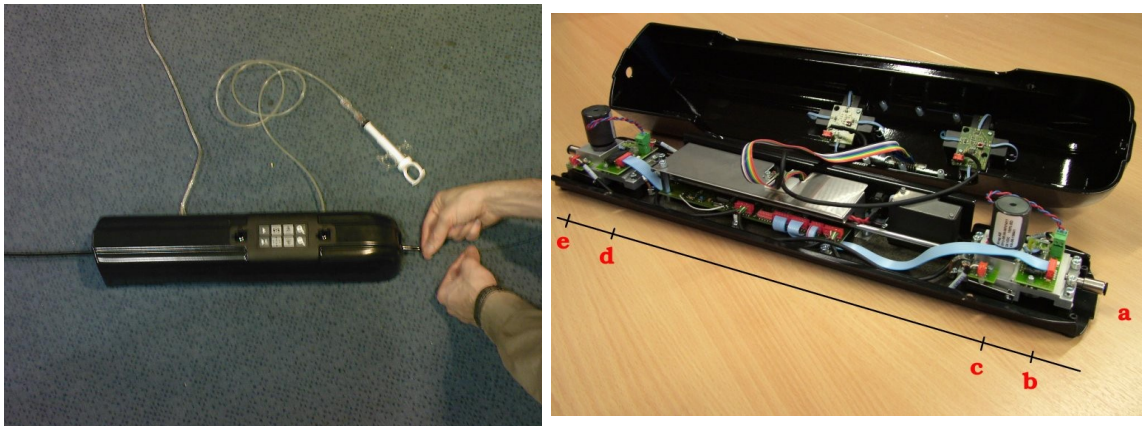

(a) (b)

Figure 2.30: (a) Insertion of instruments into the VSP during operation (b) View of the the VSP components with the chassis removed

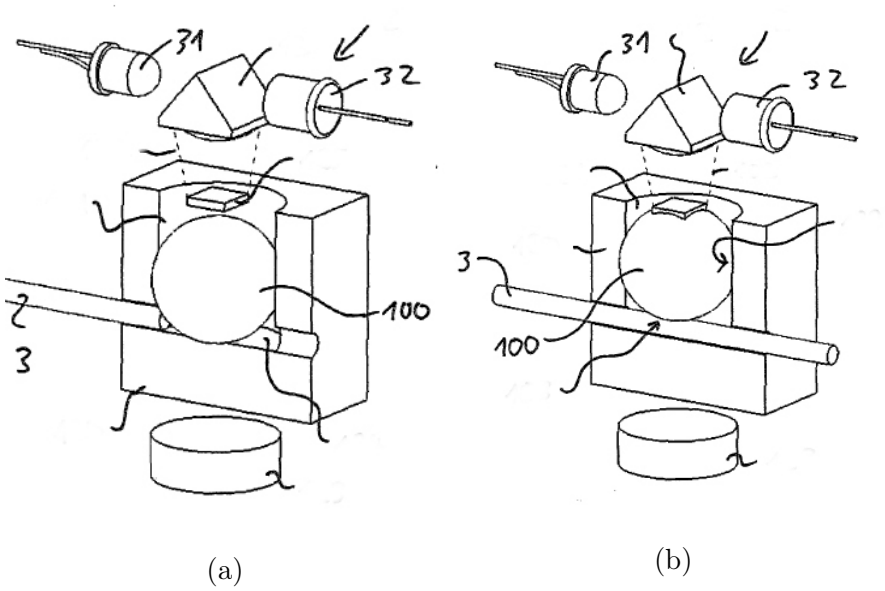

(a) (b)

Figure 2.31: (a) Illustration of effect of instrument insertion to the tracking system (b) Tracking mechanism for tools of varying diameter]

2.3.6 VSP-VISTC

Another endovascular simulation system, called the Vascular Simulation Platform or VSP was developed and sold commercially by Xitact, a company based in Switzerland. The VSP haptic interface device is long and rectangular as shown in Figure 2.30(a). Instruments enter the VSP at one end and exit it at the opposite end. Figure 2.30(b) shows the internal assembly of the VSP. The sensors and actuator for the most external instrument, (b) and (c) respectively, are located at the entrance of the device, (a). The sensors and actuators for the internal instrument, marked (d) and (e) respectively, is positioned right before the exit. Therefore, there is about 30 cm of distance between both sensor-actuator pairs.

In 2005, Xitact was granted a patent, EP1574825 A1 titled "Device for determining the longitudinal and angular position of a rotationally symmetrical apparatus" [76]. The instrument tracking system of the device utilises a spherical object like a roller ball (100) and an optical sensor (32). As shown in Figure 2.31(a), the roller ball (100) is arranged so that it comes into contact with the rotationally symmetrical apparatus (3) upon insertion into the device. The apparatus or instrument will then push the roller

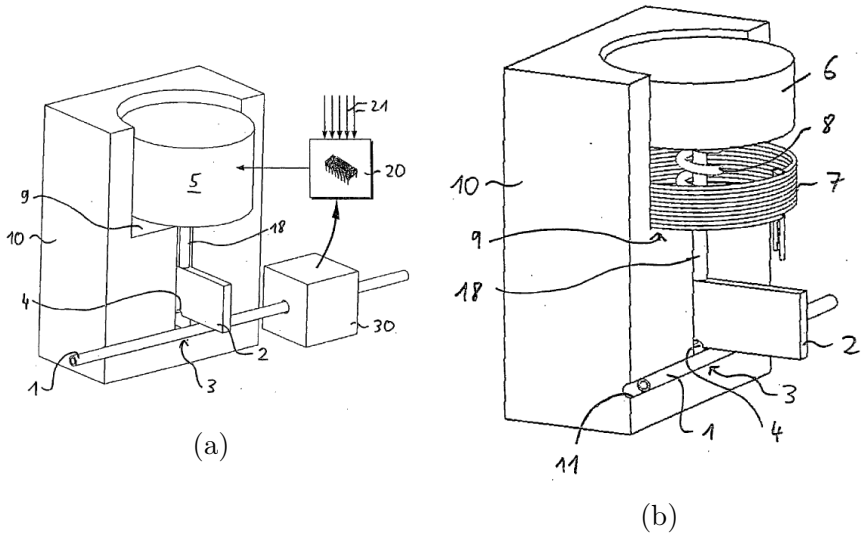

Figure 2.32: (a) Overview of haptic feedback mechanism(b) Haptic feedback actuator using an electromagnetic mechanism

ball vertically where it will be in close proximity to the optical sensors which comprises of a light source (31) and a light detector (32). As the roller ball moves in either axis due to instrument movement, the pattern of light bouncing off the roller ball will be captured by the light detector and the resulting electrical signals can then be interpreted by a processor as measured displacement. The design in Figure 2.31(b) is meant to cater for use with instruments of different diameters. Upon insertion, the instrument (3) will be pushed into contact with the roller ball by a centering mechanism (127) that is either actively controlled via a separate sensor dependent actuator, or passively through the use of a spring (128).

In 2007, Xitact was awarded another patent: Patent US20070063971 titled "Actuator for an elongated object for a haptic feedback generating device" [77]. The device is stated to work in conjunction with a tracking device for a rotationally symmetrical instrument similar to that described in the previous patent. As shown in Figure 2.32(a), when the instrument (3) is inserted into the device, it will first pass through the tracking unit (30) before going under a clip/clamp (2). A control signal sent by the computer software will tell the control unit to activate the linear actuator, either a hydraulic piston or a stepper motor, when needed. Upon activation, the clip will be lowered to clamp the instrument to provide the haptic effect. Figure 2.32(b) shows a different embodiment of the actuator which utilises a brake (2), coil (7), a permanent magnet (6) and a spring (8) instead. When the control unit sends a signal for the actuator to be activated, current will firstly be supplied to the coil attached to the brake. The current in the coil generates an electromagnetic field that will then react to the megnetic fields of the permanent magnets. This produces an electromagnetic force that will push the coil and brake downwards to clip or clamp the instrument. The spring (8) serves to retract the brake to its initial position when deactivated or idle. The design shown in Figure 2.33 is a different embodiment of the device that allows haptic feedback to be applied to an individual axis. The inserted instrument will be in contact with two sets of rollers (40 and 41) and (50 and 51). Each roller will move with the instrument as it is moved in translation and rotation respectively. When the signal is sent to the linear actuator(s), either one or both rollers can be lowered to clamp the instrument depending on which direction of movement needs to be actuated with haptic feedback. The VSP was used in several research studies such as the ImaGine system for simulating needle insertion and Seldinger technique procedures [78]. In 2005, Xitact was acquired by Mentice Corp and today it is made commercially available by Mentice as the VIST-C (Figure 2.34).

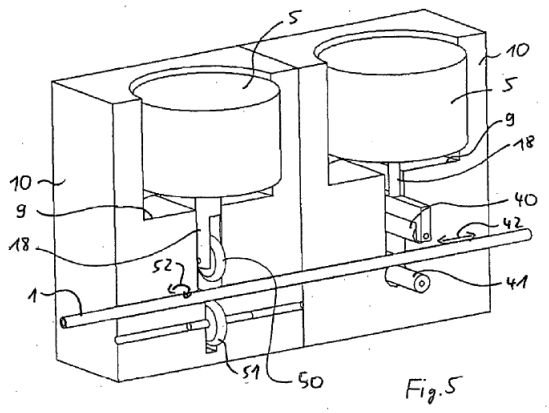

Figure 2.33: Actuator arrangement for axis specific haptic feedback [77]

Figure 2.34: The VIST-C as commercially available today [79]

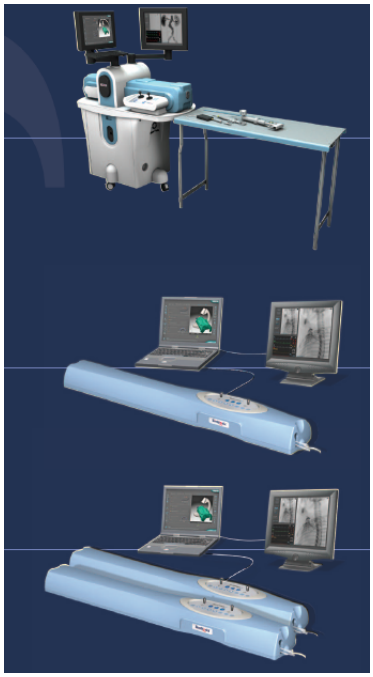

Figure 2.35: AngioMentor Ultimate (top), AngioMentor Express (middle) and AngioMentor Dual Express (bottom) product line by Simbionix [80]

2.3.7 AngioMentor

Another well known producer of endovascular simulator systems is Simbionix, who are the developers of the AngioMentor system. The current Angiomentor line of products, seen in Figure 2.35, include AngioMentor Ultimate, Angiomentor Express and Angiomentor Dual Express [80]. The Angiomentor Ultimate device represents the full simulated cathlab environment, whereas the AngioMentor Express products are designed for portability. In 2009, Simbionix was granted a patent, patent US 20070134637 for a "Medical Simulation Device with Motion Detector". The overall view of the device is as shown in Figure 2.36 [81]. In operation, instruments are inserted into the device and follow the straight path. Along the path are pairs of sensor (41,42 and 43) and actuator (45) units for each instrument (38A, 38B and 38C). The instruments can be a dummy catheter, guide wire or deflated balloon. The sensor unit can be seen with more detail in Figure 2.37(a). The instrument inserted will pass under a bounded working area (13) that is in range of the optical sensors. The focusing element, (14), will focus the light emitted by the IR photodiode (10) onto the surface of the working area which

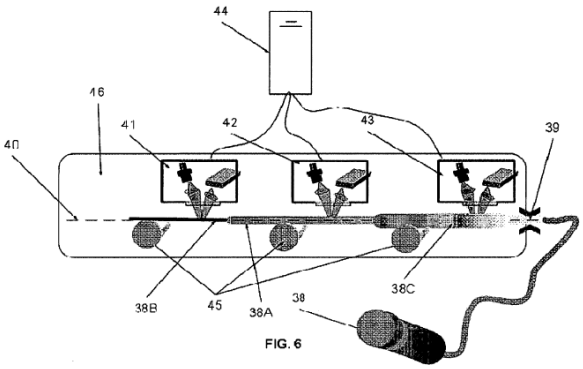

Figure 2.36: The design protected by Simbionix patent [81]

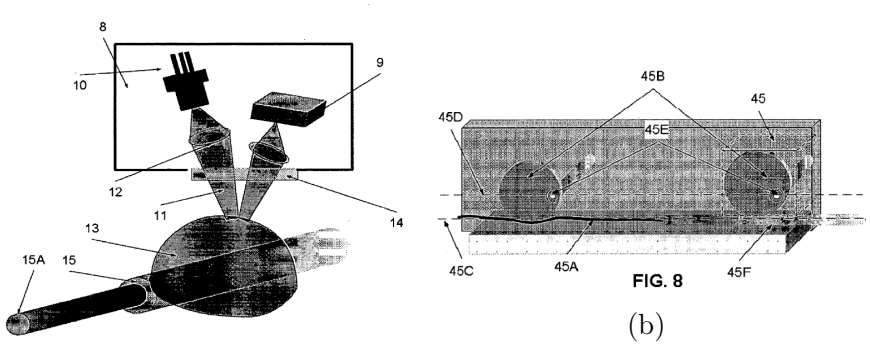

Figure 2.37: (a) Tracking mechanism and (b) Haptic feedback mechanism from Simbionix patent [81]

will then bounce light into the photosensor (9). Movement of the instrument will produce a pattern of light that is translated to measured displacement by a processor. The setup used for providing haptic feedback can be seen in Figure 2.37(b). The brake or actuator used in this design is a wheel (45B) that is connected to a motor shaft at its off centre (45E). Due to the location of its center of rotation, turning the wheel will cause varying degrees of pressure to be applied to the instrument (45A) or (45F) as a type of controllable haptic effect.

2.3.8 Simsuite-Simantha

Colorado based Medical Simulation Corporation has also been actively producing and selling medical simulators commercially. In fact, they are well known for taking endovascular simulator training mobile when they engineered a 35-foot bus that comes complete with a mock cardiology catheterization lab, an operating table and a computerised mannequin patient named Simantha (Figure 2.38). The Simantha endovascular simulator system can be used to train both cardiovascular and peripheral vessel procedures [82]. The system employs a carriage-based pulley system where each carriage is interconnected.

In 2005, Medical Simulation Corporation was granted patent US 20050277096 titled "Medical simulation system and method". The designs within it are for a portable medical simulation system that features an artificial patient housing a haptic interface device [83]. The device uses a multi-carriage system (Figure 2.39), to engage rotationally symmetrical instruments of different diameters. There are instrument stabilisers, that fold and retract with lateral motion similar to an accordion, that connect the carriages on the track. These stabilisers are meant to keep the instruments straight and stiff when inside the device. The device′s thickness is uneven at each end. This is designed so that gravity may help the navigation of the instrument or catheter within the device and into the carriages.

The design of each carriage is illustrated with detail in Figure 2.40. Every carriage (302) is meant to accept one instrument of a particular diameter. If the inserted instrument is of the right size, then it will exert a force on the walls of the lumen (452). Sensors onboard of the carriage will recognise this as the engage instrument state. They will then send signals to the Drive Motor (308), compressing spring (418) that will then open up Collet (422) to allow the instrument to move further into the carriage. Not long after, the actions are reversed which causes the spring (418) to decompress and clamp onto the tip of the instrument thus fixing it to the carriage. Once fixed, the carriage will move with the instrument when pushed and pulled. The positional and orientation information is detected by the optical sensor(436) mounted on the shaft (438) of the Magnetic Particle Brake (408). When the user wants to remove or exchange the instrument, he or she would pull on it to exert a force that is detected by the onboard sensors. The carriage will then go into instrument exchange mode and the same actions

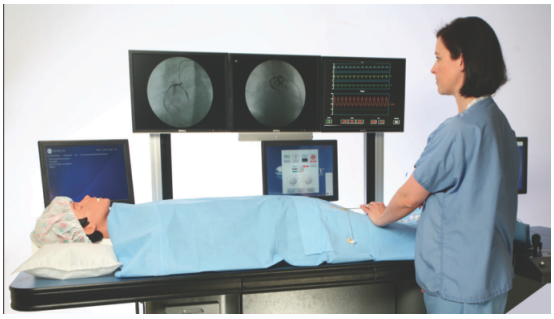

Figure 2.38: The Simantha Simulation System [82]

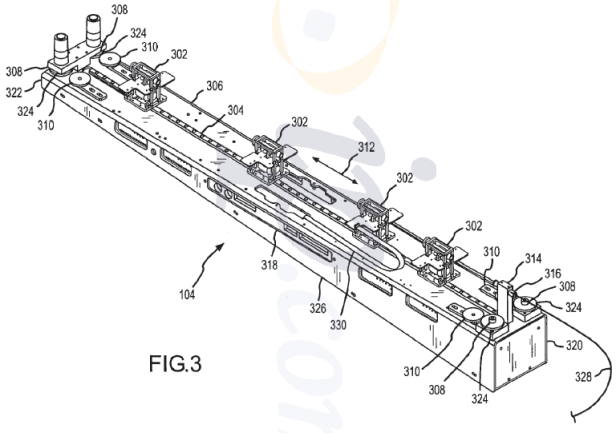

Figure 2.39: Device from Medical Simulation Corporation patent [83]

are taken to widen the lumen to enable instrument retraction. The Magnetic Particle Brake (408) functions as a mechanism for applying feedback to the user for rotational instrument movement. When current is applied to the Magnetic Particle Brake (408), the Timing Belt (446) will provide friction to the instrument and the level of friction is linearly dependent on the amount of current supplied. Each individual carriage also has a dedicated sensor to prevent collision between the carriages during operation.

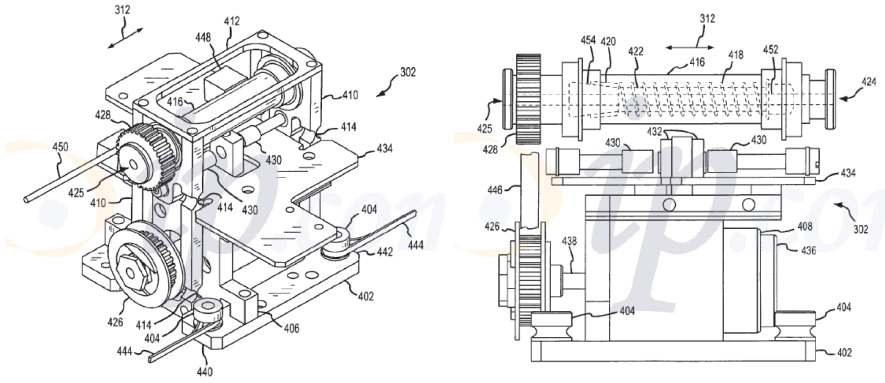

Figure 2.40: (a) Isometric and (b) Cross section (bottom) view of carriage used in patent [83]

Table 2.2: Comparison of features between reviewed haptic interfaces

System	Tracking	Haptics	No. of Tools	Channel or Carriage	Real Tools	Rotational Feedback
HT Medical Patent [63]	Optical with Rollerball	Servo motor Arm	Multi	Channel	No	No
John Hopkins Patent [69] [70]	Rotary with Rollerball	Stepper Motor Clamp	Multi	Channel	Yes	No
EVE [71]	Optical	Passive only	Single	Channel	Yes	No
Mentice Corp Patent [74]	Optical with Pulleys	Motor driven and clamp	Multi	Carriage	No	Yes
HERMES [75]	Optical with Pulleys	Motor driven	Single	Carriage	No	Yes
Xitact VSP and patents [76] [77]	Optical with Rollerball	Electromagnetic Clamp	Multi	Channel	Yes	No
Simbionix Patent [81]	Optical	Motor driven wheel clamp	Multi	Channel	Yes	No
Medical Sim Corp Patent [83]	Optical with Pulleys	Motor Driven and Clamp	Multi	Carriage	Yes	Yes

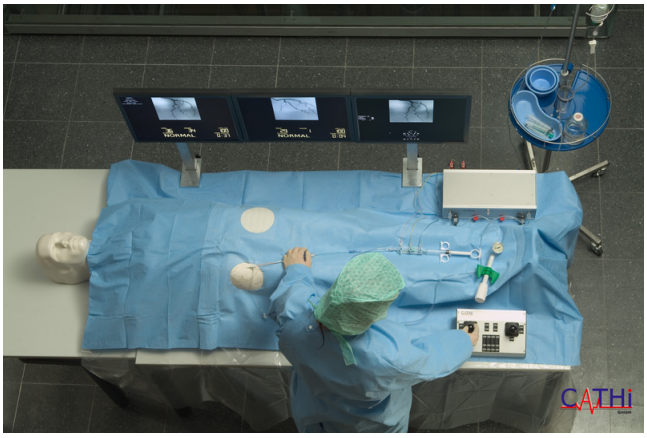

Figure 2.41: Photo from the CathI brochure [84]

2.3.9 CathI

The Catheter Instruction System or CathI is an endovascular simulator system produced by Germany based CATHi GmBh. The system has been in development since 2002, as shown in Figure 2.41 [85], and places a heavy emphasis on using actual instruments in the simulation interface. Very little information is publicly available regarding the CathI's design, although it is known that it utilises optical and pressure sensors, together with microcontrollers [85]. In 2013, the system is still being used in many training courses in Germany [84].

2.3.10 Interface Comparison

In this section, the differences and similarities between the designs examined in the previous section will be highlighted and discussed. Table 2.2 summarises the key features of the 8 interface designs that was found in the literature. This summary assumes that the owners of the patent would implement the design they have patented in their flagship device. For example, it is considered highly likely that the inner mechanisms of the Angiomentor [80] would look similar to the illustrations in Simbionix's patent [81].

As can be observed from the table, all of the interfaces utilise a type of sensor/encoder to measure the 2-DOF movements of the rotationally symmetrical instrument and an actuation system for applying haptic feedback. For sensing, rotary or optical encoders are used to either track the movements of the instruments directly or

through a proxy such as a roller or ball in contact with the instrument. For haptic feedback, all of the systems use a type of real-time (actively controllable) haptic feedback except for the EVE which uses passive haptic feedback via simple friction or collision between the instrument and the physical model. In the active haptic feedback systems, the simulation program sends a signal to the control unit to activate an actuator to apply haptic feedback on cue. Some of the actuators seen in the designs are in the form of stepper motors, servo motors and electromagnetic coils with brakes. When activated, these would position a braking mechanism to come into contact with the instrument. The resulting haptic feedback felt is in the form of controllable resistance that can produce a clamping effect at its maximum level. In some of the designs such as the VIST, motors are used to resist instrument movement. However, experienced physicians often comment that the haptic feedback generated in these devices are too simplistic and far from realistic. This is especially true for rotational haptic feedback, which is not even a feature in most of the designs.

The overall concept of the prior designs can be divided into two main categories by appearance. In category I , the instruments pass through a single channel and pairs of actuator and sensor units are strategically fixed along that channel. The Neurocath, VSP and AngioMentor all belong in this category. In category II, a carriage or conveyor system is used and the instruments will pass through the carriages and its interconnecting bodies. Sensors and actuators are positioned within each carriage which is mobile along the track. In operation, the carriages will move with the instruments along the conveyor system. Systems using the carriage or conveyor approach, ie. the Mentice VIST and the Simantha Simsuite, tend to involve more complicated mechanical parts compared to those in category I. This is best illustrated by the designs in the latter′s patent [83], which feature many intricate parts. The large number of parts increases the need for frequent maintenance and calibration due to wear and tear. Also, there is the issue of the carriages and conveyor producing unwanted mechanical friction or resistance to the instrument as it is translated and rotated.

It is also important to observe that several of the systems reviewed are compatible with real tools, like the CathI, while others rely on mock instruments to operate, like the ICard [68]. Systems that are compatible with original instruments are often considered to offer more realism in the simulation experience. In addition, the interfaces differ in terms of the number of compatible instruments. Single instrument interfaces

like the EVE, the ICard and the HERMES limit the number of compatible instruments to only one, usually a catheter. However, this is not ideal because it limits the number of procedures that can be recreated in simulation. In multiple instrument interfaces, because the guide wire is concentrically within the catheter, the sensors and actuator are arranged in the configurations of design category I and II. In both designs, there is a considerable distance between each unit pair to allow for instrument extension. There is an inherent problem with this approach as the inserted instrument has to travel a fair amount of distance before it can be detected by the sensors. For instance in the Mentice patent [74], the instrument with the smallest diameter has to pass through three carriages before it is finally locked in and tracked in simulation. Another drawback of this design is that there is a limited range of movement for the instrument's extension. For example, in the Xitact VSP, it is possible to overextend the catheter during simulation and obstruct the guide wire sensor which causes the positional information of the guide wire to be lost thus disrupting the simulation.

The examination of prior and existing designs for endovascular simulator haptic interfaces has revealed previous attempts to overcome the 'concentric occlusion' problem which produced several shortcomings. Factors like a delay in tracking the instruments upon insertion, limitations to the instrument's range of movement, errors that cause the system to lose track of an instrument's position and unrealistic haptic feedback affect the face validity of the simulation. This underlines a need for a new design for a haptic interface device that addresses these shortcomings. In order to do this, alternative technologies or approaches are considered as the starting point for the development of an improved haptic interface.

2.4 Sensor Technology

A sensor is a device that receives some form of input physical property as a stimulus and responds with an electrical signal [86]. The primary function of these devices is to inform a system about external conditions or internal within the device itself. There are generally two types of sensors: passive and active. Passive sensors do not need any additional energy source as they can directly generate an electrical signal in response to a stimuli. Examples of passive sensors include thermocouples, photodiodes and piezoelectric materials. Active sensors require external power for operation, mainly

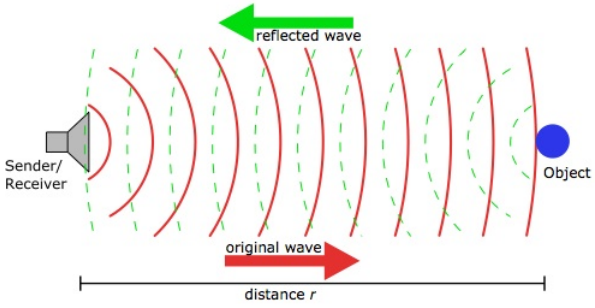

Figure 2.42: Ultrasound transmitted will bounce back to the receiver [87]

to produce an excitation signal. The properties of these sensors change in response to an external signal. A typical example of an active sensor is the thermistor, which is a temperature sensitive resistor.

An important part in sensor system design is to identify the stimulus that needs to be detected. For this application, there is a need to be able to measure any movement of the catheter and guidewire while inside the device. Both the guidewire and catheter are able to move translationally and rotationally, which means that they have two degrees of freedom (DOF) of movement each. Therefore, it is important to examine what physical properties change or can be manipulated to change when the instruments are put into motion in either of these DOF. A review of such properties is presented next.

2.4.1 Ultrasound

Ultrasound are sound waves above the range of human hearing with a frequency greater than 20kHz. Ultrasonic sensors work based on the mechanical wave properties of sound. First, a ceramic material inside the sensor is excited by an electrical signal and produces a vibration. This vibration causes the air at the surface of the sensor to compress and expand, thus creating a sound wave propagating perpendicular to the sensor surface. The time taken for the wave to travel from a transmitter to a receiver (t) can be used to determine the distance between the two by using Equation 2.1 since the speed of sound (v) is a constant value in a temperature controlled environment. Figure 2.42 illustrates this concept for a transmitter that is also a receiver, otherwise known as transceiver.

$$s = v \times t \tag{2.1}$$

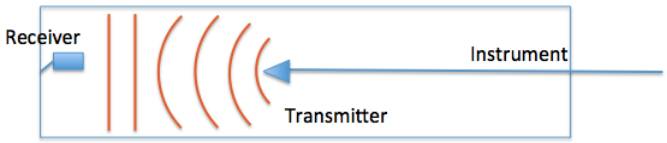

Figure 2.43: Concept design for ultrasonic translational movement technique

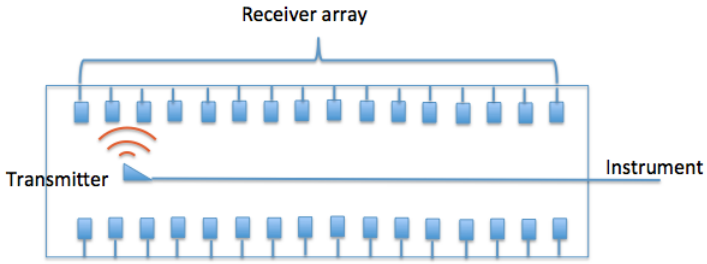

Figure 2.44: Concept design for ultrasonic rotational movement technique

Ultrasound sensing is used for a variety of applications, including motion detection in burglar alarm systems, wind direction and speed measurement, and tank water level measurement. Ultrasound is especially suited for detecting clear objects or liquids such as water since sound waves won't diffract.

A design to apply ultrasound for tracking the motion of the instrument inserted into the interface device would require substantial modification of the instrument itself. By placing an ultrasonic transmitter at the tip of the guidewire and a receiver at the far end of the device chassis, instrument depth can be known by measuring the distance between the transmitter and the receiver. As the instrument is inserted further, the distance between the two will decrease and vice versa. This is illustrated in Figure 2.43.

In a similar conceptual design, the transmitter is once again fitted to the tip of the instrument. However, the transmitter now emits ultrasonic waves to the sides of the device chassis. By placing ultrasonic receivers around and along the chassis of the device, as illustrated in Figure 2.44, it would be possible to determine both the depth and orientation of the instruments. This design is more complex, since it would involve an array of receivers, and would also be more costly. Also, the receivers have to be at an appropriate distance from the transmitter, since sound waves disperse the further they are from the source. If the dispersion is too large, the resolution of the sensing in this

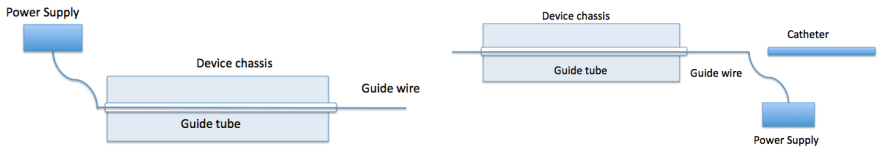

(a) (b)

Figure 2.45: Illustration of a guide wire pre inserted into device and connected to power supply through the (a) distal end and (b) proximal end in reference to the operator position

design might not be sufficient to track the small scale movements of the instruments.

While the ultrasonic approach is technically feasible, there are several issues to be considered. With this design, the catheter can never be extended beyond the tip of the guidewire due to the presence of the ultrasonic transmitter. Even if it was physically possible, this would occlude the sound waves's propagation. Another issue is that the transmitter at the tip of the wire has to be actively powered since electrical energy is required to transmit the ultrasonic waves. Regardless of whether a battery or a voltage supply is used, this would affect the realism and effectiveness of the simulation. This is because, if the wire is connected to the power supply through the proximal end (closest to the operator) , the trainee will not be able to experience the practice of inserting the instrument into the device during the simulation, since the wire would have to be pre-inserted into the device as illustrated in Figure 2.45(a). On the other hand, if it is connected through the distal end (furthest from the operator), the trainee will not be able to experience the process of advancing a catheter over the guidewire as shown in Figure 2.45(b). Either way, an important step of endovascular surgery training may be missed by the trainee. Another point of concern is that sound is very reflective and therefore it could be possible that the bouncing sound waves inside the device would cause erroneous readings from the various sensors. Also, it should be noted that sound moves at a relatively slow speed, especially when compared to light as used by optical sensors. Thus, it is feasible that the detection or tracking rate of the sensor would not be fast enough for this application, resulting in a noticeable lag during the simulation.

One of the physical characteristics of sound waves is that when they bounce off of a static target object, the frequency of the reflected wave remains the same as the initial wave. However, if the target object was in motion, the frequency of the wave would have shifted. This is known as the Doppler effect.

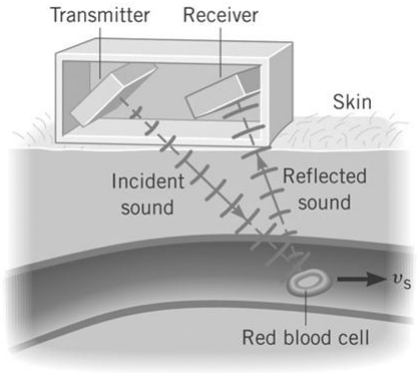

Figure 2.46: Doppler effect used to measure flow [88]

There are existing commercial sensors that operate based on this effect, which are primarily used to detect motion and flow of liquids that require a non contact approach. Figure 2.46 shows how a Doppler effect sensor is able to measure the flow rate of the blood cells externally.

One can the consider placing a similar type of sensor on the outside of a channel and using it to detect motion of the guidewire and catheter (both rotational and translational) passing within it. However, there are two main issues with this design. First, the uncertainty of whether the guidewire, which is has a small diameter, could produce a significant enough shift in frequency when hit by the ultrasonic waves. This is especially considering its movement pattern, which is usually very subtle. Secondly, it is very likely that, when the catheter is advanced over the wire, the sound waves would be occluded and blocked from reaching the guidewire, thus making it undetectable. The first two concept designs here place the transmitters on the instrument and the receivers in the device chassis, whereas the third places transmitters in the device chassis and uses the instrument itself as the target. Also, in both designs, significant modifications to the instrument are required, which may affect the realism and feel of the simulation.

2.4.2 Capacitance

Capacitive sensors measure the electrical property of capacitance as a stimulus. Capacitance exists between any two conductive objects or surfaces in close proximity with each other. In Figure 2.47 it can be seen that there are two metal plates connected to the positive and negative terminals of a battery, respectively. When the battery is switched

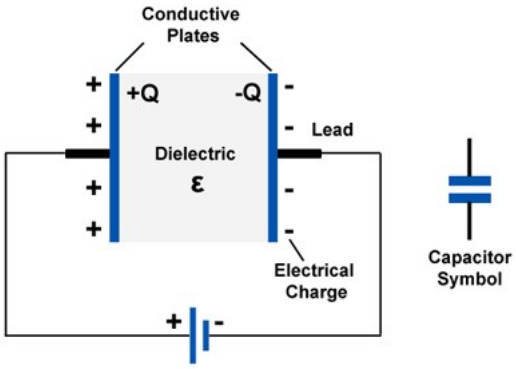

Figure 2.47: Capacitance illustrated with two metal plates [89]

on, the difference in voltage will cause the electrons from the battery to accumulate on one of the plates making it negatively charged. This creates a lack of electrons on the other plate, thus making it positively charged. If the battery connections are reversed, the polarities of the plates would also be reversed.

Capacitive sensors use alternating current (AC) resulting in the polarities of the plates switching back and forth at a fast rate. This creates a current that is influenced by the value of the capacitance, since current is a function of Charge (Q) over Time (t) (Equation 2.2) and Charge (Q) is the product of Capacitance (C) and Voltage (V) (Equation 2.3).

$$I = \frac{Q}{t} \tag{2.2}$$

$$Q = C \times V \tag{2.3}$$

Referring again to Figure 2.47, the capacitance value of this setup is directly correlated to the surface area A of the plates (the larger the surface area, the more charges are present) and the dielectric constant e of the medium between the two plates. Capacitance is also inversely correlated to the distance d between the two plates. Therefore, capacitance can also be expressed as in Equation 2.4.

$$C = \frac{e \times A}{d} \tag{2.4}$$

Based on this characteristic, capacitive sensing is very widely used in the industry today to perform certain tasks such as displacement measurement, dynamic motion

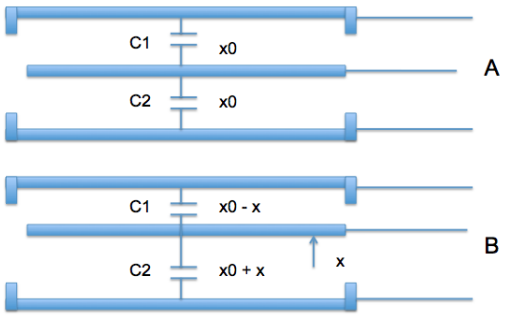

Figure 2.48: Capacitive displacement sensors

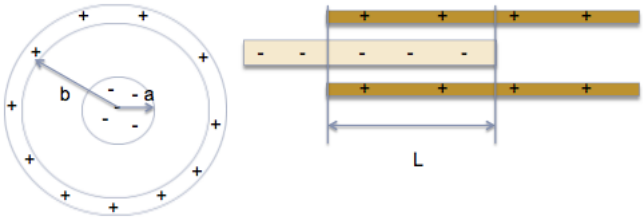

Figure 2.49: Cylindrical capacitive sensor

measurement and material thickness measurement. The basics of capacitive displacement sensing are as illustrated in Figure 2.48. It shows that in its initial condition A, there exist two capacitance values in the setup, which are the capacitance between the conductive plate in the middle and both upper and lower plates. As the centre plate experiences displacement in the vertical axis shown in B, the distance between the plates would change, causing a change in the capacitive values between the plates as well, as characterised by Equation 2.4. By measuring the change in the capacitance, the amount and direction of displacement can also be determined.

In the context of this project, however, the displacement of the wire is in the horizontal and rotational axis, therefore, the configuration in Figure 2.48 is not applicable. Instead, the configuration used in a different kind of capacitive sensor called a cylindrical capacitive sensor would be more suitable. As illustrated in Figure 2.49, this sensor is in the shape of a hollow cylinder that acts as one conductive object, and a rod in the centre of the cylinder acts as the other. The capacitance value that exists between the two objects is described by Equation 2.5.

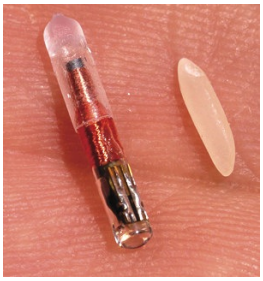

Figure 2.50: Passive RFID tag next to a grain of rice [90]

$$C = \frac{2 \times \pi \times e \times l}{ln(\frac{b}{a})} \tag{2.5}$$

In this sensor, capacitance is directly related to the length (l) of the inner conductor inserted into the cylinder. It is also inversely related to the logarithmic ratio of the distance or radius (a and b) between the conductors. This would be useful in the sense that, if the inner conductor is assumed to be a modified version of the guidewire, then when the guidewire is inserted into the cylinder, the value of the capacitance (C) would directly increase and the opposite would happen when it is withdrawn. Therefore, the capacitance value can be used to track instrument insertion depth through this method. However, this method requires the wire to be charged, which means that the wire needs to be connected to a power supply unit. As explored before, this cannot be done without affecting the simulation procedure experience and, more importantly, exposing the operator to an electrically charged wire. Also, through this method alone, there is no way to detect rotational movement of the rod or wire. It is therefore likely that a separate tracking system for measuring rotational movement would be needed.

2.4.3 RFID

Radio Frequency Identification (RFID) is a non contact information transfer system between a reader and an RFID tag via radio waves. RFID's applications include tracking of an unfinished product going through its manufacturing stages at the factory, identification of livestock and pets, payment for access to toll roads or parking and inventory management.

RFID tags can either be passive or active. Passive tags transfer information using the energy generated by the radio waves received, whereas active tags require some

Figure 2.51: Configuration of RFID tags embedded into mock guidewire

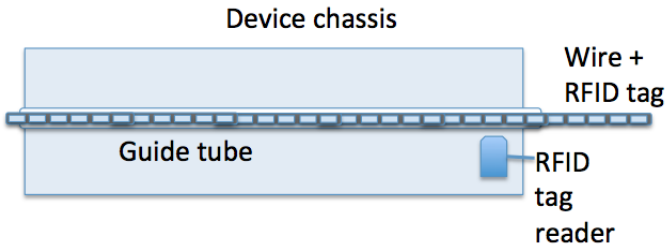

Figure 2.52: Concept for using RFID technology to determine instrument depth

sort of onboard power source such as a battery. An inductor coil within the tag reader generates a magnetic oscillatory pulse at a particular frequency. When an ID tag with a specific frequency comes into close proximity with the reader, inductive coupling causes it to oscillate. At this point, the reader would then stop oscillating and begin to "listen" for persisting oscillations, interpreting the frequencies as meaningful data.

The cost of these tags differs according to specifications such as type, size, frequency range and storage system, but most cost between USD 0.07 - 0.20 each. Size wise, active tags are usually larger than passive tags due to the onboard battery they require. Passive tags are tiny with some measuring at 1 mm x 1 mm x 0.18 mm, more or less the size of a grain of rice as shown in Figure 2.50. However, newer passive tags called Powder RFID now can measure about up to 64 times smaller.

RFID's ability to store information in such a tiny package leads to a consideration of whether it could be of any use in this project. One design possibility involved manufacturing a wire that looks and feels similar to an actual guidewire, which carries passive RFID tags spaced out equally along its length as shown in Figure 2.51. An RFID reader is placed at the entrance of the device and each RFID tag read would be identified as they pass under the reader. As the location of the tags along the wire is already known, the current instrument insertion depth can be determined. This approach is illustrated in Figure 2.52.

There are, however, two main problems with this approach. Firstly, it would be very difficult to customise or manufacture a guidewire in such a way and maintain the

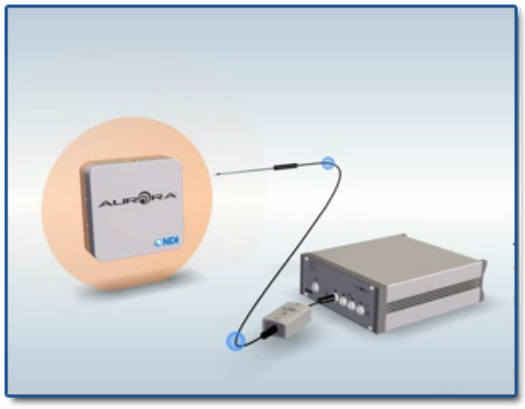

Figure 2.53: Illustration of using electromagnetic tracking for in vitro application [91]

feel of the original guidewire in terms of weight, diameter and texture. Even if it was possible, RFID will not be able to detect and track rotational movement. It can only read what is stored on the tag and not relay any real time information. Secondly, RFID is not capable of small scale tracking as required in the task investigated. Ideally, the tracking mechanism to be implemented needs to have a high resolution (millimetres) since the movements of the instruments can be very fine. However, RFID does not have the sensitivity or resolution to read different data from two different tags about 1 cm apart. Tracking using RFID is usually at a much larger scale, such as tracking a package stored inside a warehouse.

2.4.4 Electromagnetic Tracking Systems

Electromagnetic tracking systems consist of two main components, which are the field generator and the sensor coils. The field generator produces a 3-dimensional electromagnetic field. When a sensor coil enters this field, a current will be induced in the coil. The magnitude of this current will reflect the position and orientation of the coils inside the field. This system is illustrated in Figure 2.53, which demonstrates the Aurora system by NDI Technologies [91].

There are generally two types of electromagnetic tracking systems based on the the type of current used to produce the magnetic field. For example, the Aurora system developed by NDI Technologies, runs on alternating current (AC), whereas the Polhemus system runs on direct current (DC). For AC systems, the magnetic field is always varying in a controlled way, whereas for a true DC system, the magnetic field is always static.

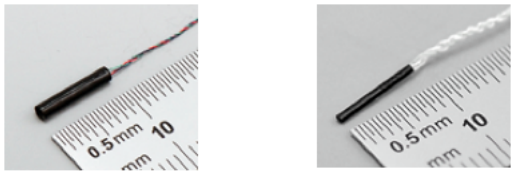

Figure 2.54: The mini (left) and micro (right) 6 DOF sensor coils produced by NDI for its Aurora system [92]

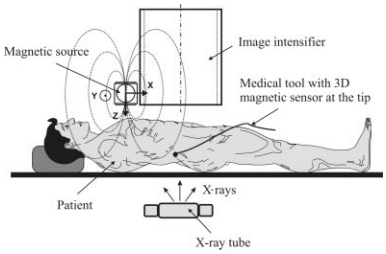

Figure 2.55: Illustration of the application of the Aurora in medical research [93]

The main advantage of a true DC magnetic field is that, unlike AC magnetic fields, no eddy currents are generated in nearby ferromagnetic objects. This would often cause a distortion of the generated field and cause erroneous sensor readings.

However, there is technically no true DC generated magnetic field. Some systems use a switching mechanism to produce a pulsing DC magnetic field by rapidly turning the circuit on and off. This approach will also produce disruptive Eddy currents, therefore, in reality, there are no significant differences between existing pseudo-DC driven and AC driven tracking systems.

Electromagnetic tracking systems are gaining popularity lately because of several factors. Firstly, the sensor coils are diminutive in size as shown in Figure 2.54. The size of the coils depends on the specific resolution and accuracy needed of the tracking system. The Aurora has coils as small as 0.5 mm x 8 mm in dimension. This makes it possible for embedding or attaching the coils onto target objects without adding to their size and weight. Secondly, the sensor coils are able to measure movements in 5 to 6-degrees of freedom, which includes x,y,z positions in the magnetic field as well as yaw, pitch and roll. Finally, electromagnetic tracking does not require contact or line of sight to operate. This makes it especially useful for use in in vitro tracking applications as illustrated in Figure 2.55. These characteristics make electromagnetic systems seem like a very suitable choice for tracking the instruments in this project.

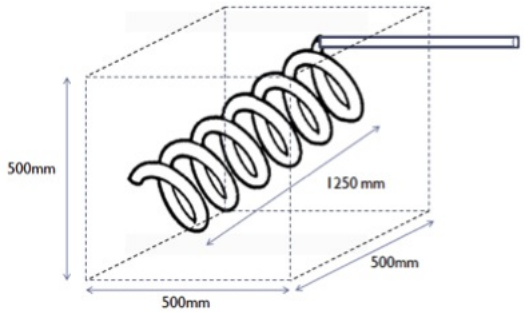

Figure 2.56: Illustration of the spring helix guide tube design

However, this approach is not without its drawbacks. The sensor coils are only trackable by the system while they are inside the electromagnetic field and the size of the field is limited. For example, the Aurora's magnetic field has a dimension of 50 cm x 50 cm x 50 cm. This complicates its use in this application since the target instruments for tracking are at least 80 to 100cm in length and they would not fit into the generated field.

A few concept ideas on how this limitation can be overcome now follow. The first approach is to replace the tube or passage into which the instruments are inserted. Instead of a horizontal and straight tube, one that resembles a spring helix design as shown in Figure 2.56 could be used. This would allow more of the instrument to fit within the field than before. The design of the helix is the most challenging part of this approach because it must be not too compressed. A compressed helix will dramatically apply external pressure on the instruments when they are advanced due to the tight curvature.

Alternatively, this limitation can be solved using multiple sensor coils. Sensor coils are placed along the instrument at a fixed distance apart from each other so that when one coil leaves the magnetic field, it will be immediately replaced by another. By keeping track of the number of times a coil exits the field, the current instrument depth can be calculated through simple programming. This approach is illustrated in Figure 2.57.

However, the sensor coils need to have a wired connection to the system control unit to function. Wireless sensor coils do exist, but currently their size is still too large for use in this application. This need for physical connectivity is similar to the requirement described in the ultrasound and capacitance systems. Like those systems, there is no

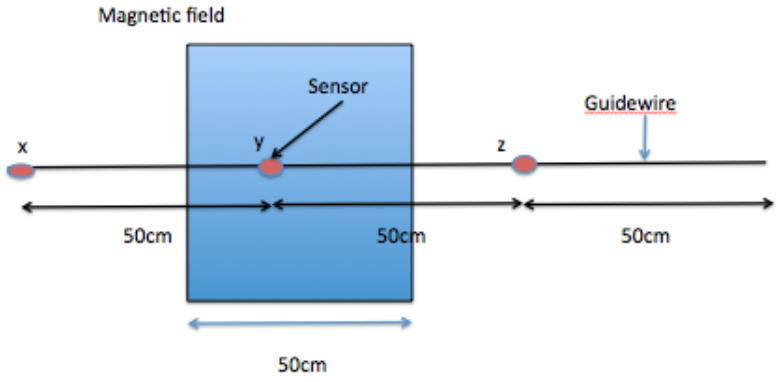

Figure 2.57: Illustration of the multi sensor coil approach

way the connection can be made without sacrificing the realism and effectiveness of the simulation training process. Electromagnetic tracking systems like the Aurora seem to be the perfect solution with its small sensor size and 6-DOF in vitro tracking capabilities. Nevertheless, issues like limited working space and need for wired connections make it difficult to implement. Equally, the fact that these system are quite costly and sensitive to disruption caused by the presence of any nearby ferromagnetic objects are important disadvantages.

2.4.5 Optical

Optical sensors gather and interpret light and other waves in the electromagnetic spectrum to obtain useful information. They are found in cameras all over the world, including digital cameras, video cameras, security surveillance cameras, smartphones and even in the typical optical mouse. Optical sensors produce an image based on the intensity and wavelength of the light they receive. The rate by which this image is produced differs according to camera specifications, but typical video cameras generate 25 frames of images per second. Security cameras use the differences between these images to detect motion for alerting the user of intruders or burglars.

As mentioned in the previous section, optical sensors have been used quite successfully in previous simulation interfaces, namely the Xitact VSP and the AngioMentor. These devices have shown these sensors to be responsive, reliable, accurate and sensitive enough to detect the subtle movements of the guidewire and catheter. The only

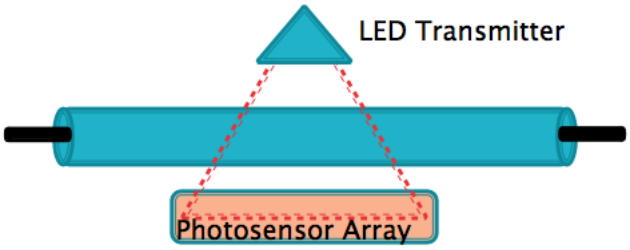

Figure 2.58: Illustration of the optical penetration approach

requirement for its application is line of sight to the target. This made it necessary to compromise on the realism of the simulation in terms of limiting the movement range of the instruments through strategic sensor placement.

The sensors in those devices are used in the same way as in a typical optical computer mouse, except that, instead of setting the sensors to monitor the work desk surface, they are set to monitor closely positioned instruments and their movements. Therefore, these sensors are not able to measure the absolute position of an object within an environment, rather they measure displacements based on the pattern of movements judged from the image differences. They then use that information to deduce the position of the target and its orientation.

Optical sensors need light to operate successfully. The reason they cannot be used to detect the movements of the guidewire when inside the catheter is because light can not penetrate through the synthetic material of the catheter. Therefore, an investigation was needed to determine whether any of the other waves in the electromagnetic spectrum are able to penetrate the thickness of the catheter and produce an image that is useful for detecting movement as shown in Figure 2.58. However, upon discussing the topic with experts on optics and researching related literature, it was found that this approach was not feasible as no light from any part of the electromagnetic spectrum would be able to penetrate the catheter.

The second approach was to investigate if the line of sight problem could be solved by using a catheter that is translucent. If the sensor was positioned close enough, light may then pass through the catheter material and be reflected off the guidewire back onto the sensor to produce a meaningful image. One possible issue with this technique is that movement of the catheter, and not just the guidewire, would also cause a displacement reading in the optical sensor. In an attempt to enable simultaneous movement tracking

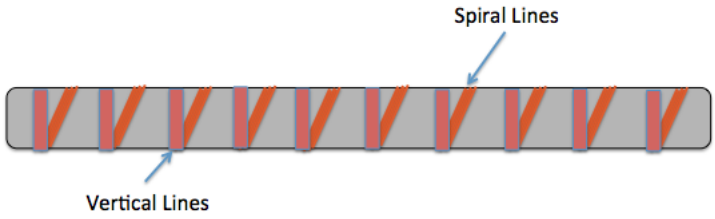

Figure 2.59: Markings on wire to indicate movement to optical sensors

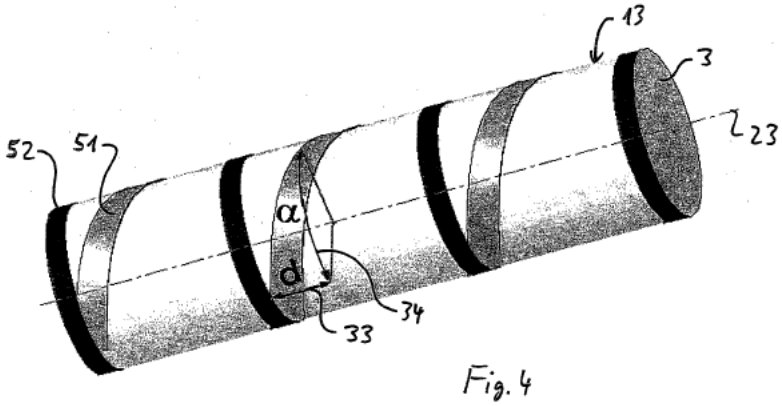

Figure 2.60: Markings on rod from Patent EP 1 517 119 A1 [94]

of the guidewire and catheter, a third approach was proposed. This approach also uses a translucent catheter to detect guidewire movement. However, here the guidewire is modified to have markings as shown in Figure 2.59. These markings will be observed by a second optical sensor to identify instrument position and orientation.

Two sets of markings were suggested. The first set of markings are simply vertical lines. When the guidewire is moved translationally, the direction and speed of movement of these markings will indicate the current movement of the wire. The second set of markings is in the form of a line that spirals around the instrument's body. Similar to the first, these markings will produce a movement effect when the guidewire is rotated. The detection and interpretation of these markings can be done through simple image processing techniques via software such as MATLAB. Upon further investigation, it was discovered that these markings and in fact this third approach is very similar to the work in the Patent EP 1 517 119 A1 [94] as shown in Figure 2.60.

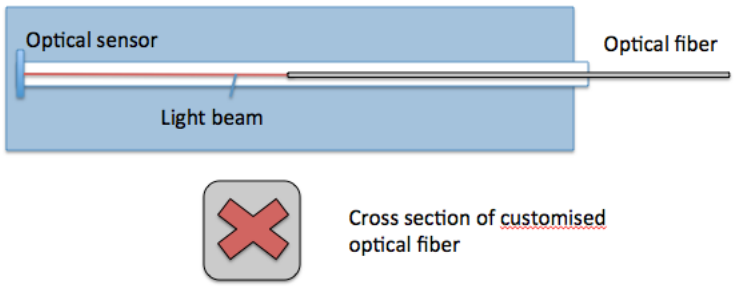

Figure 2.61: Optical fiber approach for sensing instrument position

2.4.6 Fibreoptics

The last optical approach considered involves the use of optical fibres. Optical fibres are flexible fibres made of transparent glass that are used as a waveguide to transmit light between its two ends. Light travels within the fibre by the process of total internal reflection as the hollow core of the fibre is usually covered by a material with a low refraction index. Its main application is in data transmission with its best feature being the ability to transmit data at a faster rate over longer distances. They are also a popular choice for lighting and illuminatiing building interiors.

In one design approach, the optical fibre inserted into the device would project a beam of light that is captured by an optical sensor at the end of the device as shown in Figure 2.61. As the instrument is inserted further, the intensity of the light captured would increase and vice versa. Rotation on the other hand is impossible to detect via light intensity alone. Some customisation of the fibre is thus needed to make a noticeable difference of the light captured by the sensor when the fibre is rotated. For example, instead of projecting an ordinary beam of light, the fibre tip can be shaped to form an X. This way, the translational movement of the wire can be known through analysing the intensity of the light, whereas its rotational movement is calculated based on the orientation of the image itself, represented by an X in Figure 2.61. Such modification on a fine piece of fibre is not a simple task and would presumably require special tools or machinery. Even then, with this design there is still the problem of the catheter not being extendable over the the fibre tip, since this would cause the light beam to be occluded from reaching the optical sensor. Finally, fibres need a light source at one

Figure 2.62: Rotary encoder [95]

Figure 2.63: Examples of potentiometers [96]

end to produce the light beam at the other. This results in the same problem discussed previously for the ultrasonic, capacitance and electromagnetic approaches, namely, the need to physically connect a wire to an electrical circuit, thus potentially affecting the realism of the simulation.

2.4.7 Mechanical

Mechanical sensors were a common feature in previous designs for an endovascular instrument tracking device in the form of rotary encoders (Figure 2.62). There are two main types of rotary encoders: absolute encoders and incremental encoders. Absolute rotary encoders are fitted with a shaft that is designed to touch metal contacts as it turns in such a way to produce a unique binary code for every significant shaft angle. On the other hand, incremental rotary encoders have an engine that produces pulses in channels and offsets in these pulses give relative positioning measurements of the target. There are also linear encoders that function in the same way but measures linear motion instead.

The potentiometer is another type of mechanical sensor which operates on the principle that electrical resistance (i.e. a hindrance to charge flow) is linearly correlated

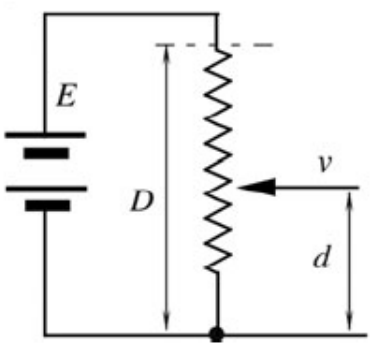

Figure 2.64: Potentiometer as a position sensor[86]

with electrical wire length. Electrical resistance is a result of collisions between the electrons/protons with the wire atoms. Thus, there would be more resistance in a longer wire as there would be more collisions occurring [97] . In its application, the moving object is mechanically coupled to the potentiometer's wiper and thus its movement causes the resistance to change as the wire length changes. The potentiometer is an active type sensor as it requires an excitation signal to measure resistance (by passing direct current through the potentiometer wire). Measurement of voltage drop instead of resistance change is more practical for some applications. It can be obtained by using Equation 2.6 since the voltage across the wiper would be proportional to the displacement d where the full scale displacement is D and the voltage across the pot is E (Figure 2.64).

$$V = \frac{E \times d}{D} \tag{2.6}$$

Physical displacement can also be measured mechanically using a Linear Variable Displacement Transducer (LVDT), which is fundamentally a transformer with a mechanically actuated core [86] (Figure 2.65). The primary coil of the transformer is driven by a sine wave with a stable amplitude, whereas the secondary coils are induced with an alternating current signal and connected in the opposite phase. Between the primary and secondary coils is a ferromagnetic core that does not physically touch any of the coils. When the core is positioned in the central magnetic point of the transformer, no output voltage is generated since the secondary output signals cancel each other. However, movement of the core away in any direction would cause an imbal-

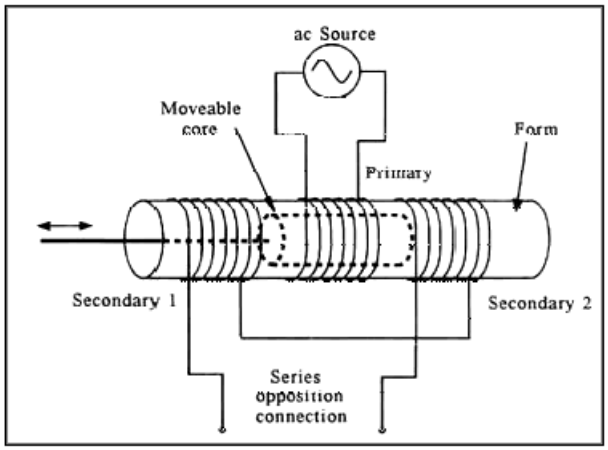

Figure 2.65: General assembly of LVDT sensor [98]

ance of the induced magnetic flux ratio between the secondary coils, thus producing an output. This is due to the change of the flux path reluctance .

One feature that every mechanical encoder, potentiometer and LVDT has in common, is that a point of contact with the moving object is required for operation. For the application of this work, points of contact with the guidewire are severely reduced when the instruments are arranged in a concentric configuration. A creative approach is needed to place and apply these sensors for tracking the movements of the concentric guidewire, such as those that were used in previous haptic interface designs. Alternatively, in another design concept, the tracking approach consists of two units. The first is the main unit containing encoders ready to accept and measure catheter movements. The second is also a unit containing encoders, but it is designed to accept and measure guidewire movements. During simulation, the catheter is first pre inserted into the main device. The guidewire is then inserted through the second unit and then immediately into the first. As the sensors are located at opposite ends, the instruments have increased range of movement since there is no chance of one instrument disrupting the sensor readings for the other. This also solves the problem of delay of tracking after insertion since the guidewire is trackable as soon as it is inserted into the second unit. This approach is illustrated in Figure 2.66.

The drawback of this design is that, with the catheter being pre inserted, an important part of the simulation experience may be missed out by the operator. Also,

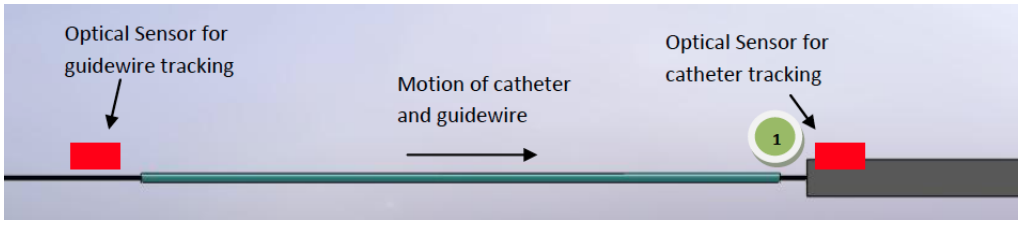

Figure 2.66: Design for tracking guidewire movement outside device [99]

the presence of a second unit located near the insertion point of the main unit could be intrusive to the workspace during the simulation. Lastly, as with all contact sensors, the encoders need to be carefully calibrated so as to avoid causing unwanted friction that would affect the feel of instrument manipulation during the simulated procedure.

2.5 Actuator Technology

As haptics technology has progressed over the last decade, the number of haptic actuators available for selection has also increased. Generally, there are four types of widely used haptic actuators, depending on the source of force that causes the initial displacement in the actuators [100]. As any of the technologies reviewed here can be used to apply haptic feedback to the external instrument (catheter), focus will be on considering how each actuator type may be used to apply force to the internal instrument (guidewire) as a solution to the concentric occlusion problem.

2.5.1 Electrodynamic

Electrodynamic actuators are very popular because the force or torque generated can be directly controlled by varying the current supplied. The basic electrodynamic actuator is made of three main parts:

i. The generator of the magnetic field (could either be in the form of an electromagnetic coil or a permanent magnet)

ii. The magnetic flux conductor (the magnet core or the iron circuit)

iii. The electrical conductor (which forms the coil and winding)

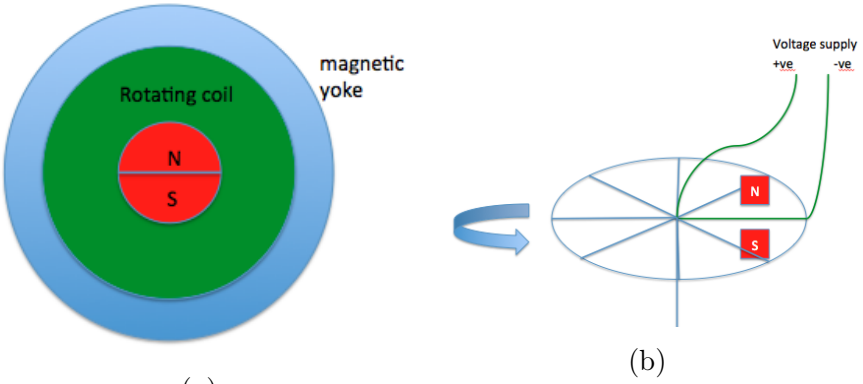

Figure 2.67: Electrodynamic actuators in the form of (a) Rotating coils and (b) Disc winding [100]

These actuators operate based on Lorentz law. Equation 2.7 represents the law where the force F acting upon the charges moving in a magnetic field is proportional to the current I, the magnetic induction B and the effective length of the conductor l.

$$F = I \times l \times B \tag{2.7}$$

Figure 2.67 shows two basic electrodynamic actuator designs for applying rotational force. The first ((a)) has a centre or core that is formed by two permanent magnets, which is concentrically within a layer of conductor coils. When current is supplied to these coils, a force as a result of the magnetic field induced produces a rotary motion of the coils.

Alternatively, a disc winding design can be used to produce a similar effect. Figure 2.67(b) shows a disc with wires that connect the disc edge with the disc centre. One of these wires is connected to a power supply source and is positioned in a magnetic field created by two permanent magnets above and below the disk. As the current flows through the conductor wire, the magnetic induction will produce a force that pushes the wire laterally in one direction. The wire will then revolve around the disk centre before experiencing the same force when it passes under the permanent magnets once more. This repetition will create a rotary motion of the disk that can be used for applying haptic feedback.

Figure 2.69 shows designs for translational force actuators under the principle of electrodynamics. In Figure 2.69 (a), the permanent magnets form the moving compo-

Figure 2.68: Illustration for placing an actuator within the catheter hub

nent of the actuation. When current passes through the coil, the Lorentz force will push the magnets outwards in a linear motion. Figure 2.69 (b) shows a similar design with the main difference being that the coil is the moving component used.

Electrodynamic actuators are contact actuators. If they are to be used in a solution for the concentric occlusion problem, then they have to be placed in contact with the inner instrument somehow. Previous designs have placed the actuators for the inner instrument at positions past the distal end (furthest from the operator) of the external instrument placing but, as mentioned before, that approach has several disadvantages. A novel approach would be to place the actuator at the proximal end (nearest to the operator) of the instrument, as illustrated in Figure 2.68 where it will not intrude on the user's workspace. The location suggested here is in the hub or head of the external instrument or the catheter hub. This involves the development of an actuator that would be very small in size to fit inside the hub of the catheter or a casing at the tip of a mock catheter. If implemented correctly, it would be a solution to the concentric occlusion problem without any of the drawbacks of previous designs.

The development of such an actuator will not be trivial since there are many factors to consider. Firstly, is it possible to design and produce an actuator at that scale? Secondly, can the actuator provide the range of forces required to simulate haptic feedback in endovascular interventions? Thirdly, would the weight of the actuator in the catheter hub affect the feel of the catheter in an unrealistic manner? Lastly, how would the actuator be actively controlled and how will it be powered? All of these issues will need to be addressed if this approach is to be implemented.

2.5.2 Electromagnetic

Electromagnetic actuators are the most frequently used actuators in the industry, where their main use is in providing vibrotactile feedback in handphones. These actuators use magnetic energy that is stored in the components that conduct flux to initialise movement and displacement. The main components of these actuators are the magnet core and the air gap. In order to minimise the energy in the system, the air gap's

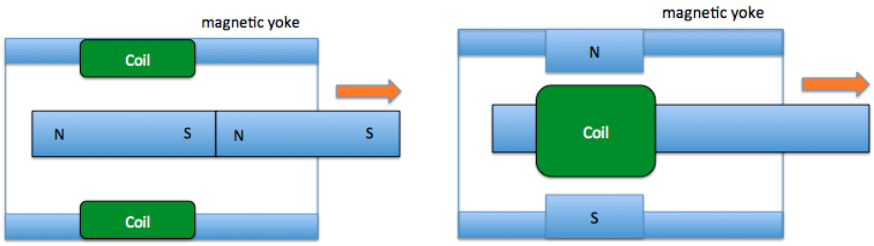

(a) (b)

Figure 2.69: Electrodynamic actuators with moving (a) permanent magnets and (b) coils [100]

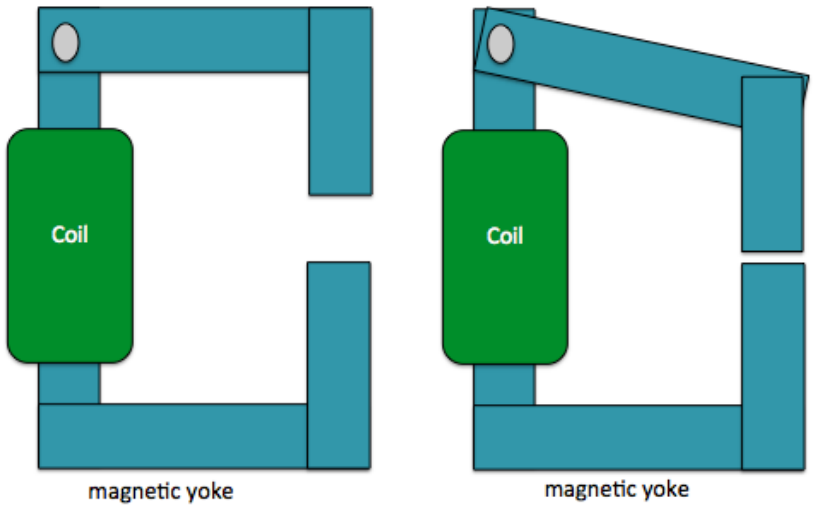

(a) (b)

Figure 2.70: Air gap reduction in electromagnetic actuators from (a) position to (b) [100]

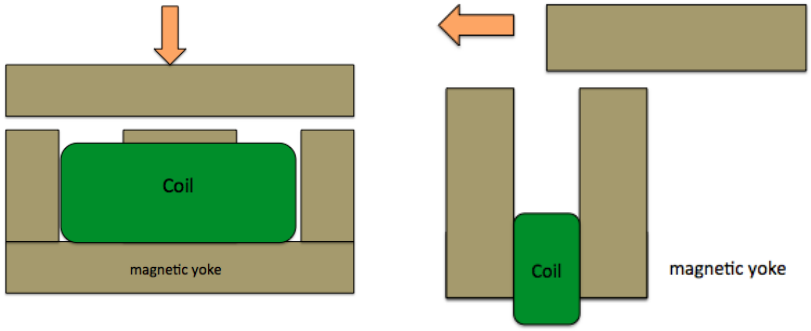

Figure 2.71: Electromagnetic actuation in (a) vertical and (b) longitudinal direction [100]

magnetic resistance is almost always reduced and this change can be used to achieve electromagnetic transversal and longitudinal displacement, as shown in Figure 2.70.

Some of the basic designs used for electromagnetic actuation are shown in Figure 2.71. The illustration in (a) shows an E-shaped magnetic core with a coil wound in the centre. The current flowing through the coil generates a magnetic flux circuit that flows through the core, although most of the flux would escape via the air gaps. When a ferromagnetic material is brought near, the flux will flow through the material and complete the magnetic circuit. The density of the flux through the material will create a magnetic force that attracts or pulls the new material to the core. This is the mechanism or technique that is used in electromagnetic brakes or locks. The magnetic force is dependent on several factors, such as the number and size of the coil winding, the material of the core, the exact magnetic properties of the new material and the amount of current supplied to the coil. Figure 2.71 (b) shows how different placement of the coil and core shape can have an effect in different force directions.

There are two possible approaches to using electromagnetic actuators for the task in mind. The first is to use them as contact actuators. As discussed previously, placing them in the catheter hub would be the most logical solution, although that comes with several challenges. The second is to use electromagnetic actuators in a non contact manner. The concept here is to place a strong electromagnet in contact with the non ferromagnetic external instrument so that it would exert a strong attraction force on the ferromagnetic inner instrument. For this concept to work, several factors need to be controlled and set. Firstly, the electromagnet must be sufficiently powerful to attract the

inner instrument with enough non contact force. Secondly, the inner instrument must be strongly ferromagnetic so that it would be sufficiently attracted by the electromagnet. Thirdly, the 'wall gap' between the electromagnet and the inner instrument, represented by the wall thickness of the outer instrument, must be minimised to maximise flux flow through the inner instrument.

The second factor raises several important questions. How many guidewires are ferromagnetic ? Ferromagnetism studies done on guidewires used in similar applications (e.g. biopsies) show that most guidewires are ferromagnetic to an extent [101, 102]. This in turn raises the question whether the level of attraction or the magnitude of the magnetic force pulling on the ferromagnetic guidewire is sufficient to produce the feel of significant resistance that is the desired outcome of this conceptual approach. Lastly, if the guidewires used are found to be non ferromagnetic, would it be possible to create a "mocked up", ferromagnetic version of the guidewire while maintaining its "feel", compliance and torque ? This question could only be answered by conducting discussions with guidewire manufacturers such as Terumo Inc., which is considered to be a possible approach should this conceptual technique show potential for success after further testing. Despite all the uncertainties mentioned, the non contact nature of this approach makes it one worth investigating.

2.5.3 Piezoelectric

The use of piezoelectric materials as actuators is still relatively recent. Their name is taken from the Greek word 'piezin', which means to press. They are called so because, when these materials are pressed, they displace charge which results in a dipole through what is called the "reciprocal piezoelectric effect". The inverse is also true. When a voltage is applied to a piezoelectric material, it becomes mechanically deformed along the crystal's orientation. This is called the "direct piezoelectric effect". This effect is illustrated in Figure 2.72.

There are two main types of piezoelectric materials: monocrystals and piezoelectric ceramics. The latter have less long term stability and are more prone to pyroelectricity. An example of a monocrystal is quartz and a common piezoelectric ceramic is barium titrate. Piezoelectric materials in general are direction dependent. When designing one for actuation, the direction of the electrical field and the angle between the desired movement direction has to be considered, together with the plane of polarisation.

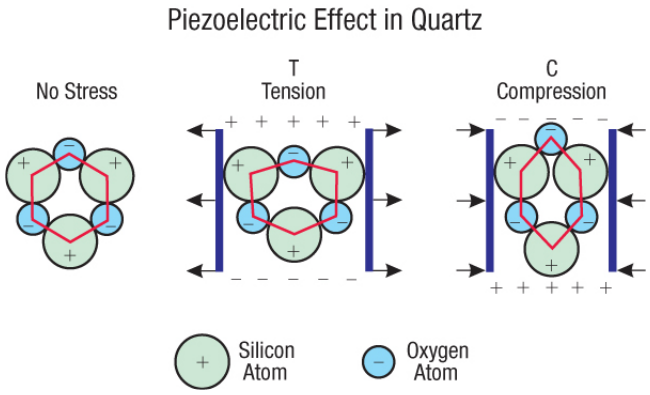

Figure 2.72: Illustration of piezoelectric effect in quartz [103]

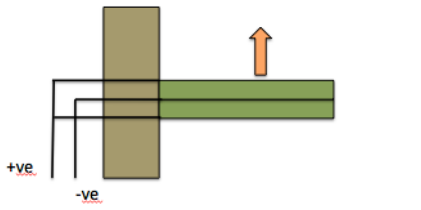

(a)

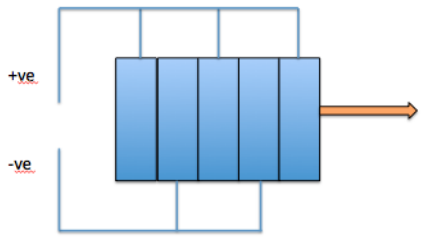

(b)

Figure 2.73: Basic design for piezoelectric (a) Bending actuator and (b) Stacked actuator [100]

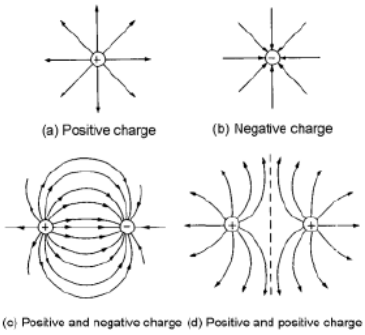

Figure 2.74: The interaction between charges of the same and opposite polarity [104]

Figure 2.73 shows the design of some of the common piezoelectric actuators available today. Figure 2.73(a) shows the bending type piezoelectric actuators which uses the bimorph principle. These actuators are made up of two active layers and use comparably low control voltages to produce large displacements. In both designs, when voltage is applied, the piezoelectric material will bend resulting in displacement. The stacked actuator design shown in Figure 2.73(b) is useful for producing a longitudinal piezoelectric effect. With this, several ceramic layers of opposite polarity are stapled above each other with a layer of contact electrodes. When voltage is supplied to the electrodes, the stacked materials will bend resulting in an accumulated force or displacement in the direction of F. Stacked actuators, however, need much higher voltage to drive that ranges in the hundreds.

Piezoelectric actuators are contact actuators and as such need to be in contact with the inner instrument at some point. It is suggested that a piezoelectric actuator can be placed in the hub of the catheter as mentioned previously. In fact, the piezoelectric actuator could be the most suited for such application as it does not have any moving parts, except for the actuator itself. However, there are still issues to be considered such as the cost of developing such an actuator as piezoelectric materials are still relatively expensive. Aside from that, the range of forces it produces during actuation needs to be investigated to ensure that it meets the requirements of the task. There is also the challenge of preparing a power source and controller for its activation in a way that does not affect the realism of the task during simulation.

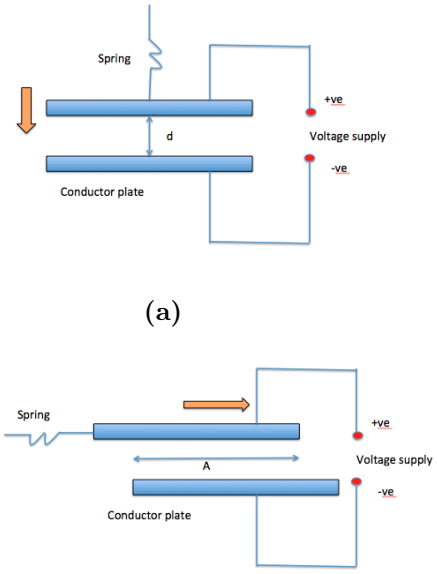

Figure 2.75: Basic design for electrostatic actuation (a) in the same direction as the electric field and (b) normal to the electric field [100]

2.5.4 Electrostatic

Two different charges sharing a space or area produce an electric field E, which in turn generates a force F that acts on the charges.The direction of the Force depends on the polarity of the charges as shown in Figure 2.74. On the other hand, its magnitude is proportional to the two charges' magnitude $Q1$ and $Q2$) and inversely proportional to the distance between them, r as described in Equation 2.8

$$F = \frac{k \times Q1 \times Q2}{r^2} \tag{2.8}$$

Some of the basic designs used in electrostatic actuators are shown in Figure 2.75. As seen in Figure 2.75 (a), two plates are placed parallel to each other. One of the plates is bound to a spring, while the other is fixed to a position. Displacement of the unfixed plate in the direction of the electric field would produce the actuation action, but that would require work. The work required to do so is proportional to the charge magnitude Q, and the amount of voltage supplied to the plates U as represented in Equation 2.9. This results in a force that would act against the pull of the spring to cause the desired displacement.

(a) (b)

Figure 2.76: Effects of the bending actuator (a) before activation and after (b) after activation] [100]

$$W = \frac{1}{2}Q \times U \tag{2.9}$$

The design in Figure 2.75 (b) is similar to that of Figure 2.75 (a), but results in displacement in a direction that is normal to the electric field. This is because the unfixed plate is attached to the spring on its side, which means that the distance between the plates is a constant. The changing variable now during actuation is the amount of surface area that they share as this influences the number of charges that are involved. In Figure 2.76, the parallel plates are replaced by electrodes. The uppermost layer is made up of a flexible counter electrode fixed to one end, and the bottom layer is made up of a regular counter electrode. A layer of insulation separates the two layers. The flexible electrode layer is fixed to one end and specially designed to form a wedge shape when it is not activated. Once activated, the flexible electrode would become rigid and straighten up, thus causing the displacement for the actuation.

Electrostatic actuators are non contact actuators. If the inner instrument was carrying charge, then, by placing a surface plate with charges of the opposite polarity nearby, the electrostatic attraction force generated should cause actuation on the inner instrument. Changing the polarity of the surface plate could produce the opposite effect. However, for this approach to be feasible, the inner instrument needs to not only be a conductor, but also be conducting sufficient current to have the required number of charges. As mentioned previously, it is not recommended to have the operator handling a live wire during simulation as it would be an unnecessary risk. Also, supplying the inner instrument with power is an issue which may negate the advantages of its non contact actuation.

2.6 Chapter Summary

This chapter opened with a concise introduction to the core skills in endovascular interventions and the tools involved. While it is recognized that the development of a Cognitive Task Analysis (CTA) and its validation would be the ideal method of studying these skills, this challenging and time consuming approach was not considered feasible due to the constraints of this project. Instead, this understanding was achieved through the review of literature (which includes a CTA for one of the stages of interventions) and the many meetings and interviews arranged with subject matter experts, with an understanding of the limitations of their subjective input. Nonetheless, useful details of endovascular interventions and tool manipulations were obtained with this approach. This was then reaffirmed through observation of the procedures being performed in the operating room and in the Cath Lab.

The chapter followed with a review of the designs of haptic interfaces used in previous and existing endovascular simulators. In this process, it became evident that every interface requires two systems. One for tracking the position and orientation of the instruments, and another for applying haptic feedback in order to emulate the forces felt during real life endovascular interventions. The two systems are controlled by a control unit that sends and receives signals based on input from the simulation software program. Upon further study, it became apparent that there are several shortcomings to the interfaces available today in terms of face validity, such as a delay in instrument detection and unnatural limitations to instrument range of movement, both of which disconnects the operator from simulation immersion. This underlines the need for a new design or approach. The remainder of the chapter studied the fundamentals of sensors and actuators as the key elements of the haptic interface device, exploring alternative conceptual approaches. From this examination, it became obvious that certain techniques employing optical tracking and electromagnetic actuators have the most potential. These techniques are further explored in the remainder of this thesis.

In the next chapter, the intricacies of haptics and how they are perceived by the operating interventionists are investigated. This includes a formal study on the type and range of forces involved, whose outcome is expected to influence the development process of the improved haptic interface.

3

Haptics and Endovascular Forces

3.1 Haptics

In the previous chapter, it was concluded that, in order to support the simulation of endovascular interventions, a haptic interface device needs to incorporate and integrate two different components: an instrument tracking system and a haptic feedback system. The requirements of the tracking system are straightforward and objective: it must be able to accurately and continuously detect both translational and rotational movement of the long, cylindrical tools. Failure to do so could result in a noticeable lag in the response of the virtual tools, negatively affecting the level of immersion or cause the loss of their positional information entirely. Furthermore, the tracking system must be able to operate whilst enabling the correct sequence of tool manipulation and exchange. These requirements are based on the acquired understanding of typical endovascular interventions and the instruments involved. Developing the haptic feedback system is much more challenging as the perception of subtle haptic effects is, by definition, very subjective. To better understand this challenge, the meaning of haptics and its main characteristics, both in generic terms, as well as in the context of endovascular interventions are studied in this chapter.

The term haptics originates from the Greek word "haptesthai", which means *to touch*. The sense of touch is naturally associated with the largest organ of the human anatomy: the skin. The human body is covered with biological sensors (receptors) located underneath the skin that inform the brain of various external stimuli (Figure 3.1). For example, if a hot iron comes into contact with the skin at whichever part of the

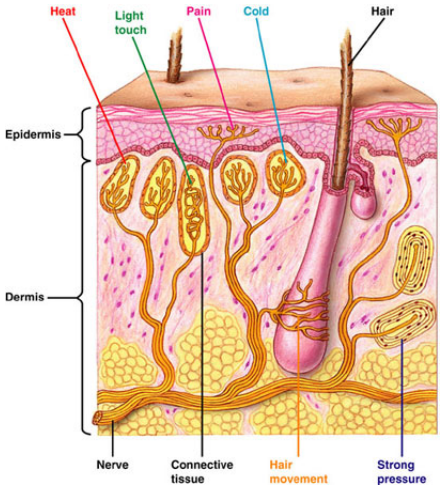

Figure 3.1: Biological receptors underneath the skin [105]

Figure 3.2: Shape of the human hand holding a glass [106]

body, the central reflex system will detect and respond to this instantly by pulling the contact region away from the iron. In the scope of this project, haptics refers to the multimodal touch senses and signals that are involved when objects are manipulated and explored by human hands.

The human hand is made up of 19 bones with as many frictionless joints that are covered by soft tissues and skin. The bones are attached via tendons to 40 intrinsic and extrinsic muscles that enable the hand to move with its 22 degrees of freedom [107]. There are receptors underneath the skin called proprioreceptors, which are located in the joints, muscles and tendons. Examples of these receptors include the muscle spindle

and Golgi tendon that measure muscle length and tension, respectively. When a person is holding a glass in his/her hand, as shown in Figure 3.2, the hand adapts to or forms itself around the glass. The shape of the hand around the glass represents a set of data points in terms of joint angles, muscle stress and length, and other biological parameters. This configuration is sensed by the receptors, and the relevant signals are then sent to the somatosensory region of the brain to be processed. The brain will then have an understanding of the weight, size and hardness of the glass, as well as its position in relation to the hands, arms and body. This represents the *kinaesthetic* portion of haptic feedback. The highest concentration of touch and thermal receptors is located at the fingertips. When holding the tall glass, these receptors tell the brain about the smoothness of the glass surface, the roughness of any markings, and the coldness of the glass to the touch. These represent some of the *tactile* information sent to the brain. Thus, the *kinaesthetic* and *tactile* elements combine to make up haptic feedback. All exploratory and manipulation tasks require a degree of both types of feedback.

In the haptic interface designs reviewed in Chapter 2, the main haptic feedback effect produced is the translational resistance effect. During simulation, when the instrument enters a vessel with a narrowing or stenosis that reduces lumen diameter to be smaller than or close to the diameter of the instrument, an actuator will apply force to the real life instrument, making it more difficult to advance and/or withdraw it. Similarly, the review also included actuator designs to resist rotational movements although to a lesser extent. However, there are several unanswered questions, such as how are these effects triggered during real life interventions ? Furthermore, what is the range of forces involved and would the range vary significantly according to the patient and / or anatomy?

Ideally, such questions would be answered through a combination of in vivo force measurements and a validated Cognitive Task Analysis (CTA) similar to the work done in [30] and [29], respectively. Such an approach presents significant challenges (specialist instruments to enable force measurements, access to patients, ethical approvals, etc) that by themselves would constitute a worthy area of research. As the focus of this work is the development of haptic interfaces to support the simulation of endovascular interventions, and recognising the time constraints of a PhD project, it was decided to instead review the literature and consult expert interventionists through an online questionnaire and experimental study.

Figure 3.3: The physical vascular model made from PVA [108]

3.2 Haptic Feedback in Endovascular Interventions

In [108], the presence of different forces (haptic effects) felt during endovascular interventions are discussed. The first force is described as: "When pushing or pulling the guidewire or catheter inside a small diameter blood vessel or inside a narrow passage or stenosis, the rubbing on the vessel wall causes a friction force". This description resembles the translational resistance effect mentioned earlier. On the other hand, the second force is described as: "When passing curves, the pre shaped tip of the catheter is bent to facilitate the navigation of the tools inside the vessels. The result is an elastic force on the instrument", which is similar to the effect of rotational resistance. They also claim that "In IR (interventional radiology), forces and torques estimated for a 5F catheter through a series of lab experiments, are in the range of $\pm$ 1.5 N and $\pm$ 4.5 mNm. Force and torque resolution shall be of $\pm$ 0.02 N and $\pm$ 0.04 mNm, respectively to meet human sensory system".

In order to study the effects and magnitude of each force type, the authors of [108] proceeded to build a physical vascular model made of Polyvinyl Alcohol (PVA) (Figure 3.3). A fibre optic gauge sensor (Figure 3.4) was then used as a mock catheter inserted within and navigated through the model. All of the force readings detected were recorded and plotted against time. Unfortunately, the PVA vascular model was very deformable, which caused the gauge to puncture through the physical arteries numerous times, limiting the number of tests that could be conducted. The resulting data (Figure 3.5) indicates that the magnitude of the force involved ranges from -70 to 85 mN, with the negative force representing the instance where the gauge penetrated

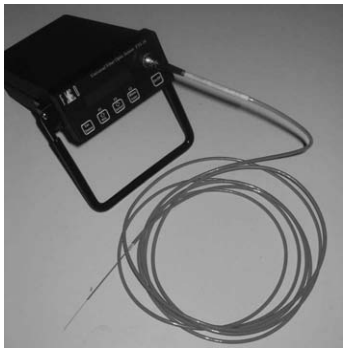

Figure 3.4: The fibre optic gauge used to measure forces inside the model [108]

the model.

Nonetheless, the fibre optic sensor does not have the same rigidity as a catheter and the elasticity of the PVA model is also different from that of actual arteries. Therefore, a separate test was performed in order to relate the rigidity of the gauge to a catheter using the setup shown in Figure 3.6 (a). The result was a Force vs Displacement plot (Figure 3.6 (b)) which showed that the catheter is roughly five times more rigid than the gauge, indicating that the force magnitude would need to be five times larger, thus suggesting that the catheter in the PVA model would have a maximum operating force of 425 mN. Also, considering that the average modulus of elasticity of a small artery is three times larger than the PVA model [108], this force would have to be further scaled by a factor of three to 1.275 N. This maximum force was then approximated to 1.3 N. Force and torque resolution were cited from [25]. Clearly, the ideal and most accurate way to obtain this information (forces resulting from instrument-vessel wall interaction) would be by using direct measurement through in vivo testing with specialised tools. However, as explained previously, such approach would be very challenging due to the constraints of this project. Therefore, while the data obtained from [108] lacks relevance to the real world anatomy and does not reflect the real world accurately, they are useful in providing a rough estimation of the magnitude of forces involved.

More recently, in [109], a master-slave robotic catheter teleoperating system was developed (Figure 3.7). The catheter movements performed by an expert are detected at the master unit and replicated with high fidelity at the slave unit where the catheter is inserted into a commercial endovascular physical phantom [110]. The vessel walls

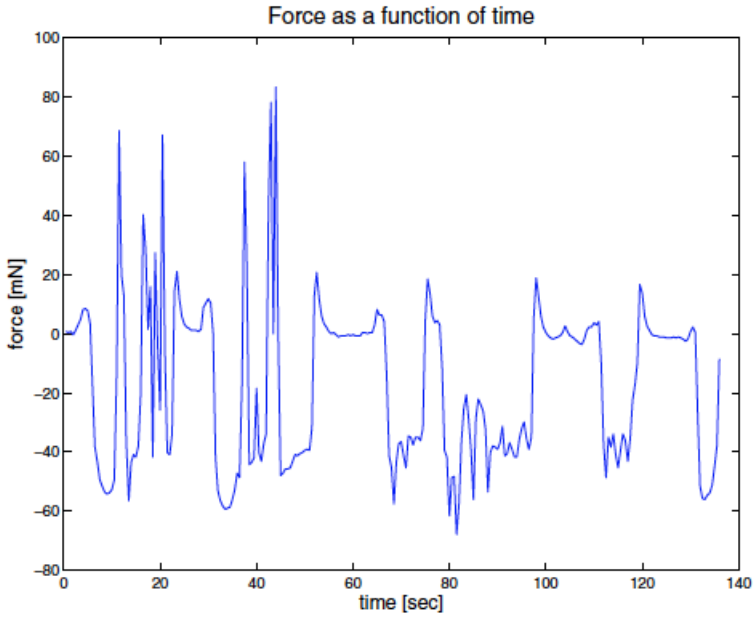

Figure 3.5: The force measurements taken from the fiber optic gauge [108]

of the phantom are made of specially manufactured materials that reportedly have the same elasticity as actual blood vessels.

Similar to the previous paper, [109] also reports the presence of a force that is caused by "friction between catheter and blood vessel". When the catheter comes into contact with the phantom vessel walls in the slave unit, the resistance forces are detected via a load cell and a fiber optic sensor. The forces are then recreated at the master side using 2 DC motors, one for each DOF. The unit on the master side is also fitted with a load cell sensor to record the forces used by the interventionist. The test results are shown in Figure 3.8 (a) and indicate that the average operating force is around 1.5 N. The forces recorded on the slave end, which are the same as those relayed to the interventionist at the master side, are shown in 3.8 (b). Lastly, Figure 3.8 (c) shows the forces as detected by the optical fiber sensor. These results suggest that the resistance forces measure around 2 N.

Similar to [108] and [109], the work in [111] aims to quantify the force interactions between the instruments and the vessel wall, specifically within the upper urinary tract. Figure 3.9 shows the rig used in [111] consisting of a computer, a motorised test stand and a charge coupled device (CCD) camera. The test stand consists of a motorised

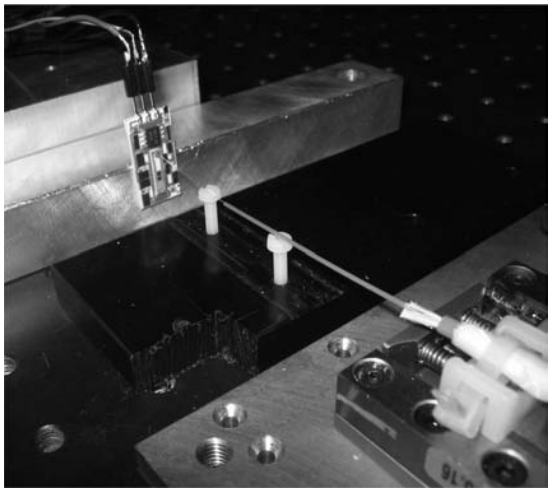

(a)

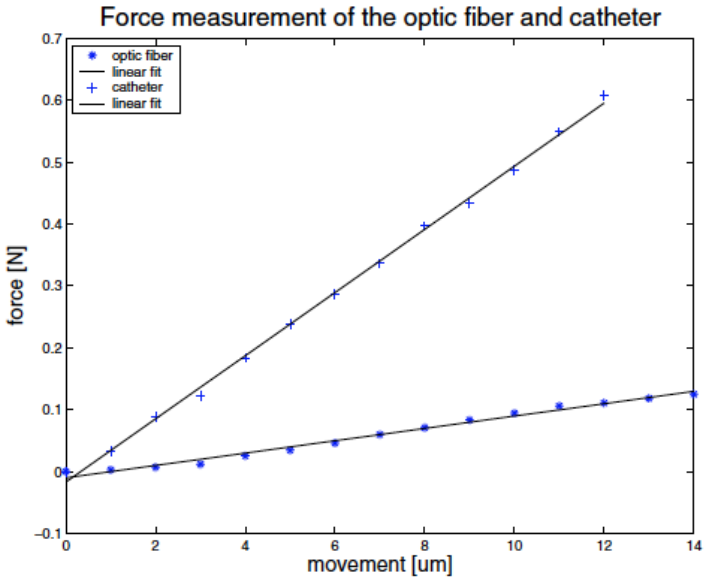

(b)

Figure 3.6: (a) The setup used to test the difference in rigidity between the catheter and the fiber optic gauge (b) The results of Force vs Displacement for the catheter and the fiber optic gauge [108]

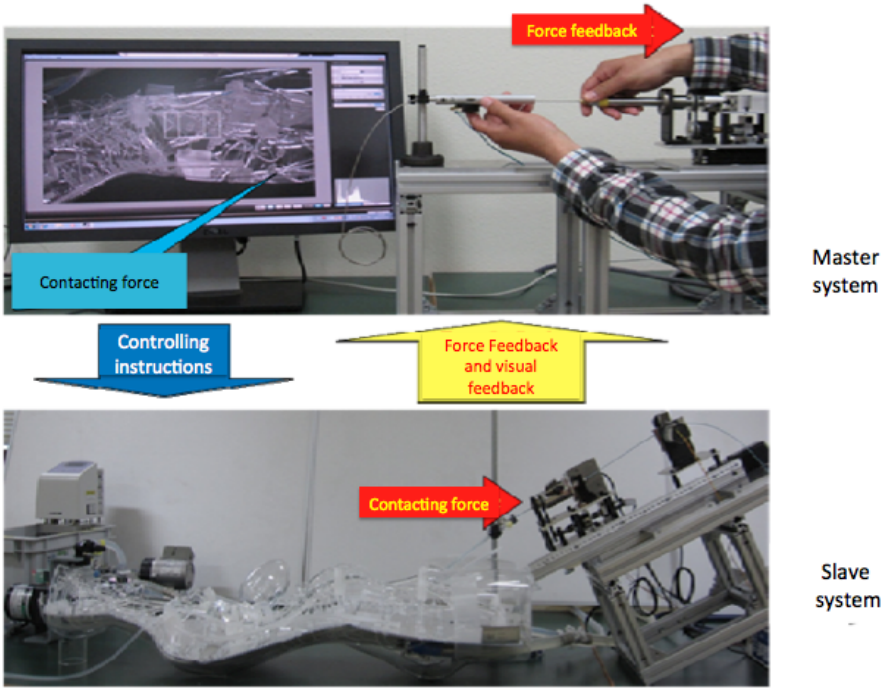

Figure 3.7: The master-slave catheter teleoperation system [109]

instrument (guidewire/catheter) driver and a path for the instruments' advancements. The path has three stages designed to recreate the three main types of obstacles typically experienced when pushed up the urinary tract. In the first stage, the instrument path is straight and clear. This stage is fitted with force sensors to measure axial forces applied by the instruments. In the second stage, the vessel becomes more tortuous. A CCD camera is placed to capture the movements of the instruments through the tortuous vessel pathways from above. Its purpose is to measure the position of the wire in relation to the closely spaced markers on the surface of the pathway. Using a discrete, mechanical model, the configuration of each point mass can be used to compute the force applied to each point mass and the transverse forces applied to the model walls (Figure 3.10). Finally, in the third stage, the pathway is obstructed by a plastic ball to emulate a stone obstruction. Force sensors are also attached to this stage to obtain an objective measurement.

Unlike [108] and [109], the modeling and measurement approach in [111] allows actual instruments to be used in testing. The test includes the use of six guide wires

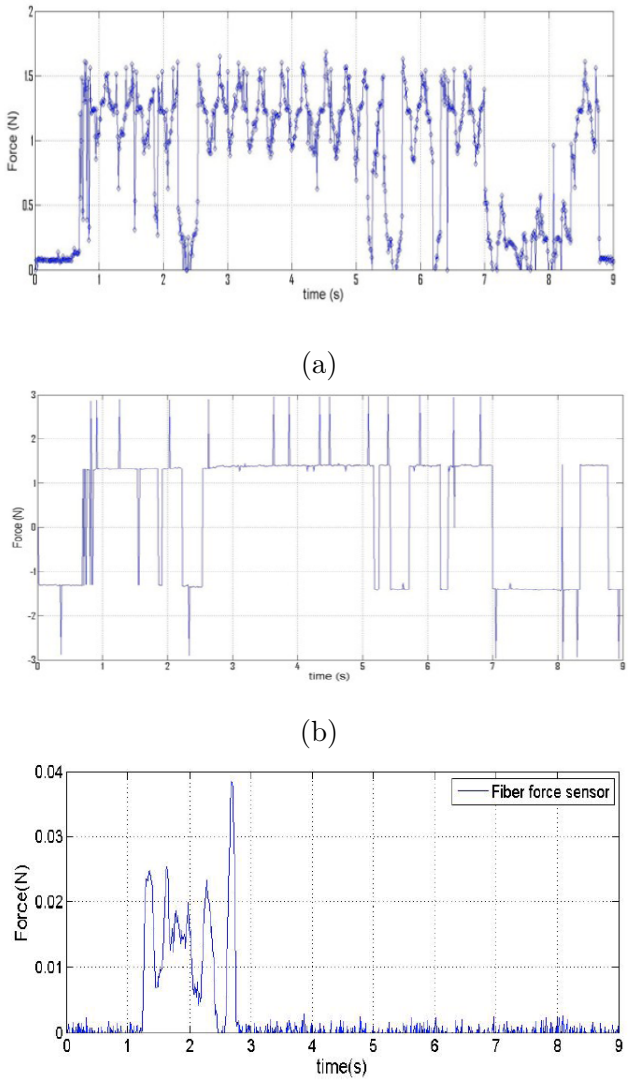

Figure 3.8: (a) The force measured at the operator's hand (master) (b) The force output measured at the slave system (c) The recorded force of catheter and vessel wall interaction [109]

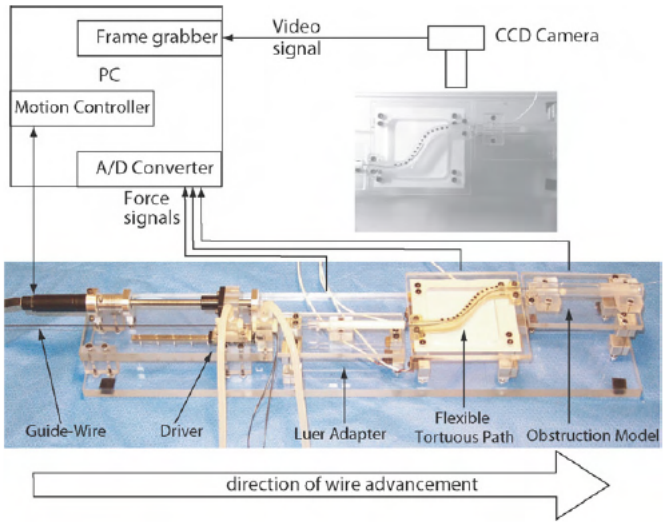

Figure 3.9: Guidewire and catheter test stand from [111]

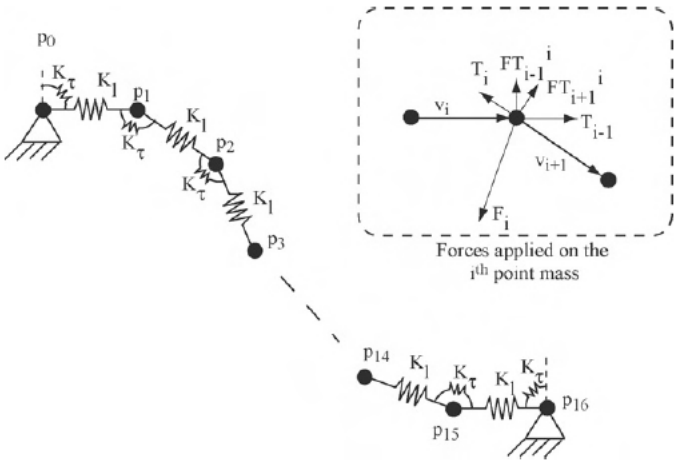

Figure 3.10: Tortuous path elastic model from [111]

that were chosen based on the estimation that they are frequently used for urological procedures. These are the HydroGlide from Bard, the Glidewire with straight tip from Boston Scientific, the Lubriglide from Boston Scientific, the Sensor from Boston Scientific, the Hiwire from Cook Urological and the PTFE coated guidewire from Cook Urological. Recognising the guide wires would perform differently when advanced individually compared to when advancing to support a catheter, the tests performed includes both instrument configurations: A lubricated test involving a single guidewire and a catheter-over-wire lubricated test. A 6 Fr "open end tapered tip urological catheter" from Cook Urological was used for the latter. A prototype everting film catheter from Percutaneous Systems Inc., which does not require a guidewire, was also tested. Each of the tests were performed 25 times for each wire type and catheter combination.

The results of measured axial forces and radial forces are shown in Figure 3.11 and Figure 3.12. For the obstruction model, the force exerted is found to be between 0 - 1.4 N and for the tortuous path, the force ranges between 0 - 2 N. The transversal forces exerted on the tortuous path are estimated to be between 0 - 3 N. The HydroGlide wire from Bard and the PTFE coated guidewire were highlighted as the best performers in terms of lowest axial and transversal force exertion, respectively. The everting film catheter by Percutaneous Systems was found to be the best performing catheter in both aspects. However, the authors in [111] summarized that there is not an overall "best" or "worst" instrument, but instead, certain instruments are better suited for certain procedures than others.

The literature discussed in this section presented a basic understanding and examination of the resistance haptic effects that exist during endovascular interventions. Their research and experiments indicate that the these effects involve forces in a range of 0 - 2N, although this was estimated using a series of approximations and assumptions which potentially imply a wide margin of error. Based on this review and initial informal discussions with subject matter experts (SMEs), an online survey and experimental study was then conducted to investigate these effects further. The following sections will present and discuss the findings obtained.

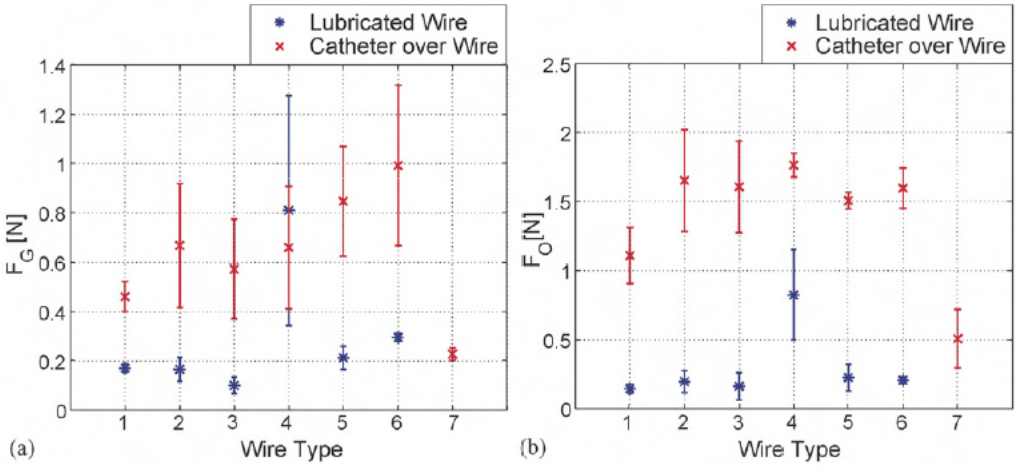

Figure 3.11: Axial forces acting on the model wall by the instruments in the (a) obstruction stage and (b) tortuous path [111]

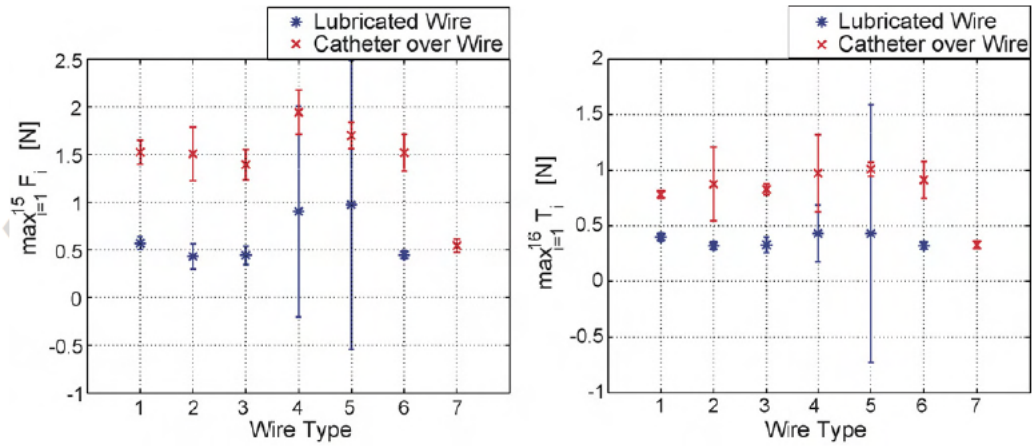

Figure 3.12: (a) Transversal forces exerted on the tortuous path and (b) Stress induced in each segment of the tortuous path [111]

3.3 Online survey

The primary objective of the online survey was to elicit the type of haptic effects or tactile sensations perceived during endovascular interventions, and their characteristics. To achieve this objective, several assumptions were made:

i. Upon insertion into the human body, the instruments can experience physical changes due to the increase in environment temperature. For example, guidewires with Nitinol (45-50% Titanium & 50-55% Nickel) cores have the special characteristics of being superelastic and having shape memory effects [112]. It would be able to recover its original shape if it is plastically deformed at a low temperature. Thus, when it is deployed and exposed to body temperatures, it would be able to return to its expanded and deformed shape. As a result, these alterations can reduce torque and change the amount of resistance felt when passing around tortuous vessels. In the survey introduction, this is intrinsically relayed to the participants through the context provided, which asks them to take into account that the instruments are "within the human vascular system, traveling from the insertion point (eg. femoral artery) to the target vessel (eg. renal artery)".

ii. Advancing instruments into a 'vessel narrowing' or 'narrowed vessels' indicates that the instrument is moving into a vessel with a lumen diameter that is smaller than or close to the diameter of the instrument, which should generally result in a resistance effect. This information was relayed to the survey participants by an accompanying illustration, (Figure 3.14), which shows the instrument being advanced into a vessel narrowing (due to the lesions) with a lumen diameter that is smaller than the diameter of the instrument.

iii. The term 'tortuous vessels' refers to vessels that are assumed to be inherently tortuous and would maintain its tortousity as the instruments are passed through it. This would often occur when the instruments used do not have a sufficient level of stiffness to cause the vessels to straighten as illustrated in Figure 2.2. This was illustrated by the accompanying figure (Figure 3.13), which showed the instrument being deformed (from its natural shape) as it passes through the tortuous vessel and not causing the tortuous vessel to straighten instead.

iv. It is assumed that the term 'occluded vessels' refers to vessels that are occluded due to longstanding fibrotic material and not due to recently formed soft thrombus. Often, the former can produce high levels of resistance to instrument advancement, while the latter would have much less of an impact on the instruments. The type of fibrotic material was suggested to the participant by the accompanying figure (Figure 3.14), which shows that the lesions/plaque forming within the vessel are sufficiently hard to deflect the instruments into a narrowing and is not easily dissolved/displaced by instrument insertion or dissection. A careful operator should minimize force and the resultant risks of dissection.

As mentioned previously, informal interviews with several interventionists (3 cardiologists, 3 interventional radiologists and 1 vascular surgeon), as well as observations of real procedures performed in the Cathlabs at Hammersmith Hospital and St Mary's Hospital in London, and the review of related literature presented earlier, provided useful details about the two types of resistance forces.

Translational Resistance

This effect is generally defined as feeling that the pushing/pulling movement of the instrument is being restricted or resisted by a certain force. Such force or resistance could be due to intrinsic or extrinsic conditions. Intrinsic resistance is the result of the instrument being bent or out of its initial shape. Guidewires and catheters are highly flexible but, when deformed, they will automatically tend to regain their initial shape and this may cause a build up of inner torsion and tension. This effect is most obvious when the instruments are inserted into a tortuous pathway that causes them to loop or distort (Figure 3.13). It is also more apparent in stiffer instruments. The feel of resistance in this context is due to the stored tension, which may also result in a reduction of controllability of the instrument. An example of this is when advancing the instrument by a certain amount at the proximal end (closer to the operator) results in only a fractional translation of the instrument tip.

Similarly, translational resistance may also be caused by extrinsic conditions, namely, a narrowing of the vessel (Figure 3.14). If the instrument is of smaller diameter than a stenosis, generally, there will be no perception of physical interaction with the stenosis as the instrument passes through. However, if the wire or catheter is passing through

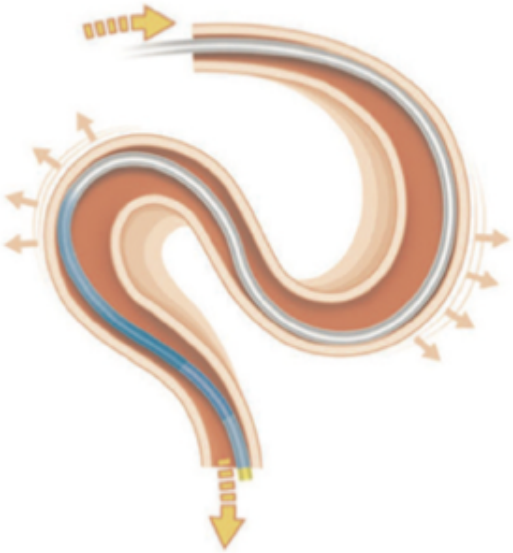

Figure 3.13: Illustration of vessel with tortuous pathway [113]

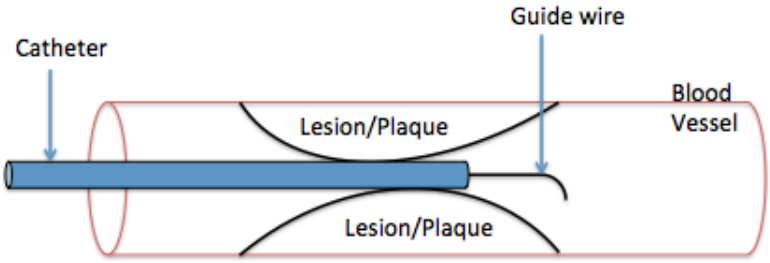

Figure 3.14: Illustration of vessel with narrowing/stenosis

a vessel or stenosis that is of equal or smaller diameter, there will be some translational and rotational resistance. This narrowing can be due to a natural reduction in vessel diameter (i.e. moving into a vessel with a naturally smaller lumen diameter) or by diseased vessels with stenosis and/or calcified lesions. Furthermore, the resistance strength would be directly proportional to the degree of the vessel narrowing (i.e. how much smaller the vessel lumen diameter is relative to the instrument diameter). I posit that the resistance felt increases as follows: Healthy vessel < Tortuosity < Stenosis < Calcified Lesion < Occluded Vessel. It is recognised that, whenever the interventionist feels an unexpected resistance, s/he will automatically and immediately cease advancing the instrument, requesting a fluoroscopic image to check its current position and the condition of the vessel. This is in order to reduce the risk of dissection of a wire into the layered elements of vessel wall anatomy, perforation of the vessel, or the dislodging of plaque that could later cause a blockage in other vessels.

Rotational resistance

Rotational resistance is similar to the previous haptic effect, with the only difference being that the resistance is felt in the rotational direction. I also theorise that, in the vast majority of cases, rotational resistance is caused exclusively by intrinsic conditions. When passing through tortuous vessels, the deformed instruments will store torsion energy as they naturally try to regain their initial shape (Figure 3.13). This energy resists the rotational movements performed by the clinician. Such resistance is detected by the sense of touch, and also visually since it reduces the controllability of the wire. For example, the interventionist would have to rotate the proximal end of the instrument multiple times to cause the tip to rotate once. It is assumed here that the rotational resistance due to external conditions such as friction resulting from the tool rubbing against the vessel is so small that it is unnoticeable. This is because the instruments are designed to have minimal friction, with some guidewires and catheters being equipped with hydrophilic coating for this purpose. This allows the instruments to move smoothly through the wet and slippery endoluminal environment created by the blood flowing through the vessels.

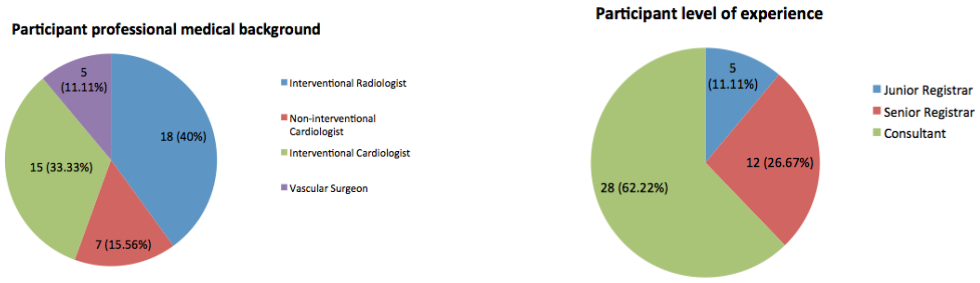

Figure 3.15: Distribution of participants in terms of (a) professional background and (b) level of experience

3.3.1 Questionnaire

The survey, as attached in the appendix, consists of two sections. The first section is for gathering participant information such as professional background and level of experience. The questions in this section are in the form of single response, objective questions, with the exception of one open ended question enquiring the number of years each participant has performed/assisted interventions. The haptic effects discussed above constitute a large majority of the questions in the second section of the survey. The questions are designed to confirm or deny the characteristics of the effects as described. Thus, a Likert scale system was utilised with the following options: Strongly Disagree, Disagree, Neutral, Agree and Strongly Agree. Based on the the feedback received from experts in the informal interviews, the inclusion criteria were that participants must have either undergone at least one year of endovascular intervention training, or performed/assisted as an interventionist in at least 100 endovascular interventional procedures. Further details of the protocol used for the study, approved by the Imperial College Research Ethics Committee (ICREC), can be found in Appendix A. In what follows, the responses gathered from the survey are presented and key findings discussed.

3.3.2 Survey Findings

The responses gathered from the survey are analysed using both descriptive and inferential statistics. For the former, the analysis includes examination of frequency and percentage response distributions, whilst for the latter, inferences on the consensus of

the population (i.e. interventionists) are made using the z-test, a test of statistical significance, with a significance level of 95%. The z-test is a hypothesis test for a proportion based on the z statistic. It returns a p-value dependent on the expected consensus in the population against the actual consensus found in the sample [114] [115]. Consensus here refers to the collective responses of Agree and Strongly Agree for each statement/question in the survey. The combination of categories for the purposes of hypothesis testing is a common practice as described in [116]. The test follows the standard normal distribution under the null hypothesis. Since the general hypothesis is: *"More than x % of interventionists Agree or Strongly Agree with the statement."*, the null and alternate hypothesis are:

$$\text{Null Hypothesis: P} < \text{x \%}$$

$$\text{Alternate Hypothesis: P} \geq x\%$$

The z-test is repeated for varying values of x to identify the percentage where the null hypothesis can be rejected. This will enable the estimation of consensus percentage within the population regarding a specific statement.

Participant Information

A total of 46 participants were recruited for the study. One participant was later withdrawn because it was discovered that her experience was mostly related to the early stages of endovascular interventions, such as needle puncture and initial vessel access. The distribution of the remaining 45 participants in terms of professional background is shown in Figure 3.15(a). They consisted of 15 (33.33%) Interventional Cardiologists, 7 (15.56%) Non Interventional Cardiologists, 18 (40%) Interventional Radiologists and 5 (11.11%) Vascular Surgeons. In terms of experience, 5 (11.11%) participants were Junior Registrars, 12 (26.67%) Senior Registrars, and 28 (62.22%) Consultants (Figure 3.15(b)). Figure 3.16 compares the minimum, maximum and mean years of experience of these group of participants. Junior Registrars had 1-3 years of experience (M=2.2), Senior Registrars 2-8 years of experience (M=4.58), and consultants 3-35 years of experience (M=15.1 years). However, the actual number of cases performed by the participant is significantly more important than the years of experience he/she has. As mentioned previously, an interventionist who has worked a minimum of 100 cases is

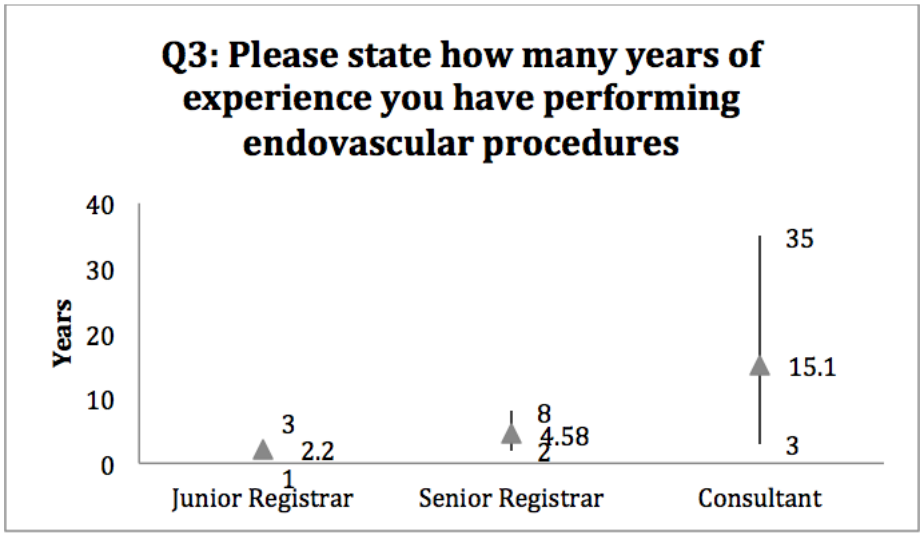

Figure 3.16: Minimum, maximum and mean number of green) years of experience for each group of participants

considered to have relevant experience in this study. In this aspect, there could be consultant interventionists that are relatively "inexperienced" in terms of case throughput.

Figure 3.17 shows the distribution of participants in terms of the type of training methods to which they have been exposed. 15 (33.33%) of the participants have trained purely on real patients without using any alternative training methods. 5 (11.11%) of the participants have complemented their real patient training with bench top model training only, whereas 9 (20%) complemented them with virtual simulator training only. A total of 16 (35.56%) of the participants have trained with both bench top models and virtual simulators, in addition to the real life training they have experienced. In the following sections, the responses to the questions regarding the haptic effects are analysed and discussed.

Translational Resistance

Figure 3.18 shows a diverging stacked bar graph of responses regarding translational resistance. Each bar corresponds to a specific question. Positive results are grouped in blue (strongly agree and agree) whereas negative results are grouped in red (strongly disagree and disagree) and are distributed right and left of neutral respectively. Bars

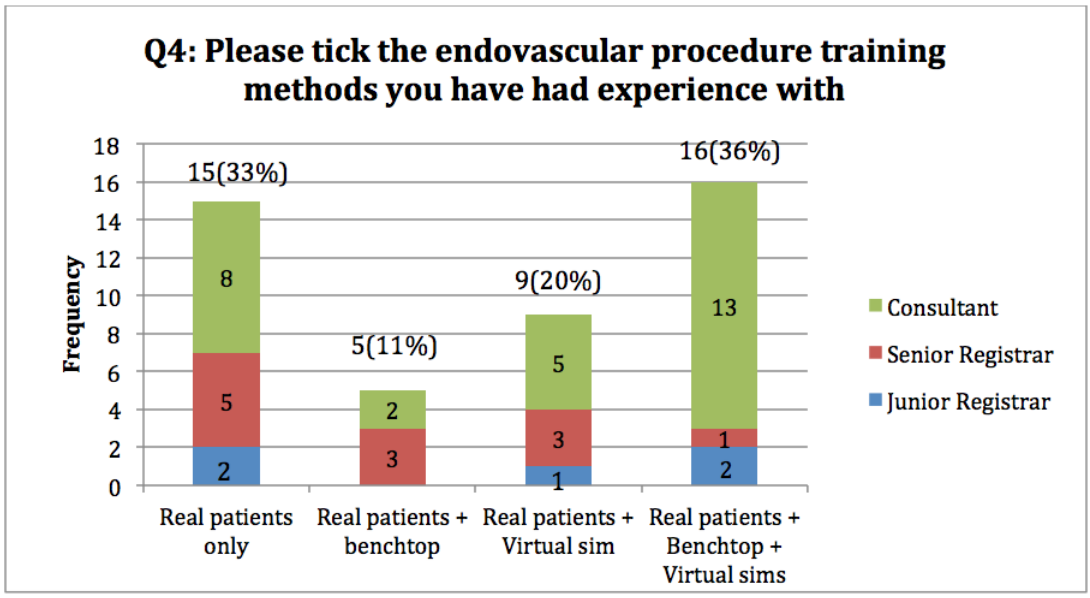

Figure 3.17: Distribution of participants in terms of experience with alternative training methods

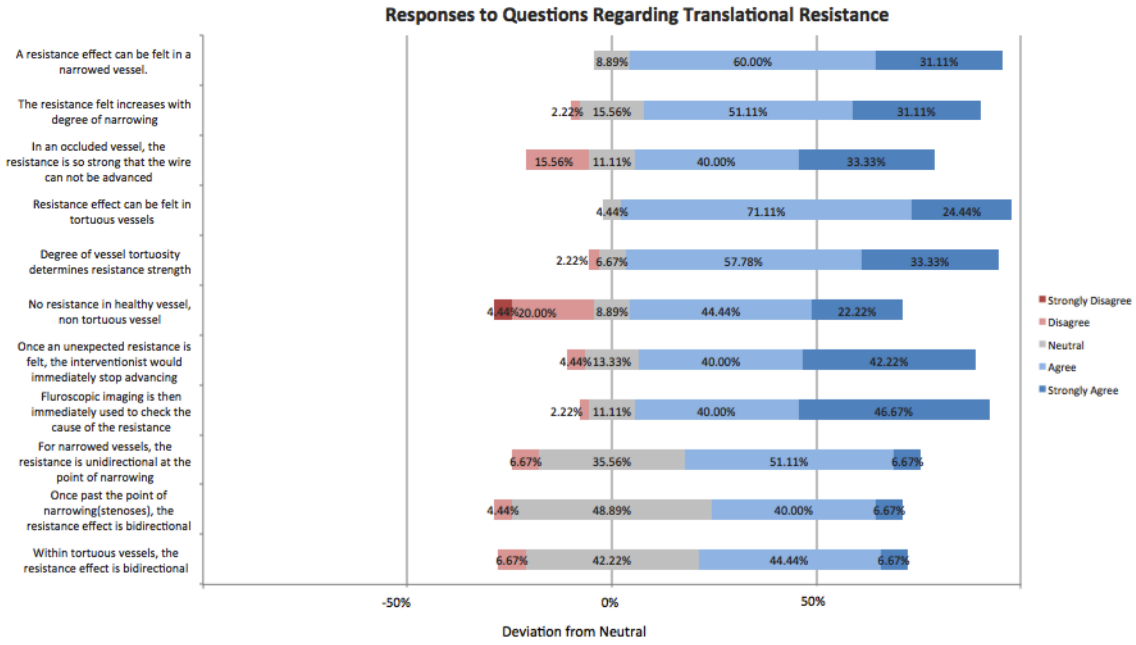

Figure 3.18: Diverging stacked bar graph of survey responses regarding translational resistance

are thus skewed in the direction of the overall trend. As can be seen, a majority of the participants, 27 (60%) agreed with the statement that a resistance effect can be felt when advancing the instruments through a narrowed vessel. A further 14 (31.11%) participants strongly agreed with the statement while the remaining 4 (8.89%) participants opted to be neutral in their responses. This resistance is said to increase with the degree of narrowing experienced by the vessel, as agreed by 23 (51.11%) participants and strongly agreed by 14 (31.11%). Only 1 (2.22%) participant disagreed as the remaining 7 (15.56%) responded neutrally. When the vessel becomes occluded, the resistance felt increases significantly and stops the instrument from being advanced further, as agreed by 18 (40%) participants and strongly agreed by 15 (33.33%) participants. It is important to note that the 7 (15.67%) participants that disagreed and the 5 (11.11%) that were neutral are 11 interventional radiologists and 1 vascular surgeon. This, and the fact that all of the participating Interventional/Non Interventional Cardiologists agreed with the statement, seems to suggest that vessel diameter might be a factor. Cardiologists operate on cardiac vessels, which are commonly smaller in diameter to the peripheral vessels more familiar to interventional radiologists and vascular surgeons. Thus, there is a higher probability of a cardiac vessel being completely occluded, preventing the instruments from advancing.

Aside from narrowed vessels, translational resistance can also occur in tortuous vessels as agreed by a majority of 32 (71.11%) participants and strongly agreed by 11 (24.44 %) participants, whereas 2 (4.44 %) participants responded neutrally. Similar to narrowed vessels, the strength of the resistance increases with the degree of vessel tortuosity as agreed by 26 (57.78%) participants and strongly agreed by 15 (33.33%) participants. From the remaining participants, 3 (6.67%) responded neutrally and only 1 (2.22%) disagreed. From the 45 participants, 20 (44.44%) participants agreed and 10 (22.22%) participants strongly agreed that no resistance is felt when advancing instruments through a healthy, non tortuous vessel. However, 9 (20%) participants disagreed with the statement and 2 (4.44%) strongly disagreed. A total of 4 (8.89%) participants were undecided and responded neutrally. Since almost a quarter of participants feel resistance even when advancing into healthy and non tortuous vessels, this highlights a possible limitation in the interpretation of "no resistance" in this question. As it was not stated, the participant could interpret "resistance" as the sensation beyond the

frictional effects of sheath or skin entry site or otherwise, thus producing the spread of responses seen here.

As many as 19 (42.22 %) participants strongly agreed and 18 (40%) participants agreed that the standard practice is to immediately stop advancing the instruments once an unexpected resistance is felt. However, 6 (13.33%) participants responded neutrally and 2 (4.44%) participants disagreed. The fact that nearly 18% of participants would advance the wire further even when unexpected resistance is felt is concerning since interventionists are extensively trained to stop in such cases. Assuming that all of the participants received correct training, these surprising responses could possibly be attributed to a misunderstanding or misinterpretation of the question.

Following the previous question, the next step is to obtain a fluoroscopic image to examine the cause of the detected resistance. This was strongly agreed upon by 21 (46.67%) participants and agreed by 18 (40%) participants. Only 1 (2.22%) participant disagreed and 5 (11.11%) others responded neutrally.

The survey then includes three questions that address the direction of resistance felt when manipulating the instruments. 23 (51.11%) of the participants agreed that resistance in narrowed vessels is only felt in one direction, i.e. the direction of instrument advancement leading up to the point of stenosis or narrowing and only 3 (6.67%) participants agreed. 16 (35.56%) participants responded neutrally to this statement, whereas 3 (6.67%) disagreed. Once past the point of narrowing (stenosis), however, 18 (40%) participants agree that the resistance effect is then bidirectional, and can be felt when both advancing and withdrawing the instrument. A further 3 (6.67%) participants strongly agreed with the statement while 22 (48.89%) participants chose a neutral response and 2 (4.44%) disagreed . In the case of tortuous vessels, the resistance effect is present for both instrument advancement and withdrawal, as agreed by 20 (44.44%) participants and strongly agreed by 3 (6.67%) participants. However, 19 (42.22%) participants responded neutrally to this statement and the remaining 3 (6.67%) disagreed.

As established earlier, the strength of the resistance felt through the instruments varies according to the level of vessel narrowing, which is dependent on the type of vessel pathology. In the survey, participants were asked to rank the strength of resistance felt in different types of vessels using a 1-5 scale system (1 - highest resistance; 5 - least resistance). Participants ranked healthy vessels to be the vessel type with the least

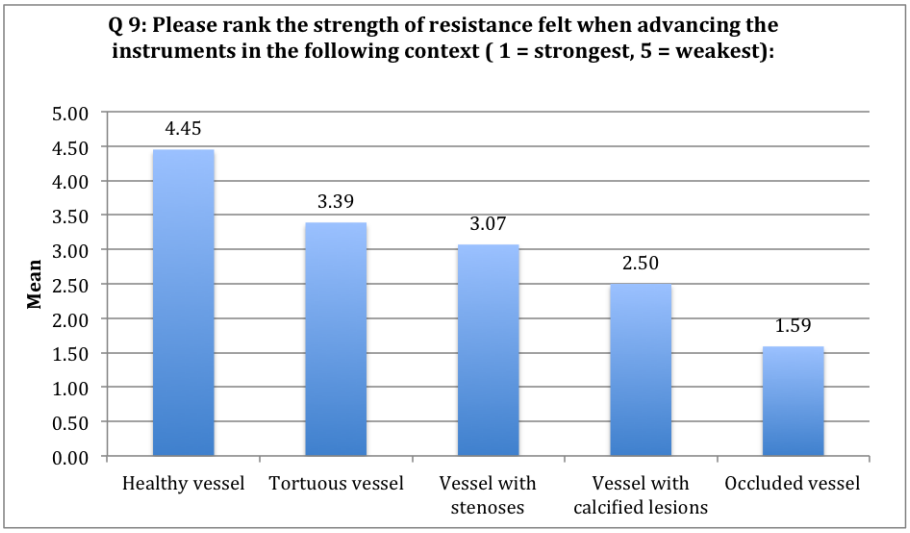

Figure 3.19: Ranking of resistance according to vessel pathology

amount of resistance (M=4.45) (Figure 3.19). The resistance feels more substantial in tortuous vessels (M=3.39) and increases slightly in vessels with stenosis (M=3.07). It grows stronger in vessels with calcified lesions (M=2.50) and is at a maximum in occluded vessels (mean=1.59).

Figure 3.20 and Figure 3.21 show the change in the p-values from the z-test for statements regarding translational resistance (Questions 1 to 11 based on Fig 3.18) as the expected consensus percentage is changed. From Figure 3.20, it can be seen that, since the p-values for statements 1, 4 and 5 are less than 0.05 when the expected consensus, $x = 80\%$, it can be inferred that at least 80 % of interventionists agree with each of those statements: there is a resistance felt when advancing instruments through a narrowed vessel (Question 1), there is a resistance felt when advancing instruments through a tortuous vessel (Question 4) and the amount of resistance depends on the degree of tortuosity of the vessel (Question 5). The other three statements from Questions 2, 3 and 6 only produce a p-value of less than 0.05 when $x = 70$ %, $x = 60$ % and $x = 50$ %, respectively. In other words, the null hypothesis is rejected at those values and it can be inferred that at least 70 % of interventionists would agree that the strength of resistance increases with the degree of narrowing (Question 2) and at least 60 % would agree that the resistance in a an occluded vessel is so strong that the instrument cannot be advanced further (Question 3). Also, at least 50 % would

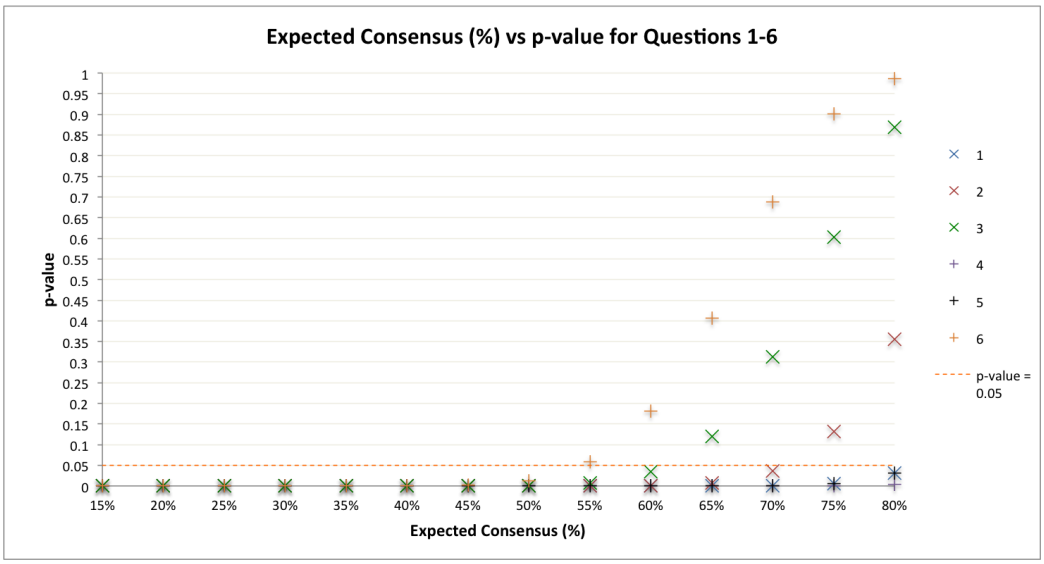

Figure 3.20: Expected Consensus (%) vs p-value for Questions 1 to 6

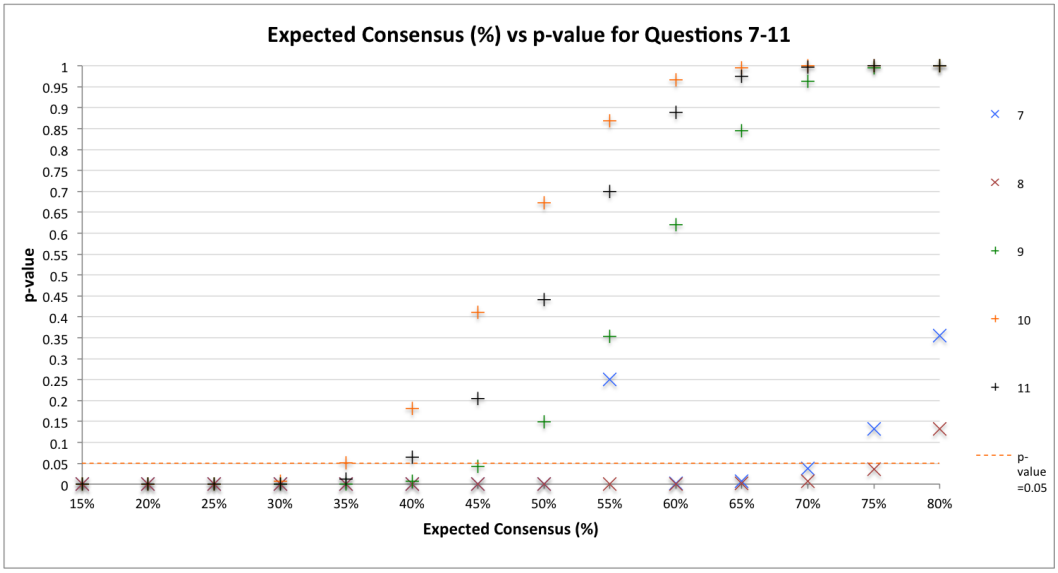

Figure 3.21: Expected Consensus (%) vs p-value for Questions 7 to 11

agree that there is no resistance felt in a healthy and non tortuous vessel (Question 6). From Figure 3.21, it is inferred that at least 70 % of interventionists would agree that instrument advancement is ceased as soon as an unexpected resistance is felt (Question 7) and that at least 75 % of interventionists would agree that fluoroscopic images are immediately obtained to check the cause of the unexpected resistance (Question 8). It can be further deduced that at least 45 % would agree that the resistance in a vessel narrowing is unidirectional, or felt only when advancing and not when withdrawing (Question 9), whereas 30 % would agree with the statement in Question 10, where the resistance is said to be present when advancing and withdrawing, once the instrument moves past the point of stenoses. Lastly, the statistical test suggests that at least 35 % would agree that the resistance effect applies in both directions (i.e. advancing and withdrawing) in a tortuous vessel (Question 11).

It is noted that there are certain known limitations to the survey and the conclusiveness of its findings; namely the small sample size and the questionable relevance of the participant's level of expertise. Nonetheless, there is statistical evidence suggesting a large consensus among the interventionists confirming the existence of the translational effect due to vessel narrowing and vessel tortuosity. Similarly, there is also evidence of a large consensus confirming that the strength of both effects would vary according to the degree of narrowing and tortuosity. However, it is deduced that there is less consensus regarding the details or characteristics of the translational resistance effect, such as direction of resistance, strength of resistance in an occluded vessel and the presence of resistance in a healthy non tortuous vessel. It is possible that there is less consensus in these statements given the general clinical context provided and the variability in the procedures and patients.

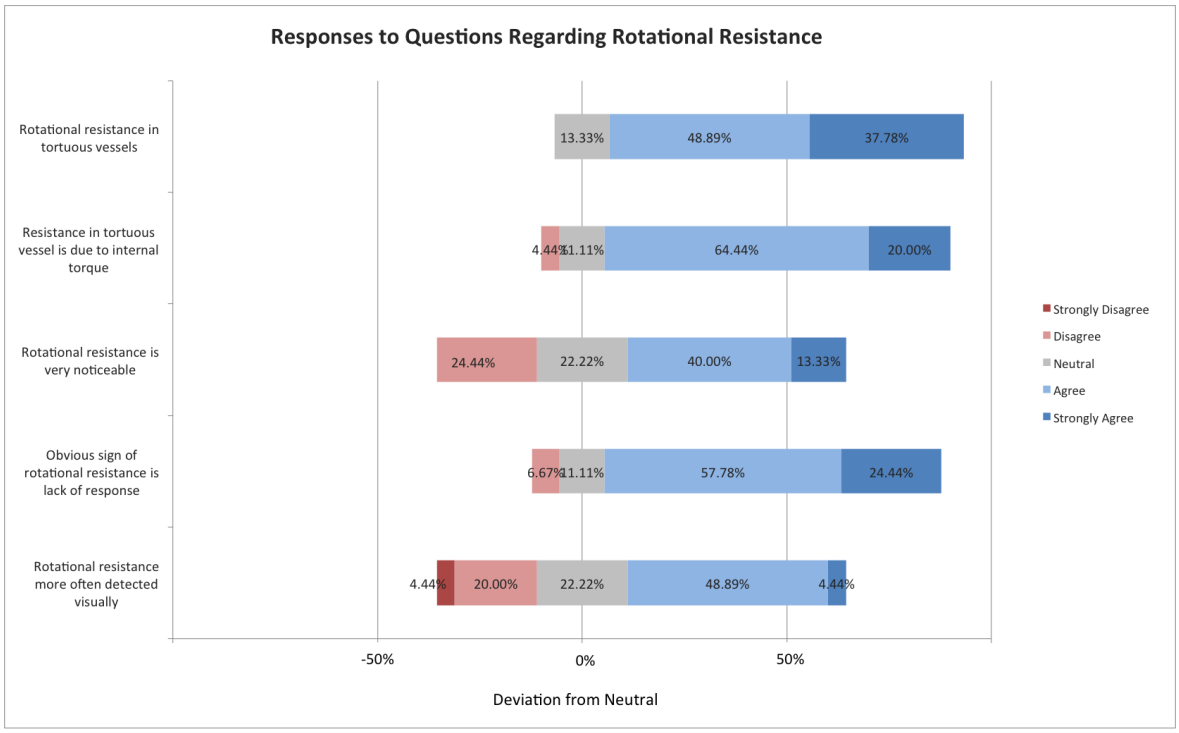

Figure 3.22: Diverging stacked bar graph of survey responses regarding rotational resistance

Rotational resistance

A diverging stacked bar graph of rotational resistance responses is shown in Figure 3.22. 22 (48.89%) participants agreed and 17 (37.78%) strongly agreed that there is a resistance felt when rotating instruments within tortuous vessels, while the remaining 6 (13.33%) responded neutrally. Furthermore, 29 (64.44%) participants agreed and 9 (20%) more strongly agreed that the rotational resistance is caused by torque that is stored within the instrument(s) as it is bent/twisted. From the 7 participants that replied otherwise, 5 (11.11%) were neutral, while only 2 (4.44%) disagreed. As many as 18 (40%) participants disagreed and 6 (13.33%) participants strongly disagreed with the statement that rotational resistance is not noticeable to the operator's touch. 10 (22.22%) participants replied neutrally and only 11 (24.44%) others agreed. This would suggest that rotational resistance can be considered to be haptically noticeable.

Rotational resistance can often be observed through fluoroscopic imaging as it might

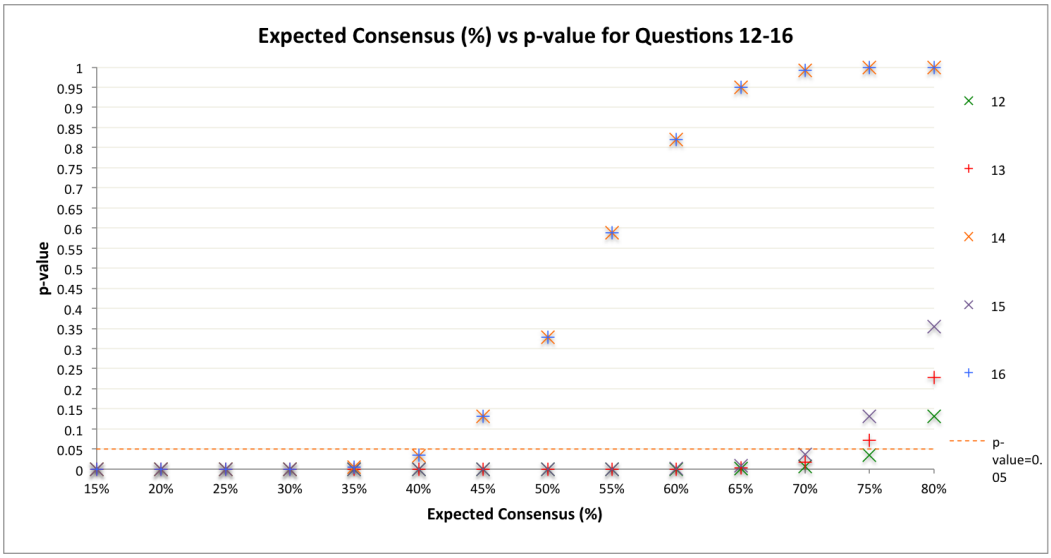

Figure 3.23: Expected Consensus (%) vs p-value for Questions 12 to 16

take several rotations at the proximal (closest to the operator) end of the instrument to visibly rotate the instrument tip slightly. This statement was agreed by 26 (57.78%) participants and strongly agreed by 11 participants (24.44%). From the remaining 8 participants, 5 (11.11%) responded neutrally and 3 (6.98%) disagreed. Following this, 22 (49%) of the participants agreed and 2 (4.44%) more strongly agreed that the rotational resistance is more often detected visually than through the resulting haptic effect. However, 9 (20%) participants disagreed and 2 (4.44%) participants strongly disagreed with this statement while 10 (22.22%) others remained neutral. This would suggest that the importance of the visual detection of rotational resistance might depend on the specific vessel. For instance, vessels with higher tortuosity may produce stronger resistance, which would then be first detected through the sense of touch rather than through sight.

Figure 3.23 shows the p-values for the z-test corresponding to statements regarding rotational resistance (Questions 12 to 16). From the figure, it can be deduced that at least 75 % of interventionists have consensus that rotational resistance is felt when rotating instruments within a tortuous vessel (Question 12). Moreover, at least 70 % of interventionists can be said to agree that rotational resistance exists due to stored torque within the instrument (Question 13) and a common sign of rotational resistance

is the loss of instrument response where the instrument needs to be rotated more to produce a rotation at its tip (Question 15). Lastly, at least 40 % of interventionists would agree/strongly agree that rotational resistance can be detected through tactile sensations (Question 14) although at least 40% agree/strongly agree that rotational resistance is more often detected by observing the instrument's movement pattern in fluoroscopic imaging than through those tactile sensations (Question 16). These findings suggest that there is generally large consensus on the existence, effects and causes of rotational resistance during interventions. However, the reduced consensus in statements comparing the importance of visual and haptic senses in the detection of rotational resistance could be due to the variability in the procedures and patients, as well as the lack of a specifically defined clinical context. When asked to compare the importance between translational and rotational resistance effects, a majority of 33 (73.33%) participants selected translational resistance as the more important between the two. Thus, for the remainder of this project, the aim of the haptic feedback system would be to focus on applying only translational resistance to the instruments during simulation, with developmental efforts for rotational resistance being reserved for future work. In the next section, an experimental study is conducted to estimate the range of forces involved to produce the desired translational resistance effect.

3.4 Resistance Force Range Experimental Study

Thirteen participants were recruited in this study, where each participant was asked to perform experiments using the custom rig shown in Figure 3.24. In the experimental setup, the guidewire was passed through both a horizontal channel and then into a vertical channel at an angle that allows the wire to extend downwards in a right angle. The aim of the study was to obtain an estimate of the range of forces that constitute the haptic presence of translational resistance in vessels of varying anatomy and/or pathologies. A known force is applied in the direction opposite to instrument advancement in order to provide the resistance effect. This was done by attaching calibrated weights (50g, 100g, 150g and 200g) to the proximal end of the instrument using the custom rig, allowing the weight to be attached at a 90 degree angle. As the participants advanced the instrument into the channel, they were asked to match the current level of translational resistance provided (through the weights) with that felt when navigating

Figure 3.24: The custom rig used for the weights force estimation test

through a specific vessel type, namely: healthy vessel, tortuous vessel, stenosed vessel, or vessel with calcified lesions (occluded). This test was repeated three times for each weight and three more times in the absence of any weight in random order. Participant responses were recorded through the survey included in Appendix C. Once again, the detailed protocol of the experimental study is also included in Appendix A.

3.4.1 Translational Resistance Experiment Findings

The responses of the participants are shown in Figure 3.25. Analysing vessel conditions individually, 39 (68.42%) responses agree that the 0g weight best represents the resistance felt in healthy vessels. For narrowed vessels or vessels with stenosis, 100g was chosen as the best representation of the resistance in narrowed vessels on 22 (40.00%) occasions. The mode weight for resistance in tortuous vessel was also 100g as it was selected 24 (42.50%) times. The 150g weight was chosen to be the best representative of the resistance in vessels with calcified lesions as it was selected 28 (50.00%) times. Lastly, the resistance in occluded vessels, which is expected to be the strongest, was associated with the 200g weight on 41 (72.41%) occasions.

Table 3.1 shows the calculated weighted average for each vessel type, together with the mode value of weights selected. It should be noted that the values presented here are

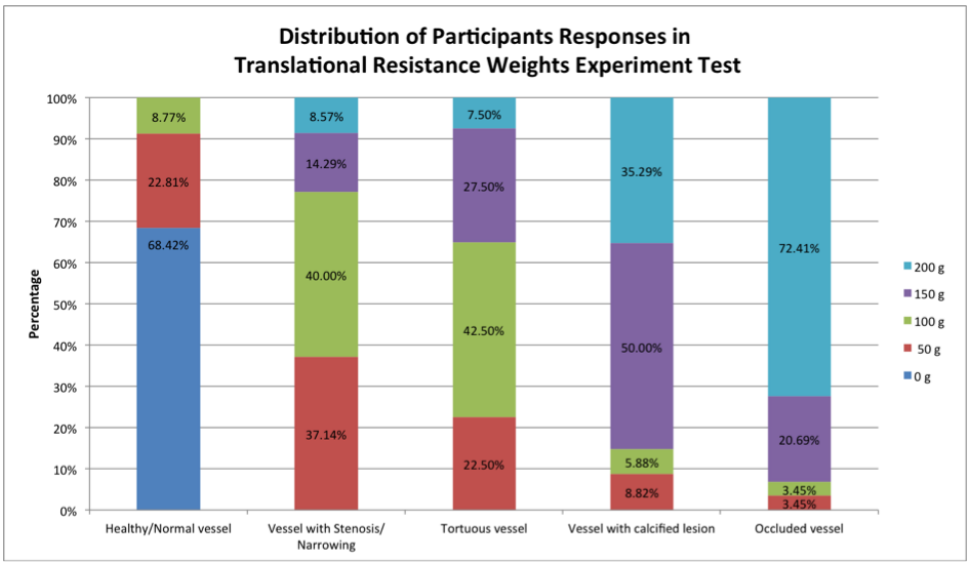

Figure 3.25: Responses matching experienced resistance with vessel condition

Table 3.1: The Mode and weighted average values of the estimated resistance for different vessel types

Vessel type	Mode weight (% voted)	Weighted average (g)
Healthy vessel	0 g (68.42%)	20.18
Narrowed vessel (stenosis)	100 g (40.00%)	97.14
Tortuous vessel	100 g (42.50%)	110.00
Vessel with calcified lesions	150 g (50.00%)	155.8
Occluded vessel	200 g (72.41%)	181.03

only meant to estimate the range of forces involved in translational resistance according to vessel type, recognising the limitations and subjective nature of the experimental study and a potentially wide margin of error for the values presented here. In healthy vessels, the mode value is 0g. This corresponds with the findings from the survey where 30 (66.67%) participants agreed that there is no resistance felt when advancing the guidewire and catheter within a healthy and non tortuous vessel. Conversely, the weighted average calculated for healthy vessels is 20.18g, corresponding to a subtle resistance that coincides with another finding from the survey where at least 11 (24.44%) participants indicated that there is some resistance felt in the instruments, even when passing through healthy and non tortuous vessels. For narrowed vessels or vessels with stenosis, the resistance felt is estimated to be around 100g based on a mode value of 22. The weighted average falls within that range with a value of 97.14g. The weighted average for tortuous vessels was calculated as 110g, although the mode value is 100g. It can thus be observed that, according to the weighted average, the resistance in tortuous vessel is slightly stronger than in narrowed vessels. This differs slightly from the responses of the survey suggesting that the strength of resistance due to vessel narrowing or stenosis is higher than the resistance due to vessel tortuosity (Figure 3.19), although there is only a small difference between the two mean response values (3.39 for tortuous vessels and and 3.06 for narrowed vessels). The mode weight value for vessels with calcified lesions is 150g and the weighted average value is 155.8g. Lastly, the mode weight value for occluded vessels is the highest, 200 g, with a weighted average of 181.03g.

Ideally, the findings of the survey and experimental study should be consistent and support each other. The experimental study has indeed implied the existence of a translational resistance effect on the instruments, and that this resistance can be felt in both narrowed and tortuous vessels, with the strength of resistance increasing according to the degree of narrowing or tortuosity. In addition, the majority of participants agreed that there is no resistance in healthy and non tortuous vessels, with those not agreeing indicating instead that there is subtle resistance even in healthy and normal vessels, which was also reflected in the experimental results. The ranking of translational resistance obtained from the survey and experimental study are also similar. The lowest form of resistance, usually very subtle, is felt in healthy and non tortuous vessels. This is followed by moderately strong resistance around 100g felt in tortuous vessels and

in narrowed vessels with stenosis. In the survey, participants rated the latter stronger than the former, but only just. The strongest form of translational resistance, found in vessels with calcified lesions and in occluded vessels, ranges between 150g - 200g, with occluded vessels providing the strongest level of resistance in both the survey and the experimental study.

3.5 Chapter Summary

This chapter opened with a general overview of haptics and its importance. The perception and measurement / estimation of haptic effects in the scope of endovascular interventions was then explored by reviewing relevant publications studying the details of haptic feedback in this context. From the review and informal discussions with experts, the most important haptic effects identified were the translational and rotational resistance effects. However, the details (i.e. the triggering and magnitude) of each haptic effect were still unclear. These questions led to the design and execution of a study consisting of two components: an online survey and a force range measurement experimental study.

Responses gathered from the study suggest that translational resistance is the main haptic effect present in real life endovascular interventions. This resistance is said to occur mainly in narrowed vessels (i.e. due to stenosis) and/or in tortuous vessels, but there is also the possibility of some form of subtle resistance present even in healthy and non tortuous vessels. The resistance in narrowed vessels increases with the degree of narrowing and, in an occluded (cardiac) vessel, the resistance can potentially be sufficiently strong as to completely prevent instrument advancement. Similarly, the resistance felt in tortuous vessels increases with the degree of tortuosity. The direction of resistance felt in these two types of vessels (narrowed or tortuous) is most likely dependent on other factors such as instrument type, vessel physiology, type of stenosis, degree of tortuosity and others. In some cases, the resistance can only be felt when pushing or advancing the instrument, whereas in others, resistance may also be felt when retracting the instruments. The strength of the translational resistance effect and the estimated average force in varying vessel types in ascending order are: healthy vessel (0.2018N), vessel with stenosis(0.9714N), tortuous vessel (1.1N), vessel with calcified lesions (1.558N) and occluded vessels (1.81N).

A majority of the study participants provided positive responses on the existence of rotational resistance felt in the manipulation of instruments within tortuous vessels. Most of the participants claim that this resistance effect is a result of the force or tension stored within the instrument as it is deformed and tries to regain its natural shape. Thus, the effect can be present even if the tortuous vessel is healthy. Rotational resistance may cause considerable loss of control of the instrument tip as it may take more than one turn of the instrument at the proximal end (closer to the operator) to produce an equivalent turn at the distal end. It is claimed that rotational resistance can normally be easily detected by observing fluoroscopic images, although the majority of participants commented that they feel the resistance first before it is visually evident.

A study of statistical significance was also conducted based on the survey findings in the form of a z-test. The hypothesis testing for proportions technique allows one to infer the consensus of the population regarding a particular statement presented to the sample (i.e. question from the survey). From the findings, it can be deduced that the minimum percentage of consensus among the interventionists regarding the translational resistance (due to vessel narrowing and vessel tortuosity) and rotational resistance is considerably large.

In summary, the findings of this study serve to inform the haptic interface design and development process in this work. From the responses gathered, it was evident that the most important haptic effect to recreate in simulation is the translational resistance effect, which will be the focus of this work. In the next chapter, the work done towards implementing haptic feedback and sensing systems into a prototype haptic interface will be described in detail.

4

Prototype Development

In Chapter 2, the requirements of a haptic interface for the simulation of endovascular interventions were examined. Prior interface designs known to have several shortcomings were then critically studied to investigate how those requirements were met. This was followed by a conceptual discussion of alternative technologies that may be used to overcome these shortcomings and exploration of some of the more feasible approaches. In this chapter, these approaches are further investigated through several experimental and simulation tests. The findings of these tests will influence the prototype development process detailed in the rest of the chapter.

4.1 Proof of Concept Investigations

The instrument sensing approach that is to be investigated here involves the use of an optical sensor to detect/track the guidewire as it moves concentrically within a transparent catheter. Replacing a normal catheter with a transparent catheter allows the optical sensor to have improved visibility of the guidewire where typically it would be occluded by the opaque catheter wall. The testing of this concept consists of several stages and involves the use of different types of guidewires and catheters. In the first stage, the ability to detect guidewire movements with an optical sensor is tested in two different conditions: by itself under direct line of sight and concentrically within a translucent catheter. For both phases of testing, the guidewire is advanced/rotated a set distance and the sensor readings for each movement recorded. The total displacement is then averaged and the mean values for both tests (where the higher value reflects

better tracking performance and sensitivity) are used to analyse the difference in tracking performance. Ideally, both mean values should be similar. If there is a significant difference, the performance of concentric tracking will be improved by making modifications to the sensor and/or the guidewire until satisfactory before proceeding to the next stage. A translucent catheter was used at this stage (and not a transparent/clear catheter) because it was the first catheter with the right diameter size and some degree of transparency that became available. During the course of this project, there was an ongoing search for new, more transparent catheters. This led to the discovery of the other translucent and transparent/clear catheters that are then used in the second stage of testing (following on the promising results from the first stage of tests).

In the second stage, similar tests were conducted, with the guidewire (positioned concentrically within translucent and transparent catheters in separate occasions) advanced/rotated a set distance in 10 steps. Both translucent and transparent catheters are used in testing to examine the effects of increased catheter transparency on the optical sensor's ability to detect guidewire movements. I posit that the guidewire can be tracked with better precision within a transparent/clear catheter compared to a translucent catheter due to the increased visibility. The data obtained is then used to create a scatter plot which will be studied to establish the sensitivity and linearity of the configuration, with precision determined through standard deviation calculations. A flowchart for these tests is shown in Figure 4.1

The second and third conceptual approaches investigate novel techniques for applying force to the guidewire concentrically within the catheter in order to recreate the effect of translational resistance during simulator operation. For the second approach, an attempt is made to apply non contact force to the guidewire using an electromagnetic actuator. To do this, the electromagnetic parameters required to produce the target non contact force are first studied and determined through a series of computer simulations. After the suitable parameters have been identified, electromagnetic actuators are created based on those parameters and used in tests where the force output of the actuators on the guidewire is analysed and recorded. Parameters such as current supply, electromagnet core size and guidewire diameter are varied to study the effects of each on the generated force. The data obtained is then compared to the findings from the simulation and the comparison is used to determine the feasibility of the approach.

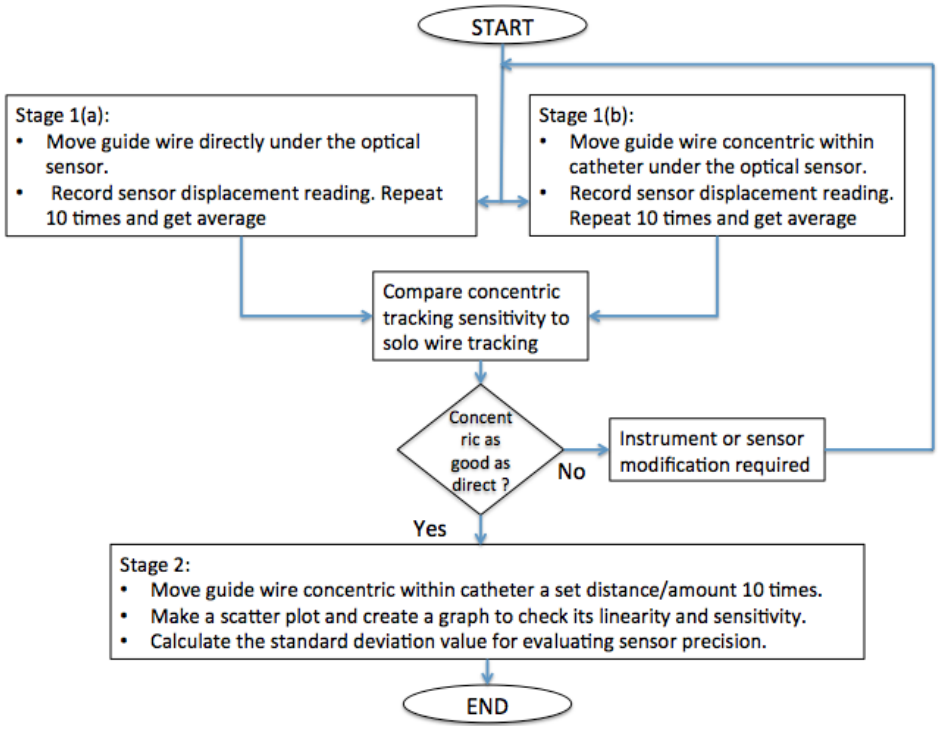

Figure 4.1: Test methodology for concentric instrument tracking

This process is summarized in Figure 4.2. The final approach researches the hub actuator technique, which explores the possibility of placing an actuator within the catheter hub. The effects of the hub actuator on the guidewire are then studied as the current supply is varied. The process is repeated with different guidewires to investigate the force effect on different instrument types. These steps are summarized in Figure 4.3. It should be noted that, in the interest of time, the experimental tests conducted at this early stage are strictly qualitative. However, the findings of the tests would be sufficient to ascertain the most feasible approach to develop further (as described later in the chapter) that includes quantitative testing of the actuator output.

4.1.1 Concentric Tracking of Guidewire

As concluded from the review in Chapter 2, no existing sensor technology is able to perform the concentric instrument tracking task without sacrificing some of the realism and feel of the simulated procedure. Nonetheless, the concentric tracking approach

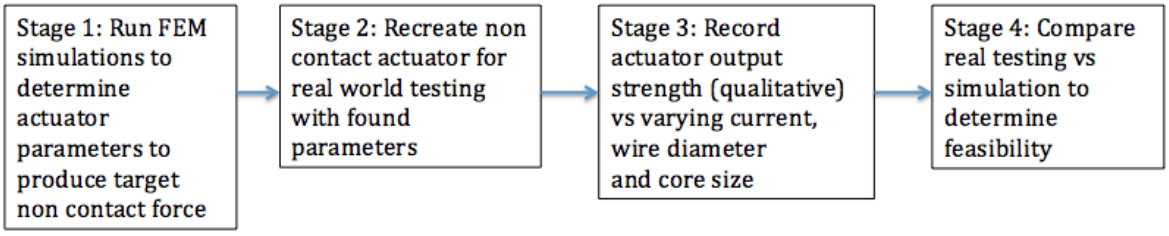

Figure 4.2: Test methodology for non contact actuator approach

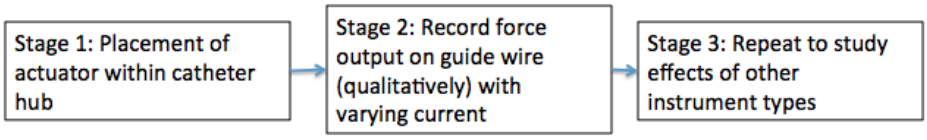

Figure 4.3: Test methodology for hub actuator approach

proposed in Chapter 2 was considered to be one of the most promising approaches to overcome the concentric occlusion problem. The approach involves the use of an optical sensor to detect and track the guidewire through a transparent catheter. As such, instrument modification is a prerequisite for the approach to be successful and this could impact on the instrument's properties, namely diameter, weight, friction coefficient and flexibility. These changes will be examined later in this chapter, but the preservation of other physical aspects, such as instrument tip shape and behaviour, are much less important as these are represented virtually within the simulation software. However, it must be emphasised that the modified instrument(s) are not meant to be the final version of the proposed solution. Instead, they are used to show proof of concept (i.e. whether or not it is possible for an optical sensor to detect guidewire movement within a transparent catheter). For this purpose, the preservation of the exact feel and weight of the modified instrument(s) is not considered vital at this stage. It is considered that, once proof of concept is achieved, it should be possible to manufacture replacements (e.g. transparent catheter) with very similar properties to their original counterparts. Through various discussions and meetings with Osco Ltd. UK (a catheter manufacturing company that has been assisting and supplying materials for this project), I was made to understand that it would be feasible to do so.

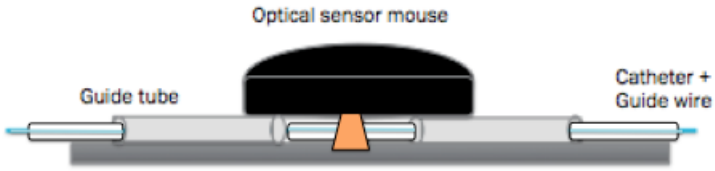

Figure 4.4: Test bed design for testing optical sensor tracking

Translucent Catheter

The initial test to investigate this approach involved a simple experiment using an optical sensor that is positioned to detect the guidewire by 'seeing through' a translucent catheter. The translucent catheter used here was a 5F umbilical catheter obtained from a Subject Matter Expert (SME), an interventional cardiologist, who was interviewed as part of the informal discussions to learn more about interventional tools and procedures, as mentioned in Chapter 2. It was chosen for convenience as it was the only catheter with some degree of opacity and a suitable diameter that was available at the time.

This experiment was conducted using the optical sensor from a computer mouse, a 0.035" hydrophilic guidewire and the umbilical catheter. A basic testbed was built (Figure 4.4), where a guide tube was fixed onto a base plate. The guide tube acts as the channel in which the instruments are inserted. The optical sensor is positioned above the tube, looking down towards the instrument passing underneath, and wired to a micro controller board (Arduino Uno) connected to a PC through a USB port. A program was written for the Arduino in order to extract the sensor readings from the optical sensor. These readings correspond to the X and Y axis position of the cursor on a virtual screen, and therefore do not directly relate to actual displacement of the instrument(s) in mm.

A series of tests were performed using this testbed. These involved moving an instrument on its own (guidewire or catheter), or a combination of instruments (guidewire concentrically within a catheter) a specific distance through the channel (i.e. 20mm) and recording the resulting sensor reading. The same test was then repeated for capturing the sensor reading caused by 360 degrees of instrument rotation. Each measurement

Figure 4.5: Calibration software tool for the Xitact VSP Interface Device

was performed ten times and an average of the resulting sensor reading was calculated for each instrument type or configuration.

While measuring translational displacement is relatively straightforward and can be achieved by using a ruler or protractor, rotations are much harder to measure precisely. For this reason, a commercial haptic interface device called the VSP [51] (as described in Chapter 2) was used as a tool to measure both translational and rotational displacement for these tests. The VSP is connected to the PC via USB and is used with a first party calibration tool software that displays the outputs of the sensors and actuators within the device (Figure 4.5). The testbed is placed at the entrance port of the VSP device so that as the guidewire exits the testbed, it would be advanced into the VSP (Figure 4.6). From then onwards, all guidewire movements would be tracked by the VSP and displayed on screen through the calibration software. As the VSP has been discontinued (due to the merger of its developer Xitact with Mentice Corp), no data sheet of the VSPs technical specs can be found. However, since the VSP utilises optical sensors to track instrument movements, it is expected that the precision of these sensors would be comparable to one of the most popular optical sensors from the same period, the ADNS 2610 from Agilent with a resolution of 400 counts per inch(cpi) and rates of motion of up to 12 inches per second (ips) [117].

The results of this test are shown in Figure 4.7. It is important to note here that the optical sensor (taken from the optical mouse) does not measure absolute position, but relative position or displacements. For this reason, the sensor readings here on the Y axis do not have any units of measurements. At this stage of testing, guidewire visibility to the optical sensor is gauged by the amount of displacement readings produced for a

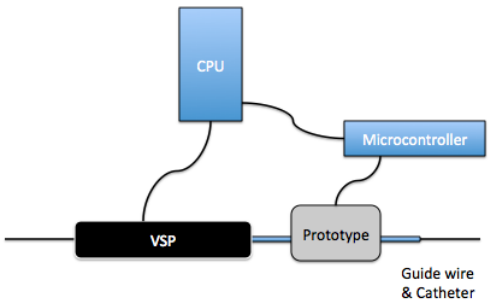

Figure 4.6: Arrangement of the prototype and calibration used together to measure displacement and the resulting sensor readings

set amount of physical wire movement/rotation. For example, a wire that is inserted 20mm and results in a sensor reading of 1000, would be more visible than a wire that is inserted by the same amount, but produces a reading of only 200.

The results confirm the expectation that each instrument can be individually tracked well on its own. The movements of the normal guidewire by itself (i.e. not used within a catheter) were detected with good responsiveness and sensitivity, and producing an average reading of 20.6 and 441.1 for 20 mm translation, and 360 degree rotation, respectively. The tracking performance for the individual catheters was found to be equal or better than that of the guidewire, which can be due to the catheters having a larger diameter and surface area to reflect light to the sensor. In an ideal condition, the tracking performance of the guidewire while within a catheter would be equally good and produce similar readings. However, this is not the case when placed inside a normal catheter, as the guidewire is undetected by the optical sensor due to the lack of line of sight. When inserted into a translucent catheter, the guidewire becomes detectable, but its tracking performance (compared to being outside the catheter) is diminished with an average sensor reading output of 9.8 for translational motion and 152 for rotational motion. This represents a 52.4% and 65.5% drop from the average sensor readings obtained from testing the guidewire individually. There are possibly two other factors contributing to this finding.

Firstly, the positioning of the sensor might not be optimal in relation to its distance to the guidewire and, since the sensor is mounted on a fixed platform, this cannot be adjusted. Secondly, as the guidewire is originally dark in colour, the movement of

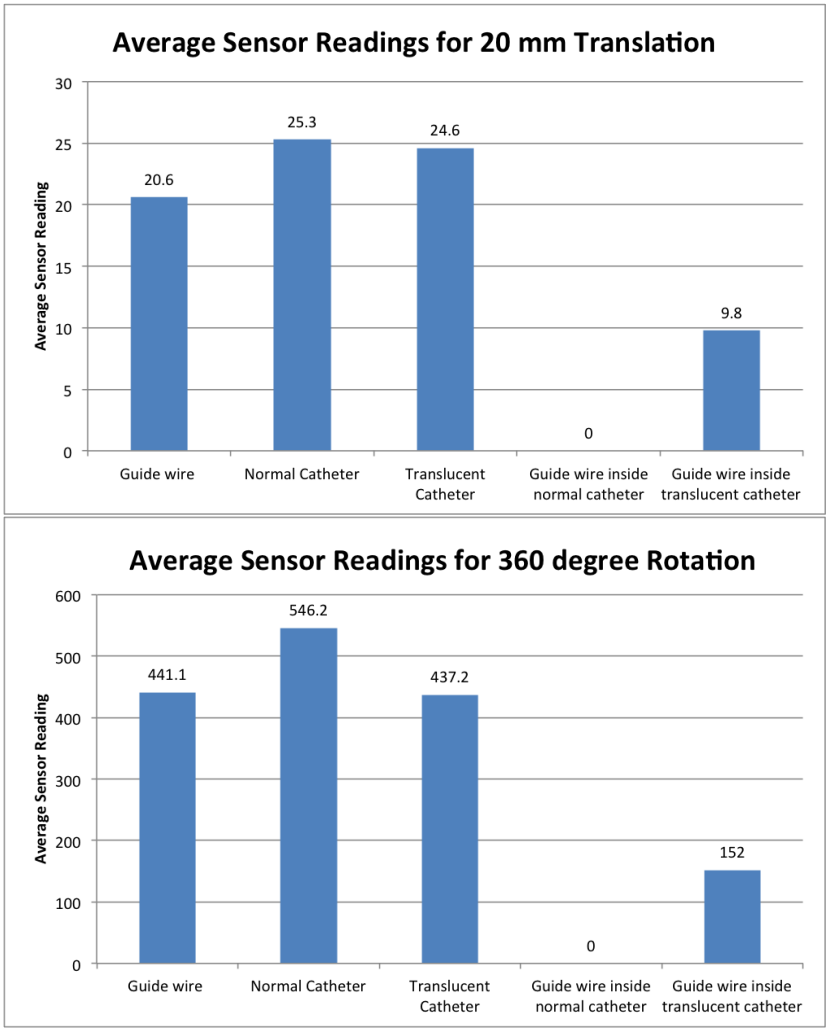

Figure 4.7: Average Optical Sensor Readings for (a) 20mm Translation and (b) 360 rotation in Test 1: Investigation on Sensor Sensitivity to Movement of Concentric Guidewire within a Translucent Catheter

the guidewire inside the translucent catheter does not reflect sufficient light back to the optical sensor, resulting in the significantly reduced sensor readings for equivalent displacements. Therefore, the reflectiveness of the wire needed to be increased. The sensor positioning issue was addressed by producing a second testbed with the optical sensor mounted on an adjustable platform (i.e. the height of the platform can be adjusted using screws). The improved testbed was then used in another series of tests to improve guidewire visibility to the optical sensor.

Enhanced Guidewire Visibility

Using the improved testbed, the second set of tests examined the effect of different colours/surface on the visibility of the concentric guidewire to the optical sensor through the translucent catheter. The guidewire was divided equally into seven segments, six of which were modified to increase reflectivity, and one segment maintaining its original appearance as a control. The six segments were: grey, silver, white, gold, nail polish and reflective tape. These colours/surfaces were chosen based on the assumption that they would reflect more light to the optical sensor (thus improving tracking performance), compared to the original color/surface of the guidewire. The paints were applied using enamel modelling paints. This results in an uneven layer of paint on the instrument which causes an increase in the diameter, weight and friction coefficient of the instruments. These changes will be examined in more detail in the next section. A repeat of the translation and rotation tests was performed for the different segments of the guidewire. The sensor readings were recorded and the average readings for each section are tabulated in Figure 4.8.

From these results, it is observed that the positional tracking of the normal segment guidewire has improved significantly with the adjustments done to the optical sensor. In fact, the average sensor readings for translational movement of the normal segment was the highest compared to all the other segments, with a reading of 21.1. However, the results show that the rotational movements of the normal segment are still poorly tracked. The average sensor readings for its rotational movements (123.5) were the lowest in the test. Therefore, while the normal guidewire tracking has been improved due to better sensor positioning, its rotational movements are still less visible compared to the others.

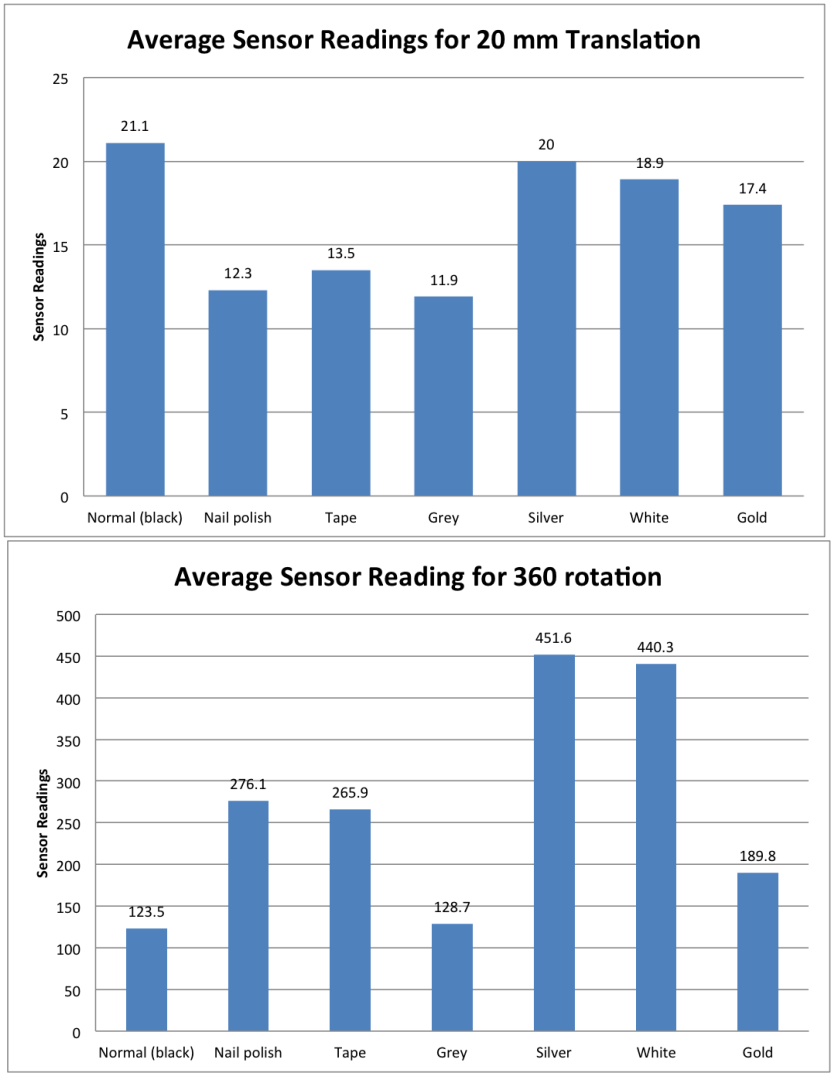

Figure 4.8: Average Sensor Readings for (a) 20mm Translation and (b) 360 rotation in Test 2: Investigation of the Effects of Guidewire Colours/Surface on Sensor Sensitivity to Concentric Guidewire Movement in Translucent Catheter

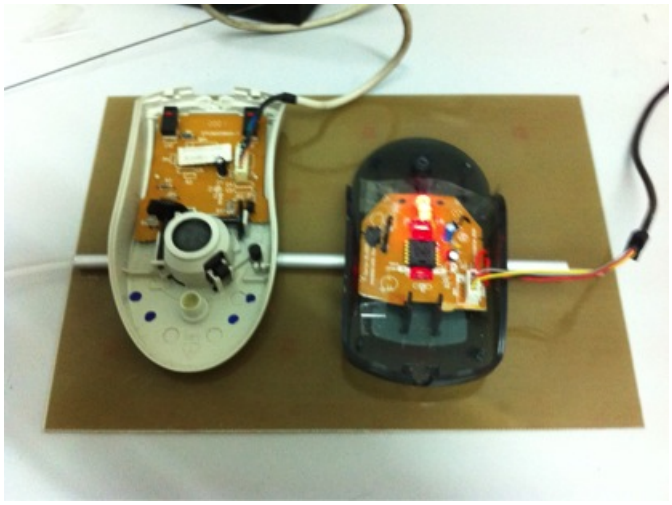

Figure 4.9: Testbed with implemented dual sensor design

Furthermore, the results show that, overall, the best tracked guidewire segment is the silver segment as this segment is second best in terms of translational movement (average sensor reading of 20) and the best in terms of rotational movement (average sensor reading of 451.6). Therefore, it is shown that, by modifying the appearance of a normal guidewire, its visibility to the optical sensor when concentrically placed within a translucent catheter can be increased significantly. However, with this configuration, it is not possible to discriminate between displacement of the catheter and the wire as the readings from the optical sensor are indistinguishable. In order to detect the movements of the catheter, a second sensor is needed.

Dual Sensor Tracking Approach

To investigate this approach, a new testbed was made that included a mechanical encoder from a roller ball mouse as a second sensor (Figure 4.9). When the guidewire and the catheter are concentrically within the guide tube, the roller ball sensor will be activated as the catheter is moved and, in turn, the optical sensor will be deactivated. Likewise, when the catheter is not moving, the optical sensor will remain active. This way, the movements of each instrument will not disrupt the sensor tracking readings for the other. While this configuration is only useful for non-simultaneous instrument movement detection, it overcomes a key shortcoming of the tracking mechanisms seen

in previous systems, namely the ability to continuously track the guidewire whilst inside the catheter with no limit to the range of movement of each instrument. Another advantage of this approach is that, since the sensors for both instruments are positioned close to each other and also located close to the instrument insertion port (entry point for the prototype), the instruments can be detected and tracked as soon as insertion occurs. This is in contrast to previous designs that placed the instrument sensors further away from each other, with the result that instruments would only be detected after travelling a certain minimum distance from the insertion point, or between sensors.

The next series of tests aimed at investigating the performance of the dual sensor tracking design for different guidewire and catheter combinations. Three different types of catheters were selected to study the effects of increased catheter transparency on the concentric guidewire tracking performance. The catheters (6F in diameter) were: a regular diagnostic catheter, a translucent catheter tube, and a fully transparent or clear catheter tube. The translucent and clear catheters used here were obtained from the aforementioned Osco Ltd. U.K. Similarly, three different types of guidewires were used to illustrate the effects of increasing guidewire visibility on concentric guidewire tracking performance. The guidewires (0.035" or 0.89mm in diameter) were: an original Hydrophilic coated guidewire, a silver-painted Hydrophilic guidewire (hereafter known as Hydrophilic Painted) and an original J-tip guidewire. Silver coloured acrylic paint was applied to the hydrophilic wire with a spray can. As the application was performed manually, the actual thickness of the uneven paint is unknown. Ideally, this can be measured with great accuracy by using electro or confocal microscopy. However, at this current stage of establishing proof of concept, it is believed that an estimation would suffice. Based on the lumen size of the 6F original catheter of 1.67 mm (from the manufacturer specification sheet), and the guidewire diameter of 0.89 mm, the thickness of the paint layer must be less than 0.78 mm (i.e. the space between the guidewire and the catheter wall). If the paint layer thickness was equal or close to 0.78 mm, there would be a feel of resistance when advancing the wire through the catheter due to the tight fit, which was not present in the tests conducted.

As mentioned previously, the physical properties of the modified instruments (translucent catheter, clear catheter and painted hydrophilic wire) would inevitably differ from their original counterparts. For instance, there would be a change in the smoothness of their surface (friction coefficient) and their flexibility (flexural modulus). Table 4.1

summarises the general differences between the modified and original instruments used in the tests. The length, weight and diameter of each guidewire/catheter were measured using a measuring tape, weight scale and Vernier caliper, respectively. Details concerning the friction (i.e. static friction against stainless steel) and flexibility of each instrument were either provided by the manufacturer, cited from other studies/references [118, 119] or approximated based on the general properties of the known constituent material(s) [120–122]

From the Table 4.1, it is shown that the layer of paint applied to the hydrophilic guidewire has increased its weight and diameter by 0.759 g and 0.04 mm, respectively, compared to the original hydrophilic guidewire. In terms of surface friction, the original hydrophilic guidewire has the smoothest surface (due to its hydrophilic coating) with the lowest coefficient of friction, estimated to be between 0.025 - 0.06 [119]. Once painted, the hydrophilic coating on the surface of the guidewire is replaced by that of acrylic paint, which has a higher coefficient of friction, and this reduces the smoothness of the guidewire surface. The hydrophilic guidewire is also highly flexible with an estimated flexural modulus of 8 kpsi [118]. However, the layer of paint on the guidewire would increase its rigidity to a certain extent, causing its flexural modulus to increase. Comparing the physical properties of the original catheter, transparent catheter and clear catheter relative to one another, reveals that the translucent and clear catheters were slightly lighter than the original catheter by 0.813g and 0.6953g, respectively. The surface of the original catheter is the smoothest of the three,with an estimated friction coefficient of 0.05-0.08 [120] while the friction coefficient for the transparent and clear catheters are estimated from the related material specifications sheet to be between 0.1 - 0.9 [121] and 0.22- 0.61 [122] respectively. In terms of flexibility, all three catheters are fairly flexible. Nonetheless, the original catheter is still the most flexible, with an estimated flexural modulus of 22.48 kpsi [118]. This is followed by the more rigid clear catheter (75 kpsi) and transparent catheter (78.32 kpsi) based on the specifications provided by the manufacturers. Given that the purpose of these instruments is to obtain proof of concept and not as final versions of suitable replacements, additional testing to further quantify the differences between them was deemed unnecessary at this stage.

The three modified instruments were presented to two SMEs (registrars in interventional cardiology and interventional radiology), to obtain their feedback on the feel and handling of each instrument. Both SMEs concluded that each modified instrument

Table 4.1: Comparison between the properties of the original and modified instruments

Instrument	Length (cm)	Weight (g)	Diameter (mm)	Friction Coefficient	Flex Modulus (kpsi)
Hydrophilic guidewire	120	2.75	0.89	0.025-0.060 [119]	8 [118]
Painted hydrophilic guidewire	120	3.51	0.93	>0.060 [119]	>8 [118]
Original catheter	100	4.09	2	0.05-0.08 [120]	22.48 [118]
Transparent catheter	100	3.28	2	0.1-0.9 [121]	78.32
Clear catheter	100	3.39	2	0.22-0.61 [122]	75

feels and handles similarly to its original counterpart. The SMEs also agreed that the modified instruments would be sufficiently adequate for use in experimental tests to show proof of concept. It should be noted that the J-tip guidewire is chosen for testing despite the fact that it is not a torque wire, since it is of interest to study how its colour and more reflective surface performs under this tracking approach.

There were two stages to the tests. The first stage explored tracking performance of the instruments individually. The aim of this stage was to review the effectiveness of both the ball sensor and the optical sensor for tracking the catheter and guidewire, respectively. The second stage focuses on the sensor's ability to track the guidewire concentrically through the catheter as its visibility is increased. While the instruments or combination of instruments vary for each test, the methodology and procedures involved are the same:

- Linearity: A measure to show that the readings of the sensor have a linear correlation with the quantity measured. The instruments are moved incrementally in each direction and the sensor readings are recorded. The data are plotted in a scatter plot and the relationship between the sensor reading and instrument displacement (in mm) is studied for linearity.

- Sensitivity: A measure of the sensor's ability to pick up the smallest changes in the quantity measured. The device's sensitivity is measured through the ratio of change in sensor readings to the amount of displacement. Therefore, the same data used to determine linearity is used here. Sensitivity is directly correlated to this ratio. The larger the ratio, the more sensitive the measuring device, and vice versa.

- Precision: A measure of how often the sensor can produce the same reading when conducting repeated measures of the same phenomena. The instrument is displaced a certain quantity (i.e. 50 mm for translational displacement and 360 degrees for rotational displacement) a set number of times (ten) and the displacement is recorded each time. The data is then averaged and calculated for standard deviation. There is an inverse relationship between the standard deviation and the precision of the prototype measurements. The smaller the standard deviation, the more precise the prototype's measurement.

The catheter tracking performance of the rollerball sensor was examined first. Figure 4.10 shows that there is a linear relationship between catheter displacement and the sensor readings in both directions. The linear equation that best fits the data obtained for each instrument is also shown. The slope of this line is equivalent to the ratio of change in sensor readings to the amount of displacement and is therefore indicative of the tracking system's sensitivity.

The sensitivity ratio and the precision for each catheter are presented in Table 4.2. The sensitivity ratio or value shows that, for every 1mm displacement of the normal catheter, a reading of 6.745 will be produced by the roller ball sensor. Similarly, for rotational displacement, for every 1 degree of rotation, a reading of 0.0957 is produced by the same sensor. While this seems very small, it should be noted that this displacement is in the smallest scale possible. Using examples to put these values in context, a 10mm displacement would then produce a sensor reading of 67.45 whereas a 90 degree rotation would produce a reading of 8.613.

The results indicate that there is only a slight difference between the tracking performance of the three catheters due to the variation in their material, allowing for the different levels of transparency. The translucent catheter is made of polytetrafluoroethylene (PTFE), which has a slightly smoother surface than the normal catheter, whereas

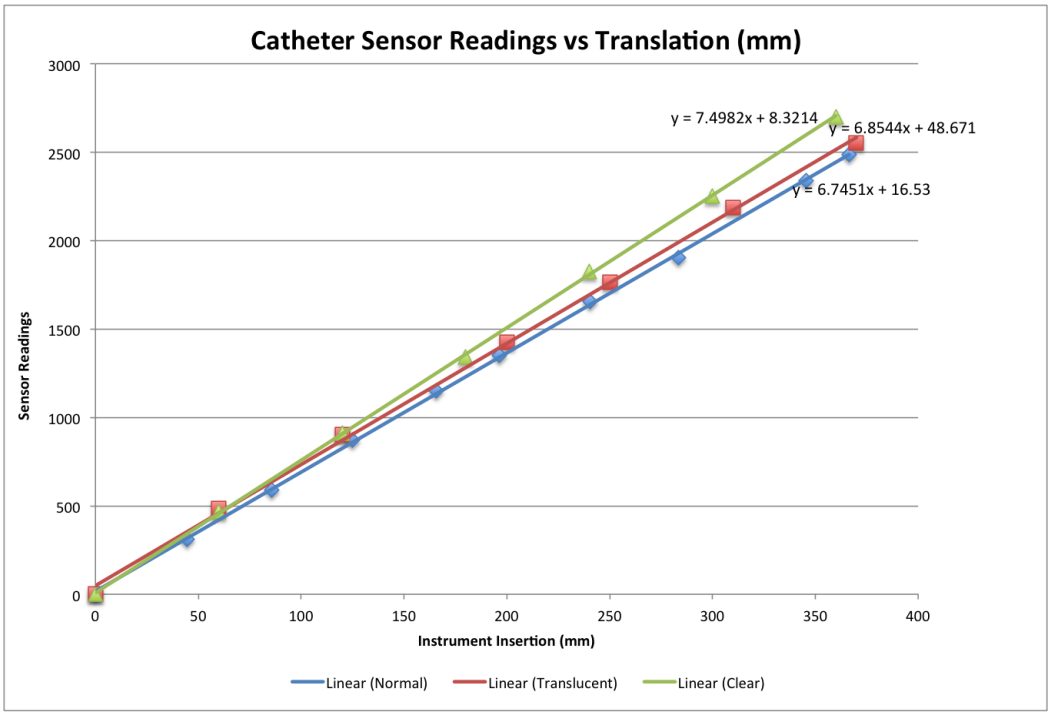

(a)

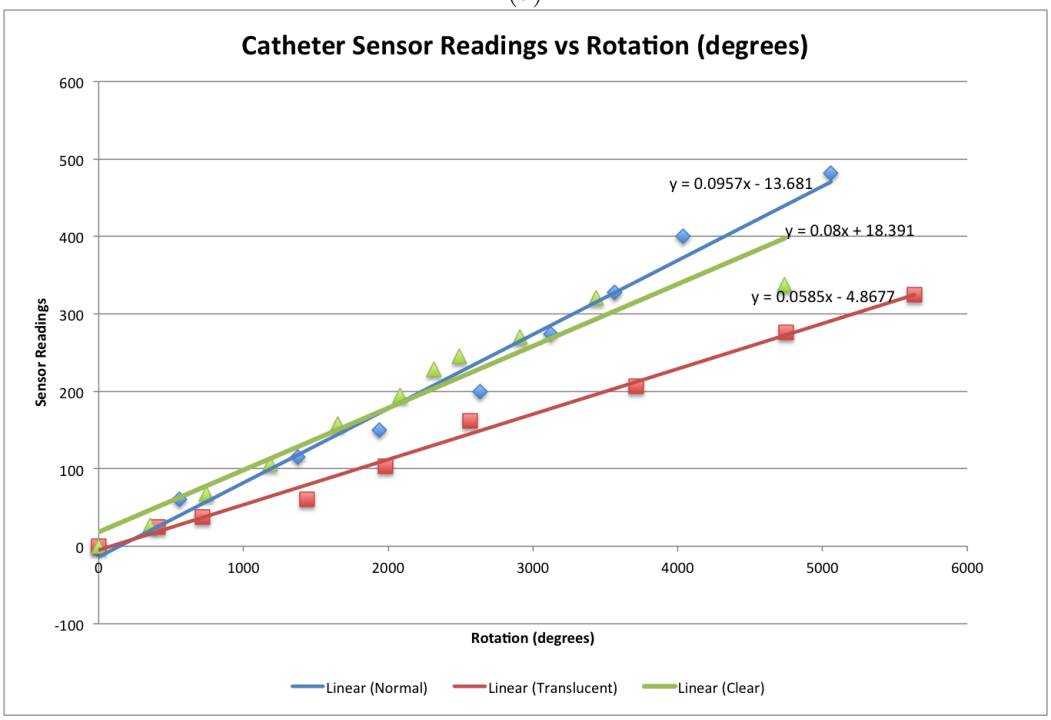

(b)

Figure 4.10: Graph showing the relationship of single catheter displacement against sensor readings for (a) translational and (b) rotational movement.

Table 4.2: Sensitivity and precision test results for single catheter insertion

Feature		Catheter type		
		Normal	Translucent	Clear
Sensitivity	Translation	6.745	6.854	7.498
	Rotation	0.0957	0.0585	0.08
Precision	Translation			
	Mean	362.1	374.5	422.7
	Std Dev	7.723	10.66	17.436
	Rotation			
	Mean	35.9	13.9	20.6
	Std Dev	3.348	3.14	4.087

the clear catheter is made of nylon and has the smoothest surface of the three. On the whole, the roller ball sensor is able to track each catheter's movement with the same level of sensitivity and precision.

Figure 4.11 presents the results for guidewire tracking performance. There is a linear relationship between the displacements and sensor readings, as described by the respective best fit linear equations. The sensitivity and precision of the tracking is shown in Table 4.3. As expected from previous findings, the results show that there is no significant difference in the translational movement tracking performance between the three guidewires, and that painting the guidewire silver has the effect of improving its rotational tracking performance, as shown by the 100% increase in sensitivity between the Hydrophilic wire and the Hydrophilic Painted wire. The J wire was more difficult to rotate in a controlled manner due to the fact that it is not a torque wire. This is reflected by the data points in Figure 4.11 (b), which did not produce a good linear fit.

The next set of tests relate to tracking the movement of the guidewires whilst inside and covered by the translucent catheter. Figure 4.12 and Table 4.4 show that there is an overall slight decrease in sensitivity in tracking translational motion due to the partial occlusion caused by the translucent catheter. For example, the Hydrophilic mean wire sensitivity is down to 29.41 from 33.243 and the mean precision is also down to 1487.9 from 1842. The precision of tracking the J-wire and hydrophilic wire has also improved as the standard deviation has decreased from 202.75 and 261.35 to 50.83 and 83.35 respectively. This is in sharp contrast to the standard deviation of the hydrophilic

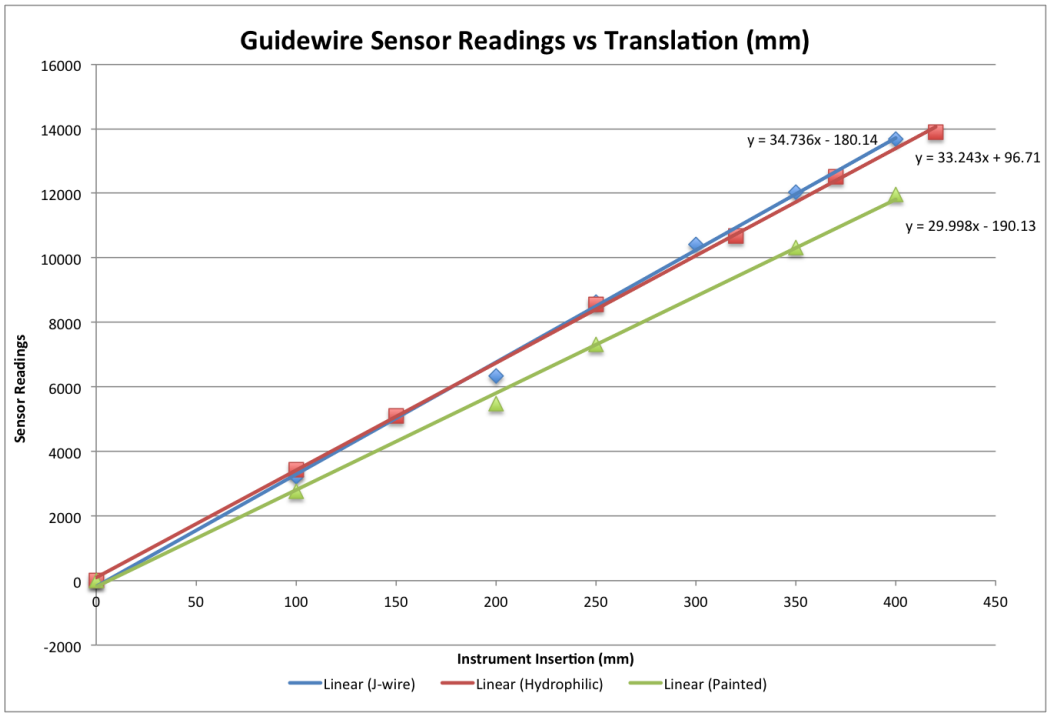

(a)

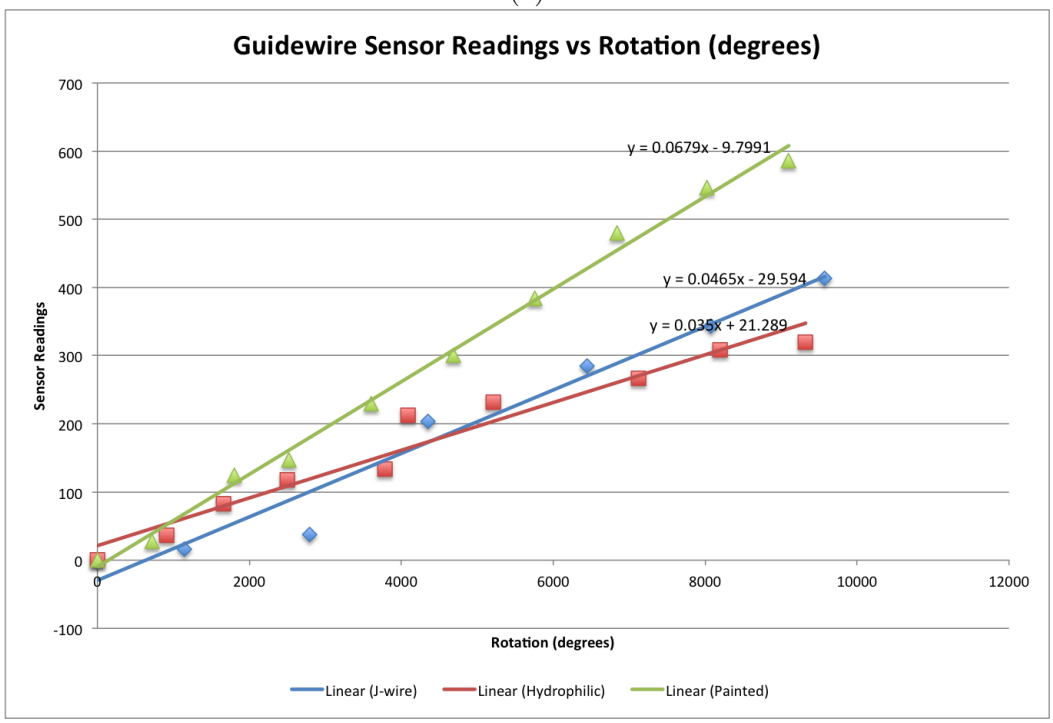

(b)

Figure 4.11: Graph showing the relationship of single guidewire displacement against sensor readings for (a) translational and (b) rotational movement.

Table 4.3: Sensitivity and precision test results for single guidewire insertion

Feature		Guidewire type		
		J-wire	Hydrophilic	Hydrophilic Painted
Sensitivity	Translation	34.736	33.243	29.998
	Rotation	0.0465	0.033	0.0679
Precision	Translation			
	Mean	1436	1842	1677
	Std Dev	202.75	165.73	261.35
	Rotation			
	Mean	24.3	21.1	23.1
	Std Dev	12.23	8.53	7.59

Table 4.4: Sensitivity and precision test results for guidewire insertion within the translucent catheter

Feature		Guidewire type		
		J-wire	Hydrophilic	Hydrophilic Painted
Sensitivity	Translation	29.21	29.41	29.8
	Rotation	0.0638	0.0452	0.0521
Precision	Translation			
	Mean	1526.4	1487.9	1558
	Std Dev	50.83	208.12	83.35
	Rotation			
	Mean	47	45.3	40.1
	Std Dev	10.1	11.69	5.28

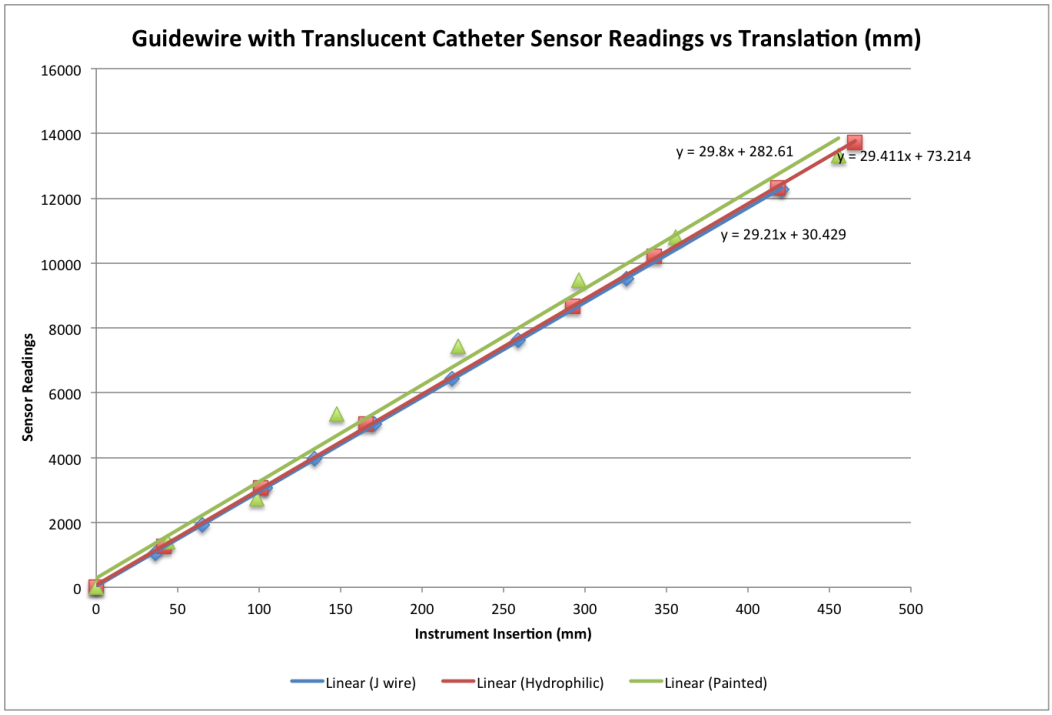

(a)

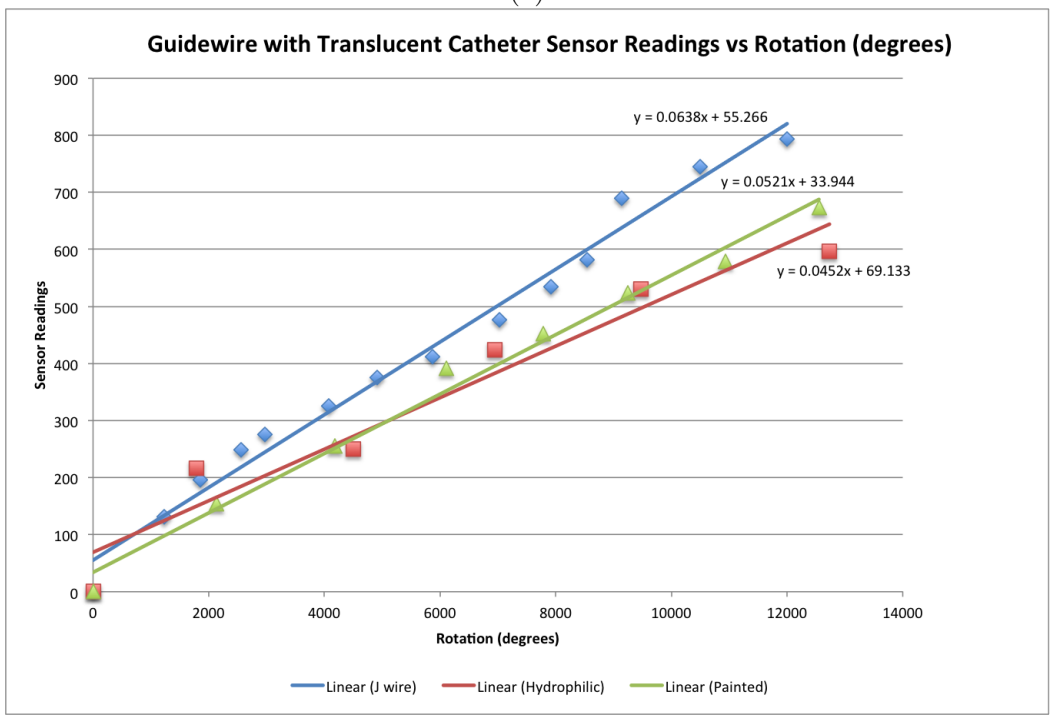

(b)

Figure 4.12: Graph showing the relationship of guidewire displacement inside a translucent catheter against sensor readings for (a) translational and (b) rotational movement.

Table 4.5: Sensitivity and precision test results for guidewire insertion within the clear catheter

Feature		Guidewire type		
		J-wire	Hydrophilic	Hydrophilic Painted
Sensitivity	Translation	26.688	29.336	23.49
	Rotation	0.0345	0.0554	0.1582
Precision	Translation			
	Mean	1419.5	1451.2	1508
	Std Dev	100.66	149.41	146.26
	Rotation			
	Mean	22	43.7	70.6
	Std Dev	9.175	15.06	12.72

guidewire where its standard deviation has increased from 165.73 to 208.12. It should be stressed that this is not an outlier value since it is an average calculated from a total of 10 measurements. This could suggest that, being concentrically inside the catheter has brought the guidewires closer to the optical sensor, thus improving the tracking precision, with the hydrophilic guidewire being the only exception. A possible reason for this is its unique dark surface and coating, limiting its visibility to the sensor through the translucent catheter.

Nonetheless, the new configuration (i.e. guidewires covered by the translucent catheter) did not produce a dramatic change in the readings of sensitivity and precision across the three guidewire types in terms of translational movements as the mean for sensitivity and precision lie within the range of 29-30 and 1400-1600, respectively. It is important to note that, being covered by the translucent catheter has actually improved the rotational motion tracking performance for all the guide wires. The average precision has nearly doubled from tests where the guidewires were not covered by the translucent catheter (mean sensor readings increased from 24.3 to 47 for the J wire; 21.1 to 45.3 for the hydrophilic wire and 23.1 to 40.1 for the painted guidewire). As mentioned previously, being concentrically inside the catheter has changed the position of the guidewire and brought it closer to the optical sensor. This would explain the improved tracking performance seen in the results.

The final test for the tracking system aims at reviewing guidewire tracking perfor-

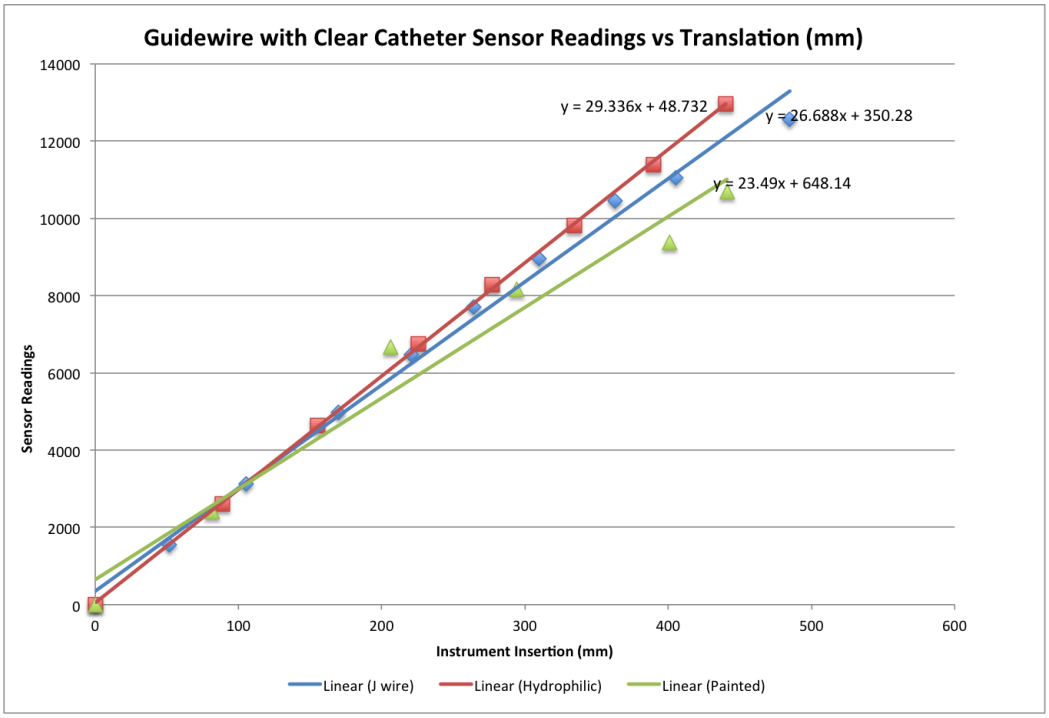

(a)

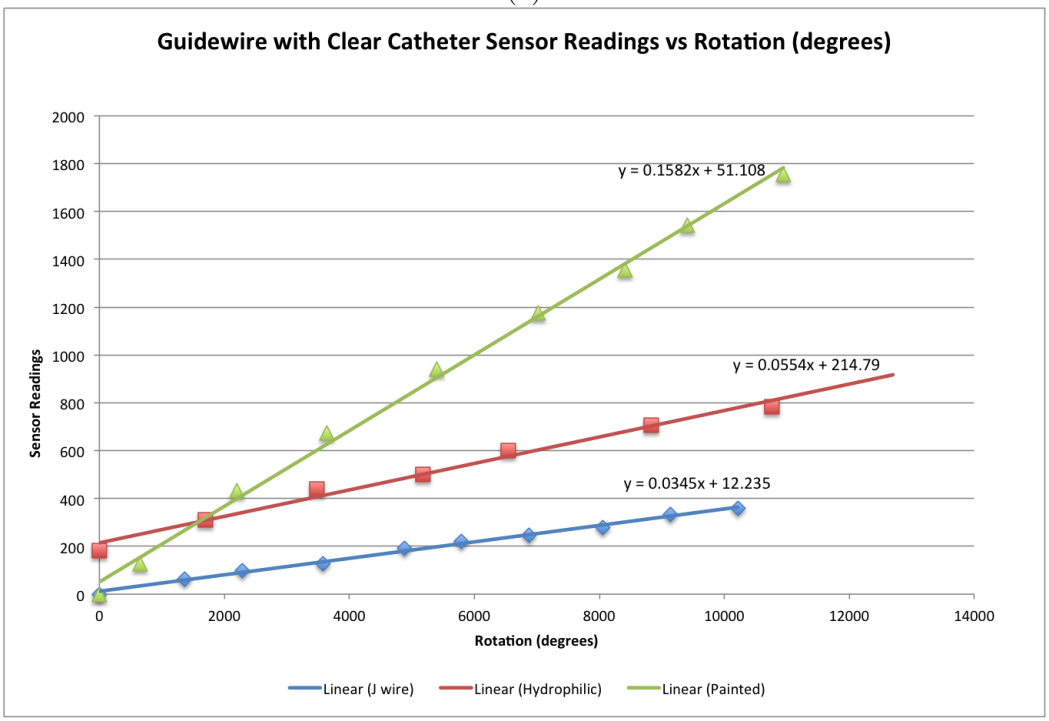

(b)

Figure 4.13: Graph showing the relationship of guidewire displacement inside a clear catheter against sensor readings for (a) translational and (b) rotational movement.

mance through the clear catheter. It was estimated that the wire would be tracked with greater sensitivity and precision in the clear catheter than in the translucent catheter. It was also expected that the tracking performance for the painted guidewire would be the best due to its enhanced reflectivity. The graphs in Figure 4.13 show that the sensor readings are linear to the displacement changes. The sensitivity and precision data in Table 4.5, however, indicates that the assumptions made were only partially correct. The rate of translational movement detection is the same, if not lower for two of the three guidewire types, compared to the results from tests with the translucent catheter. Nonetheless, the three guidewires exhibit distinctively different characteristics in terms of rotational motion tracking, which is shown to be low in sensitivity and precision for the J-wire. This can possibly be attributed to the fact that the J wire is not a torque wire and is therefore not designed to facilitate rotational movement. The poor rotational tracking performance of the J wire can thus be attributed to its inability to turn/rotate effectively and the sensing approach used. Its inclusion in the test is to investigate if its unique surface coating (green and more reflective than the standard Hydrophilic wire) makes it more visible to the sensor in this tracking approach. The measurements obtained indicate that the J wire's surface appearance does not add considerably to its visibility since the mean sensitivity and precision values do not differ dramatically from the other guidewires. The sensor manages to detect rotational motion significantly better when the clear catheter is combined with the Hydrophilic guidewire, and best when combined with the Hydrophilic Painted guidewire. This could be due to the increased visibility of the guidewire as a result of its enhanced reflectiveness, and/or the increased transparency of the catheter.

Summary of Concentric Tracking Results

The tests and investigations performed here confirmed the potential of the 'concentric tracking' approach. It was observed that the translational and rotational movements of the guidewire can be tracked reliably when it is concentrically within the catheter. This is made possible by increasing the guidewire's visibility to the sensor through the combined use of a clear catheter and a brightly painted guidewire. However, this configuration requires the use of a second sensor for tracking the movements of the catheter. Data from the tests performed have shown that a mechanical roller ball sensor would be suitable for this application. Overall, the findings of these tests are

very encouraging, suggesting that it is feasible to design a dual sensor tracking system that is able to solve the 'concentric occlusion' problem and overcome the shortcomings of previous interfaces.

4.1.2 Non Contact Haptic Actuator

In the conceptual approach for a non contact haptic actuator, the guidewire experiences a pulling force from a non contact actuator that is activated in close proximity. This force will produce a resistance effect to the translational movements of the guidewire. Electrostatic and electromagnetic actuators are popular sources for non contact force. Electrostatic actuators require the guidewire to be conductive (i.e. be made of a material that allows the passage or flow of charge carriers such as electrons within itself). While the inner core of the guidewire is commonly made of steel and therefore conductive, guidewires such as the hydrophilic guidewire are wrapped by a non conductive material and coating. As the guidewire is not naturally conductive externally, this would need a significant modification that may result in a change in the weight and/or feel of the original guidewire. This approach is also undesirable as it may present a potential hazard or health risk due to handling instruments conducting an electric current. Electromagnetic actuators do not need the actuation target to carry charge to operate. Instead, the only requirement is for the material to be ferromagnetic. Therefore, this approach was considered to have potential and is further explored here.

Electromagnetic Force Generation

The magnetic flux density of an electromagnet, B is given by Equation 4.1. It represents the amount of magnetic flux within a unit area. The higher the magnetic flux density, the stronger the magnetic field.

$$B = \frac{Mo \times Mr \times I \times N}{l} \tag{4.1}$$

From the above equation, the various parameters involved in designing an electromagnet are:

i. l: the shape and dimensions of the electromagnet core, which determines the effective length of the solenoid. It depends on the function of the magnetic circuit. An example of a typical core shape is the E-shaped cores found in transformers

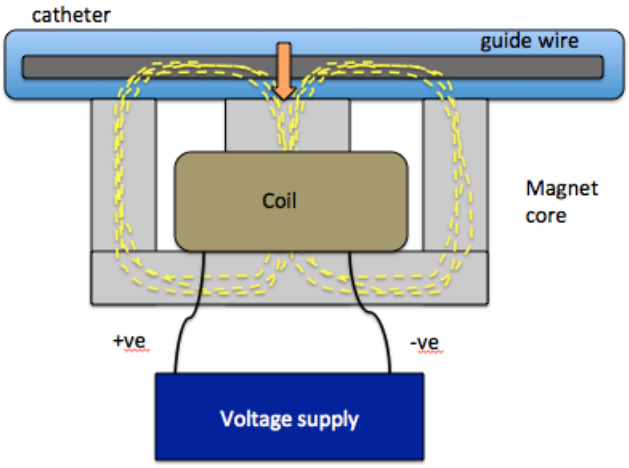

Figure 4.14: Applying non contact force for simulating force feedback

ii. Mr: the flux permeability coefficient of the core. Materials with higher permeability allow more flux to flow through them. Mo is a permeability constant

iii. N: the number of turns of the copper coil. It depends on the diameter of the copper wire used in the coil, as well as the dimension of the coil, which relates to the dimensions of the core

iv. I: the current supplied to the copper coil. The higher the current, the more flux is generated

The flux generated by the electromagnet must flow through the guidewire and complete the magnetic circuit for there to be a pulling effect (Figure 4.14). As mentioned previously, the strength of the magnetic force F increases with the flux density B and also with the surface area of the actuation target, S. This is shown by Equation 4.2

$$F = \frac{B^2 \times S}{2 \times Mo} \tag{4.2}$$

Taking both equations into consideration, the following parameters need to be determined when designing an electromagnetic non contact actuator for this application:

i. Core shape and dimension: variable to a certain extent as permitted by the size of the haptic interface device

ii. Core material: variable according to availability of material, cost, and the target output magnetic field of the electromagnet

iii. Number of copper wire turns on coil: variable according to copper wire diameter and the size/dimensions of the core used

iv. Gap distance between electromagnet and guide wire: varies depending on the size of catheter used. It is equivalent to the thickness of the catheter wall.

v. Guide wire diameter: variable. Ideally, it should be fixed and equal to the diameter of the guidewire used to maintain the realism of the simulation

vi. Guide wire material: needs to be modified/changed to a ferromagnetic material. At this stage, the assumption is that this change of material would not have a significant impact on the properties of the guidewire. This is to enable the conducting of tests and computer simulations required to investigate the feasibility of the non contact actuator approach.

Magnetostatic Simulations

A series of magnetostatic simulations were performed in ANSYS 13, a Finite Element simulation software. The objective of the simulations was to estimate the appropriate values of the listed parameters in order to generate the target magnetic force on the guidewire (maximum of 1.5N). This target maximum force value is based on the results of the study conducted in Chapter 3 and supported by the reviewed literature [108, 109]. The following parameters were set in the simulation:

i. Core shape and dimension: Two electromagnet cores with a basic E shape, Core A (66 mm x 44 mm x 22 mm) and Core B (32 mm x 25mm x10 mm), were modelled in a 3-D mechanical Computer Aided Design (CAD) program, Solidworks [123] and imported into ANSYS. The two cores, pictured in Figure 4.15, were considered to be within reasonable size limits and able to show the effects of core size on the strength of the electromagnetic field.

ii. Core material: The material of the cores used in simulation was set as M22 steel, which is the standard core material used in similar electromagnetic simulations.

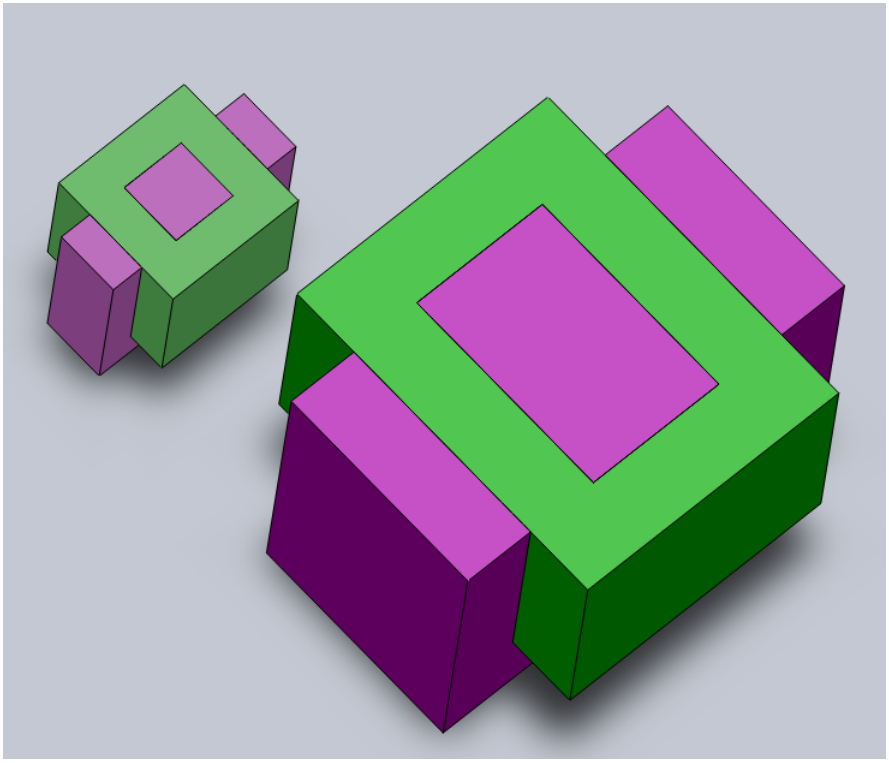

Figure 4.15: The E-shaped magnetic cores modeled in Solidworks and imported into ANSYS. The larger model represents Core A whereas the smaller model represents Core B)

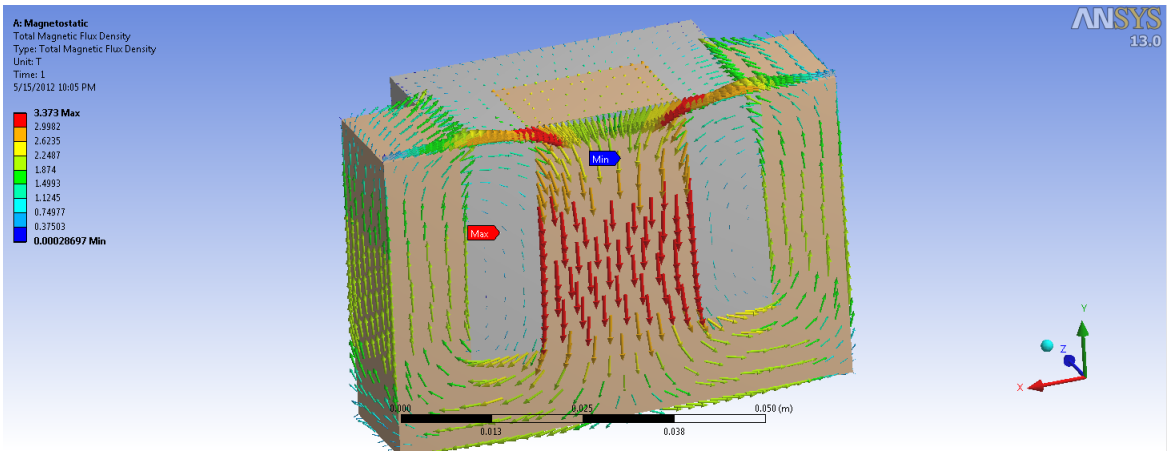

Figure 4.16: Simulation results for magnetic flux density direction

iii. Number of copper wire turns on the coil: As mentioned previously, the number of turns on the coil depends on the dimension of the core and the diameter of the copper wire used. In this simulation, three different copper wires of varying diameters were used with each magnet core. The three wires had diameters of 0.36 mm, 0.54 mm and 0.89 mm each, resulting in a total number of 756, 408 and 152 turns in the copper coil for Core A, respectively. The number of turns for Core B with the same copper wire diameters were 2716, 1199 and 445.

iv. Gap between electromagnet and wire: It is a constant equal to the thickness of the catheter wall. For the 6F catheter used in the experimental work so far, this value is 0.333 mm based on its specification sheet.

v. Diameter of the wire: A constant depending on the diameter of a typical guidewire, 0.89 mm or 0.035"

vi. Material of the wire: The wire material is set to Silicon Core Iron, a typical ferromagnetic material used in similar simulations.

ANSYS simulates the total flux density of the electromagnet and the direction of the flux generated (Figure 4.16). The simulation also computes the directional force experienced by the guidewire. From the simulation results in Table 4.6, it can be seen that only magnet Core A with 0.89 mm diameter copper wire is able to reach (and

Table 4.6: Simulation results for Core A and Core B, with wire diameter = 0.89 mm and V = 12 V

	Copper Wire Diameter/mm	Number of turns (N)	Current (I)/A	NI	Force/N
Core A	0.36	926	0.82	759	0.385
	0.54	408	5.54	2500	1
	0.89	152	36	5466	1.62
Core B	0.36	2716	0.1137	308.8	0.054
	0.54	1199	0.7207	864.1	0.137
	0.89	445	4.98	2213	0.329

surpass) the target force actuation of 1.5 N. However, the amount of current needed to generate that force is 36 Amp, which is extremely high, unsafe and impractical for this application. A more realistic approach is to use the combination of a slightly larger core with 0.54 mm copper wire coil since it can produce 1N of force with a current of 5.54 Amp using the same Core A.

In order to observe the effects of varying core size on the magnetic force produced, the same combinations of copper wire and guidewire diameters were repeated in simulation using Core B. The results arranged in Table 4.6 show that none of the simulated outputs using Core B are able to produce the target force. Moreover, the simulated force for Core B is actually lower than Core A, despite its larger size. This could be due to the fact that, although magnetic flux density is increased with the larger core, the guidewire covers a smaller percentage of the core surface, which causes the amount of flux flowing through the wire to be less than that with Core A.

Next, the effects of varying the materials of the guidewire and core were studied in simulation. Commonly used ferromagnetic materials with unique B-H magnetic curves were selected to replace the material used in the original simulation (using only Core A and copper wire diameter = 0.36 mm). A comparison of the simulated force produced by the different cores and experienced by the different wires (Table 4.7 and Table 4.8) showed that changes in the material of the guidewire produces only a slight change in the force generated. Also, changes in the core material do not seem to affect the force output. This suggests that core and guidewire material are not the key factors affecting the strength of the magnetic field produced.

Table 4.7: Simulation results for different Core A materials with copper wire diameter = 0.36 mm

Core Material	M22 Steel	M3 Steel	M50 Steel	Moly Permalloy	Iron Ingot Annealed
Simulated Force on Core(N)	0.385	0.386	0.383	0.381	0.384

Table 4.8: Simulation results for different guidewire materials with copper wire diameter = 0.36 mm

Guidewire Material	Silicon Core Iron	Gray Cast Iron	Moly Permalloy	Iron Ingot Annealed	Nodular Cast Iron
Simulated Force on Guidewire (N)	0.385	0.345	0.204	0.479	0.354

Table 4.9: Simulation results for core A and B, with guidewire diameter = 1.5 mm and V = 12 V

	Copper Wire Diameter/mm	Number of turns (N)	Current (I)/A	NI	Force/N
Core A	0.36	926	0.82	759	1.47
	0.54	408	5.54	2500	3.42
	0.89	152	36	5466	5.28
Core B	0.36	2716	0.1137	308.8	0.254
	0.54	1199	0.7207	864.1	0.552
	0.89	445	4.98	2213	1.27

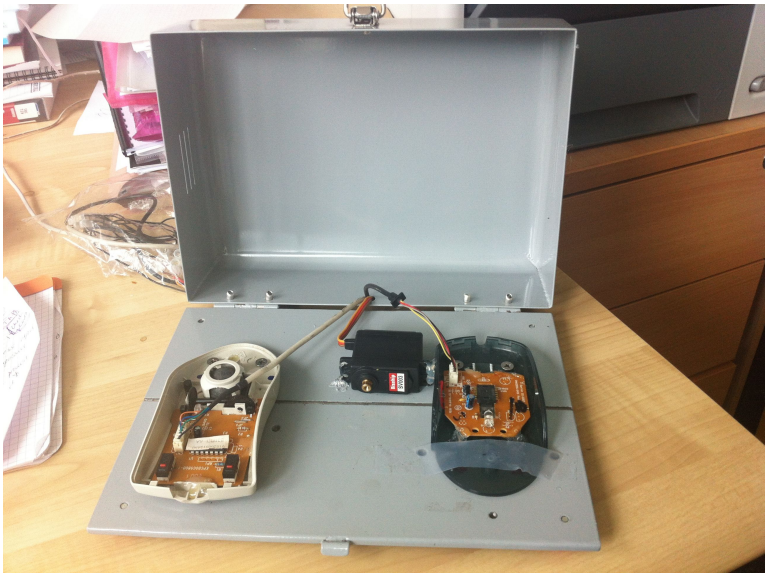

Figure 4.17: Second iteration of the prototype made of ferromagnetic material

The simulation was then repeated with a 1.5 mm guidewire to investigate the effects of varying guidewire diameter on the force generated. From the simulation results in Table 4.9, it can be seen that increasing the guidewire diameter has caused an increase in the magnitude of the force acting on the guidewire. The larger diameter guidewire has increased the amount of ferromagnetic material, enabling more flux to flow through the guidewire resulting in a stronger magnetic force. Whilst all of the copper wire combinations using Core A are close to or above the target force of 1.5 N, this is still not the case for Core B. Although the magnitude of the force acting on the guidewire has increased to the desired value for Core A, increasing the guidewire diameter by 0.6 mm represents a significant change in this application and would greatly affect the realism of the training experience. According to informal discussions held with the two SMEs mentioned earlier, a guidewire with a larger diameter would feel heavier to the touch and be more difficult to manipulate than the original. Furthermore, the non standard guidewire diameter would mean that it would no longer be compatible with certain catheters due to the end hole diameters.

In order to confirm the findings of the simulation, several qualitative tests were conducted using actual electromagnets. The two E-shaped cores used in the simulation were recreated with the same dimensions (Figure 4.18). Measures were taken to set

Table 4.10: Comparison of equipment parameters used in simulation and real life testing

Equipment	Features	Simulation	Testing
Core A	Dimensions(mm)	32 x 25 x 10	32 x 25 x 10
	Number of copper wire turns	926	1200
	Copper wire diameter (mm)	0.36	0.3
Core B	Dimensions(mm)	66 x 44 x 22	66 x 44 x 22
	Number of copper wire turns	2716	2500
	Copper wire diameter (mm)	0.36	0.3
Catheter	Wall thickness(mm)	0.333	0.3

the other parameters as similar as possible to those in the simulation (Table 4.10). Electromagnet Core A was coiled with 0.3 mm diameter copper wire, 1200 turns and 0.9 Amp current. The ferromagnetic 'guidewire' used was made of galvanized steel of a diameter of 0.8 mm. It was placed within a 6F catheter resulting in a gap of 0.333 mm between the 'guidewire' and the electromagnet due to the thickness of the catheter wall. In order to ensure that the magnetic flux generated by the electromagnet does not escape into the air, a ferromagnetic testbed was used. This testbed (Figure 4.17) allows for the placement of an electromagnet above the channel through which the instruments pass. It is expected that, when the electromagnet is activated, the generated flux will flow through the testbed, the catheter wall gap, the guidewire and then back to the electromagnet, thus completing the electromagnetic circuit.

The testbed was used in a qualitative test to evaluate the effects of guidewire diameter variation on the strength of the force felt. This phase of testing was meant as a precursor to investigating the feasibility of the non contact approach and will be followed up by quantitative testing if positive results are obtained. The ferromagnetic guidewire was passed under the electromagnet as voltage and current supplied to it increased. The effect of the magnetic field on the guidewire was rated by the author using the scale shown in Table 4.11. For a *Very Weak* force, the effect was very low and more noticeable visually than by touch or feel. In contrast, a *Very Strong* force becomes so strong that it is significantly harder to advance/withdraw the guidewire. This test was performed for both 1 mm and 1.5 mm diameter guidewires with Core A and Core B. The results are shown in Table 4.12. Core A with the 1.0 mm guidewire resulted in a force or resistance that was only felt when the current was 1 Amp, but the maximum

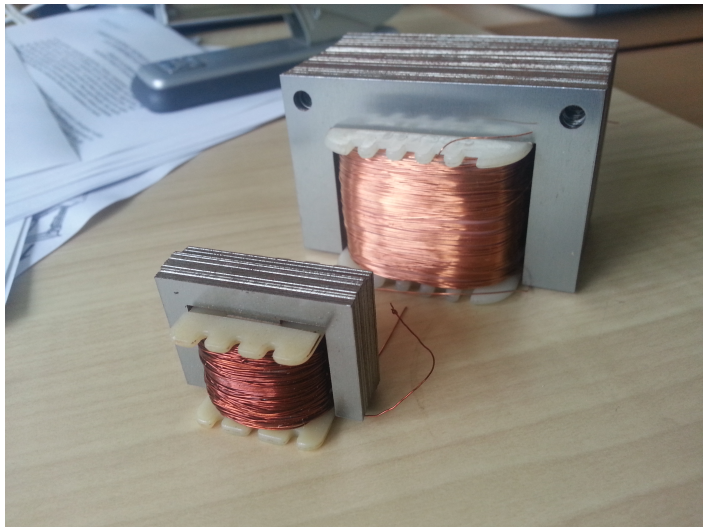

Figure 4.18: The two E-shaped cores used in the qualitative tests, Core A (left) and Core B(right)

Table 4.11: Force scale used in the qualitative tests

Force Level	Rating	Description
0	None	No effect felt or observed on the guidewire
1	Very Weak	Observed and not felt
2	Weak	Minimal force felt and observed as slight attraction
3	Light	Force effect felt is noticeable, guidewire visibly attracted
4	Moderate	Noticeable force felt when moving guidewire, guidewire attraction is quite apparent
5	Strong	Force effect on guidewire makes manipulation difficult, guidewire attraction is more apparent
6	Very strong	Guidewire movement becomes extremely difficult, guidewire attraction is very apparent

Table 4.12: Comparison of test results between 1 mm and 1.5 mm guidewires with Core A and Core B

	Core A			Core B		
Voltage (V)	Current (A)	1mm	1.5 mm	Current(A)	1 mm	1.5 mm
0	0.000	0	0	0.00	0	0
5	0.245	0	0	0.08	0	1
10	0.49	0	0	0.18	0	2
15	0.734	0	1	0.25	1	3
20	1.0	1	1	0.36	1	4
25	1.175	2	2	0.45	2	5
30	1.362	2	3	0.57	2	6

level of force felt was *Weak*, even when the voltage and current were increased. The result was similar when using the 1.5 mm guidewire, with the only difference being that the strength of the magnetic field reached a maximum of *Light* force. The effect of the magnetic field from Core B is much more noticeable as it is first felt for lower voltage and current, even when using the 1mm guidewire. The maximum force output from Core B was much stronger, resulting in a *Very Strong* force. In addition, the force output when testing Core B was more controllable and gradually ranged from *Very Weak* to *Very Strong*, depending on the the voltage and current supplied.

In sum, for both cores, the maximum magnetic force achievable on the 1.0 mm guidewire was *Weak* and negligible. The force effect was enhanced when Core B was used, especially with the 1.5 mm guidewire, where the effect was linearly controllable and reached a maximum force on the wire rated as *Very Strong*. These results reflect the findings from the simulation, where an increase in the magnet core size and the wire diameter produce a stronger force acting on the wire. While increasing the core size is an acceptable approach, increasing the diameter of the instrument used during simulation is not. Interventional experts confirmed that using a significantly larger diameter guidewire would have a distinctly negative effect on the simulation experience in terms of both realism and training effectiveness. Since the force felt with a 1.0 mm ferromagnetic wire (which is already 0.11 mm thicker than the original 0.89 mm wire) is too weak and insignificant, it was concluded that there is no feasible way to achieve the desired force strength level without changing the wire diameter significantly,

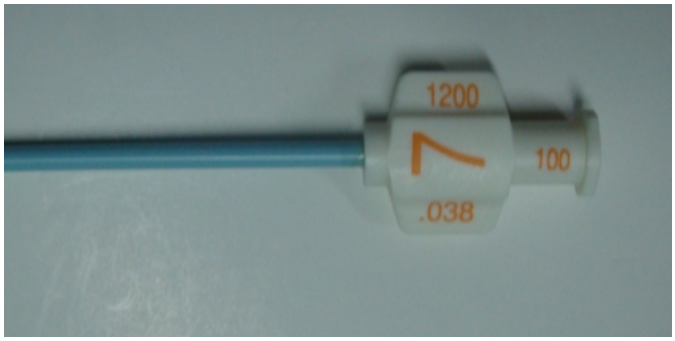

Figure 4.19: Catheter hub for 7 F diagnostic medical catheter

or supplying an impractically large electrical current. Such increase in wire diameter, added to the change to a ferromagnetic wire, is likely to significantly affect the properties and handling of the guidewire compared to the original. For these reasons, the non contact electromagnetic force actuation approach was not pursued further.

4.1.3 Catheter Hub Actuator

The catheter hub refers to the plastic case that forms the entrance at the proximal end of the catheter (Figure 4.19). It has a unique cylindrical shape measuring 8 mm x 20 mm (Diameter x Length) with 'wings' extruding from the sides. During operation, the guidewire will always pass through the catheter hub to enter the catheter tubing. Therefore, by placing an actuator within the hub, it will have direct contact with the guidewire at any time without requiring or causing any movement restrictions. This is a useful feature, which could potentially lead to a solution to the concentric occlusion problem. In this subsection, the feasibility of this approach is explored together with possible designs for further testing.

An actuator using the same principle as the four basic actuators described in Chapter 2 can be specifically designed and miniaturised for implementation within a custom catheter hub. Between the many different actuator types, the electromagnetic actuator was selected due to the minimal parts required that are relatively simple to miniaturise, easy to obtain and with the potential for producing varying levels of resistance. The illustration in Figure 4.20 shows an example of how an electromagnetc actuator can be utilised in this approach. When actuation is required, current will be supplied to the coil, thus producing an electromagnetic field. Next, the magnetised coil is pulled down

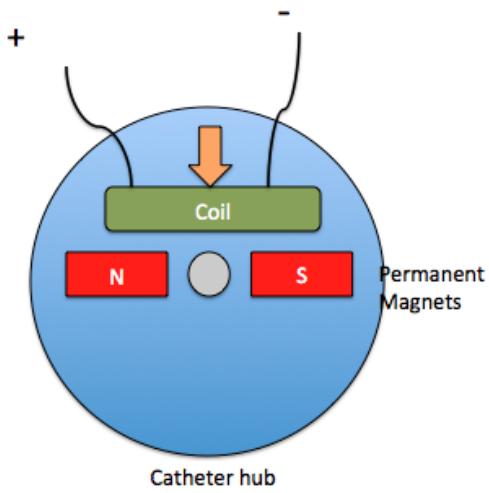

Figure 4.20: Electrodynamic microactuator design for catheter hub replacement

by the permanent magnets, thus applying friction and force to the guidewire passing through.

Proof of Concept

For initial testing purposes, a large scale basic catheter hub prototype with an electromagnetic actuator was developed, measuring 35mm x 25.4mm x 25.4mm (H x L x W) as shown in Figure 4.21. The purpose of testing with the hub prototype was to investigate if it would be possible to recreate the resistance effect by applying force/friction to the

Table 4.13: Comparison of resistance effect felt between J wire and Hydrophilic wire using the Hub Actuator approach

Voltage (V)	Current (A)	J wire	Hydrophilic Wire
0	0	0	0
5	0.089	0	0
10	0.184	0	0
15	0.276	3	4
20	0.361	4	5
25	0.443	5	6
30	0.505	6	6

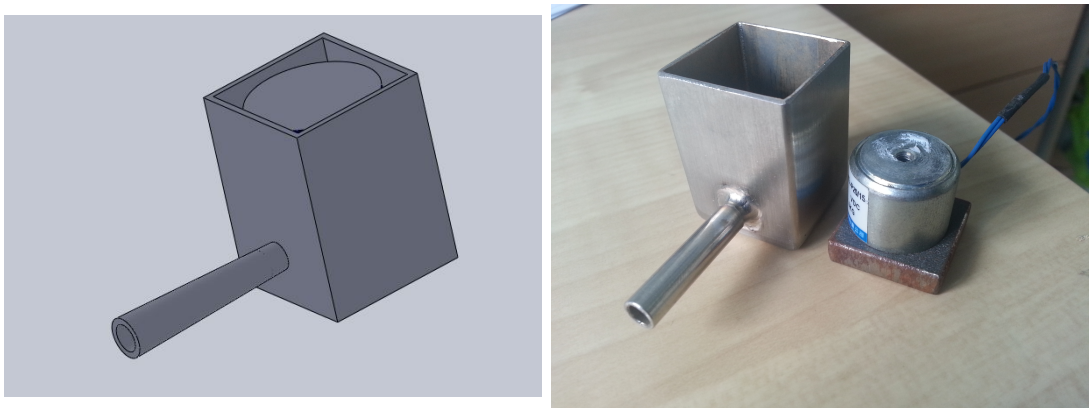

(a) (b)

Figure 4.21: (a) Design of catheter hub measuring 35mm x 25.4mm x 25.4mm (H x L x W) (b) Prototype catheter hub with electromagnetic actuator

guidewire from within the catheter hub. The resulting clamping effect was evaluated qualitatively in a series of experimental tests, where a guidewire was inserted into the hub and the resulting force actuated on the wire rated according to Table 4.11. The test was repeated for different levels of voltage and current supplied, and also with two different guidewire types. The results of this test are shown in Table 4.13. There is no effect felt on either wire until V=15 V, I=0.276 Amp, when the force felt is *Light* and *Moderate* for the J and hydrophilic guidewire, respectively. The strength of the force felt increases gradually with the increase in Voltage/Current until the maximum point is reached (*Very Strong*) when V=30V, I=0.505 Amp for the J wire, and V=25 V, I=0.443 Amp for the hydrophilic wire. At this point, the guidewire becomes unmovable due to the clamping effect of the actuator.

These findings indicate that it is possible to create varying levels of resistance through this actuator. However, the modifications made to the catheter hub add significant weight to the catheter, which drastically changes the feel of the instrument, especially during rotational movements. Therefore, the main challenge is to develop a custom actuator hub that is specifically designed to produce a suitable resistance, while also replicating the feel, weight, and controllability of the original catheter at an acceptable level. Efforts to develop such an actuator are described in detail in the next section.

4.2 Hub Actuator Development

In this section, the design process involved in the development of the haptic interface prototype is described. The novel key component of the prototype featured here is the hub actuator, which was designed specifically for the application of force to the guidewire from within the catheter hub to generate the feel of translational resistance. In the next subsection, the mechanism and implementation of the actuator in its different iterations are explained. This is then followed by a description of how the actuator integrates with the other components (ie. sensor/actuators/controllers) to form a working haptic interface prototype.

From the proof of concept tests detailed earlier in the chapter, it was established that it is possible to use an actuator to exert force onto the guidewire from within the catheter hub, in order to produce a strong resistance effect. In addition, the generated force can be varied in magnitude and the maximum force was found to be sufficiently strong as to resist guidewire movements completely. However, the proof of concept tests used an off-the-shelf electromagnetic actuator that was too large and heavy to be embedded within the catheter without affecting its weight and feel. Thus, the aim is to design and implement an actuator that fits within the actuator hub and has the ability to provide the necessary level of force to the guidewire. This presents the main design challenge, which is to achieve an acceptable balance between size constraints and the force output requirements of the actuator.

First Design Iteration

The hub actuator was designed based on the moving copper coil casing (hereafter referred to as coil casing) concept. The actuator features a ferromagnetic steel frame with a channel for the guidewire to pass through inside its middle shaft. In its first iteration, the actuator consisted of 3 segments, where each segment has two slots for the placement of permanent magnets and the coil casing (Figure 4.23(a)). For each segment, there are also two small openings on the top and bottom surface of the middle shaft, which is meant to enable the interaction of the coil casings with the guidewire. The frame was constructed from individual parts that were manufactured using machining techniques and the coil casing was fabricated with 3-D printers.

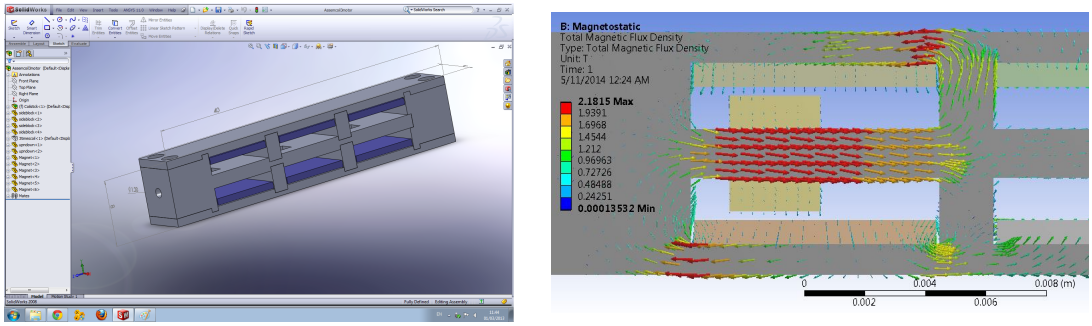

(a) (b)

(b)

Figure 4.22: The three segment actuator prototype (a) modeled in Solidworks, (b) simulated for flux density in ANSYS and (c) after fabrication

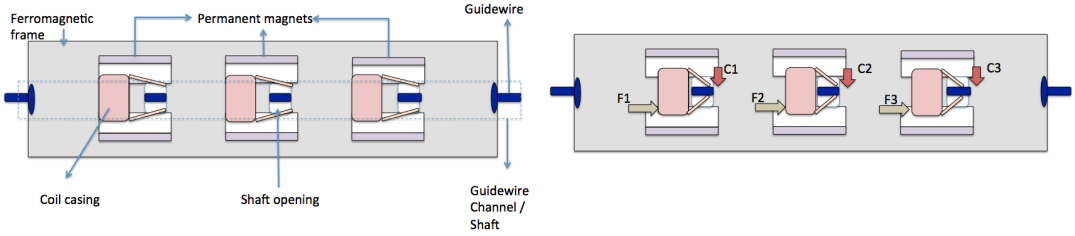

(a) (b)

Figure 4.23: Three segment actuator in (a) Off position and (b) On position

A pair of permanent magnets are placed in each top and bottom slot of each segment whereas the coil casing is placed on the middle shaft. The polarities of the magnets are arranged in such a way that, when the coil is supplied with current, the electromagnetic field produced reacts to the magnetic field of the permanent magnets and pushes the coil casing towards the slots on the shaft openings. The coil casings would then produce a resistance effect to guidewire movement by putting pressure or friction on the guidewire. The operating mechanism of this actuator is illustrated in Figure 4.23(b). The resulting electromagnetic force (F1, F2 and F3) pushes the coil casing towards the shaft opening, resulting in pressure being applied onto the guidewire via a pair of coil casing arms that flex inwards (C1, C2 and C3), thus generating the resistance effect.

The actuator was designed with specific size and force output requirements established earlier in mind. It features a long and horizontal profile, measuring 8mm x 6mm x 40mm (H x W x L). Also, the direction of actuator movement is perpendicular to the direction of actuated force. This feature is important to minimise the width and height of the actuator. The ability to activate each of the three segments individually gives it the flexibility of producing either a strong (when all segments are activated simultaneously) or subtle resistance effect (when only one or two of the segments are activated).

The dimensions of the three segment actuator were selected based on the results of FEM simulation performed in ANSYS (Figure 4.22 (b)). From the simulation, each segment (with the chosen dimensions) is estimated to be able to produce around 0.5 N of force upon activation (when current is supplied), which drives the actuation of the coil casing. These would result in the target 1.5N force when all three individual segments are activated simultaneously.

Initial tests conducted with the three segment actuator revealed several shortcomings. Firstly, the actuator was found to be too long and this made the catheter difficult to manipulate, especially for rotational movements. Secondly, the sliding coil casing did not exert enough force on the guidewire. Whilst the force produced by the electromagnetic field manages to push the coil casing onto the guidewire, there is no resistance felt on the wire, even when all three segments are activated. One possible explanation for this is that the magnetic force generated by the actuator during testing is weaker than the magnetic force that is expected through simulation. This could be due to a number

of factors such as different materials used, as well as the tolerance values in the dimensions of the instruments or equipment used. The other possibility is that the magnetic force generated with the actuator could actually be similar to the force simulated, but the lack of any resistance effect on the guidewire is due to the ineffectiveness of the coil casing arms to exert force or produce friction on the guidewire. The smooth surface of the guidewire and the flexibility of the coil casing arms (made of plastic) could also be major factors to why this coil casing design did not produce the expected effect. This suggests the need for a specialised braking mechanism that can translate the horizontal motion of the copper coil casing into a downward thrust/force that brakes and resists guidewire movements.

Second Design Iteration

A second iteration of the hub actuator featured only two segments (Figure 4.24(a)) in order to reduce the overall dimensions (Figure 4.24(b)). However, this would also reduce its total output force. To compensate for this, the two segment actuator has more space between the middle shaft and the top and bottom shafts, allowing for a larger copper coil around the middle shaft, which should produce a stronger electromagnetic force when current is supplied. The final dimensions of this actuator are 12mm x 20mm x 6mm (H x L x W).

Another significant modification was the removal of the column separating the two segments, which enabled the use of more varieties of copper coil designs, such as using two copper coils around a single casing for combined actuation, instead of being restricted to single copper coils as in the previous design. This changes the flow and density of the magnetic flux and was shown through simulation (Figure 4.25) to be able to match and even surpass the force output of the actuator with certain parameters set.

Similar to the previous three segment design, this actuator can be controlled in an ON / OFF manner. By applying current to the coil in one direction, the coil casing will be pushed to one side (i.e. braking the guidewire movements). When the current direction is reversed, the coil casing will be pushed to the other side (i.e. disengaging the brake on the wire). The redesign managed to address the size issues of the three segment actuator, while maintaining the level of force output required. However, as discussed previously, generating a strong electromagnetic force does not directly produce a strong resistance effect to guidewire movement. A brake is needed to translate the

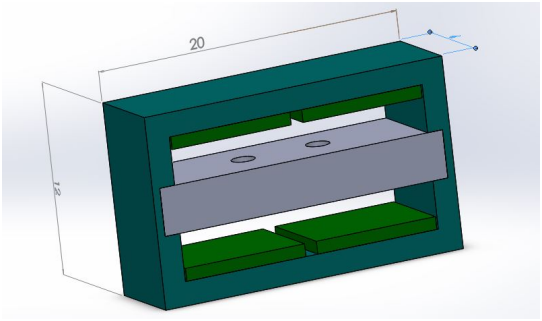

(a)

(b)

Figure 4.24: Two segment actuator (a) Modeled in Solidworks and (b) Comparison with three segment actuator and the catheter hub

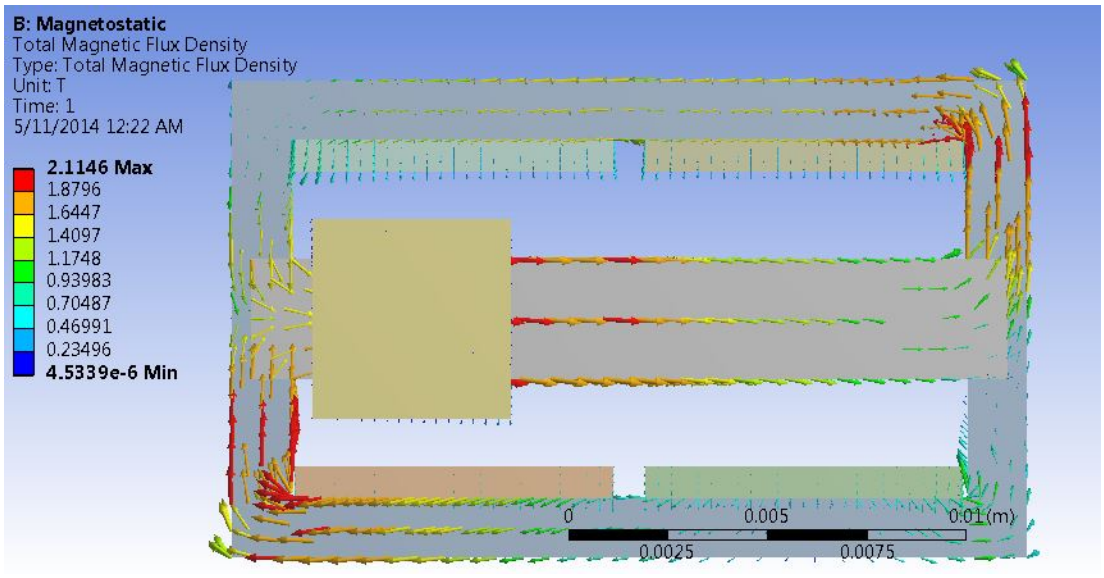

(a)

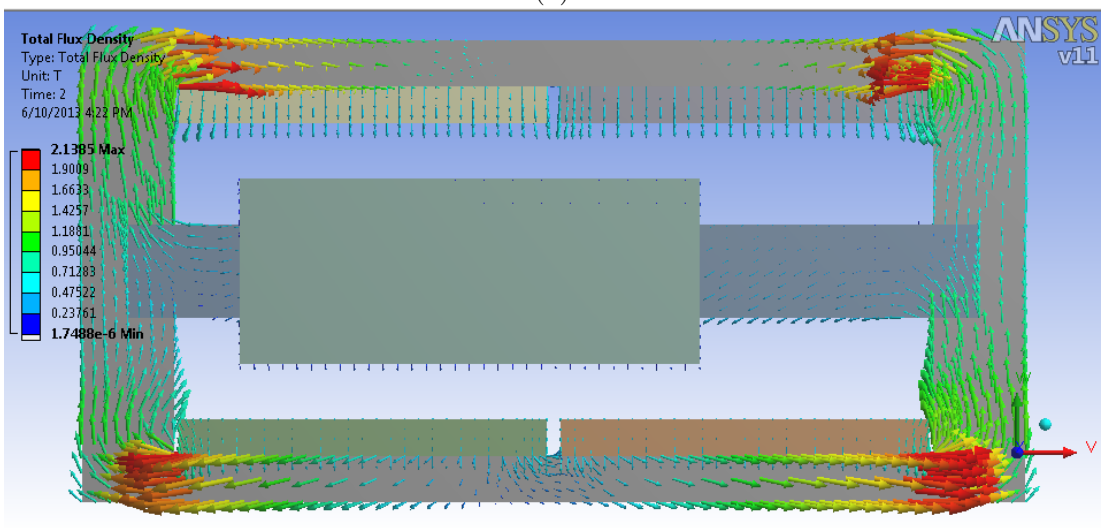

(b)

Figure 4.25: Two segment actuator simulated with (a) Single coil casing and (b) Dual coil casing

strong horizontal force pushing the coil casing into a downward force on the guidewire, resulting in a resistance effect.

Braking Mechanism and Coil Casing

A plastic sphere (made of Delrin) was considered to be a good candidate for such a brake since it is not deformable/malleable, light and effective in any direction of movement. In order to brake the guidewire with the plastic spheres, the coil casing had to be redesigned to perform several tasks. First, the coil casing had to secure the sphere within the opening of the middle shaft at all times. Second, when deactivated, the coil casing must give the sphere room to move freely with the guidewire to prevent any unwanted resistance. Third, when activated, the coil casing must push the sphere onto the guidewire with enough force to create a resistance effect.

Several coil casing designs were tested before an optimal design was identified. There was some variation in the design of the coil casings, but the principle remained the same. Every coil casing features a pair of arms that keep the sphere in the opening of the shaft (fulfilling the first required task). While the specific tips and edges of the arms are different for each design, they are all shaped at an angle so that, as the coil moves horizontally during activation, the sloping edge and/or tip of the arm will push the sphere onto the guidewire (fulfilling the third task). In addition to keeping the sphere in place when the actuator is deactivated, the sloping arms also give room to the sphere to move within the shaft opening (fulfilling the second task). Figure 4.26 shows a sample of the different arm designs considered for this application. From these, the sliding arm in Figure 4.26 (c) was chosen to be most suitable as it was shown through experimental testing to perform all of the required tasks best, especially the application of force to the guidewire.

Four braking mechanism designs were considered (Figure 4.28) and tested for the implementation of the sphere brake. Only the brake mechanism was changed between tests with all other parameters, such as the number of turns on the coil casing and the current supplied, were kept constant through the different tests.

The tests involved moving the guidewire while each brake was activated and rating the level of resistance felt on the wire (if any). The findings of the tests are summarized in Table 4.14. While testing the effectiveness of each braking approach, it was discovered that the guidewire - brake interaction is more complex than was initially thought. The

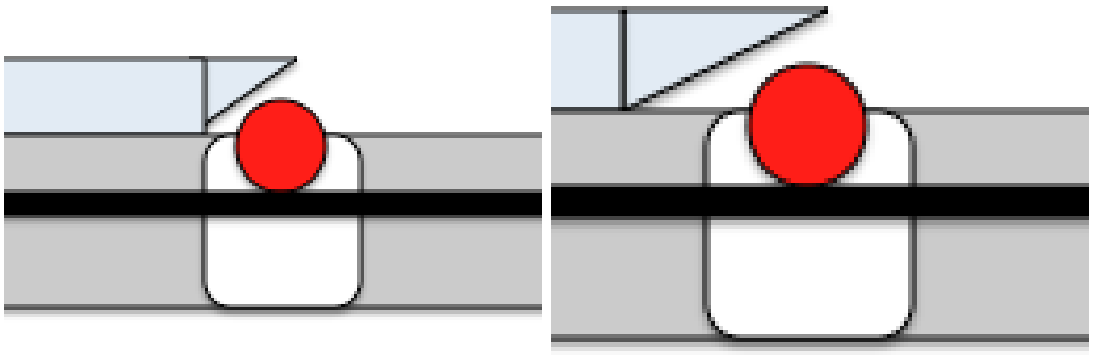

(a)

(b)

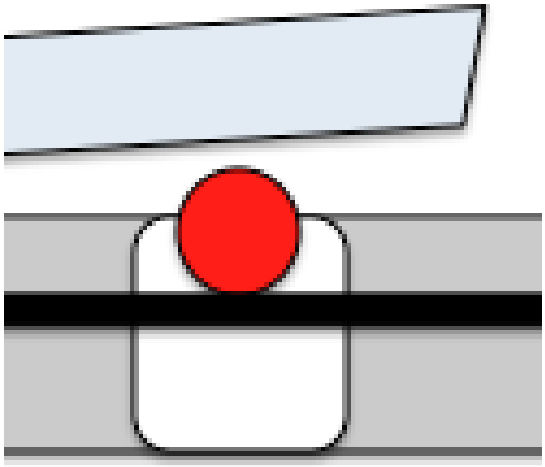

(c)

Figure 4.26: Coil casing arms designs considered

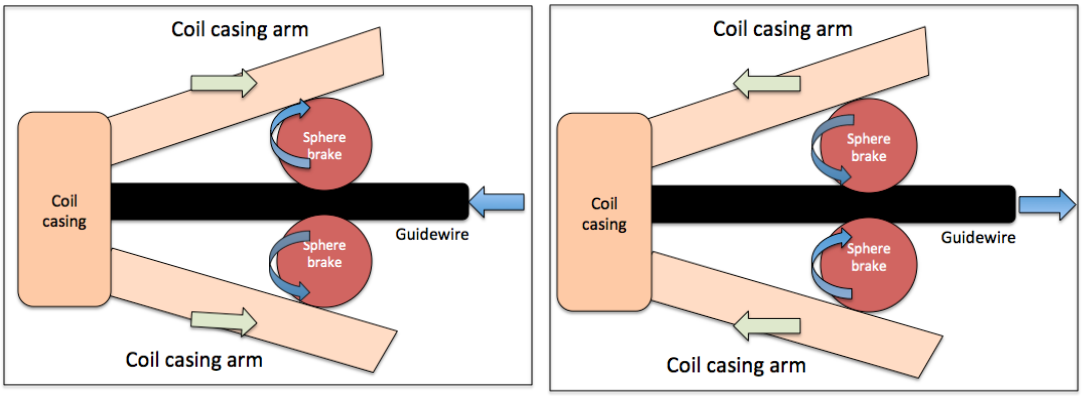

(a) (b)

Figure 4.27: The (a) pulling and (b) pushing effect on the coil casing resulting from the actions of the sphere brake and guidewire

Table 4.14: Comparison summary of different braking mechanisms tested

Brake mechanism	No. of coils	No. of brakes (pairs)	Brake location	Resistance
A	1	1	Center	Strong
B	2	1	Center	Very Subtle
C	2	1	End	Subtle
D	1	2	End	Very Subtle

spheres do not simply brake the guidewire when activated, and roll along with the wire when disengaged. Instead, wire movements cause the spheres to rotate, which would in turn push the coil casing away (releasing the brake) or pull it closer (engaging the brake).

This interaction heavily influenced the resistance felt during the tests, where the only significant level of resistance was felt with brake mechanism A (Figure 4.28. This was because only brake mechanism A allows for the coil casing to be pulled closer (due to the added space at the shaft end) when the guidewire is advanced, thus engaging the brake fully. This in turn pushes the spheres into the channel and pins the guidewire against the inner wall of the shaft, creating the strong resistance effect (Figure 4.27(a)). When the guidewire is pulled, the spheres will rotate and push the coil casing, which in turn will release the guidewire from being clipped (Figure 4.27(b)). The other three brake mechanisms only managed to produce subtle resistance.

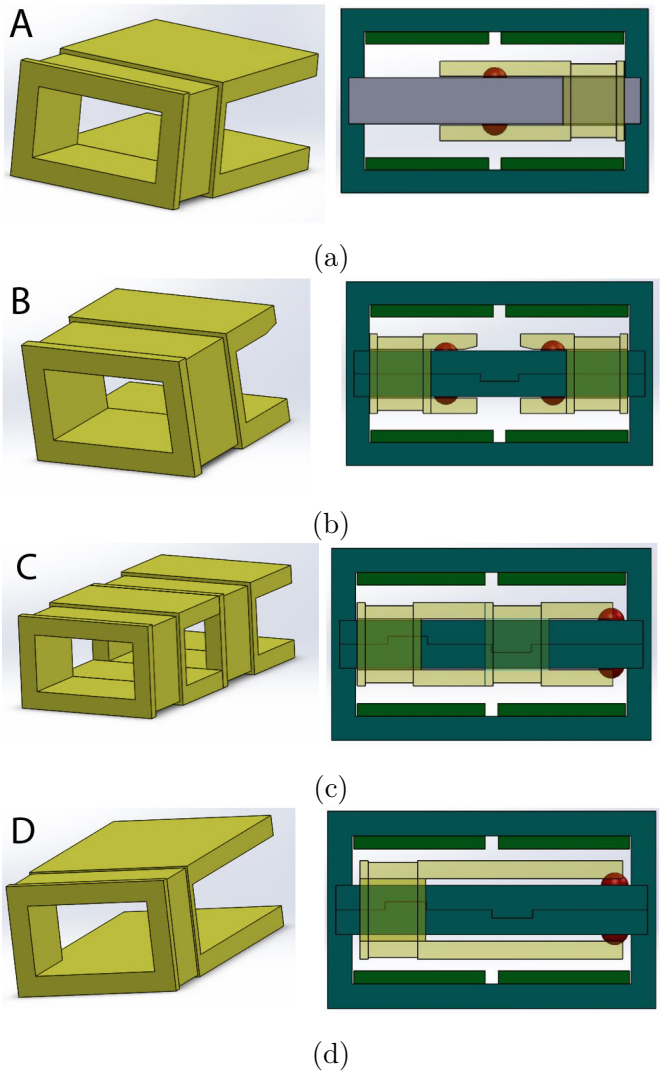

Figure 4.28: Coil casing and actuator design featuring (a) Single coil and single central brake pair (b) Double coils and double central brake pairs (c) Double coil and single end positioned brake pair and (d) Single coil and single end positioned brake pair

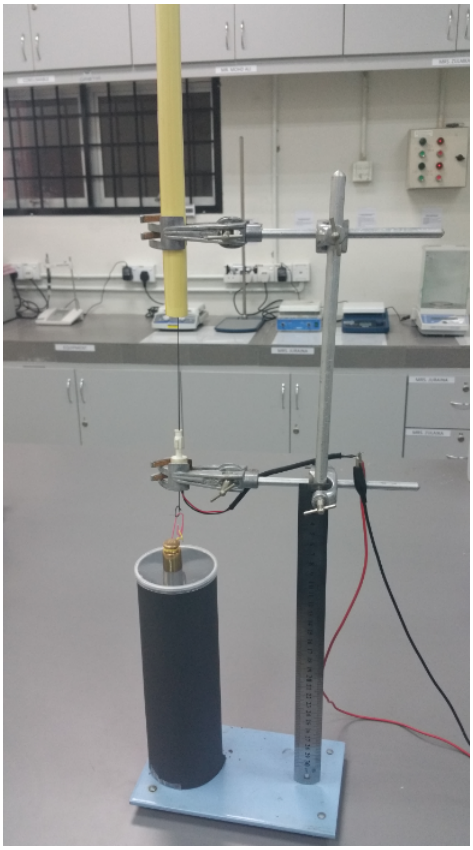

Figure 4.29: Setup for measuring the resistance provided by the activated actuator

Thus, brake mechanism A was selected as the most suitable design as it has managed to produce the most significant level of resistance. The chosen mechanism was then assembled together and used in a pilot test with a senior cardiologist registrar. In the pilot test, the participant (the cardiologist) was asked to move the guidewire as the actuators were activated. He was then asked to provide feedback on the resistance effect produced and how it felt compared to real life instrument resistance. After testing, the participant confirmed that the resistance effect generated by the actuator was distinctively noticeable and resembles its real life counterpart.

4.2.1 Actuator Resistance Measurement Test

Feedback from the initial qualitative tests performed indicated that the actuator hub design has potential to generate resistance haptic effects. In order to determine the

range of resistance forces that it can apply, an experiment was performed using the setup shown in Figure 4.29. The actuator hub was placed in the gripper on the lower arm of the retort stand while a tube is placed in the upper arm. A guidewire is then passed through the tube (needed to keep the guidewire straight) and into the actuator hub. Calibrated weights were then attached to the guidewire tip, pulling the guidewire downwards (with a quantifiable force F=mg). A cylindrical block was placed at the base of the retort stand to serve as a platform to attach/remove weights to/from the guidewire and to release the weights without introducing any additional force. This is done by slowly removing the platform as the weights are kept in place.

The weights attached to the guidewire varied from 10g - 100g, whilst the current supplied to the actuator was kept constant at 0.4 A (the maximum level of current that can be supplied before the actuator overheats) in order to estimate the maximum amount of force or resistance that can be applied by the actuator. The main outcome of the experiment is the observation of whether or not the actuator was able to keep the guidewire from dropping to the base of the retort stand for the given weight attached. If so, this would indicate that the resistance force applied by the actuator was equal to or greater than the pulling force of the attached weight. Otherwise, the force produced by the weights was larger and overcomes the resistance of the actuator. Ten different sets of weights were used and each weight was tested for a total of ten times. The results of the tests are shown in Table 4.15.

In an ideal system, the outcomes for each weight are expected to be consistent (e.g. the actuator always holds the 50g weight in place and the 60g weight always drops to the bottom). However, as shown in Table 4.15, such results are difficult to achieve with the prototype actuator, given the limitations of its manufacturing process. For example, the coil casing had to be shaped manually with files to obtain the required dimension and shape since the 3D printing technology used did not have the level of resolution needed. This causes the coil casing to be asymmetrical (between its top and bottom arm/wing), which contributes to the variability of the maximum force applied. The plastic spheres used as brakes in the actuator were also potentially asymmetrical since these are manufactured with a tolerance value, which although relatively small, could have a large impact on the mechanics of the system.

Nevertheless, the findings in Table 4.15 can be used to estimate the resistance force output of the actuator by identifying the most frequently occurring (i.e. the

Table 4.15: Findings of actuator resistance measurement test (A "✓" signifies that the weight is held whereas a "×" signifies that the weight drops to the bottom.)

Weight (g) / Run	1	2	3	4	5	6	7	8	9	10
10	✓	✓	✓	✓	✓	✓	✓	✓	✓	✓
20	✓	✓	✓	✓	✓	✓	✓	✓	✓	✓
30	✓	✓	×	✓	✓	✓	✓	✓	✓	✓
40	✓	×	✓	✓	✓	✓	✓	✓	×	✓
50	×	✓	×	×	✓	×	✓	✓	×	×
60	×	✓	×	×	✓	✓	×	✓	×	×
70	✓	×	×	✓	×	×	×	×	×	✓
80	×	×	✓	×	×	×	✓	×	×	×
90	×	×	×	×	×	×	×	×	×	×
100	×	×	×	×	×	×	×	×	×	×

mode) outcome for each weight applied. The mode outcomes for each applied weight is summarised in Table 4.16. 100% of tests performed with weights 10g and 20g resulted in the guidewire being held in place. It remains the mode outcome as the weights are changed to 30g and 40g with 90% and 80% occurrence respectively. However, the mode outcome switched, from 50g onwards, where the weights begin to drop to the bottom with greater frequency. The percentage of such occurrence increases from 60% with the 50g and 60g weights, to 70% with 70g, 80% with 80g and 100% with weights 90g and above. Thus, based on the transition in the mode outcome (from the weights being mostly held, to being mostly dropped) between weights 40g and 50g in the tests, it can be estimated that the maximum resistance force output by the actuator is within the range of 40g-50g or 0.3923 N - 0.4903 N (with F=mg using g=9.806). It is considered feasible that, having obtained proof of concept in this work, the actuator (and its components) could be manufactured with greater precision in the future to improve the consistency of its performance. The next section presents the integration of the hub actuator into the prototype haptic interface system.

4.3 Haptic Interface System

This section presents the integrated haptic interface system including both *sensors* and *actuators*. First, the sensors and actuators utilised in the prototype are described

Table 4.16: Outcome summary for individual weights based on mode value (A "✓" signifies that the weight is held whereas a "×" signifies that the weight drops to the bottom.)

Weight (g)	10	20	30	40	50	60	70	80	90	100
Weight held %	100	100	90	80	40	40	30	20	10	0
Weight drop %	0	0	10	20	60	60	70	80	90	100
Mode outcome	✓	✓	✓	✓	×	×	×	×	×	×

(a) (b) (c)

Figure 4.30: The sensors used in the prototype (a) Roller ball sensor (b) Parallax Inc trackball and (c) Paralllax Inc optical sensor

individually in their respective subsections. Then, the *system* subsection explains how these components are integrated in the prototype to form a working system.

4.3.1 Sensors

The sensors component performs a vital function as its role is to continuously track the position and orientation of the instruments used with the prototype. It comprises three different types of sensors. A roller ball sensor was used to track the movements of the catheter (Figure 4.30(a)). This sensor was found to be most reliable since the roller ball surface grips the surface of the catheter without creating a noticeable resistance. A second, trackball sensor (Parallax Inc) similar to those used in smartphones (Figure 4.30(b)) was mounted to track the movements of the guidewire outside the catheter. Lastly, an optical sensor (Parallax Inc) resembling that found in an optical mouse (Figure 4.30(c)) was used for concentric tracking of the guidewire. This follows the proof of concept tests performed previously, which established that the concentric

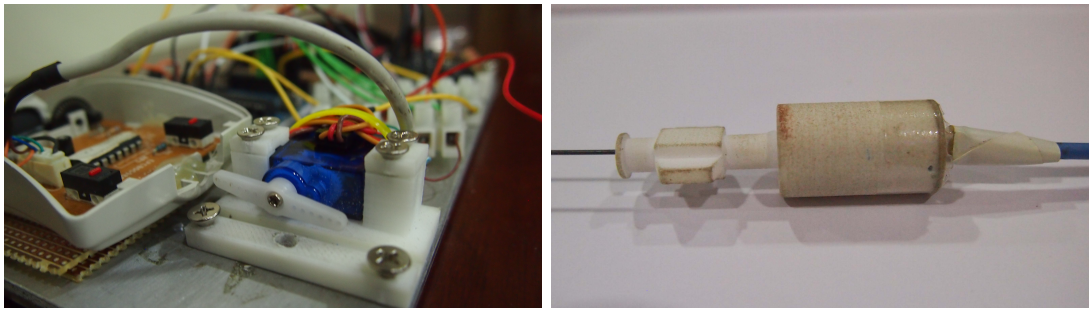

(a) (b)

Figure 4.31: Actuators implemented into the prototype interface (a) Servo motor and (b) Custom hub actuator

tracking approach was feasible after modifications were made to the instruments.

4.3.2 Actuators

Since haptic feedback is required for both the guidewire and catheter, two actuators are used in the prototype. One of them is a popular option in the literature reviewed, a servo motor, which is used to apply force and resistance to the catheter. Depending on the required level of force, the servo motor arm will rotate to a set position to clip the catheter (Figure 4.31(a)). The concentric occlusion issue makes it more difficult to apply force to the guidewire whilst inside the catheter. Thus, the need for a second actuator - the hub actuator described earlier. While the current version of the hub actuator does not yet fit inside a true catheter hub, a customised catheter hub with larger dimensions, but without significantly affecting the weight and feel of the instrument was designed and 3D printed (Figure 4.31(b)). The servo motor runs its power directly off the Arduino board. However, the hub actuator, operates at 0.4 A and needs a connection to a power supply to be activated.

4.3.3 Integrated System

The integrated haptic interface system features a multi port design (Figure 4.32.), where instrument insertion and/or interaction occurs at one or more ports. Several factors led to the implementation of this design:

i. The need to implement the concentric guidewire tracking approach to obtain proof of concept

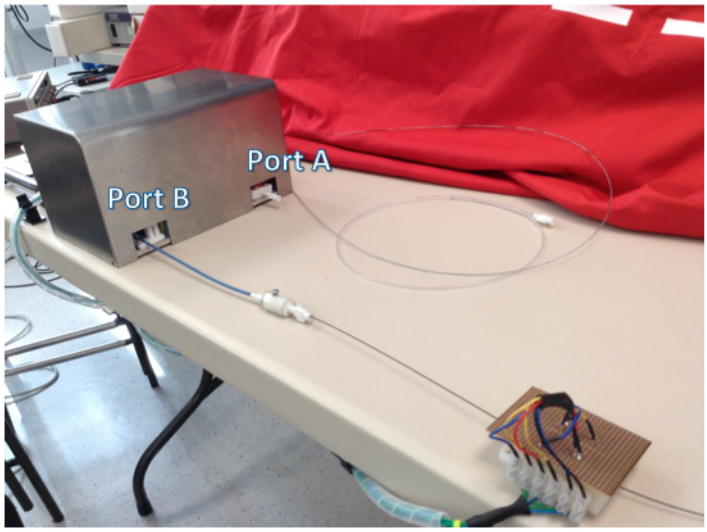

Figure 4.32: Haptic interface prototype with Port A and Port B highlighted

ii. The need to implement the actuator hub approach to obtain proof of concept

iii. The need to allow for the practice of the correct sequence of interventional procedures: starting from initial insertion of the guidewire into a major artery, to the advancement of the instruments to reach a target point in the vasculature.

There is a conflict between the second and third factors described. In order to implement the actuator hub approach, the catheter hub needs to be tethered to a power supply and a micro controller. It also requires the catheter to be pre-inserted into the prototype since it is wired to the micro controller at the tip of the catheter. These current restrictions make it impossible to perform the procedures of initial guidewire insertion and instrument exchange in a single port.

Therefore, a two port design was used to meet all of the three requirements. The first, Port A, is designed to accommodate for procedures such as initial guidewire insertion and instrument exchange. Also, since these procedures often involve the movement of one instrument at a time, the concentric tracking approach is most suited for implementation in Port A. On the other hand, Port B is designed to accommodate the key step of manipulating both instruments to a target vessel. The hub actuator approach is implemented at Port B since this stage of the intervention involves interaction with

smaller diameter vessels and vessels that may have lesions/plaques where haptic feedback is necessary. Ideally, in future work, the instrument ports must be improved so as to enable haptic feedback to be applicable at any point in simulation since tactile sensations are vital indicators of potentially hazardous collisions that can occur at any stage of a procedure. This is particularly relevant during the initial guidewire insertion stage.

The multi port design enables the practice of the following instrument manipulation steps:

i. *Initial guidewire insertion*: The simulation in this work does not facilitate the needle puncture process, which has been previously undertaken by [29, 124]. Instead, it takes place at the end of the vessel puncture process and the beginning of the initial guidewire insertion stage. For this reason, a mock "needle" (in the form of an introducer sheath) is already pre-inserted in Port A and the hub of the "needle" can be seen in Figure 4.32. While a wide-bore needle could also be used (to improve face validity), an introducer sheath was used at this stage for safety reasons. The introducer sheath is used to facilitate the advancement of the guidewire through the needle and the removal of the needle later on. As the simulation begins, the operator is prompted to insert the guidewire through the needle into Port A to a certain pre-determined insertion depth (Figure 4.33(a)). Upon insertion, guidewire movement is tracked by the optical sensor (Sensor 1) on Port A. Once the guidewire reaches the desired insertion depth, the simulation program prompts the operator to pull out the needle, while leaving the guidewire inside the patient.

ii. *Catheter sheath over guidewire and catheter insertion*: The operator will then be prompted to sheath a catheter over the guidewire in Port A. The catheter is then inserted into Port A, while the guidewire is held firmly in place (Figure 4.33(b)). The insertion depth of the catheter is measured by a trackball sensor (sensor 2). Once the desired insertion depth is reached, the operator will be directed to the next step.

iii. *Guidewire and catheter navigation to target vessel*: The operator will be instructed to switch to Port B and all sensors and actuators on Port A will be deactivated.

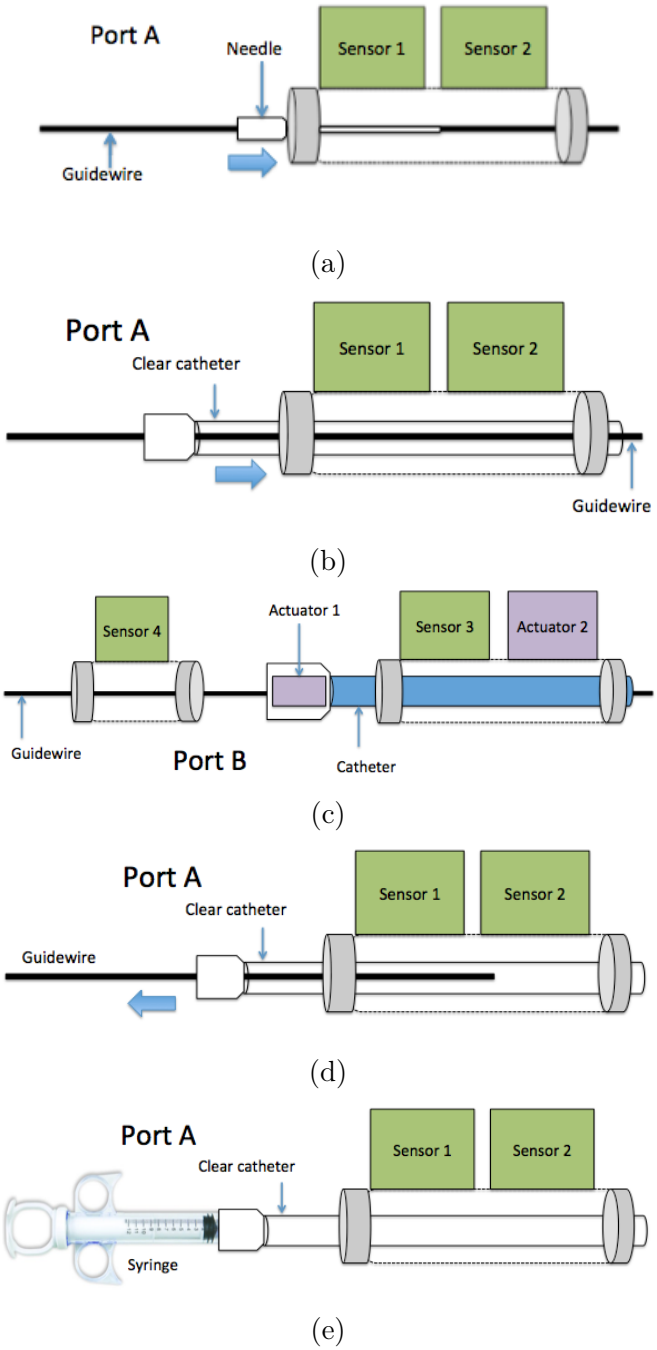

Figure 4.33: Illustration of the instrument configurations with the multi port interface (a) Initial guidewire insertion (b) Catheter sheathing over guidewire (c) instrument navigation to target vessel and (d) instrument extraction and (e) dye injection

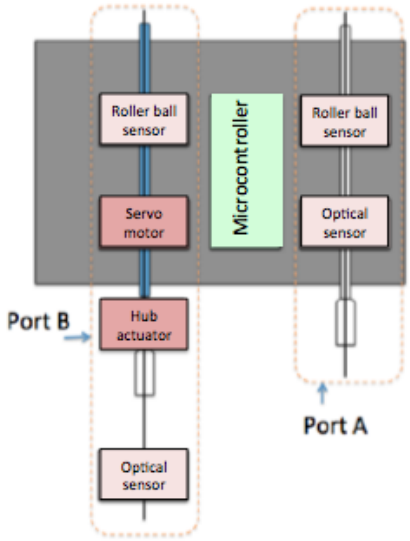

Figure 4.34: Layout of components for the prototype interface

Figure 4.33(c) shows the pre inserted catheter and guidewire on Port B, following the previous steps in the procedure performed at Port A (i.e. both instruments inserted at a certain depth). The operator will then be prompted to move the guidewire and catheter to the target vessel. The catheter and guidewire are tracked by Sensor 3 and Sensor 4 respectively. When activated by the simulation software, Actuators 1 and 2 will provide force and haptic feedback to the guidewire and catheter, respectively. Once the branch of the target vessel is reached, the next step will be prompted.

iv. *Guidewire extraction and dye injection*: Port B is deactivated at this point and Port A reactivated. The operator will be instructed to pull out the guidewire inserted in Port A (Figure 4.33(d)) and attach a syringe to the catheter in order to inject contrast agent as necessary (Figure 4.33(e)). Pressing a foot pedal will capture simulated radiographic images displayed on a screen. Once this task is completed, the operator will be instructed to remove the syringe and reinsert the guidewire into Port A and repeat steps (iii)-(iv) as necessary.

Figure 4.34 shows the arrangement and layout of sensors and actuators used in the prototype. As mentioned previously, this prototype is designed with a focus on training

the core skills of endovascular interventions: the manipulation of the guidewire and catheter to advance from the insertion point (often at the femoral artery) to the target vessel (e.g. coronary artery or renal artery). Port B of the prototype is dedicated to the task of tracking the movements of and applying haptic feedback to both instruments at this simulated stage of intervention. This is performed by the combination of two sensors and two actuators placed in Port B. However, Port A is meant to facilitate auxiliary tasks such as initial insertion of the guidewire and instrument withdrawal/exchange. Due to time constraints, haptic feedback was not implemented for the tasks in Port A, which feature only sensors and not actuators. This does not imply that these auxiliary tasks can be considered unimportant, but rather, they were not the main focus of the present prototype. Therefore, the aim of the implementation of Port A in the prototype is (1) to provide a platform that allows for the performance of initial guidewire insertion and instrument exchange (albeit without haptic feedback), and (2) evaluate SMEs receptiveness to the multi port approach that can potentially be expanded in future work to include more complex tasks such as needle puncture and/or supporting complex, multi port interventions.

The sensors in Port A are a roller ball sensor for tracking catheter movements and an optical sensor for tracking concentric guidewire movement. A silver painted hydrophilic guidewire (from the preliminary testing) is used with a clear catheter to enable this tracking technique. This dual sensor combination has shown to provide good tracking performance in previous tests, despite the fact that it does not allow for simultaneous tracking of guidewire and catheter. This is because, once activated, the optical sensor is able to sense the movements of both instruments (the catheter and the silver guidewire within the catheter), but is not able to distinguish between them. Thus, the system is programmed to deactivate the optical sensor when the roller ball sensor detects catheter movements. This ensures that the optical sensor will only detect guidewire movements, which is key to the concentric tracking approach. In previous discussions with SMEs (2 Interventional Radiologists and 1 Interventional Cardiologist), it was concluded that the lack of simultaneous instrument tracking for the tasks at Port A would not be a major issue since the initial manipulations performed mostly involve the movement of a single instrument at any one time. This is especially true for new trainees, who are often advised against simultaneous instrument advancements. Therefore, at this stage, Port A operates within this assumption. In future work, depending on SMEs validation

and feedback, simultaneous tracking can possibly be implemented in Port A by utilizing an optical sensor that is specialized and is able to differentiate guidewire and catheter movements exclusively. Likewise, the concentric tracking approach can also be applied to Port B or any additional ports in the future.

Port B of the prototype consists of a pair of sensors and actuators. Similar to Port A, a roller ball mouse is used to track the movements of the catheter. Unlike Port A, however, the guidewire is tracked using a trackball sensor as the one shown in Figure 4.30(b). The purpose of this sensor is to track the movement of the guidewire outside the catheter, hence it is positioned separate from the main unit close to the proximal end of the guidewire. It is connected by a length of cable (about 30 cm) to the Arduino micro controller within the prototype chassis. The guidewire is pre inserted into the trackball unit and the catheter hub for every procedure. This is in line with its function, which is to facilitate the tasks performed after the instruments have already been inserted into the patient through Port A.

As for haptic feedback, Port B utilises a servo motor to apply force and pressure to the catheter. The orientation of the servo arm can be changed to press onto the catheter directly depending on the level of force required. A custom hub actuator is placed at the proximal end of the catheter (replacing the original catheter hub) in order to apply haptic feedback to the guidewire whilst inside the catheter. The hub actuator is connected to the micro controller and power supply at its distal end. For this reason, the catheter is pre inserted into the prototype. It should be noted that a heat shrink sleeve was used to cover the wiring over the catheter, which removes any potential health risks posed by the current carrying wire. Each of the components in Port A and B are connected to the Arduino micro controller board as its source of power and control signals. The hub actuator uses an additional H bridge circuit to control the direction of the current, which in turn controls the activation of the actuator. The components in the main prototype unit and the wiring that connects them can be seen in Figure 4.35 (a) and (b) respectively.

However, for a majority of interventions, only a single port (or point of entry into a major artery) is used for instrument insertion and manipulation. Therefore, it can be expected that the presence of the two instrument ports and the need to switch between them during simulation would cause a decrease in face validity and affect the immersion of the simulation. Due to this potential shortcoming, the two port approach

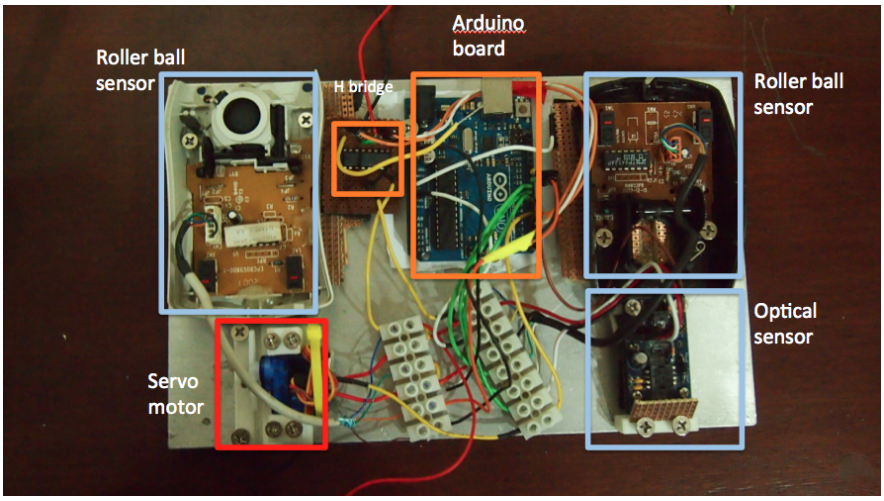

(a)

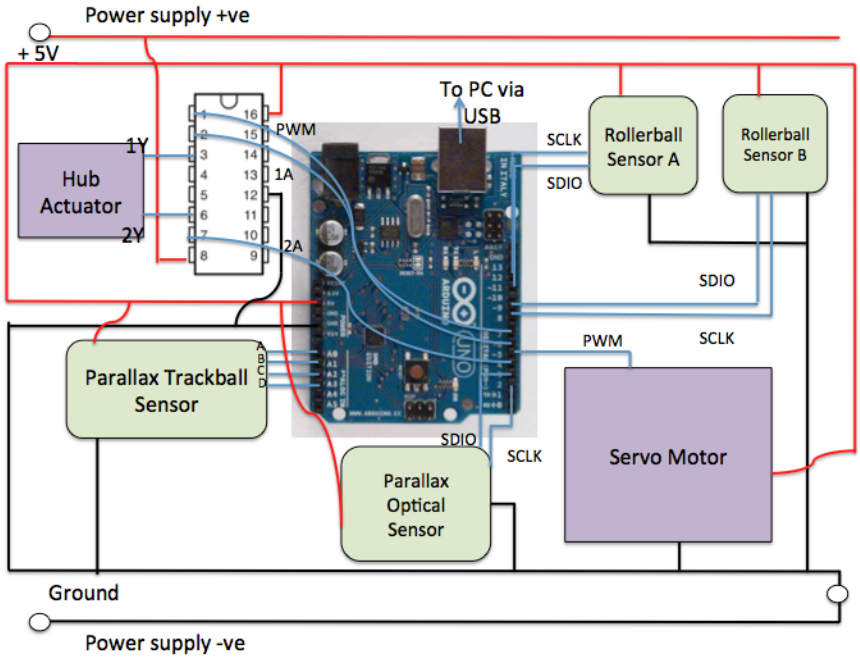

(b)

Figure 4.35: (a) A top down view of the innards of the main prototype unit. Sensors are marked in blue boxes, controllers in orange boxes and actuators in red boxes (b) The circuit diagram of the prototype components

was implemented in the prototype not as a final or optimal solution, but as a means to obtain proof of concept for the novel techniques developed in this project: the concentric tracking approach and the actuator hub approach. Also, through its implementation in the prototype, investigations can be carried out to determine how much it actually impacts face validity and if it can become a useful approach for training and transfer of skill despite this. If found to be useful, then there is the potential for adding further ports if necessary, such as to accurately accommodate the simulation of other interventional procedures. The merits of this design will be tested in the next chapter when the prototype is presented to SMEs for testing and validation.

4.4 Chapter Summary

This chapter began with a series of experimental tests and simulations to investigate several conceptual solutions to the guidewire tracking and haptic feedback issues caused by the concentric occlusion problem when the wire is manipulated inside the catheter. The concentric guidewire tracking approach, which used modified instruments (i.e. translucent / clear catheter and touched-up guidewire) to increase the visibility of the guidewire of the optical sensor, was found to be a feasible approach based on the test results obtained. Experiments for the non contact electromagnetic actuator approach revealed the impracticalities of such approach due to the potentially high level of current required, and possible alterations to the guidewire in terms of both material and dimensions. Interviewed SMEs claimed that this would greatly affect the instrument feel and weight significantly. Notwithstanding, the alternative approach of a bespoke hub actuator was found to be feasible from the experimental tests conducted. The main challenge for this approach is the miniaturisation of the actuator while maintaining the level of force output needed.

Initially, FEM simulations were used to determine the suitable dimensions of the hub actuator. This led to the fabrication and testing of the first actuator prototype with three segments. The flaws of the three segment design (large size, low level of resistance) prompted a second iteration of the actuator with only two segments and an improved coil casing size. Several tests were then conducted to establish the best coil casing and brake mechanism design to apply haptic feedback to the guidewire in an effective, repeatable and reliable manner. A key finding from these experiments was that plastic spheres are

the most effective brakes, while the coil casing with the sloping straight arm is the most effective design compared to other possibilities considered. Quantitative experimental tests were then performed using calibrated weights to estimate the resistance forces produced by the hub actuator with the selected sphere brakes and coil casing design. The test results suggested that the maximum resistance force output by the hub actuator is between 0.3923 N - 0.4903 N.

The components and findings of the proof of concept tests were then implemented into a dual port prototype integrated haptic interface system. The concentric tracking of the guidewire was performed using the optical sensor at Port A, whereas the hub actuator was embedded into the catheter hub of the catheter at Port B. A dual port approach was chosen to test and obtain a proof of concept of the two novel techniques developed in this project. Port A features the concentric tracking approach for procedures such as initial guidewire insertion and guidewire withdrawal before angiography whereas Port B features the hub actuator that will provide resistance to the guidewire when traversing narrowed vessels. Component layout for the two ports is different and specific to the tasks that they are meant to simulate.

In the next chapter, the overall performance of the integrated haptic interface system as part of a simulator for endovascular interventions will be examined, detailing the initial validation study conducted involving several experts interventionists who were asked to rate the performance of the sensing, haptic feedback and two port system approach.

5

Prototype Evaluation and Discussions

In this chapter, the prototype haptic interface is tested in terms of its instrument tracking and haptic feedback performance, as well as its system design. The purpose of the tests is twofold. First, to verify that the sensors can reliably track the instruments and that the actuators are able to generate the desired type and magnitude of haptic feedback. Second, to investigate if the new design can avoid the shortcomings of existing haptic interfaces, and how it might improve upon them.

5.1 Validation Study

A validation study consisting of two stages was conducted. In the first stage, participants were asked to perform a series of interactions using guidewires and catheters using the prototype, based on the context provided via a computer generated 3D virtual environment. Once all the interaction sequences have been performed, the second stage consisted in participants completing a questionnaire to gather their feedback regarding the prototype. The design and methodology of the validation study was reviewed and approved by the Imperial College Research Ethics Committee (ICREC_14_2_9). The hardware equipment, software setup, participants and questionnaire involved are described in more detail in the next section. The chapter then continues with an analysis on the findings of the questionnaire and discussion about the feedback received.

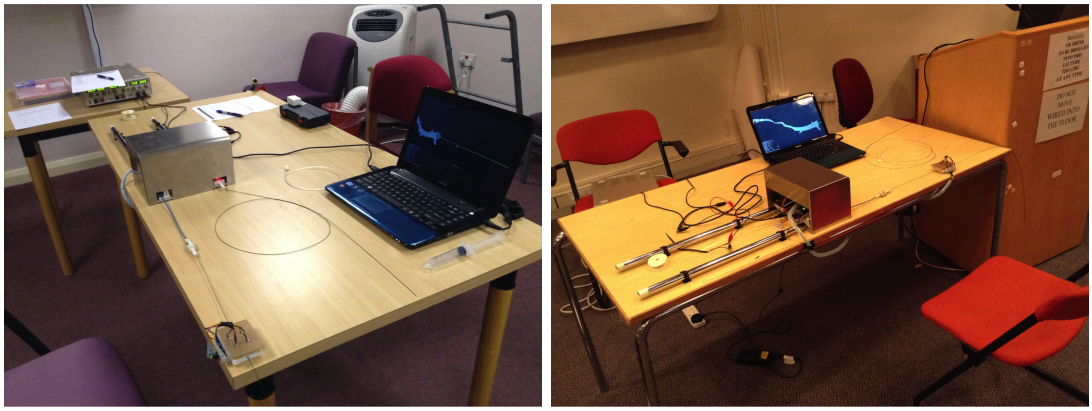

(a) (b)

Figure 5.1: Prototype equipment setup during a test session from the (a) front and from the (b) rear

5.1.1 Prototype Setup

Figure 5.1(a) shows the physical setup of the prototype and its components during one of the validation study sessions. The prototype was arranged along the side of a long table to accommodate its profile and to enable easy access to the instruments during testing. The setup used here was finalised with the assistance of a cardiology SpR, who provided useful advice during pilot test sessions.

One of the discoveries of the pilot test sessions was that, after the instruments exit the prototype, the distal tips of the guidewires and catheters would naturally tend to curl up due to their material make up. This made the instruments very difficult to handle, especially for rotational movements. To avoid this problem, metal tubes were placed at the rear of the prototype to provide a passage or channel that will keep the instruments straight (Figure 5.1) after they exit. This added tubing, and the placement of the external tracker sensor on the right side of the operator causes the prototype to have a long profile.

Two sets of guidewires and catheters were used during the study as shown in Table 5.1. The dimensions and weight of each instrument were obtained by direct manual measurement, whereas the surface friction and level of flexibility were approximated based on the general properties of the constituent material(s). All of the instruments listed here were previously used in the conceptual tests described in Chapter 4. Also, the properties of the instruments were summarised in Table 4.1 with the exception of

Table 5.1: Comparison between the properties of the original and modified instruments

Instrument	Length (cm)	Weight (g)	Diameter (mm)	Friction Coefficient	Flex Modulus (kpsi)
Port A					
Painted hydrophilic guidewire	120	3.51	0.93	>0.060 [119]	>8 [118]
Clear catheter	100	3.39	2	0.22-0.61 [122]	75
Port B					
Hydrophilic guidewire	120	2.75	0.89	0.025-0.060 [119]	8 [118]
Modified catheter	100	16.14	3.00	0.15-0.22 [125]	>78.32

the modified catheter, which was constructed specifically for this study. The modified catheter is the result of the combination of the translucent catheter with a 3D-printed hub containing the actuator developed in this work, as featured previously in Chapter 4 (Figure 4.31(b)). An opening in the hub allows the actuator's wiring to be coiled around the translucent catheter and connected to the Arduino micro controller at the opposite end of the catheter. In order to protect the wiring from damage, a heat shrink sleeve is applied to the catheter and a blue coloured heat shrink was used here to increase its resemblance to an original catheter.

As seen in Table 5.1, due to its construction, the weight and size of the catheter has increased significantly. It is 12.05 g and 12.86 g heavier than the original catheter and the original transparent catheter, respectively (Table 4.1). This is largely due to the actuator hub. In terms of size, it is 1mm larger in diameter than the other catheters previously used in this work (Table 4.1). The modified catheter would also have more surface friction (estimated friction coefficient of 0.15-0.22) compared to the original catheter (estimated friction coefficient of 0.05-0.08) due to the properties of the heat shrink sleeve, which is made from polyolefin. While there is a small but significant increase in friction coefficient, this was deemed acceptable in the context of a proof-

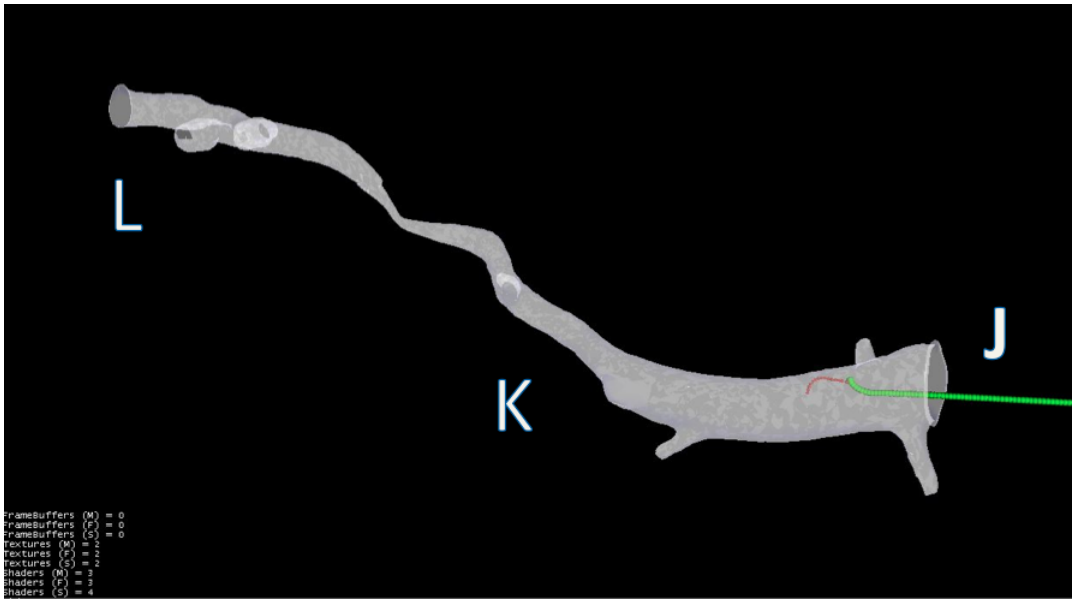

Figure 5.2: 3-D geometry used as instrument pathway in prototype testing [Red = Guidewire; Green = Catheter; Grey = Vascular Anatomy]

of-concept. In addition, the heat shrink has increased the rigidity of the transparent catheter (with estimated flex modulus of 78.32 kpsi initially) since the shrinking has produced a straightening effect. As the purpose of these instruments is to obtain proof of concept and not as final versions of suitable replacements, additional testing to further quantify the differences between them was deemed unnecessary at this stage.

In order to keep the tabletop tidy during use, the actuator prototype connects to the power supply at the far end of the table and the wiring of the external tracker to the prototype is routed underneath the table using cable clips and hooks. At the beginning of the testing, the instruments for Port B are pre-inserted into the prototype, while the instruments for Port A are arranged on top of the table. Finally, a Toshiba laptop with Windows 7 was placed in front of the participants seat. The laptop was used during the study to run a 3D virtual environment (VE) that functions as the visual display of a simulator of endovascular interventions.

5.1.2 Endovascular Simulation

The simulation VE was generated and run in Eclipse, a Java Programming environment, with the purpose of providing a useful and effective way to show the correspondence of movements between the real and virtual instruments, and the translation of haptic cues from the VE into real haptic effects in the prototype interface (Figure 5.2). For this purpose, the rate of physics simulation for the VE was set to 4 kHz, which far exceeds the required rate of haptic interactivity (1 kHz). The protocol of testing involving the VE was as follows:

i. The guidewire (red) enters the vessel at point **J**. It is then advanced to point **K**. Along the way, the wire is rotated to ensure that its tip does not hook into any of the branch vessels leading to point **K** (Figure 5.3(a)).

ii. Upon reaching point **K**, the catheter is then advanced over the guidewire (in real life practice and not depicted within the VE). Next, the catheter (green) is inserted into the vessel at point **J**. It is then advanced to reach the position of the guidewire at point **K** (Figure 5.3(b)).

iii. From point **K**, the guidewire is advanced first, followed by the catheter, while being careful not to move it beyond the guidewire tip. Both instruments are advanced intermittently in this sequence with the goal of reaching point **L**, while avoiding entering other branch vessels located just past point **K** (Figure 5.3(c)).

iv. After successfully progressing past the branch vessel, the operator then encounters a narrowing en route to point **L**. Unlike previous steps, this time the instruments need to be manipulated so that they are able to pass into the narrowing. Once access is gained, the instruments are then advanced through to the final section of the vessel (Figure 5.3(d)).

v. At this final section, the operator was instructed to continue advancing to reach point **L** as the final destination in the vasculature without entering any of the branch vessels. Once this is achieved, the first stage of the test is completed. The operator was then asked to complete the questionnaire and give feedback on the prototype (Figure 5.3(e)).

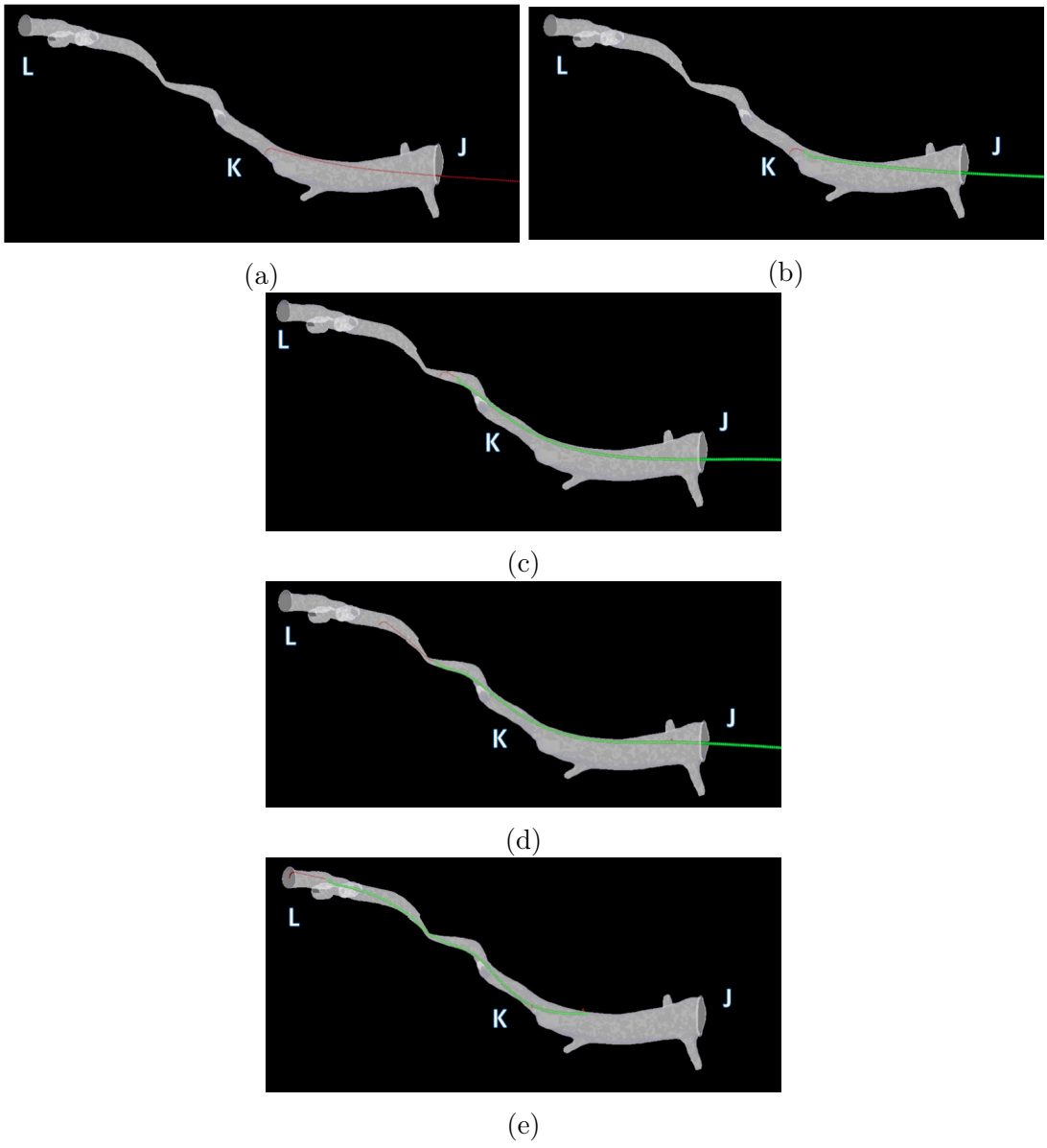

Figure 5.3: Illustration of virtual instruments progressing through the virtual blood vessel in sequence (a) guidewire insertion to point K (b) Catheter insertion to point K (c) Approaching vessel narrowing (d) Entering vessel narrowing (e) Reaching final checkpoint L

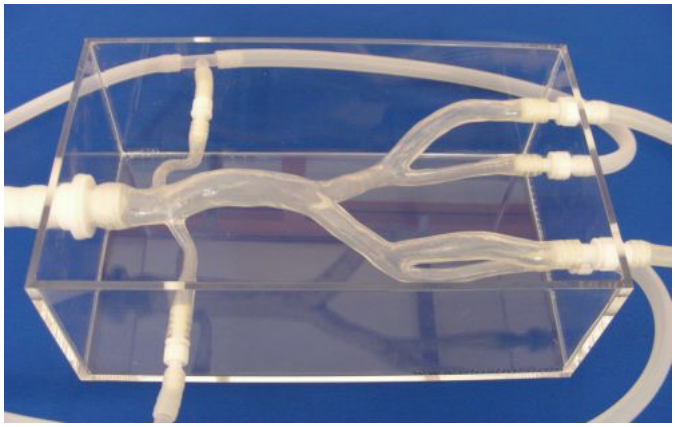

Figure 5.4: Silicone Phantom Vascular Model produced by Elastrat [126]

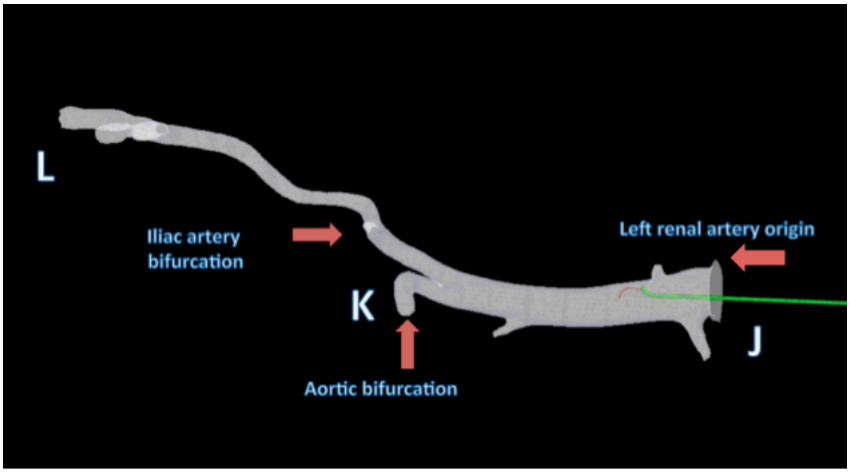

Figure 5.5: 3D geometry scanned in CT and imported into Virtual Environment as a blood vessel and pathway for the virtual instruments

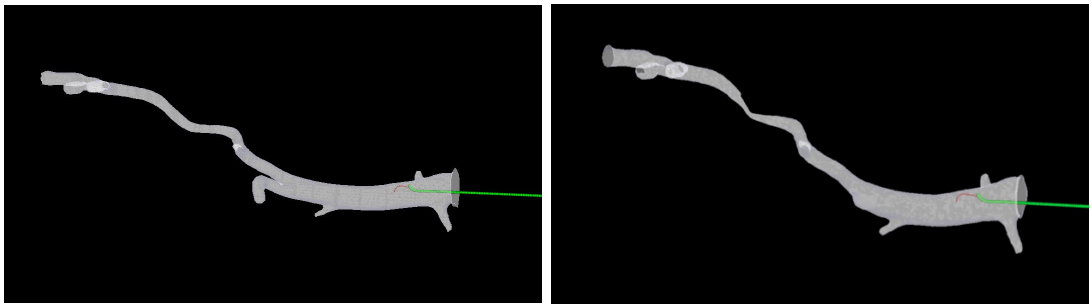

(a) (b)

Figure 5.6: Change in 3D pathway model (a) before and (b) after modification

Virtual Environment

The VE was adapted from previous work in my research group [127]. A silicone phantom vascular model (Figure 5.4) produced by Swiss based company *Elastrat*, was scanned using multi detector Computed Tomography (resolution of 0.53 mm x 0.53 mm x 1 mm). The resulting 3D geometry was imported into the VE. The scanned phantom model corresponded to a large blood vessel in the abdominal region, featuring branch vessels leading to the iliac artery, the aorta and the left renal artery (Figure 5.5). However, this model was modified in *Blender* to accommodate the protocol for the test study as shown in Figure 5.6.

One major change is that the aortic branch vessel has been removed. This was done because progression from point **J** to **K** represents the traversal of instruments in large diameter arteries (i.e. femoral). In certain conditions, haptic cues caused by the presence of unknown atheromatous plaques or stenoses may be felt during this process. These cues would alert the operator to advance the instruments carefully in order to avoid dissection or perforation of the vessel. However, due to time constraints, this feature and haptic feedback in general in Port A could not be implemented in the simulator. Thus, an assumption that the large major arteries are healthy and clear from any obstruction was used for the purpose of the validation tests. In future work, implementation of haptic feedback to allow for plaque interactions in such major arteries should be feasible with the correct application of actuators in Port A. On the other hand, the branch vessels between points **K** and **L** has not been modified as this is meant to challenge the user to rotate the instrument and avoid the instrument tip from entering the branch vessel.

The other major change is that the path from **K** to **L** has been narrowed in such a way that the diameter of the channel or vessel lumen is smaller than the diameter of the catheter. This was in order to simulate natural vessel narrowing due to stenosis or calcified lesions. When passing through this part of the vessel, a significant haptic cue would be dynamically triggered by the simulation software, which is then translated to real haptic effects by the prototype. In most cases, the instruments would need to be rotated to enter the narrowing (stenosis) at the right angle to enable progression to point **L** successfully.

Modelling the blood vessel in the VE was simplified by considering this as a static and rigid geometry. The guidewire and catheter are much more complex to model as they are both mobile and flexible. Such modelling was also based on previous published work within my research group [127].

The instruments (guidewire and catheter) are both modelled as elastic rods, with each rod consisting of a discrete and finite number of nodes or spheres. An elastic rod can be defined as a "curve-like elastic body with one dimension (length) that is much larger than the others (cross section)" [128]. More specifically, the instruments are modelled as Cosserat rods, i.e. "Non linear elastic rods with an orientated centerline, enabling the modelling of bending and twisting deformations" [127]. The reader is referred to [127] for a more detailed explanation of the underlying mathematical model.

In the VE, each rod is made up of 200 discrete nodes. The nodes of the guidewire rod are bound to the constraints of the catheter rod. Increasing the amount of discrete points that make up each rod would possibly improve the realism of each instrument's behaviour, but this would also increase the computational complexity of the VE and introduce significant lag. Therefore, this number of nodes was chosen as it was found to produce a good balance between behaviour realism and performance.

The position of the last node of the rod (located at its proximal end) within the 3D space of the VE can be set manually (Figure 5.7). However, aside from manual designation, the position of the node can also be determined by offsetting its initial position with displacements in translational and rotational directions. This technique is used to link the virtual instruments with the real instruments manipulated through the prototype haptic interface.

When the position of this particular node is changed translationally, it will drive the entire rod to move forward/backwards. Like wise, rotational movement of the node will also cause the rod to rotate following the rules of the Cosserat rod implementation [127]. The virtual guidewire and catheter are originally placed at the entrance of the blood vessel model. As the real instruments are inserted into the prototype and manipulated, the sensors will detect the displacements made and transmit the data to the Arduino board, which then relays them to the Java program. The transmitted data here consists of four variables that span across the two ports: Guidewire position, Guidewire orientation, Catheter position, Catheter orientation. Next, these displacements are offset with the initial position of the instruments in the VE, which results in movements

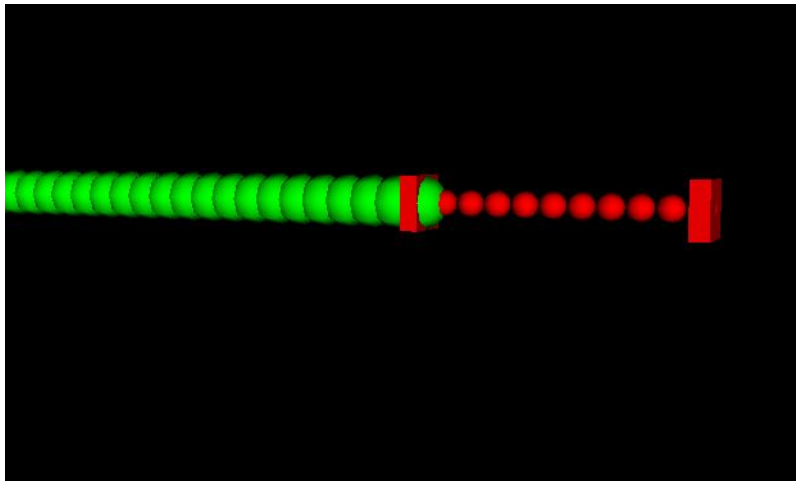

Figure 5.7: The controllable nodes of the virtual instruments marked by the red squares

of the virtual instruments that mirror the movements made to the real guidewire and catheter.

Force Feedback

As the virtual instruments are moving within the VE, each node of the rod has the potential to collide with the geometry of the blood vessel wall. The resulting collision effects on the rod in terms of bending or twisting are handled by the simulation software, which controls the timing and magnitude of the output of the prototype haptic interface. A unique threshold value, called a Force Trigger, is set for each virtual instrument. If the bending force experienced by a rod (either the guidewire or catheter) exceeds the corresponding Force Trigger, a signal will be sent by the simulation VE to the Arduino board to activate the respective actuator. The value of each Force Trigger was tuned heuristically to ensure that the prototype is not too sensitive and only delivers haptic feedback in the correct collision conditions.

For the servo motor, the signal received is a digital signal of either 0 or 1, where 0 sets the servo motor arm to the OFF position and 1 sets the arm to the ON position (i.e. pressing against the catheter). Similarly, for the hub actuator this signal is also a digital signal which is output from one of the pins of the Arduino board to pin 1 (the Enable pin) of the H bridge op amp used, L293NE (Figure 5.8). Pin 8 of the H bridge is connected to the power supply, which supplies up to 0.45 Amp of current to the hub

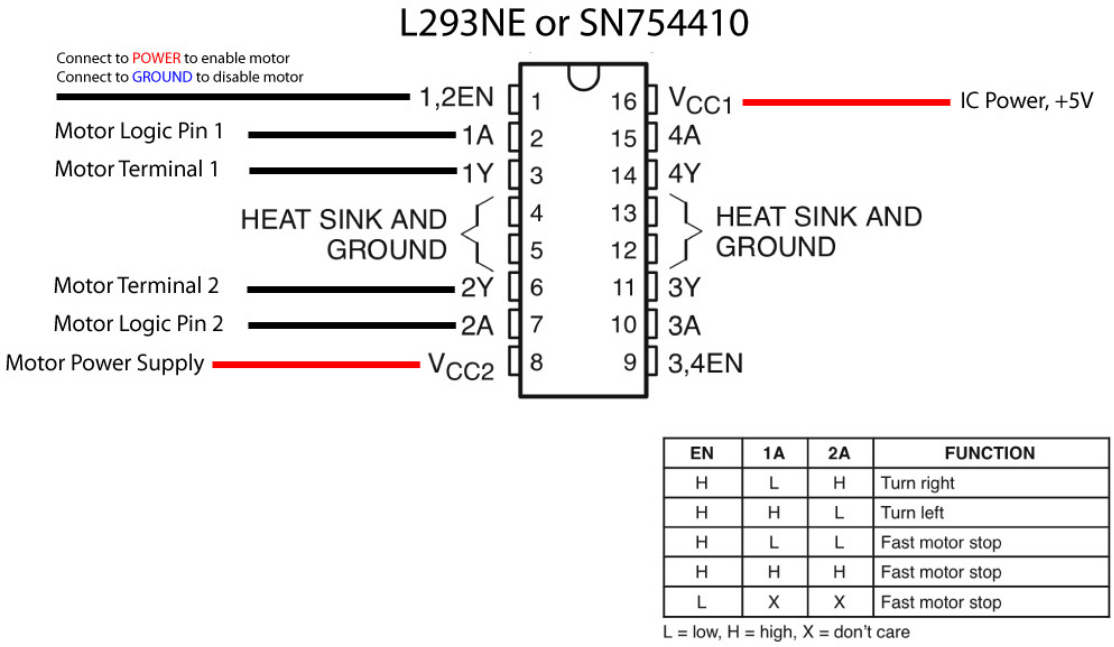

Figure 5.8: Connections to and from the H bridge op amp L293NE

actuator as needed. Pins 2 and 7 are connected to the digital output pins of the Arduino board, whereas pins 3 and 6 are connected to the terminals of the hub actuator.

As shown by the legend in Figure 5.8, the outputs of pin 2 and 7 dictate the direction of current flow across pins 3 and 6. However, the magnitude of the current to the hub is determined by the current supplied to pin 1. A logic HIGH signal would enable current to flow across the terminals of the motor, whereas a logic LOW signal would disable it. Digital signals are used to control the actuators in the prototype because only ON-OFF operation of the actuators are implemented in the test to examine the strength of each actuator. If a more linear or varying force is needed, then an analog signal (via pulse width modulation techniques) can be used to substitute the digital signal sent to the H bridge. It is highly likely that such application of variable force would be needed in the future, where a full physics VR simulator is to be used for training/credentialing.

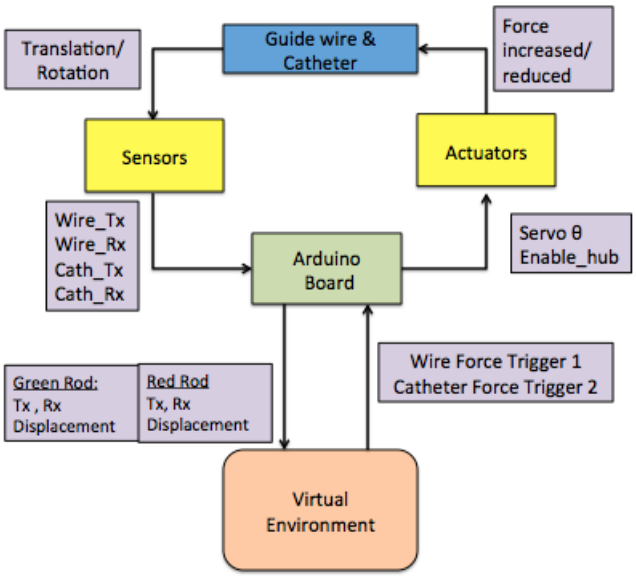

Figure 5.9: Flow of data between prototype and Virtual Environment software

Data Exchange

The exchange of information and variables involved in the operation of the prototype is summarised in the flowchart of Figure 5.9. The main input to the Arduino board is the translation and/or rotational motion of the instruments, as detected by the sensors which produce displacement readings represented as four variables: WireTx, WireRx, CathTx and CathRx. These variables are transferred by the Arduino board to the VE simulation software as displacement and rotation of the guidewire (red rod) and catheter (green rod), and are used to update the position of the virtual instruments in real time.

If the virtual catheter movements result in geometric collisions where a significant force/resistance is generated (i.e. larger than the set catheter Force Trigger), the servo motor actuator is activated by sending the digital HIGH signal. Similarly, If the virtual catheter movements result in collisions where a significant force/resistance is generated (i.e. larger than the set guidewire Force Trigger), then a logic HIGH signal is sent to the H bridge circuit to supply current and trigger the hub actuator. This process enables the application of force on the real instruments through the prototype haptic interface, thus reflecting the actions and conditions of both instruments in the VE.

5.1.3 Participants and Study Protocol

Study Demographics

The inclusion criteria of the study was that participants must have undergone at least one year of training in endovascular interventions or performed/assisted in 100 interventional procedures. A recruitment email was sent to the British Society of Interventional Radiology (BSIR), as well as to the administrative and research contacts of various medical institutions such as the Manchester Royal Infirmary, London Heart Hospital, London Chest Hospital and London St. Bartholomew's Hospital. The emails generated considerable interest and positive replies were received from several individuals willing to participate. Subsequently, meetings over several days were arranged to conduct the study at the respective institutions. Both the equipment and questionnaire were transported to meet the participants at their workplace according to the set schedule.

A total of 14 participants were recruited for the study. 5 participants were from the London Heart Hospital, 4 from the London Chest Hospital, 4 from the Manchester Royal Infirmary and 1 from St Bartholomew's Hospital. In terms of specialities, 6 (43%) participants were interventional cardiologists; 4 (29%) non interventional cardiologists; 2 (14%) interventional radiologists; 1 (7%) vascular surgeon and 1 (7%) experienced radiographer (Figure 5.11(a)). Regarding level of experience, 4 (29%) were junior registrars; 3 (21%) senior registrars and 7 (50%) consultants (Figure 5.11(b)). It should be noted that, at the time of testing, the radiographer was considered to have consultant level experience as she had been in practice for over ten years. Table 5.2 shows the minimum, maximum and mean number of years for each experience category. Aside from the number of years in practice/training, the participants' experience with virtual simulators was also examined. From the 14 participants, only 7 (50%) had prior experience training with virtual simulators. The other half were trained exclusively following the apprenticeship model on patients.

Protocol

At the beginning of the test, each participant was given a short briefing about the prototype haptic interface that included an explanation of the aim of the prototype, the range of interventions it allows for simulation, and the implemented dual port approach. Participants where then allowed to ask any questions before the test commenced. Once

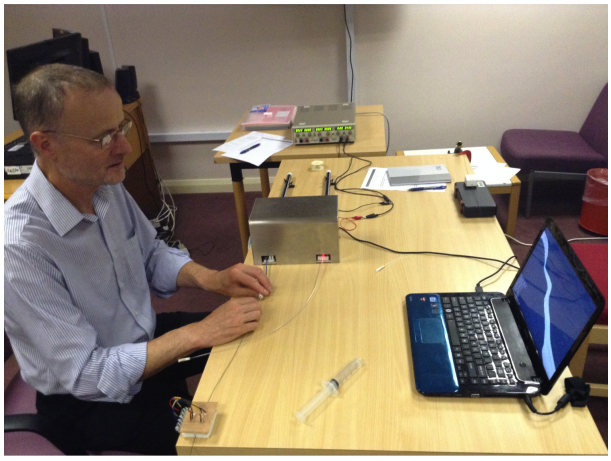

(a)

(b)

(c)

Figure 5.10: Photo of participant interacting with the prototype taken at (a) Manchester Royal Infirmary (b) St Bart's Hospital and (c) London Heart Hospital

(a) (b)

Figure 5.11: Distribution of participants according to (a) Professional background and (b) Level of experience

Table 5.2: Minimum, maximum and mean of years for each participant experience category

Professional background	Minimum (years)	Maximum (years)	Mean (years)
Junior Registrar	1	2	1.5
Senior Registrar	3	5	3.8
Consultant	3	20	8.1

the participant was ready, s/he was given step-by-step instructions on how to use the supplied instruments with the prototype in sequence (full task sequence list shown in Table 5.3). By completing each task one by one, s/he would be able to progress through the first stage of the study.

After the tasks had been completed and s/he was confident that s/he had gained a good understanding of the prototype haptic interface, the participant entered the second stage of the study, where s/he was asked to complete a paper questionnaire. The questionnaire contains 23 questions (5-point Likert scale) divided into three sections: *instrument Tracking, Haptic Feedback and Multi Port Design*. For the *Instrument Tracking* section, the participant was asked to rate the perceived sensitivity of the tracking system (i.e. how responsive is the virtual instrument to movements in the real instrument). Participants were also asked to rate how closely the movement of the virtual instruments corresponds to the movement of the real instrument. For example, if the instrument is rotated twice in real life, would the virtual instrument be rotated by the same amount in the VE? In the *Haptic Feedback* section of the questionnaire, the par-

Table 5.3: Tasks involved in prototype testing and the respective ports for each task

Task Number	Task Description	Port
1	Initial guidewire insertion from point J to K	A
2	Catheter sheath over guidewire	A
3	Catheter insertion from point J to K	A
4	Switching ports	B
5	guidewire and catheter navigation from point K to L	B
6	Extraction of the guidewire	B
7	Manipulation of syringe to mimic dye injection	B

ticipant was asked to rate the suitability of the resistance effect on both the guidewire and catheter, according to the context provided by the VE, and to rate if the resistance effect is acceptable for use in simulation training.

The *System Design* section of the questionnaire covered much wider aspects of the prototype haptic interface. Participants were asked to rate the workspace provided to him/her during the testing. A pair of questions request the participant to rate the guidewires and catheters used with the prototype haptic interface. The final four questions in this section asked for feedback on the dual port design approach. First, the participant was asked to rate the ability of this design to enable acceptable instrument manipulation practice. Second, s/he was asked if the sequences performed using the two ports are an adequate representation of the sequences performed in real life. Third, the difficulty of switching between the two ports was rated and, lastly, the participant was asked if switching between the two ports affected the immersion of the simulation. These questions are important in evaluating the effectiveness of the dual port approach as a tool for teaching and training. The full questionnaire can be seen in Appendix D. The responses obtained are discussed in the next section.

5.2 Study Results and Discussion

Out of the 14 participants who tested the prototype, two participants had to be removed from the final result evaluation, leaving a total of 12 participants. One of them was the first participant when it was discovered that the parameter values for the actuator were not correctly set. It is important to note that this was the only alteration done

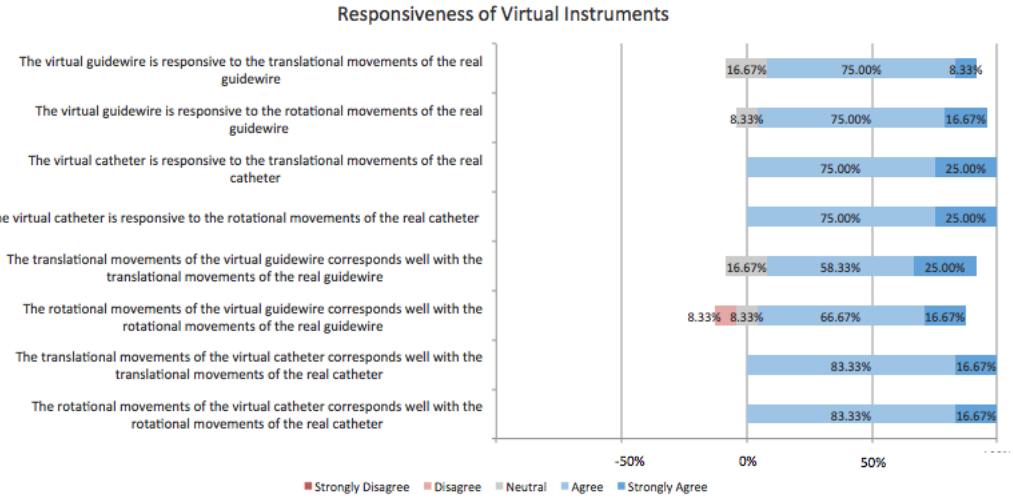

Figure 5.12: Responses to questions regarding virtual guidewire and catheter movements

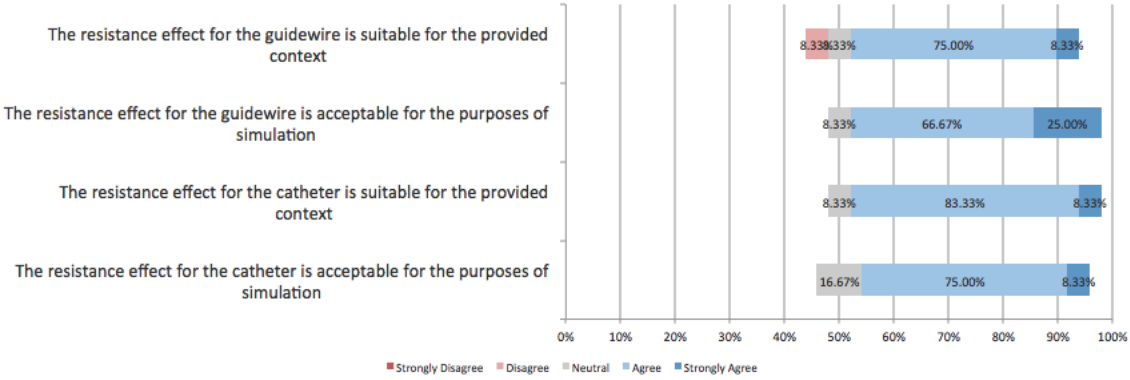

Figure 5.13: Responses to questions regarding haptics and force feedback

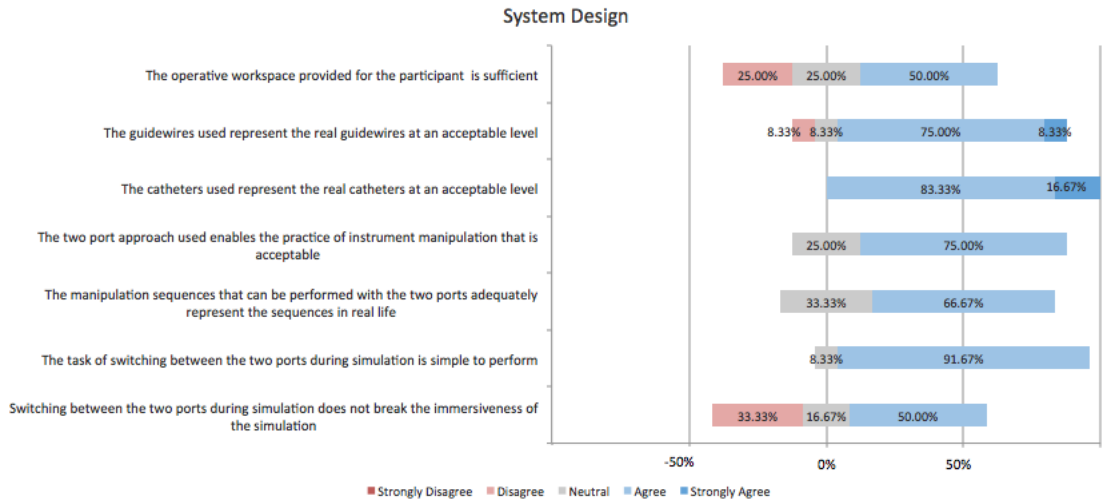

Figure 5.14: Responses to questions regarding prototype system design

to the system throughout the testing stages and the system was then unchanged for the remaining 13 participants. The second participant removed from the study was the senior radiographer mentioned earlier as she admitted to lacking experience in hands on procedural work.

The findings of the survey are summarized by the diverging stacked bar graphs of Figures 5.12 - 5.14. Each bar corresponds to a specific question. Positive results are grouped in blue (strongly agree and agree), whereas negative results are grouped in red (strongly disagree and disagree) and are distributed right and left of neutral, respectively. Bars are thus skewed in the direction of the overall trend. A majority of participants rated instrument tracking performance of the prototype positively. 9 (75%) participants agreed and 1 (8.33%) more strongly agreed that the virtual guidewire was responsive to translational movements of the real guidewire, whereas 2 others (16.67%) responded neutrally (Figure 5.12). Furthermore, 9 (75%) participants agreed and 2 (16.67%) more strongly agreed the same for rotational guidewire movements, while 1 (8.33%) responded neutrally. Also, 7 (58.33%) participants agreed and 3 (25%) more strongly agreed that the translational movements of the virtual guidewire correspond well to the movements of the real guidewire, while the remaining 2 (16.67%) participants responded neutrally. For the correspondence of the guidewire rotational movements, 8 (66.67%) participants strongly agreed that it corresponds well and 2 (16.67%) more

strongly agreed on the matter. However, 1 (8.33%) participant disagreed and 1 (8.33%) more remained neutral.

Participants rated the catheter tracking performance of the prototype very positively with 9 (75%) participants agreeing and 3 (25%) participants strongly agreeing that the movements of the virtual catheter are responsive. Equally positive, 10 (83.33%) participants agreed and 2 (6.67%) more strongly agreed that the virtual catheter corresponds well to the movements (both translational and rotational) made to the real catheter. The use of contact sensors, such as the roller ball and the trackball, have been proven to be very effective in the literature. Therefore, the most significant finding here is that the novel guidewire tracking technique (concentrically through a clear catheter) was both successful and reliable.

Participant responses regarding the haptic feedback output of the prototype are similarly positive. 9 (75%) participants agreed and 1 (8.33%) strongly agreed that the resistance felt on the guidewire is suitable for the context provided. From the remaining two participants, 1 (8.33%) disagreed and 1 (8.33%) was neutral (Figure 5.13). 8 (66.67%) of the participants agree and 3 (25%) others strongly agreed that the resistance effect produced on the guidewire is acceptable for simulation. Only 1 (8.33%) participant disagreed with the former statement (i.e. believed that the resistance felt on the guidewire is not suitable). For the resistance effect produced on the catheter, 10 (83.33%) participants agreed and 1 (8.33%) strongly agreed that the effect is suitable for the context given, whereas 1 (8.33%) participant responded neutraly. 9 (75%) participants agreed and 1 (8.33%) more strongly agreed that the generated effect is acceptable for simulation purposes, while 1 (8.33%) participant was neutral on the matter.

Since the servo motor has been established in the literature as an effective tool for providing haptic feedback, the positive response about the haptic effect provided by the hub actuator on the guidewire is the most significant finding here. From the testimony of the majority of participants, it may be concluded that the novel actuation technique manages to produce a noticeably strong, but subtle resistance effect to the guidewire, while also overcoming the drawbacks of previous designs caused by the 'concentric occlusion' problem.

The final set of questions gather participant's opinions on the dual port design of the prototype. Only 6 (50%) of the participants agreed that the workspace provided to them

during testing was sufficient. From the remaining participants, 3 (25%) disagreed as they felt that the workspace was insufficient and 3 (25%) others were neutral or undecided (Figure 5.14). The workspace here refers to the amount of space the participant had to insert and manipulate the instruments when interacting with the prototype. Typically, this is defined by the distance between the prototype and the external tracker unit at Port B. During testing, this distance was set to 40 cm. The negative responses received seem to suggest that this distance needs to be increased to provide a larger workspace. This can be easily rectified by placing the external tracker unit further away from the main unit (e.g by another 20 cm) by either extending the wiring of the external tracker or, more ideally, by manufacturing a wireless version of the external tracker.

The guidewires and catheters used with the prototype haptic interface are altered versions of the real life instruments as explained earlier in this chapter. However, these changes do not seem to be detrimental to the simulation experience based on the responses of the questionnaire. 9 (75%) participants strongly agreed and 1 (8.33%) more agreed that the guidewires used were a good representation of the real guidewires. 1 (8.33%) participant was undecided and only 1 (8.33%) participant disagreed with the statement. Similarly, 10 (83.33%) participants agreed and 2 (16.67%) others strongly agreed that the catheters used are an acceptable representation of their real counterparts.

Whilst feedback regarding the prototype mechanisms and systems have been generally positive, the dual port design has received mixed reviews. 9 (75%) participants agreed that the dual port approach allows for acceptable practice of instrument manipulation. The remaining 3 (25%) participants were undecided and responded neutrally. For the next question, 8 (66.67%) participants agreed that the sequence of interventions performed at both ports are an acceptable representation of real life sequences, while 4 (33.33%) participants were undecided. Next, a large majority of 11 (91.67%) participants agreed that the task of switching between the two ports when operating the interface is trivial and only 1 (8.33%) responded neutrally. However, only 6 (50%) participants agreed that switching between ports does not break the immersion of the simulation experience. From the remaining 6 participants, 4 (33.33%) felt that switching ports negatively affects the immersion of the simulation, whereas 2 (16.67%) were undecided.

From these findings, it can be concluded that several of the participants are critical of the prototype's dual port design. The main issue raised is that the existence of the two ports (and therefore two sets of instruments), as well as having to switch between the two ports in mid intervention, disrupts the immersion of the simulation experience. For these participants, this negative effect outweighs the advantages of the two port approach. Nonetheless, the general feedback received suggests that most participants agree that the prototype is still a valid and useful tool for the teaching and practice of instrument manipulation and endovascular intervention sequences.

5.3 Chapter Summary

A study conducted to examine, test and validate the prototype haptic interface was detailed in this chapter. The objective of the study was to evaluate three aspects of the prototype: the instruments tracking system, the haptic feedback system and the multi port interface design. There were two stages to the study. In the first stage, participants were instructed to perform a series of instrument manipulations with the prototype, whilst in the second stage, they were asked to complete a questionnaire.

The prototype hardware, which includes sensors, actuators and control circuits such as the H bridge, is complemented with a 3D Virtual Environment (VE) simulation written in Java. The VE functions as a visual component of an endovascular simulator. Its main purpose is to provide a useful and effective way to show the correspondence of movements between the real and virtual instruments, and the translation of haptic cues from the VE into real haptic effects through the prototype interface. The VE consists of two main components: the blood vessel and the virtual instruments. The 3D geometry of the blood vessel was obtained by scanning a silicon phantom model in CT. The geometry was then modified in *Blender* to accommodate the requirements of the tests before being loaded by the software as a rigid model. The virtual guidewire and catheter are modelled as inextensible Cosserat rods in the VE. This allows for real time manipulation of the rods, visually realistic instrument behaviour and interactions such as bending and twisting. In operation, the movements of the real guidewire and catheter within the prototype haptic interface are detected by the sensors. The sensors produce displacement readings that are then sent to the VE, which results in movements of the virtual instruments that mirror the movements made to their real life counterparts. A

force calculation algorithm is also implemented in the VE that consistently calculates the bending or twisting deformations experienced by each virtual instrument or rod as they collide with the vessel walls. If the force involved exceeds a certain preset threshold (unique to each virtual instrument), a signal will be sent from the VE to the actuators to activate and apply the necessary haptic feedback to the instruments. The instrument tracking and haptic feedback information is updated in real time by the system throughout the testing process.

A total of 14 participants took part in this study, recruited from various medical institutions including the Manchester Royal Infirmary, London Heart Hospital and London St. Bartholomew's Hospital. This included 6 (43%) interventional cardiologists, 4 (29%) non interventional cardiologists, 2 (14%) interventional radiologists, 1 (7%) vascular surgeon and 1 (7%) radiographer. These participants also had different levels of experience, with 7 (50%) consultants, 3 (21%) senior registrars and 4 (29%) junior registrars. In terms of familiarity with virtual simulators, only half of the participants had prior experience of training with virtual simulators. The questionnaire prepared consisted of three sections: *Instrument Tracking*, *Haptic Feedback* and *System Design*. The latter includes aspects such as workspace suitability and effectiveness of the multi port approach.

Only the responses of 12 participants were processed and evaluated from the original 14 due to reasons explained earlier in the chapter. The feedback received from this initial study has been very positive with a majority of the participants highlighting the reliability of the instrument tracking system, as well as the subtle yet strong output of the haptic feedback system. This is especially encouraging considering the introduction of two novel techniques implemented in this prototype, namely the concentric guidewire tracking and the catheter hub actuator. However, the negative feedback suggests that there is still room for improvement. One of the features that needs to be improved is the workspace provided to the participants, which has been described as limited and insufficient. In future work, this issue can potentially be addressed by extending the external tracker further away from the main prototype. Participants also criticised the multi port design of the prototype, as a fair percentage of them found the presence of multiple ports (and therefore multiple instrument sets), and having to switch between the ports/instruments during simulation, to be disruptive of the simulation immersion. As mentioned in the previous chapter, the impact of this design on face validity has

been considered, and therefore these negative/neutral responses are somewhat expected. Nevertheless, the multi port design of the prototype allows for the testing of the concentric tracking technique and the actuator hub approach to obtain proof of concept. In addition, it enabled the investigation to determine if it could be a useful approach for training (i.e. enable successful transfer of skills), despite its impact on face validity. As can be interpreted from the survey results, although only 6 (50%) participants felt that the multi port approach does not break the immersion of the simulation, 9 (75%) participants agreed that it allows for instrument manipulation that is acceptable for simulation, whereas 8 (66.67%) participants agree that it allows for the simulation of manipulation sequences that are representative of the sequences in real life. While these findings suggest that the multi port approach can actually be a useful tool for training, despite the reduced face validity, its benefits do not appear to overcome its negative effect on simulation immersion. Thus, there should be concentrated efforts to combine the features of the multiple ports into a single port in future work.

Overall, based on the feedback received, the prototype interface has managed to fulfill its objectives, while avoiding the drawbacks of prior designs and introducing novel techniques for instrument tracking and haptic feedback. In the next chapter, the work done in this project is critically reviewed and future work suggested.

6

Conclusions and Future Work

6.1 Summary of Work and Achievements

This project began with the aim of designing and producing a haptic interface device for the simulation of endovascular interventions, able to address some of the major shortcomings of currently available devices. The aim was successfully fulfilled with the production of a multi port haptic interface device that has received generally positive feedback from subject matter experts, both in terms of the novel instrument tracking and haptic feedback mechanisms implemented. A review of the initial specific objectives now follows:

(a) To design and develop a sensor system that continuously tracks the position and orientation of the guidewire and catheter during simulation

The main challenge of designing a haptic interface for the simulation of endovascular interventions is caused by the configuration of its instruments, where one of the instruments, the guidewire, is concentrically positioned within the other instrument, the catheter. In this configuration, guidewire detection is challenging due to the lack of line of sight and point of contact. This is referred to in this work as the ′concentric occlusion′ problem, which also limits the selection of possible actuators for generating haptic feedback.

A variety of sensors were studied to identify new technologies that can be used as a solution to the concentric occlusion problem. However, after the technology re-

view, it became apparent that the application of most sensors that allow for wireless or non contact tracking would require significant modification of the instruments that may severely change their weight and feel. As the instruments are meant for use in simulation-based training where sufficient realism is expected, these alternative sensor designs were deemed not practical for implementation in the project.

Following the review, a series of experimental tests were conducted to investigate the possibility of detecting the guidewire (and its movements) by using the combination of a clear catheter and an optical sensor. Based on the encouraging results, this tracking approach was implemented into the instrument tracking system of the prototype. The feedback received regarding the prototype tracking system was largely positive. From the prototype validation survey, at least 80% of participants agreed or strongly agreed that the virtual guidewire was responsive to translational movements of the real guidewire and at least 90% agreed or strongly agreed the same for rotational movements. In addition, at least 80% of participants agreed or strongly agreed that both the translational and rotational movements of the virtual guidewire corresponds well with the movements of the real guidewire.

The clear catheter used in this tracking approach has different properties (e.g. weight, surface friction and flexibility) compared to the original catheter. Since the specific clear catheter used in the experiments is only temporary to obtain proof of concept, and not as a final solution, quantitative measurements of some of its properties were not performed. Instead, these properties were either obtained from the manufacturer's technical specification sheet, or estimated based on the properties of the material of the catheter. Before its implementation into the prototype, the clear catheter was presented to subject matter experts who agreed that the clear catheter sufficiently resembles the original catheter and is suitable for use in proof of concept testing. This is further confirmed by the findings of the prototype validation survey responses, where 100% of the participants agreed or strongly agreed that the catheters used with the prototype are an acceptable representation of their original counterparts.

(b) To study and understand the range and types of haptic effects as perceived by the interventionists during an endovascular procedure

Despite the popularity and commercial success of current virtual simulators for endovascular interventions, there is a lack of published research regarding the intricacies of the

haptic feedback during such procedures. [29, 30] has pioneered such investigations for the earlier stages of interventions, specifically for arterial puncture using the combination of Cognitive Task Analysis (CTA) validation and in vivo force measurements. However, this has yet to include the other stages of interventions. A possible cause for this is that the process of obtaining both CTA and in vivo measurements involves significant challenges (access to patients, ethical approvals, etc) which are not only time consuming, but also requires specialist instruments to enable force measurements. Considering the constraints of this project, both elements were not expanded in this work for these same reasons.

In this project, the haptic sensations occurring during endovascular interventions were explored based on a literature review and feedback from SMEs via interviews, experimental studies and an online questionnaire. Whilst there are inherent limitations of using SMEs to obtain this information given its subjective nature, descriptive and statistical analysis of the results have revealed useful insight on these resistance effects, for both translational and rotational movements. This includes an understanding on the conditions that would cause the effects to occur as well as an estimate of the range of forces involved. Thus, the information gathered through the study helped to influence and inspire the haptic feedback mechanism developed in this work.

(c) To design and develop a haptic actuation system that can deliver haptic feedback to both the guidewire and catheter.

The findings of the haptic feedback study, the recognition of the concentric occlusion problem and the systematic review of existing haptic interface devices, as well as possible alternative approaches, led to the design and development of a prototype actuator for the purposes of producing a continuous resistance effect on guidewire movement. The proposed actuator was designed to be placed within the hub of the catheter as a means of addressing the concentric occlusion problem. The maximum resistance provided by the actuator was estimated to be between 0.3923 N - 0.4903 N through a set of experimental tests. In the prototype validation survey, the feedback received from the participants regarding the haptic feedback produced by the actuator was largely positive. More than 80% of participants agreed or strongly agreed that the resistance felt on the guidewire is suitable for the context provided, while 90% agreed or strongly agreed that the resistance effect produced on the guidewire is acceptable for simulation.

A more conventional actuator, a servo motor, was used to generate haptic feedback on the catheter since it does not suffer from the concentric occlusion problem. More than 95% of the participants agreed or strongly agreed that the resistance effect produced by the servo motor is suitable for the context provided whereas more than 80% of them agreed or strongly agreed that it is suitable for the purposes of simulation.

(d) To combine both sensor and actuation systems into a prototype device

The prototype haptic interface device produced in this project features multiple ports for instrument insertion and manipulation, where each port is tailored for the simulation of individual stages of an intervention. This approach was designed to facilitate the steps usually performed during interventions, whilst enabling the proof of concept testing of the instrument tracking and haptic actuation systems. These systems were then integrated within a single simulation system, which includes a 3-D generated virtual environment, with real time instrument position/orientation updates, mathematically modelled instrument behaviour and collision detection.

(e) To test and evaluate the prototype based on input from subject matter experts

An initial validation study to test the tracking and haptic feedback of the integrated system was conducted with subject matter experts. Participants were asked to perform simple instrument manipulations, such as instrument insertion and navigation. The general feedback was positive, with the most favourable responses regarding the instrument tracking and haptic feedback. Also, despite the fact that 50% of the participants felt that the multi port approach has a negative effect on face validity, 75% of participants agreed or strongly agreed that the approach allows for instrument manipulation that is acceptable for simulation whereas more than 60% of participants were in agreement that it allows for the simulation of manipulation sequences that are representative of the sequences in real life.

6.2 Limitations and Future Work

As in any project and newly developed system, there are several limitations. These limitations involve tradeoffs that bring benefits as well as drawbacks, but are necessary to make progress with the work or task required. The main limitations of this work and suggested future work are summarised as follows:

(a) Instrument Modification

During the course of this work, various investigations were performed in an effort to address the concentric occlusion problem, in terms of instrument tracking and haptic feedback. For both, the selected approaches are made possible by customising and replacing most of the original instruments. These replacements also introduce a change to the feel of the instruments since their properties such as weight, friction and flexibility have been modified. Since the purpose of their use in this work is to obtain proof of concept, and not meant as a final solution to the problem, the differences between the modified instruments and their original counterparts were not quantitatively measured except for the changes in weight and diameter. The other changes were estimated based on the technical specifications provided by their manufacturers as well as the knowledge of the properties of their constituent material. In future development, progressing beyond the proof of concept stage, it is very important to manufacture replacement instruments that closely resemble the properties of the original instruments to maintain a higher degree of face validity in the simulation.

(b) Simultaneous Instrument Tracking

In the current stage, the concentric tracking approach does not accommodate for simultaneous tracking of both the guidewire and catheter due to the fact the optical sensor cannot differentiate between guidewire and catheter movements. It is expected that this task would be possible in future work if a customised optical sensor (with a lens designed to focus on the guidewire only) was used instead of the off-the-shelf sensor used in this work. Another alternative is to use the tracking technique featured in Port B of the prototype, where the guidewire movements are tracked by an external tracker positioned at the base of the guidewire (to the operator's right). For this approach however, the focus in the future will be to enable the external tracker to function wirelessly.

This would reduce the amount of wiring, increase the reliability of the system and the available workspace, which was one of the issues raised during the validation study.

(c) Hub Actuator Performance

Firstly, the hub actuator needs to be connected to the microcontroller and a power source to function. Thus, the hub of the catheter needs to be tethered and this limits the range of movements of the catheter during simulations. Developing a wireless version of the hub actuator would increase the catheter's range of movement significantly and should be a priority in future developmental work. Secondly, the resistance effects produced by the hub actuator can be inconsistent as reflected by the results of the experimental test in Section 4.2.1. This is mainly attributed to the fact that several parts of the hub actuator were manually finished. Namely, the coil casing, which is first 3-D printed and then manually filed to ensure proper angle of its edges. This was necessary as the available 3-D printers could not print at the higher resolution required for the edge and tips of the coil casing. Naturally, such manual finishing is subject to inconsistency and variability of the human operator. In the future, efforts should be made to improve the consistency of the actuator by implementing a new design or components that can be manufactured automatically (i.e. not produced by hand). Also, further miniaturisation of the actuator is equally important to reduce the impact caused by the added size and weight.

(d) Haptic Feedback Study

Aside from the arterial puncture process, there are not many publications examining the characteristics of the haptic effects present during endovascular interventions and the forces involved. A general understanding of these effects was needed to inform the design of the haptic feedback and actuation system in the haptic interface prototype. Ideally, the best method to obtain such information would be through the ongoing development of a validated Cognitive Task Analysis (CTA) and in vivo force measurements. However, performing both tasks are time consuming and highly challenging due to certain factors (e.g. ethical approvals, gaining access to patients and customised instruments to measure forces).

Due to the constraints of this project, the investigation was conducted by analyzing subject matter expert (SME) input gathered from various interviews, experimental tests

and an online questionnaire. However, this approach has several limitations: the subjectivity of the data provided by the SMEs, and the fact that the number of participants was relatively small, particularly for the experimental testing component. Expanding this study to include more participants, more detailed questions and more robust experimental testing could be of interest in future work. Although, obtaining a validated CTA and in vivo measurements would be the ultimate goal for research in this field.

(e) Dual Port Approach

The dual port approach was implemented in the haptic interface prototype mainly to allow proof of concept testing of the instrument tracking and haptic feedback systems, as well as the correct sequence of steps to be performed. While it managed to fulfil that purpose, its implementation within the prototype itself received mixed responses since a fair percentage of participants (SMEs) felt that the approach had a negative effect on the face validity of the simulation. Thus, there should be concentrated efforts to combine the features of the dual ports into a single port in future work.

This would be possible by producing an actuator hub that is wireless so that the catheter will no longer be tethered, enabling it to be inserted into the port and replaced by other instruments. Both actions are not possible at Port B in the current prototype and can only be performed at Port A. The single port may also incorporate the concentric tracking that was introduced in Port A in this prototype, but with an improved optical sensor to allow for the tracking of simultaneous instrument movements. This feature is not available in the current prototype which uses an off the shelf optical sensor. Lastly, due to certain constraints, the current prototype works under the assumption that no haptic feedback is present during the process of initial guidewire insertion into the major artery. This is not always the case and, therefore, future iterations should incorporate haptic actuators to produce specific haptic effects during this stage of the intervention.

In conclusion, whilst the haptic interface prototype designed in this work has met the original objectives, it is very much in its early stages. There are still many important aspects which need to be addressed through future work to improve the content validity and face validity of the simulation training. Nevertheless, the prototype has shown plenty of promise thus far and, with further development, it could potentially evolve and become a significant improvement over the haptic interfaces that exist today.

References

[1] World Health Organization, "Global status report on noncommunicable diseases 2010 Geneva," Accessed 17 November 2016. [Online]. Available: http://www.who.int/mediacentre/factsheets/fs317/en/

[2] S.A.Darzi and Y.Munz, "The impact of minimally invasive surgical techniques." *Annual Review of Medicine*, 2004.

[3] C. Dotter and M. Judkins, "Transluminal treatment of arteriosclerotic obstruction. description of a new technic and a preliminary report of its applications," *Circulation*, pp. 654–670, 1964.

[4] S.B. King III and B. Meier, "Interventional treatment of coronary heart disease and peripheral vascular disease," *Circulation*, 2000.

[5] T.Grunwald, D.Clark, S.Fisher, M.McLaughlin, S.Narayanan, and D.Piepol, "Using cognitive task analysis to facilitate collaboration in development of simulator to accelerate surgical training," *Stud Health Technol Inform.*, vol. 98, pp. 114–120, 2004.

[6] D.A.Gould and J.A.Reekers, "The role of simulation in training endovascular interventions," *Eur J Vasc Endovasc Surg*, pp. 633–636, 2008.

[7] D.A.Gould, "Using simulation for interventional radiology training," *The British Journal of Radiology*, pp. 546–553, 2010.

[8] M. Berry, T. Lystig, J. Beard, H. Klingestierna, R. Reznick, and L. Lonn, "Porcine transfer study: Virtual reality simulator training compared with porcine training in endovascular novices," *Cardiovascular and Interventional Radiology*, vol. 30, no. 3, pp. 455–461, 2007.

[9] M. Berry, M. Hellstroem, J. Gothlin, R. Reznick, and L. Lonn, "Endovascular Training with Animals Versus Virtual Reality Systems: An Economic Analysis," *Journal of Vascular and Interventional Radiology*, vol. 19, no. 2, pp. 233–238, 2008.

[10] L. Desender, Z. Rancic, R. Aggarwal, J. Duchateau, M. Glenck, M. Lachat, F. Vermassen, and I. V. Herzeele, "Patient-specific rehearsal prior to evar: a pilot study," *Eur J Vasc Endovasc Surg*, vol. 45, pp. 639–647, 2013.

[11] N. Rudarakanchana, I. V. Herzeele, L. Desender, and N. Cheshire, "Virtual reality simulation for the optimization of endovascular procedures: current perspectives," *Vasc Health Risk Manag.*, vol. 11, pp. 195–202, 2015.

[12] J. Lundberg, S. Jonsson, and S. Holmin, "Applied Cognitive Task Analysis (ACTA): A practitionerâĂŹs toolkit for understanding cognitive task demands," *Ergonomics*, vol. 41, pp. 1618–1641, 1998.

[13] R.E.Clark and F.Estes, "Cognitive task analysis," *International Journal of Educational Research*, vol. 25, no. 5, pp. 403–417, 1996.

[14] B.Means and S.Gott, "Cognitive task analysis as a basis for tutor development: Articulating abstract knowledge representations." *Intelligent tutoring systems*, pp. 35–58, 1988.

[15] S.Johnson, A.Healey, J.Evans, M.Murphy, M.Crawshaw, and D.Gould, "Physical and Cognitive Task Analysis in Interventional Radiology," *Clinical Radiology*, vol. 61, pp. 97–103, 2006.

[16] J. Batter and F. B. Jr, "GROPE-1: A computer display to the sense of feel," *Proceedings of IFIP 1971, North-Holland Publishing Company*, pp. 759–763, 1972.

[17] News and Events Page, "SensAble Technologies Official website," Accessed 17 November 2016. [Online]. Available: http://www.sensable.com/pr_20080125/news-press-detail.htm

[18] F. Tendick, M. Downes, T. Goktekin, M. C. Cavusoglu, D. Feygin, X. L. Wu, R. Eyal, M. Hegarty, and L. W. Way, "A virtual environment testbed for training

laparoscopic surgical skills," *Presence-Teleoperators and Virtual Environments*, vol. 9, no. 3, pp. 236–255, 2000.

[19] G. Tholey, J. P. Desai, and A. E. Castellanos, "Force feedback plays a significant role in minimally invasive surgery - results and analysis," *Annals of Surgery*, vol. 241, no. 1, pp. 102–109, 2005.

[20] G. Sela, J. Subag, A. Lindblad, D. Albocher, S. Schein, and G. Elber, "Real-time haptic incision simulation using fem-based."

[21] M. Tsai, M. Hsieh, and C. Tsai, "Bone drilling haptic interaction for orthopedic surgical simulator," *Computers in Biology and Medicine*, vol. 37, no. 12, pp. 1709–1718, 2007.

[22] D. Ni, W. Chan, J. Qin, G. Qu, Y. Chui, S. Ho, and P. Heng, "An ultrasound-guided organ biopsy simulation with 6 DOF haptic feedback," *Medical Image Computing and Computer-Assisted Intervention - MICCAI 2008, Pt Ii, Proceedings*, vol. 5242, pp. 551–559, 2008.

[23] P. Rhienmora, P. Haddawy, P. Khanal, S. Suebnukarn, and M. Dailey, "A virtual reality simulator for teaching and evaluating dental procedures," *Methods of Information in Medicine*, vol. 49, no. 4, pp. 396–405, 2010.

[24] D. Ilic, T. Moix, B. Fracheboud, H. Bleuler, and I. Vecerina, "A haptic interface for interventional radiology," *2005 IEEE International Conference on Robotics and Automation (ICRA), Vols 1-4*, pp. 2933–2937, 2005.

[25] T. Moix, D. Ilic, B. Fracheboud, J. Zoethout, and H. Bleuler, "A real-time haptic interface for interventional radiology procedures," *Medicine Meets Virtual Reality 13: The Magical Next Becomes the Medical Now*, vol. 111, pp. 329–333, 2005.

[26] E. Samur, L. Flaction, U. Spaelter, H. Bleuler, D. Hellier, and S. Ourselin, "A haptic interface with motor/brake system for colonoscopy simulation," *Symposium on Haptics Interfaces for Virtual Environment and Teleoperator Systems 2008, Proceedings*, pp. 477–478, 2008.

[27] I. Brouwer, K. MacLean, and A. Hodgson, "Simulating cheap hardware: A platform for evaluating cost-performance trade-offs in haptic hardware design," *IEEE Proceeedings for International Conference on Robotics and Automation*, vol. 1-5, pp. 770–775, 2004.

[28] M. Tavakoli, M. M. R. Patel, and A. Aziminejad, "Haptics for teleoperated surgical robotic systems (new frontiers in robotics series)," *World Scientific Publishing Company*, 2008.

[29] Collaborators in Radiological Interventional Virtual Environments (CRaIVE) website, "Projects," Accessed 17 November 2016. [Online]. Available: http://www.hpv.cs.bangor.ac.uk/CRaIVE/projects.php

[30] A.E.Healey, J.C.Evans, M.G.Murphy, S.Powell, T.V.How, D.Groves, F.Hatfield, B.M.Diaz, and D.A.Gould, "In vivo force during arterial interventional radiology needle puncture procedures," *Studies in Health Technology Informatics*, pp. 178–184, 2005.

[31] C. Chong, J. Brennan, T. How, R. Edwards, G. GillingSmith, and P. Harris, "A prototype simulator for endovascular repair of abdominal aortic aneurysms," *European Journal of Vascular and Endovascular Surgery*, vol. 13, no. 3, pp. 330–333, 1997.

[32] C. Chong, T. How, R. Black, A. Shortland, and P. Harris, "Development of a simulator for endovascular repair of abdominal aortic aneurysms," *Annals of Biomedical Engineering*, vol. 26, no. 5, pp. 798–802, 1998.

[33] R. Dayal, P. Faries, S. Lin, J. Bernheim, S. Hollenbeck, B. DeRubertis, S. Trocciola, J. Rhee, J. McKinsey, N. Morrissey, and K. Kent, "Computer simulation as a component of catheter-based training," *Journal of Vascular Surgery*, vol. 40, no. 6, pp. 1112–1117, 2004.

[34] P. Coates, I. Zealley, and S. Chakraverty, "Endovascular simulator is of benefit in the acquisition of basic skills by novice operators," *Journal of Vascular and Interventional Radiology*, vol. 21, no. 1, pp. 130–134, 2010.

[35] R. Aggarwal, S.A.Black, J. Hance, A. Darzi, and N. Cheshire, "Virtual Reality Simulation Training Can Improve Inexperienced Surgeons' Endovascular Skills," *European Journal of Vascular and Endovascular Surgery*, vol. 31, no. 6, pp. 588–593, 2006.

[36] I. Van Herzeele, R. Aggarwal, S. Neequaye, A. Darzi, F. Vermassen, and N. J. Cheshire, "Cognitive training improves clinically relevant outcomes during simulated endovascular procedures," *Journal of Vascular Surgery*, vol. 48, no. 5, pp. 1223–1230, 2008.

[37] J. Hsu, D. Younan, S. Pandalai, B. Gillespie, R. Jain, D. Schippert, C. Narins, A. Khanna, S. Surowiec, M. Davies, C. Shortell, J. Rhodes, L. Waldman, R. Green, and K. Illig, "Use of computer simulation for determining endovascular skill levels in a carotid stenting model," *Journal of Vascular Surgery*, vol. 40, no. 6, pp. 1118–1124, 2004.

[38] R. A. Chaer, B. DeRubertis., S. Lin, H. Bush, J. Karwowski, D. Birk, N. Morrissey, P. Faries, J. McKinsey, and K. Kent, "Simulation improves resident performance in catheter-based intervention," *Transactions of the ... Meeting of the American Surgical Association*, vol. 124, pp. 9–18, 2006.

[39] D. Dawson, J. Meyer, E. Lee, and W. Pevec, "Training with simulation improves residents endovascular procedure skills," *Journal of Vascular Surgery*, vol. 45, no. 1, pp. 149–154, 2007.

[40] D.A.Gould, D.O.Kessel, A.E.Healey, S.J.Johnson, and W.E.Lewandowski, "Simulators in catheter-based inteventional radiology: Training or computer games ?" *Clinical Radiology*, vol. 61, pp. 556–561, 2006.

[41] J. S. Tsang, P. A. Naughton, S. Leong, A. D. K. Hill, C. J. Kelly, and A. L. Leahy, "Virtual reality simulation in endovascular surgical training," *Surgeon-Journal of the Royal Colleges of Surgeons of Edinburgh and Ireland*, vol. 6, no. 4, pp. 214–220, 2008.

[42] M. A. Passman, P. S. Fleser, J. B. Dattilo, R. J. Guzman, and T. C. Naslund, "Should simulator-based endovascular training be integrated into general surgery

residency programs?" *American Journal of Surgery*, vol. 194, no. 2, pp. 212–219, 2007.

[43] M. M. Tedesco, J. J. Pak, E. J. Harris, T. M. Krummel, R. L. Dalman, and J. T. Lee, "Simulation-based endovascular skills assessment: The future of credentialing?" *Journal of Vascular Surgery*, vol. 47, no. 5, pp. 1008–1014, 2008.

[44] K. Ahmed, A. N. Keeling, M. Fakhry, H. Ashrafian, R. Aggarwal, P. A. Naughton, A. Darzi, N. Cheshire, T. Athanasiou, and M. Hamady, "Role of virtual reality simulation in teaching and assessing technical skills in endovascular intervention," *Journal of Vascular and Interventional Radiology*, vol. 21, no. 1, pp. 55–66, 2010.

[45] M. C. M. Willems, J. A. van der Vliet, V. Williams, L. J. S. Kool, D. Bergqvist, and J. D. Blankensteijn, "Assessing endovascular skills using the simulator for testing and rating endovascular skills (STRESS) machine," *European Journal of Vascular and Endovascular Surgery*, vol. 37, no. 4, pp. 431–436, 2009.

[46] I. Van Herzeele, R. Aggarwal, I. Malik, P. Gaines, M. Hamady, A. Darzi, N. Cheshire, F. Vermassen, and E. V. R. Endovasc, "Validation of video-based skill assessment in carotid artery stenting," *European Journal of Vascular and Endovascular Surgery*, vol. 38, no. 1, pp. 1–9, 2009.

[47] J. Lundberg, S. Jonsson, and S. Holmin, "New endovascular method for transvascular exit of arteries and veins: Developed in simulator, in rat and in rabbit with full clinical integration," *Plos One*, vol. 5, no. 5, 2010.

[48] S. Ikeda, C. Tercero, Y. Okada, T. Fukuda, F. Aral, and M. Negoro, "Patient-specific IVR surgical simulator for endovascular intervention," *2007 International Symposium on Micro-Nano Mechatronics and Human Science*, vol. 1 2, pp. 157–162, 2007.

[49] S. Hislop, J. H. Hedrick, M. J. Singh, J. M. Rhodes, D. L. Gillespie, M. Johansson, and K. A. Illig, "Simulation case rehearsals for carotid artery stenting," *European Journal of Vascular and Endovascular Surgery*, vol. 38, no. 6, pp. 750–754, 2009.

[50] W. I. M. Willaert, R. Aggarwal, D. F. Nestel, P. A. Gaines, F. E. Vermassen, A. W. Darzi, N. J. Cheshire, and Everest, "Patient-specific simulation for endovascular

procedures: Qualitative evaluation of the development process," *International Journal of Medical Robotics and Computer Assisted Surgery*, vol. 6, no. 2, pp. 202–210, 2010.

[51] T. Coles, D. Meglan, and N. John, "The role of haptics in medical training simulators: A survey of the state of the art," *IEEE Transactions on Haptics*, vol. 4, no. 1, pp. 51–66, 2011.

[52] N. John, V. Luboz, F. Bello, C. Hughes, F. P. Vidal, I. S. Lim, T. V. How, J. Zhai, S. Johnson, N. Chalmers, K. Brodlie, A. Bulpit, Y. Song, D. O. Kessel, R. Phillips, J. Ward, S. Pisharody, Y. Zhang, C. M. Crawshaw, and D. A. Gould, "Physics-based virtual environment for training core skills in vascular interventional radiological procedures," *Proceeding of Medicine Meets Virtual Reality 16 (MMVR16)*, pp. 195–197, 2008.

[53] D.Kessel and I.Robertson, "Interventional radiology: A survival guide," 2011.

[54] P. Schneider, "Endovascular skills: Guidewire and catheter skills for endovascular surgery," 2008.

[55] Jersey Medical Device website, "The hydrophilic guide wires," Accessed 17 November 2016. [Online]. Available: http://www.jerseymedicaldevice.com/content.asp?id=1532

[56] VenaCure EVLT website, "Nevertouch Procedure Kit," Accessed 17 November 2016. [Online]. Available: http://venacure-evlt.com/endovenous-laser-vein-treatment/angiodynamics/products/kits/nevertouch-procedure-kit/

[57] Component Supply Company website, "French catheter gauge size decimal and metric equivalents," Accessed 17 November 2016. [Online]. Available: http://www.componentsupplycompany.com/French-Catheter-guage-decimal-equivalents.html

[58] Stephen A Robinson website, "Portfolio," Accessed 17 November 2016. [Online]. Available: http://www.stephenarobinson.com/portfolio.html

[59] The University Hospital website, "The Stroke Center: Managing Risky Conditions," Accessed 17 November 2016. [Online]. Available: http://www.theuniversityhospital.com/stroke/risky.htm

[60] Belief.net website, "Health and Healing: Coronary Angiography," Accessed 17 November 2016. [Online]. Available: http://www.beliefnet.com/healthandhealing/getcontent.aspx?cid=14765

[61] Encyclopaedia Brittannica, "Coronary Artery: Insertion of a Stent into a Coronary Artery," Accessed 17 November 2016. [Online]. Available: http://www.britannica.com/EBchecked/media/106611/When-a-coronary-artery-becomes-narrowed-or-blocked-a-stent

[62] K. Ahmed, A. N. Keeling, M. M. Fakhry, H. Ashrafian, R. Aggarwal, P. A. Naughton, A. Darzi, N. Cheshire, T. Athanasiou, and M. Hamady, "Role of virtual reality simulation in teaching and assessing technical skills in endovascular intervention," *J Vasc Interv Radiol*, pp. 55–66, 2010.

[63] G. Merril and C.Chase, "Interventional radiology interface apparatus and method," *Patent US6106301*, 2000.

[64] Immersion.com website, "Immersion to Acquire Leading Medical Simulation Developer; Merger With HT Medical Systems Reinforces Immersion's Growth In Key Vertical Market," Accessed 17 November 2016. [Online]. Available: http://ir.immersion.com/releasedetail.cfm?releaseid=111418

[65] Diagnostic Imaging website, "Immersion enters virtual reality to solve surgical problems," Accessed 17 November 2016. [Online]. Available: http://www.diagnosticimaging.com/articles/immersion-enters-virtual-reality-solve-surgical-problems

[66] Immersion.com website, "CAE Healthcare Acquires Immersion Medical Simulation Product Lines and Licenses TouchSense Technology," Accessed 17 November 2016. [Online]. Available: http://ir.immersion.com/releasedetail.cfm?releaseid=455705

[67] J. H. Anderson and R. Raghavan, "A vascular catheterization simulator for training and treatment planning," *J. Digit Imaging*, pp. 120–123, 1998.

[68] Y. Wang, C. Chui, H. Lim, Y. Cai, and K. Mak, "Real-time interactive simulator for percutaneous coronary revascularization procedures," *Comput Aided Surg.*, vol. 3, pp. 211–27, 1998.

[69] C. Chui, P. Chen, W. Yaoping, J. M. H. A., C. Yiyu, and K.-H. Mak, "Interventional radiology interface apparatus and method," *Patent US6538634*, 2003.

[70] X.Ma, "Latest development of an interventional radiology training simulation system: NeuroCath," *Digital Human Modeling, Lecture Notes in Computer Science*.

[71] X. Wu, V. Pegoraro, V. Luboz, P. Neumann, R. Bardsley, S. Dawson, and S. Cotin, "New approaches to computer-based interventional neuroradiology training," *Medicine Meets Virtual Reality 13: The Magical Next Becomes the Medical Now*, vol. 111, pp. 602–607, 2005.

[72] S. Dawson, S. Cotin, D.Meglan, D. Shaffer, and M. Ferrell, "Designing a computer-based simulator for interventional cardiology training," *Catheter Cardiovasc Interv.*, vol. 51, pp. 522–7, 2000.

[73] Sciencedirect.com website, "Learning Curves and Reliability Measures for Virtual Reality Simulation in the Performance Assessment of Carotid Angiography," Accessed 17 November 2016. [Online]. Available: http://origin-ars.els-cdn.com/content/image/1-s2.0-S0735109706003792-gr1.jpg

[74] F. Ohlsson, "Interventional simulation device," *Patent US7520749*, 2009.

[75] M. Raspolli, C. Avizzano, G. Facenza, and M. Bergamasco, "HERMES: An Angioplasty Surgery Simulator," *World Haptics Conference: First Joint Eurohaptics Conference and Symposium on Haptic Interfaces for Virutual Environment and Teleoperator Systems, Proceedings*, pp. 148–156, 2005.

[76] S. Betrisey, I. Vecerina, and J. Zoethout, "Device for determining the longitudinal and angular position of a rotationally symmetrical apparatus," *Patent EP 1574825*, 2005.

[77] I. Vecerina, S. Betrisey, and J. Zoethout, "Actuator for an elongated object for a force feedback generating device," *Patent US 20070063971*, 2007.

[78] V. Luboz, Y. Zhang, S. Johnson, Y. Song, C. Kilkenny, C. Hunt, H. Woolnough, S. Guediri, J. Zhai, T. Odetoyinbo, P. Littler, A. Fisher, C. Hughes, N. Chalmers, D. Kessel, P. Clough, J. Ward, R. Phillips, T. How, A. Bulpitt, N. John, F. Bello, and D. Gould, "ImaGiNe Seldinger: First simulator for Seldinger technique and angiography training." *Comput Methods Programs Biomed.*, vol. 111, pp. 419–34, 2013.

[79] Mynewsdesk.com website, "VIST-C System," Accessed 17 November 2016. [Online]. Available: http://www.mynewsdesk.com/us/mentice-ab/images/vist-c-system-r-123848

[80] Simbionix.com website brochure, "Angiomentor," Accessed 17 November 2016. [Online]. Available: http://www.simbionix.com/wp-content/uploads/2011/01/ANGIOMentor_11_2012-Web.pdf

[81] R. Bronstein and S.Israeli, "Medical simulation device with motion detector," *Patent US 20070134637*, 2007.

[82] Medical Simulation Corp. website, "Simantha brochure."

[83] Y. Chen, Q. Gao, D. A. MacPhee, and D. E. Wilson, "Medical simulation system and method," *US 7862340*, 2011.

[84] CathI-Online website, "Product brochure," Accessed 17 November 2016. [Online]. Available: http://www.cathi-online.com/index.php/en

[85] P. Rebholz, C. Bienek, D.Stsepankou, and J. Hesser, "CathI âĂŞ Training system for PTCA: A step closer to reality," *Medical Simulation, Lecture Notes in Computer Science*, vol. 3078, pp. 249–255, 2004.

[86] J. Fraden, "Handbook of Modern Sensors: Physics, Designs and Applications," *SpringerVerlag*, 2003.

[87] WikiSensor, "Ultrasound sensor: Reflective mode," Accessed 17 November 2016. [Online]. Available: http://sensorwiki.org/doku.php/sensors/ultrasound?s[]=ultrasound

[88] Chegg.com website, "Doppler flow meter," Accessed 17 November 2016. [Online]. Available: http://www.chegg.com/homework-help/questions-and-answers/doppler-flow-meter-used-measure-speed-blood-flow-transmitting-receiving-elements-placed-sk-q1508919?frbt=1

[89] Freecircuits.com website, "How Capacitors Work," Accessed 17 November 2016. [Online]. Available: http://freecircuits.org/2012/01/capacitors-basics-working/

[90] RFID Journal website, "VeriChip Markets Its Implantable RFID Tags and Services Direct to Consumers," Accessed 17 November 2016. [Online]. Available: http://www.rfidjournal.com/article/view/4055

[91] NDI Digital website, "The Aurora Electromagnetic Tracking System," Accessed 17 November 2016. [Online]. Available: http://www.ndigital.com/medical/technology-em.php

[92] N.D.I Digital website, "NDI Aurora Brochure," Accessed 17 November 2016. [Online]. Available: http://www.ndigital.com/medical/aurora-accessories.php

[93] P. J. French, D. Tanase, and J. F. L. Goosen, "Sensors for catheter applications," *Sensors Update*, vol. 13, pp. 107–153, 2004.

[94] S.Betrisey, I.Vecerina, and J. Zoethout, "Optical device for determining the longitudinal and angular position of a rotationally symmetrical apparatus," *Patent EP1517119*, 2005.

[95] Industry Cortex website, "Products and services," Accessed 17 November 2016. [Online]. Available: http://www.industrycortex.com/products/results/cov

[96] Caldaro.com website, "Potentiometer," Accessed 17 November 2016. [Online]. Available: http://caldaro.com/potentiometer/

[97] Physics Classroom website, "Resistance," Accessed 17 November 2016. [Online]. Available: http://www.physicsclassroom.com/class/circuits/Lesson-3/Resistance

[98] Measuring Position and Displacement with LVDTs, "(national instruments website)," Accessed 17 November 2016. [Online]. Available: http://www.ni.com/white-paper/3638/en/

[99] A. Sarwa, *Haptic Device for Virtual Endovascular Procedural Training.* Masters Dissertation, 2009.

[100] T. Kern, "Engineering haptic interfaces," 2009.

[101] M. Moscatel, F. Shellock, and S. Morisoli, "Biopsy needles and devices: assessment of ferromagnetism and artifacts during exposure to a 1.5-t mr system." *J Magn Reson Imaging.*, pp. 369–372, 1995.

[102] J. Dulhunty, A.Suhrbier, G.A.Macaulay, J. Brett, V. van Straaten, I. Brereton, and J. Farmer, "Guide-wire fragment embolisation in paediatric peripherally inserted central catheters," *Med J Aust*, pp. 250–255, 2012.

[103] Center for Scientific Creation website, "Theories for the origin of earthâĂŹs radioactivity," Accessed 17 November 2016. [Online]. Available: http://www.creationscience.com/onlinebook/Radioactivity3.html

[104] Studentforums.biz website, "Electricity and Magnetism," Accessed 17 November 2016. [Online]. Available: http://www.studentforums.biz/references-and-resources/physics-p3-2752010/

[105] PMR Science Wikispaces website, "The sense of touch," Accessed 17 November 2016. [Online]. Available: http://pmr-science.wikispaces.com/1.2+The+Sense+of+Touch

[106] Stock Free Images website, "Hand holding glass," Accessed 17 November 2016. [Online]. Available: http://www.stockfreeimages.com/7358405/Red-wine.html

[107] Geomagic website, "What is Haptics ?" Accessed 17 November 2016. [Online]. Available: www.geomagic.com/files/7713/4857/8044/what_is_haptics.pdf

[108] O. Lambercy, T. Moix, D. Ilic, L. Sache, and H. Bleuler, "Measurement of internal constraints during an interventional radiology procedure," *Proceedings of the 2005 IEEE Engineering in Medicine and Biology 27th Annual Conference Shanghai, China*, 2006.

[109] J. Guo, S. Guo, N. Xiao, X. Ma, S. Yoshida, T. Tamiya, and M. Kawanishi, "A novel robotic catheter system with force and visual feedback for vascular interventional surgery," *International Journal of Mechatronics and Automation*, 2012.

[110] FAIN Biomedical, "Product Brochure," Accessed 21 October 2014. [Online]. Available: http://www.fain-biomedical.com/wp-content/themes/fbm_srk/images/eve_fbm_e.pdf

[111] A.Patriciu, D.Mazilu, H.S.Bagga, D.Petrisor, L.Kavoussi, and D.Stoianovici, "An evaluation method for the mechanical performance of guide-wires and catheters in accessing the upper urinary tract." *Med Eng Phys*, vol. 29, pp. 918–922, 2006.

[112] T. Fogarty and R. White, "Peripheral endovascular interventions, journal = Springer, year = 2010,."

[113] Invasive Cardiology website, Accessed 17 November 2016. [Online]. Available: http://www.invasivecardiology.com/articles/successful-transradial-intervention-switching-6-french-5-french-guiding-catheter

[114] G. Privitera, "Statistics for the behavioral sciences," *SAGE*, 2014.

[115] K. H. Zou, S. S. J.R. Fielding, and C.M.Tempany, "Hypothesis testing I: Proportions," *Radiology*, pp. 609–613, 2003.

[116] R. A. Hanneman, A. J. Kposowa, and M. D. Riddle, "Basic statistics for social research," *John Wiley and Sons*, 2012.

[117] Agilent ADNS 2610 Data Sheet, Accessed 17 November 2016. [Online]. Available: http://www.robotiklubi.ee/_media/projektid/distantsisensor/5988-9774en.pdf

[118] V. Luboz, J. Zhai, T. Odetoyinbo, P. Littler, D. Gould, T. How, and F. Bello, "Guidewire and catheter behavioural simulation," *Comput. Methods. Programs Biomed.*, 2013.

[119] "Coefficient of Friction Analysis of Commercially Available Nitinol Guidewires," Accessed 17 November 2016. [Online]. Available: http://www.bardmedical.com/media/19291/ks_nicore_whitepaper_cof.pdf

[120] Rjchase.com website, "PTFE Handbook," Accessed 17 November 2016. [Online]. Available: http://www.rjchase.com/ptfe_handbook.pdf

[121] Sunray Polyurethane Products website, "Understanding polyurethane coefficient of friction," Accessed 17 November 2016. [Online]. Available: http://www.slideshare.net/SunrayInc/understanding-polyurethane-coefficient-of-friction

[122] FosterComp website, "Pebax in medical applications," Accessed 17 November 2016. [Online]. Available: http://www.fostercomp.com/sites/default/files/Pebax%20in%20Medical%20Applications.pdf

[123] Dassault Systems website, "Solidworks page," Accessed 17 November 2016. [Online]. Available: http://www.solidworks.co.uk/

[124] N.W.John, V.Luboz, F.Bello, C.Hughes, F.Vidal, I.S.Lim, T.V.How, J.Zhai, S.Johnson, N.Chalmers, K.Brodlie, A.Bullpit, Y.Song, D.O.Kessel, R.Phillips, J.W.Ward, S.Pisharody, Y.Zhang, C.M.Crawshaw, and D.A.Gould, "Physics-based virtual environment for training core skills in vascular interventional radiological procedures." *Stud Health Technol Inform.*, pp. 195–197, 2008.

[125] Dotmar.com website, "Coefficient of friction of plastics," Accessed 17 November 2016. [Online]. Available: http://www.dotmar.com.au/co-efficient-of-friction.html

[126] Elastrat Products website, "Abdominal soft silicon model without aneurysm," Accessed 17 November 2016. [Online]. Available: http://www.elastrat.ch/models/index.php?id=114

[127] P. Korzeniowski, F. Martinez, N. Hald, and F. Bello, "Simulation of catheters and guidewires for cardiovascular interventions using an inextensible cosserat rod," *Lecture Notes of ISBMS 2014*, 2014.

[128] M. Bergou, M.Wardetzky, S.Robinson, B. Audoly, and E. Grinspun, "Discrete elastic rods," *ACM Trans. Graph.*, 2008.

7

Appendix

Appendix A: Research Ethics and Study Protocol

Appendix B: Online Questionnaire on Endovascular Haptic Feedback

Appendix C: Questionnaire for Experimental Testing with Weights

Appendix D: Questionnaire for Prototype Validation Testing

Appendix A: Research Ethics and Study Protocol

A Study of Endovascular Forces, Their Effects on Endovascular Tools and its Perception as Haptic Feedback

Imperial College London

2013

Researcher name: Hafiz Rashidi b Harun

Supervisor : Dr Fernando Bello
Reader in Surgical Graphics & Computing
Division of Surgery, Dept. of Surgery and Cancer
Imperial College London

1. Introduction

Cardiovascular diseases or CVD are the number one cause of death around the world [1]. It is estimated that 17.3 million people died from CVDs in 2008. The key advent of pinhole surgery at the end of the 20th century has enhanced the diagnosis and treatment of many major vascular diseases and has become a vital part of vascular health care today. With this approach, patients suffer much less tissue trauma, which leads to faster recovery and reduced treatment costs since they can usually be treated as day surgery cases [2]. Endovascular clinicians require extensive training and practise because endovascular procedures demand dexterity in handling the delicate guide wire and catheter tools and good hand-eye coordination.

Endovascular clinicians are largely trained using the traditional apprenticeship model where the trainee or apprentice learns first through observation, and then by gradually assisting and performing surgical procedures themselves under the direct supervision of the senior clinician. Several factors such as the increasing costs of time in the operating room [3] have resulted in a need for alternative out-of-the OR training methods such as virtual reality (VR) simulators [4]. These simulators have the advantage of being adaptable to simulate different anatomies, as well as having haptic feedback that helps to recreate the feeling of handling the tools through the sense of touch.

Despite the significant advantages of endovascular surgical training with virtual simulators, there are several factors that cause its use to be less widespread than might be expected. From our initial pilot study, the general consensus among senior endovascular clinicians is that the simulators are still lacking in realism. While the presence of haptic feedback is considered useful, many senior clinicians feel that the type of haptic sensations delivered to the user is still too basic and does not accurately resemble the forces that are felt in real life. This can be due to the fact that hardware and software developers are trying to replicate forces or haptic feedback that they have never experienced themselves, with very little published evidence of the actual requirements for such devices. Therefore, the aim of this study is to address this and fill in the gaps of information.

We aim to achieve this by conducting a study that involves gathering the opinions from medical experts through an online questionnaire and an experimental study using a bench top prototype device. The only ethical considerations for the study are voluntary participation, data confidentiality, anonymity and use of the gathered data. This study does not involve patients. It requires only the consensual participation of medical experts. The identities of the participants will

be anonymised and their responses and any other gathered data will be kept confidential at all times in accordance with the Data Protection Act.

References

[1] Global status report on noncommunicable diseases 2010. Geneva, World Health Organization, 2011.

[2] Benefits of Minimally Invasive Surgery, University of Chicago Webpage, accessed 17 Oct 2013. http://www.uchospitals.edu/specialties/minisurgery/benefits/

[3] The financial impact of teaching surgical residents in the operating room, Bridges, M. ,Diamond, D.L., American Journal of Surgery, 1999 Jan, 177(1), 28-32.

[4] Simulation in Surgical Education, S. de Montbrun, H.MacRae. Clin Colon Rectal Surg,25(3), September 2012, 156-165.

2. Study Aim & Objectives

The aim of this study is to investigate the characteristics of the forces involved in endovascular procedures and how their effects are perceived as haptic feedback by the end effector or user.

The study has the following research objectives:

a) To identify the types of forces that affect the endovascular tools.
b) To study and understand the characteristics of each type of force and how they affect the endovascular tools mechanically.
c) To understand how the mechanical changes in the endovascular tool due to the forces is perceived as haptic feedback.
d) To identify which types of forces are important and should be recreated in a simulation environment to enhance realism of the virtual experience.
e) To determine the magnitude and range of forces required to reproduce similar haptic feedback with an actuator

3. Study Design

This study is designed around the research aim of gaining an understanding of the forces involved in endovascular procedures and how their effects are perceived as haptic. We plan to achieve this with the help of two different tools. First, we intend to gather the opinions of experienced individuals using an online questionnaire to meet objectives (a)–(d). Through the questionnaire responses, we will be able to better understand the types of forces that affect endovascular instruments in vitro and their mechanical effects. This will also address how the effects are perceived as haptic feedback and which feedback is considered important or should be recreated in a virtual simulator interface to enhance realism. Secondly, as we would like to have an estimate of the range of these forces and fulfil objective (e), an experimental study will be conducted. It is expected this new found knowledge on endovascular forces and haptic feedback perception will help in the generation of more realistic haptic feedback in future haptic interfaces. The two components of the study are now explained further.

Part 1: Online Questionnaire

Materials: Internet enabled computer or tablet device

Measurement items and units: Questionnaire and its responses

Method:

i- A suitable participant will be identified through a mutual contact with a similar professional background. His or her contact details will be sent to the researcher via email.

ii- A recruitment email will be sent to the subject explaining the aim of the study as well as other related general information.

iii- The subject will be asked to click on the attached link to access the online survey.

iv- At the front page of the online survey, the subject will be provided with information about the online survey and how it is to be completed.

v- The subject will then complete the online survey and the responses will be submitted anonymously.

vi- The online survey responses are collected by the survey hosts.

vii- The researcher will repeat steps i-vi until a suitable total number of participants have been reached.

viii- Once the target number is reached, the researcher will extract the results from the survey hosts and conduct statistical analysis on the data obtained.

Part 2: Force Measurement Experiments

Materials: Guide wire, catheter, electromagnetic actuator, mechanical actuator, bench top prototype, microcontroller, notebook computer, cardboard illustrations

Measurement items and units: Current supplied to electromagnetic actuator (I/A), Degree of mechanical actuator arm (D/◦), Force applied to tools (Fa/N), Maximum force applied (Fmax/N)

Method:

i – The participant will be given an information sheet which provides a briefing on the purpose of the experiments to be conducted. The participant will also be given instructions on how to perform the experiment prior to the test. Per the participant's agreement to participate, he or she will be asked to fill in a consent form.

ii – The participant will be presented with the bench top prototype containing both actuators and the concentrically pre-inserted instruments (guide wire and catheter) to be used in the experiments.

iii - For each experiment, the participant will be provided with the context for a specific endovascular procedure at a specific location in the vascular system. The context will be explained using cardboard illustrations to help visualise the scenario. The anatomy used to describe the scenario will depend on the training background of the participant.

iv – The participant will then be asked to advance only the catheter within the bench top prototype with the scenario in mind. The test operator will increase the amount of resistance applied to the catheter in steps using the microcontroller circuit.

vi – The participant will acknowledge the strength of the current applied force in a confirmation sheet as either too low, too high or just right for the set context. This will be repeated until the maximum level of resistance is used.

viii – With the same context in mind, the experiment will be repeated with the guide wire whilst the catheter is held in place.

ix – Steps iv – viii are repeated for each instrument through the 6 different contexts, featuring 3 vessels with different levels of tortuosity, and 3 vessels with different levels of stenosis severity. This will result in the identification of the most suitable range of forces involved in each context.

4. Participant Entry Requirement

a) Inclusion Criteria

The subjects in this study are also known as endovascular clinicians. They are medical professionals that have been trained or are still in training as interventional radiologists, vascular surgeons and interventional cardiologists. From discussions with several endovascular clinicians, it is recognised that a clinician in training would need to perform a minimum of 300 procedures as the main operating clinician, either with or without senior supervision, in order to understand the types of haptic feedback felt in real interventions. Given that in the UK trainees perform an average of 20 procedures per week, our inclusion criteria is that subjects must have performed endovascular procedures for at least one year.

b) Exclusion Criteria

Subject has not performed endovascular procedures for a minimum of one year.

c) Withdrawal Criteria

This is a non-intervention study and there are no consequences for early withdrawal. The subject or participant may withdraw consent at any point.

5. Data Management

Part 1: Online Survey

The online survey does not require the participant to provide any details that reveal their personal identity other than their medical background and years of professional experience. It is is therefore not possible to link the responses of the survey to a specific participant. This ensures the anonymity of participants in the study.

Part 2: Force Measurement Experiments

Each participant will be assigned a unique identification code. Their data will be carefully anonymised to remove all personal identifiers except for their professional background, position and years of experience. This data will be stored on a secure Imperial College server. There will be a journal/notebook linking this unique code with the individual in case there is a need to go back and look at the personal details again or to exclude a participant's data. The journals will be stored in a locked filing cabinet in a secure office by the data custodian. The appointed data custodian will be Dr Fernando Bello (the study Chief Investigator).

6. Adverse Events

This study is not a clinical trial of an investigational medicinal product or medical device. It involves no drugs and no novel procedures. It involves qualitative observations and recordings. Therefore no adverse events are expected.

7. Assessment and Follow Up

There will be no clinical intervention and therefore no follow-up intervention required.

8. Statistics and Data Analysis

Part 1: Online Survey

To ensure the external validity of the study, we aim to recruit a minimum of 30 participants to complete the online survey.

Objective: To understand the types of forces involved in vitro in endovascular procedures and determining which forces in particular should be recreated in simulation training to enhance realism.

Hypothesis: There are several forces acting on the endovascular tools in vitro. These forces produce a haptic feedback to the end user. Some of these haptic feedback effects need to be recreated in simulation to enhance simulation realism.

Analysis of interest:

a) Number of participants agreeing to each force description provided in the questionnaire and the percentage of that from the total.
b) Overall evaluation of the force type descriptions provided.
c) Percentage of participants ranking a force type from strongest to weakest.

Part 2: Force Measurement Experiments

A sample size of 10 subjects is targeted for this experimental study. Data and all appropriate documentation will be stored for a minimum of 10 years after the completion of the study, including the follow-up period.

Objective: To investigate the range of forces that needs to be applied to the tools with an actuator in order to recreate realistic haptic feedback in endovascular procedure simulation.

Hypothesis: By applying forces in the range of 0 - 2 N[1] (Fa = 0.5, 1.0, 1.5, 2.0) onto the tools, reproduction of realistic haptic feedback to the end user can be created.

Analysis of interest:

a) Mean value and standard deviation for Fmax (the maximum value of suitable force applied to the tools) for the guide wire for 6 specific contexts from all 10 participants.
b) Mean value and standard deviation for Fmax for the catheter for 6 specific contexts from all 10 participants.

[1] **A real-time haptic interface for interventional radiology procedures.** 2005: **Thomas Moix; Dejan Ilic;** Blaise Fracheboud; Jurjen Zoethout; Hannes Bleuler, Studies in health technology and informatics 2005;111():329-33.

9. Regulatory Issues

a) Ethics

The main ethical considerations refer to voluntary participation, data confidentiality, anonymity and use of the gathered data. To address participation, an information sheet will be provided to ensure participants are adequately informed. The participants will be assured that the data collected will be confidential, remain anonymous and be used solely for the purposes of this study. The collection and handling of the data will be in accordance to the Data Protection Act.

The research will not involve work done under the Animals (Scientific Procedures) 1986 Act. The research will not involve the use of genetically modified tissue. The project will not involve the use of post-operative, post mortem material or access to confidential patient information.

This protocol will be submitted to the ICREC for ethical approval because this work does not involve NHS patients. It will only involve volunteer members of Imperial College NHS Trust and surgical trainees.

b) Consent

All participants will be required to sign a written consent form prior to the commencement of the study and will be free to withdraw from the study at any point.

10. Study Management

The day-to-day management of the study will be co-ordinated by the researcher Mr Hafiz Rashidi b Harun under the supervision of the Chief Investigator, Dr Fernando Bello.

11. Publication Policy

Only anonymised data will be used in publication. It is anticipated that resources acquired through the study may be included in presentations at conferences and publications in peer-reviewed journals.

Imperial College London

PARTICIPANT INFORMATION SHEET FOR THE ENDOVASCULAR FORCE AND HAPTICS STUDY

We are running a research study and we wish to enter you as a participant. We would like you to take the time to read this sheet, which explains the research. Ask us if there is anything that is not clear or if you would like more information. Please take your time to decide whether or not you wish to participate.

Thank you for reading this.

What is the purpose of the research?

We are studying the types of endovascular forces that translate into haptic feedback in endovascular tools, primarily the guide wire and catheter. Also, we are interested in finding the quantitative value of the forces so that we can faithfully reproduce said haptic feedback effects artificially. This is part of an ongoing effort to improve the haptic feedback available in haptic interfaces for endovascular virtual simulators so as to make surgical training in a virtual environment more realistic and effective.

Why have I been chosen?

You have been chosen as your surgical experience satisfies our participant selection criteria.

What are you asking of me?

We are asking you to participate in both an online questionnaire and an observational study involving a bench top prototype. The online questionnaire consists of 10 questions and should take no longer than 10 minutes to complete. The observational study consists of a series of tests where you will be asked to manipulate a guide wire and a catheter within a bench top prototype. You will be given a context scenario before each test which features a specific type of anatomy within the vascular system. While you are visualising the context and manipulating the instruments, the device will apply increasing levels of force to the instruments which also increases the strength of the haptic feedback. You are then asked to notify the researcher of when the level of applied force is suitable for the current context provided and also when it is too strong. This is so that we can identify the right level of force or haptic feedback that is correct to a given context and establish a maximum value for the force too. This test is repeated for 6 different contexts and we estimate that the whole test should not take longer than 50 minutes. Your input to the study, both from the questionnaire and the observational tests, will be recorded and kept securely on an electronic file.

What will happen if I take part?

We will ask you to sign a consent form. The form breaks down the consent process into parts. This is to help you understand what you are agreeing to. You should read the consent form carefully and, if you agree, sign each part. If you do not agree then do not sign.

If I agree?

If you agree to participate in the study then this is recorded on the consent form. We will discuss suitable times for you to participate in the experiments. Prior to that, you will be given a link to complete the online questionnaire, which will also help familiarise you with the study.

If I refuse?

If you do not wish to continue with the study then we will record this on the consent form. We will not contact you again about this research study.

What about data, confidentiality and privacy?

We plan to keep the data related to this research for 10 years. The data will be kept secure by the Data Custodian. Access to the data will only be for research staff. Data will be anonymised. If you wish to see your recorded input after providing them, this will be permitted, however you will not be allowed to view other participants' data.

What are the benefits of taking part?

Increased understanding of haptic feedback generation using force actuators.

What if something goes wrong?

If there is a technical fault with the observational setup during the tests, which prevents you from completing it, the fault and the stage in the test at which it happened will be recorded before restarting the setup to the stage at which it stopped. If needed, a separate session will be arranged to complete the tests.

What will happen to the results of the research?

We hope that the results will be published in a scientific journal. The data will be anonymised so the readers of the journal will not know who the operators were.

Imperial College London

Who is organising and funding the research?

This research is organised by the Faculty of Medicine at Imperial College London. The project has been funded by the MIDP (Malaysia-Imperial Doctoral Programme).

Who has reviewed this study?

This study was given a favourable ethical opinion for conduct in the NHS by the Imperial College Research Ethics Committee (ICREC). The ICREC was founded in 2006 to review studies which need ethical consideration, but which fall outside the remit of NHS Ethics Committees. The Committee comprises of 4 lay members and 4 members of Imperial College.

Contact for Further Information

For further information please contact Dr Fernando Bello. He can be contacted on the following telephone number: 0203312 1788

Thank you for reading this information sheet.

IF YOU DECIDE TO CONSENT TO THIS STUDY A COPY OF THIS SHEET AND A SIGNED CONSENT FORM WILL BE GIVEN TO YOU TO KEEP.

Imperial College London

Endovascular Forces and Haptic Feedback Study

Please initial box

1.	I confirm that I have read and understand the participant information sheet dated 28 Oct 2013 version 1.2 for the above study and have had the opportunity to ask questions which have been fully answered.	
2.	I understand that my participation is voluntary and I am free to withdraw and stop taking part at any time without giving a reason.	
3.	I agree to take part in this study.	

_____	_____	_____
Print name of participant	**Signature**	**Date**

_____	_____	_____
Name of person taking consent	**Signature**	**Date**

_____	_____	_____
Chief Investigator	**Signature**	**Date**

Appendix B: Online Questionnaire on Endovascular Haptic Feedback

Copy of Ultimate

Introduction

Haptic feedback is an emerging new technology based on the sense of touch in user interface design. This tactile feedback technology is developed by understanding users' sense of touch e.g. by applying forces, vibrations or motions.

We are seeking to understand and determine the characteristics of haptic feedback that are considered useful by clinicians so that they may be accurately recreated for use in high fidelity virtual simulated environments. This work is part of an ongoing effort to improve the effectiveness and realism of endovascular procedures training through the use of virtual simulators.

In the brief set of questions that follow, we would value your feedback about the types of forces that act upon the guide wire and catheter while it is within the human vascular system, traveling from the insertion point (eg. femoral artery) to the target vessel (eg. renal artery). We would also like to understand the haptic effect these forces produce as perceived by operating clinicians.

Definitions & Terms: In the following questions, the following terms apply:

- "guide wire" refers to a 0.35" (0.9mm) Terumo wire
- "catheter" refers to a diagnostic catheter of a diameter and tip shape suitable for navigating from the femoral/radial artery onwards.

For more information about our work, please contact Dr Fernando Bello, Dept of Surgery & Cancer, Imperial College London (f.bello@imperial.ac.uk) or Hafiz Harun (h.harun10@imperial.ac.uk)

1. Please state your professional medical background.

- ◯ Interventional Radiologist
- ◯ Non-interventional Cardiologist
- ◯ Interventional Cardiologist
- ◯ Vascular Surgeon

2. Please describe your current level of experience

- ◯ Junior Registrar
- ◯ Senior Registrar
- ◯ Consultant

3. Please state how many years of experience you have performing endovascular procedures

4. Please tick the endovascular procedures training methods you have had experience with

- [ ] Real life patients in the Cathlab or Operating Room
- [ ] Benchtop physical model
- [ ] Virtual simulator trainers (VIST/Angiomentor/others)

Other (please specify)

5. In a healthy and non tortuous vessel, there is no resistance felt when advancing the guide wire and catheter

Strongly Disagree	Disagree	Neutral	Agree	Strongly Agree
○	○	○	○	○

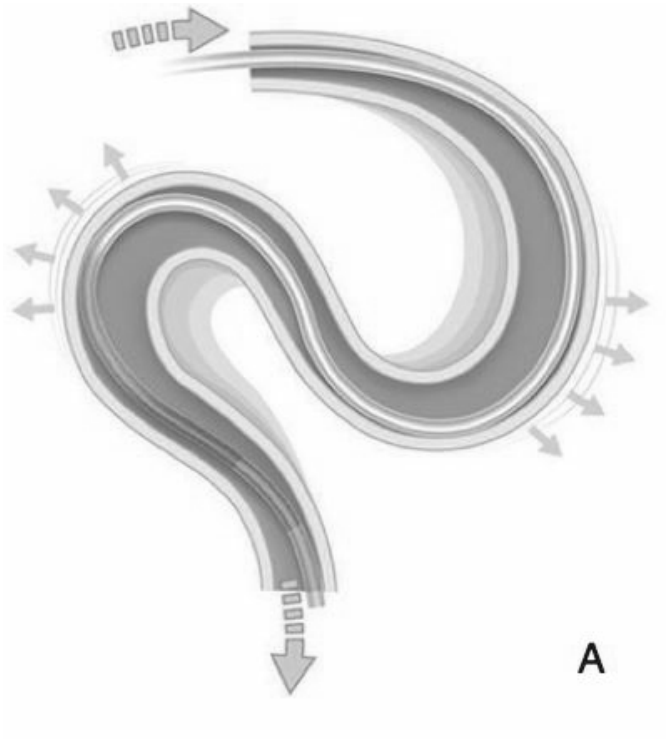

6. Tortuous vessels

	Strongly Disagree	Disagree	Neutral	Agree	Strongly Agree
There is resistance felt when moving the instruments through a tortuous vessel.	○	○	○	○	○
The strength of the resistance increases with the degree of vessel tortuousness and vessel narrowing	○	○	○	○	○
There is also resistance felt when rotating instruments within tortuous vessels	○	○	○	○	○
This rotational resistance is caused by torque that is stored within the instruments as it is bent/twisted	○	○	○	○	○
Rotational resistance is not that noticeable to the operator's touch	○	○	○	○	○
An obvious sign of rotational resistance is that it takes many rotations to cause the instrument tip to rotate as shown by fluoroscopic images	○	○	○	○	○
Rotational resistance is more often detected visually by observing than through the operator's touch	○	○	○	○	○

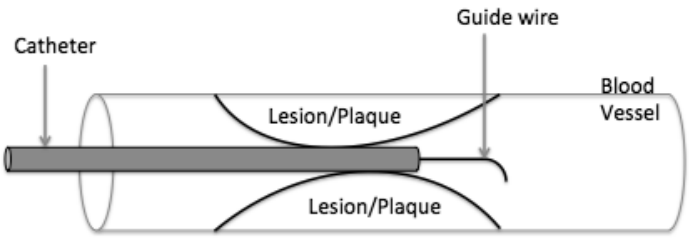

7. Narrowed vessel

	Strongly Disagree	Disagree	Neutral	Agree	Strongly Agree
A resistance effect can be felt when advancing the instruments through a narrowed vessel.	○	○	○	○	○
The resistance felt increases with the amount of narrowing experienced by the vessel	○	○	○	○	○
In an occluded vessel, the resistance is so strong that the wire can not be advanced	○	○	○	○	○

8. Please rank the strength of resistance felt when advancing the instruments in the following context (1 = strongest, 5 = weakest):

- ⠿ ▲▼ Healthy vessel
- ⠿ ▲▼ Tortuous vessel
- ⠿ ▲▼ Vessel with stenoses
- ⠿ ▲▼ Vessel with calcified lesions
- ⠿ ▲▼ Occluded vessel

9. Resistance effect and direction of movement

	Strongly Disagree	Disagree	Neutral	Agree	Strongly Agree
Once an unexpected resistance is felt by the clinician when pushing the instruments, he/she will immediately stop from advancing the instruments any further.	○	○	○	○	○
Following the above, fluoroscopic images are then obtained to examine the cause of the said resistance.	○	○	○	○	○
For tortuous vessels, the resistance effect when advancing the instrument is bidirectional until the instrument exits the tortuous vessel	○	○	○	○	○
For narrowed vessels, the resistance effect when advancing the instrument is unidirectional when at the point of narrowing(stenoses)	○	○	○	○	○
Once past the point of narrowing(stenoses), the resistance effect is bidirectional	○	○	○	○	○

10. Please rank the forces described here in terms how noticeable they are during the procedures. (1 = most important, 2 = least important)

⠿ ▲▼ Force I: Resistance due to narrowed vessel or highly tortuous vessel

⠿ ▲▼ Force II: Rotational resistance due to tortuous pathway

11. Please give any feedback that you think will be useful to this study.

Appendix C: Questionnaire for Experimental Testing with Weights

Copy of Haptics study

Thank you for your willingness to participate in this study. The objective of the study is to understand the forces involved in order to reproduce the haptic effects felt during endovascular surgery through a simulator haptic interface. In the following exercise, you will be asked to advance a guide wire/catheter through a device which will apply specific haptic effects to the instrument. You are then asked to reflect on how similar or close the haptics produced is to the ones felt in real life according to the scenarios given and record your input in this survey.

Thank you again for your time.

Part A: Quantifying contextual resistance haptic feedback

1. Please assign each level of applied resistance to one of the following contexts based on the maximum strength of resistance felt.

	Healthy/Normal vessel	Vessel with Stenosis/Narrowing	Tortuous vessel	Vessel with calcified lesion	Occluded vessel
R1	☐	☐	☐	☐	☐
R2	☐	☐	☐	☐	☐
R3	☐	☐	☐	☐	☐
R4	☐	☐	☐	☐	☐
R5	☐	☐	☐	☐	☐
R6	☐	☐	☐	☐	☐
R7	☐	☐	☐	☐	☐
R8	☐	☐	☐	☐	☐
R9	☐	☐	☐	☐	☐
R10	☐	☐	☐	☐	☐
R11	☐	☐	☐	☐	☐
R12	☐	☐	☐	☐	☐
R13	☐	☐	☐	☐	☐
R14	☐	☐	☐	☐	☐
R15	☐	☐	☐	☐	☐

Part B: Reproducing haptic effects and establishing context

2. Please assign each level of applied resistance to one of the following contexts based on the maximum strength of resistance felt.

	Healthy/Normal vessel	Vessel with Stenosis/Narrowing	Tortuous vessel	Vessel with calcified lesion	Occluded vessel
R1	☐	☐	☐	☐	☐
R2	☐	☐	☐	☐	☐
R3	☐	☐	☐	☐	☐
R4	☐	☐	☐	☐	☐
R5	☐	☐	☐	☐	☐
R6	☐	☐	☐	☐	☐
R7	☐	☐	☐	☐	☐
R8	☐	☐	☐	☐	☐
R9	☐	☐	☐	☐	☐

3. Please give any feedback that you think will be useful to this study.

Appendix D: Questionnaire for Prototype Validation Testing

1. Guide wire and Catheter Movement

	Strongly Disagree	Disagree	Neutral	Agree	Strongly Agree
The virtual guide wire is responsive to the translational movements of the real guide wire	○	○	○	○	○
The virtual guide wire is responsive to the rotational movements of the real guide wire	○	○	○	○	○
The virtual catheter is responsive to the translational movements of the real catheter	○	○	○	○	○
The virtual catheter is responsive to the rotational movements of the real catheter	○	○	○	○	○
The movement of the virtual guide wire corresponds well to the real guide wire	○	○	○	○	○
The movement of the virtual guide wire corresponds well to the real guide wire	○	○	○	○	○

2. Haptics and Force Feedback

	Strongly Disagree	Disagree	Neutral	Agree	Strongly Agree
The resistance effect for the guide wire is realistic to the provided context	○	○	○	○	○
The resistance effect for the guide wire is acceptable for the purposes of simulation	○	○	○	○	○
The resistance effect for the catheter is realistic to the provided context	○	○	○	○	○
The resistance effect for the catheter is acceptable for the purposes of simulation	○	○	○	○	○

3. System Design

	Strongly Disagree	Disagree	Neutral	Agree	Strongly Agree
The operative workspace provided for the participant is sufficient	○	○	○	○	○
The different appearance of the guide wire has no negative affect on the simulation	○	○	○	○	○
The different appearance of the catheter has no negative affect on the simulation	○	○	○	○	○
The setup and tools as presented faithfully recreate the setup in real life	○	○	○	○	○
The two port approach used enables the practice of tool manipulation that is acceptable	○	○	○	○	○
The sequences that are performed with the prototype represent closely the sequences in real life.	○	○	○	○	○
Switching between the two ports during simulation does not break the immersiveness of the simulation	○	○	○	○	○

4. Please provide any feedback you think would be useful in the further development of the prototype.